Innovative Lastmile Solutions

Integrating People and Goods Transportation

Cheng, Rong

Publication date:
2024

Document Version
Publisher's PDF, also known as Version of record

DTU Management
Department of Technology, Management and Economics

Innovative Last-mile Solutions: Integrating People and Goods Transportation

PhD Thesis

Rong Cheng

October 2023

Innovative Last-mile Solutions:
Integrating People and Goods Transportation

PhD Thesis
October 2023

By
Rong Cheng

Main Supervisor:	Otto Anker Nielsen, Professor at Department of Technology, Management and Economics, Technical University of Denmark.
Co-Supervisor:	Yu Jiang, Associate Professor at Department of Technology, Management and Economics, Technical University of Denmark.
University:	Technical University of Denmark.
Department:	Department of Technology, Management and Economics
Division:	Transportation Science Division

| Cover photo: | Solveig Béen |
| Published by: | DTU, Department of Technology, Management and Economics, Akademivej, Building 358, 2800 Kgs. Lyngby Denmark
www.man.dtu.dk |

Summary

Transportation systems are integral to modern societies' functioning, facilitating people's movement to complete their daily tasks, such as going to work and school, as well as delivering goods to meet people's diverse needs. However, the escalating transportation demands resulting from the rapid urbanization and the boom of E-commerce have exacerbated traffic congestion and given rise to environmental issues. Consequently, actions must be taken to mitigate the negative externalities of growing transportation demands.

In 2007, the "Green Paper: Towards a New Culture for Urban Mobility" presented by the European Commission advocated for better integration of passenger and goods transport in urban planning. It emphasized that "Local authorities need to consider all urban logistics related to passenger and freight transport together as a single logistics system." The integration of passenger and goods transport offers a multitude of advantages. First, it could reduce traffic congestion and environmental pollution by reducing the number of used vehicles on the road and the total vehicle kilometers traveled. This is achieved by optimizing the routes of passenger and freight vehicles to curtail the overlap between them. Second, this integration could enhance cost-effectiveness and boost the economy by efficiently utilizing transportation resources (e.g., roads and vehicles), reducing operational expenses for businesses and improving mobility for people and goods. This, in turn, increases trade and economic activity. Third, the integrated transportation system improves the equity and accessibility to transport services, particularly in rural areas, as merging logistics services with public transport makes the transportation service more viable, ultimately reducing the isolation experienced by rural residents.

This thesis comprises four papers and makes several contributions to the realm of integrated people and goods transportation. It provides an overview of the development of integrated transportation systems, introduces two novel forms to integrate passengers and goods, validates their viability, and advances mathematical optimization within this field.

The first study (Paper 1) comprehensively reviews integrated people-and-goods transportation systems. It categorizes three forms of integrating people and goods transportation: people and parcels sharing a taxi, freight on transit, and crowdshipping. For each integration form, this study introduces real-life applications and summarizes the corresponding research problems. Furthermore, this study proposes a general framework for planning integrated people-and-goods transportation systems, along with directions for future research.

Followingly, this thesis explores two innovative solutions within the concept of integration of people and goods transportation. The first solution combines passenger and parcel transportation using demand-responsive vehicles (DRBs) and drones, considering the advantages of DRBs in terms of flexibility and large capacity, as well as the fast speed and low emissions of drones. DRBs can transport both passengers and parcels, while drones are dedicated to parcel delivery. This thesis initially proposes a passenger and parcel share-a-ride problem with drones (SARP-D) to address the routing problems for DRBs and drones in this context and devises different solution approaches. Paper 2 develops an arc-based mixed integer programming model solvable by CPLEX for small instances and an adaptive large neighborhood search (ALNS) metaheuristic for large instances with 200 nodes, the largest instance in the existing literature. Paper 3 reformulates the arc-based model to a path-based model and develops a column generation algorithm to solve it. The column generation approach can produce high-quality solutions for SARP-D instances involving 50 nodes. Meanwhile, it can be used to evaluate the metaheuristics for SARP-

D.

The second solution this thesis investigates is public transport (PT)-based crowdshipping. In this concept, parcel lockers are installed in several PT stations. PT users act as crowdshippers, picking up parcels from parcel lockers at their origin PT stations, taking public transport, and delivering parcels to parcel lockers at their destination PT stations. Paper 4 develops a parcel locker location model and a vehicle routing model to simulate the PT-based crowdshipping system. A case study in a central district in Copenhagen is conducted to assess the impacts of PT-based crowdshipping.

Computation results reveal that both SARP-D and PT-based crowdshipping could decrease the number of used vehicles on the road and total vehicle kilometers traveled, effectively alleviating traffic congestion. This thesis will inspire innovation in practical applications and contribute to advancing the research on integrated people and goods transportation in academia.

Resumé (Danish)

Transportsystemer er en integreret del af det moderne samfund og understøtter personers mobilitet for at udføre deres daglige opgaver, såsom at tage på arbejde og skole, samt levere varer. De stigende mobilitetskrav og deraf følgende transport har dog forværret trængsel og givet trafikpropper i nettet, og det stigende transportarbejde har givet anledning til miljøproblemer. Derfor bør der træffes beslutninger for at afbøde de negative eksternaliteter af voksende transportbehov.

I 2007 blev "the Green Paper: Towards a New Culture for Urban Mobility" fremlagt af Europa-Kommissionen for bedre integration af passager- og godstransport i byplanlægning. Den understregede, at "De lokale myndigheder er nødt til at overveje al bylogistik relateret til passager- og godstransport sammen som et samlet logistiksystem." Integrationen af person- og godstransport giver en lang række fordele. For det første kan det reducere trængsel og miljøbelastning ved at reducere antallet af benyttede køretøjer på vejen og de samlede kørte køretøjskilometre. Dette opnås ved at optimere ruterne for passager- og godskøretøjer for at begrænse overlappet imellem dem. For det andet kan denne integration øge omkostningseffektiviteten og booste økonomien ved effektivt at udnytte transportressourcer (f.eks. veje og køretøjer), reducere driftsudgifter for virksomheder og forbedre mobiliteten for mennesker og varer. Dette øger igen handel og økonomisk aktivitet. For det tredje forbedrer det integrerede transportsystem ligheden og tilgængeligheden til logistiktjenester, især i landdistrikter, da sammenlægning af logistiktjenester med offentlig transport gør transporttjenesten mere levedygtig, hvilket i sidste ende reducerer den isolation, som landbeboere oplever.

Denne afhandling består af fire artikler og giver adskillige bidrag til området integreret menneske- og godstransport. Den giver et overblik over udviklingen af integrerede transportsystemer, introducerer to relativt nye former til at integrere passagerer og varer, validerer deres levedygtighed og formulerer matematiske modeller og formulerer optimeringsteknikker inden for dette felt.

Den første undersøgelse (artikel 1) gennemgår integrerede transportsystemer for mennesker og varer. Den kategoriserer tre former for integration af person- og godstransport: personer og pakker, der deler en taxa, fragt på kollektiv trafik og crowdshipping (deleøkonomi). For hver integrationsform introducerer afhandlingen dens virkelige applikationer og opsummerer de tilsvarende forskningsproblemer. Desuden foreslås et generel framework for planlægning af integrerede transportsystemer for personer og varer, samt retninger for fremtidig forskning.

Efterfølgende udforskes to innovative løsninger inden for konceptet integration af person- og godstransport. Den første løsning kombinerer passager- og pakketransport ved hjælp af efterspørgselsfølsomme køretøjer (DRB'er) og droner, idet man tager fordelene ved DRB'er i betragtning med hensyn til fleksibilitet og stor kapacitet, såvel som dronernes høje hastighed og lave udledning af drivhusgasser. DRB'er kan transportere både passagerer og pakker, mens droner er dedikeret til pakkelevering. Afhandlingen foreslår indledningsvis et passager- og pakke-share-a-ride-problem med droner (SARP-D) for at løse ruteproblemerne for DRB'er og droner i denne sammenhæng og udtænke forskellige løsningstilgange. Artikel 2 udvikler en buebaseret blandet heltalsprogrammeringsmodel, der kan løses af CPLEX softwaren til små forekomster og en adaptiv storkvarterssøgning (ALNS) metaheuristisk for store forekomster med 200 knuder, den største forekomst i den eksisterende litteratur. Artikel 3 omformulerer den kantbaserede model til en sti-baseret model og udvikler en kolonnegenereringsalgoritme til at løse den. Kolonnegenereringsalgoritmen kan producere løsninger af høj kvalitet til SARP-D-instanser, der involverer 50

knuder. I mellemtiden kan den bruges til at evaluere metaheuristikken for SARP-D for problemer af denne størrelse, inden SARP-D benyttes til løsning af større problemer.

Den anden løsning, der undersøges, er offentlig transport-baseret crowdshipping. Her er der installeret pakkeskabe på flere offentlige transportstationer (PT). PT-brugere fungerer som crowdshippere, henter pakker fra pakkeskabe på deres oprindelige PT-stationer, tager offentlig transport og leverer pakker til pakkeskabe på deres destinations PT-stationer. Artikel 4 udvikler en pakkeskabsplaceringsmodel og en køretøjsrutemodel for at simulere det PT-baserede crowdshipping-system. Virkningerne af PT-baseret crowdshipping er undersøgt med et casestudie i en central bydel i København baseret på data fra en større logistikudbyder i Danmark.

Beregningsresultaterne afslører, at både SARP-D og PT-baseret crowdshipping kan reducere antallet af brugte køretøjer på vejen og det samlede antal kørte køretøjskilometer, hvilket effektivt kan afhjælpe trafikpropper. Denne afhandling vil inspirere til innovation i praktiske anvendelser og bidrage til at fremme forskningen i integreret menneske- og godstransport i den akademiske verden.

Preface

This PhD thesis entitled Innovative Last-mile Solutions: Integrating People and Goods Transportation is submitted to meet the requirements for obtaining a PhD degree at the Department of Technology, Management and Economics, DTU Management, Technical University of Denmark. The PhD project was supervised by Professor Otto Anker Nielsen and co-supervised by Associate Professor Yu Jiang, both from DTU Management. The thesis is paper-based and consists of the chapters listed in the tables of content, including separate chapters for each of the following papers:

Paper 1: Cheng, R., Jiang, Y., & Nielsen, O. A. (2023). Integrated people-and-goods transportation systems: from a literature review to a general framework for future research. Transport Reviews, 1-24. DOI: 10.1080/01441647.2023.2189322.

Paper 2: Cheng, R., Jiang, Y., Nielsen, O. A., & Pisinger, D. (2023). An adaptive large neighborhood search metaheuristic for a passenger and parcel share-a-ride problem with drones. Transportation Research Part C: Emerging Technologies, 153, 104203. DOI: 10.1016/j.trc.2023.104203.

Paper 3: Cheng, R., Jiang, Y., Nielsen, O. A., & Van Woensel, T. (2023). A passenger and parcel share-a-ride problem with drones: A column generation approach. Under review in Transportation Research Part B: Methodological.

Paper 4: Cheng, R., Fessler A., Larsen, A., Nielsen, O. A. & Jiang, Y. (2023). Assessing the impacts of public transport-based crowdshipping: A case study in a central district in Copenhagen. To be submitted to Frontiers of Engineering Management.

Rong Cheng

Kgs. Lyngby, October 2023

Acknowledgements

First and foremost, I would like to thank my main supervisor, Professor Otto Anker Nielsen, and co-supervisor, Associate Professor Yu Jiang, for your expertise, continuous guidance, and meticulous paper revisions during my entire PhD journey. I am deeply grateful for the opportunities you provided me to collaborate with outstanding researchers and attend conferences, which played a pivotal role in my academic development.

I express my deep gratitude to Professor David Pisinger. Thank you for your prompt responses to my questions and your constructive comments on revising the paper that we collaborated on. Your insights significantly contributed to improving our work. Thank you, Andreas Fessler, for building connections with the logistics company, which facilitates our collaboration on evaluating the potential saving of public transport-based crowdshipping. A big thanks to Associate Professor Jesper Bláfoss Ingvardson for helping process the smart card data. I would also like to thank Professor Allan Larsen for your guidance at the initial stage of the case study and your insightful comments, which have greatly enhanced our work.

I am very grateful to Professor Tom Van Woensel for hosting me at the Operations, Planning, Accounting, and Control (OPAC) Group at Eindhoven University of Technology during my six-month external stay. It has been a pleasure to work with you. Thanks for your excellent experiences and dedication to refining our paper.

My sincere gratitude extends to both past and present colleagues at DTU Management and the OPAC group, as well as all my friends. The PhD journey can be challenging sometimes. Your companionship, fruitful discussions, and vibrant social activities brighten my days.

A tremendous thank you to my parents. Your boundless love, endless support, constant encouragement, and profound understanding over the three years have been my steadfast anchor. I cannot wait to reunite with you at home, as your presence is the most cherished treasure in my world!

Contents

1 Introduction

1.1 Background

Over the past few decades, the world has experienced a significant transformation marked by rapid population growth, urbanization, and the rise of E-commerce. Back in 1950, the global population was 2.5 billion, with the majority (75%) residing in rural areas. The urban population has outpaced overall population growth since then. By 2020, the urban population swelled to 4.4 billion, constituting 56% of the world's population. It is projected that the urban population will escalate to 6.7 billion by 2050, making up 68% of the world's inhabitants (Habitat, 2022). This urban expansion has coincided with the exponential growth of E-commerce, primarily driven by the evolution of the Internet and accelerated during the COVID-19 pandemic. Global E-commerce sales, which amounted to $1.3 trillion in 2014, soared to $5.717 trillion in 2022, and are expected to ascend to $8.1 trillion by 2026 (Statista, 2022).

The remarkable rise in urbanization and E-commerce has inevitably led to an increased demand for transportation in urban areas. This escalating transportation demand has undoubtedly contributed to economic growth, but it also placed immense pressure on urban transportation networks, increasing greenhouse gas (GHG) emissions and exacerbating traffic congestion. As reported by the European Environment Agency (2022), GHG emissions from the transport sector increased by 33% between 1990 and 2019. Furthermore, the estimated annual road congestion cost in the EU is €110 billion, exceeding 1% of the EU's GDP (European Court of Auditors, 2019).

Numerous cities around the world are grappling with the challenge of mitigating traffic congestion and environmental concerns while striving to meet people's expectations for convenient transport and cost-effective and timely delivery, especially for the last mile. To cope with the surge of transportation demands and tackle the last-mile dilemma, the European Commission (2007) has advocated for local authorities to view passenger and freight transport together as a unified logistics system, departing from the conventional practice of managing and operating them separately. While the integration of passenger and freight transportation over decades has been successfully implemented in long-haul journeys such as water and air transport, it is less prevalent for short-distance travel. Given that both passenger and freight vehicles share and vie for the capacity of the same urban transport infrastructure, integrating their transportation, particularly when they exhibit similar travel patterns, is a logical and beneficial endeavor. Moreover, the integration of passenger and freight transportation holds several compelling advantages:

Mitigated traffic congestion and reduced environmental pollution. When passengers and freight are transported simultaneously, some overlapping routes of passenger and freight vehicles could be shared. Consequently, the total vehicle kilometers traveled, along with the carbon footprints and air pollution, could be reduced. Meanwhile, the number of used vehicles to serve the same transportation demands would also be reduced, alleviating the traffic congestion.

Improved cost-efficiency and bolstered economic growth. A well-developed integrated transportation system efficiently utilizes transportation resources (e.g., roads and vehicles), leading to reduced operational expenses and labor costs for businesses. Additionally, the alleviation of traffic congestion streamlines the flow of

people and goods, benefiting both businesses and individuals, ultimately fostering economic activity and trade.

Enhanced equity and access to transport services. Integrating passenger and freight transportation contributes to bridging the urban-rural divide by extending transport services accessibility, including logistics service and public transport service, to rural areas. Rural areas often have limited public transport and logistics services due to low density and high transportation costs. Combining logistics service with public transport will augment the revenues of public transport companies and diminish the operational cost of logistics companies. Consequently, public transport companies and logistics companies will not reduce or shut down their services in rural areas. This ensures that residents in rural areas get easier access to transport services and feel less isolated.

Motivated by these potential benefits, innovative last-mile solutions have emerged in the last decade. These solutions, having various terminologies such as passenger and parcel share-a-ride (Li et al., 2014), crowdshipping (Le et al., 2019), freight on transit (Elbert & Rentschler, 2022), and cargo hitching (Van Duin et al., 2019), are all centered on the core idea of integrating people and goods transportation. Some of them leverage emerging technologies such as mobile communication technology and are the products of the sharing economy and gig economy, e.g., passenger and parcel share-a-ride and crowdshipping.

Despite these strides, the field of integrated people-and-goods transportation is still in its infancy, with new integration forms continually emerging alongside technological advancements. Two critical questions arise: Is there a unified framework capable of guiding the planning and operation of such an integrated system when a new integration form emerges? What untapped opportunities await for merging people and goods transportation within our evolving technological landscape? This thesis answers these two questions.

1.2 Objective and research questions

The objective of this thesis is thus to advance the understanding of integrated people-and-goods transportation systems and explore innovative integration forms that fuse the idea of integrating people and goods transportation with emerging last-mile solutions to improve transportation efficiency and reduce congestion in urban areas. In order to achieve the aforementioned objective, a set of research questions are formulated and addressed in corresponding chapters of the thesis.

Research question 1 (Q1). Which framework can comprehensively represent and guide the planning and operation of an integrated people-and-goods transportation system?

The integration of people and goods transportation has gained considerable attention in both literature and practice, resulting in a multitude of integration forms. What is the present status of the development of integrated people-and-goods transportation? What lessons can we learn from past successful and failed applications? Despite the diversity in integration forms, is it possible to find a unified framework that could encapsulate the characteristics of integrated people-and-goods transportation systems and serve as a guidance for planning and operation of existing integration forms and future endeavors? Such a framework is essential for understanding the integrated people-and-goods transportation system.

Research question 2 (Q2). Are there innovative solutions that incorporate the concept of integrating people and goods transportation with other last-mile solutions?

Besides integrating people and goods transportation, various solutions have been proposed to address the last-mile problem from distinct angles. Concerning transportation means, one notable initiative is Amazon's introduction of drone delivery services in California and Texas. Drone delivery has been regarded as a promising last-mile solution owing to its fast speed and environmental benefits. Regarding handover ways, parcel lockers have been developed rapidly in recent years, especially in Nordic countries, as they could reduce the number of not-at-home deliveries and the last-mile delivery cost. As reported by the European Regulators Group for Postal Services (2022), the counts of parcel lockers in Denmark and Norway in 2021 quadrupled compared to 2017, reaching 1740 and 2288 in Denmark and Norway, respectively. This research question seeks to explore the synergy between integrating people and goods transportation and emerging last-mile solutions. By delving into this synergy, researchers and practitioners can unlock new opportunities to mitigate adverse impacts of transportation while meeting peoples' expectations for swift and reliable last-mile services.

Research question 3 (Q3). What are the benefits of the proposed innovative solutions, and how can they be quantified?

This research question shifts the focus from theoretical concepts to practical outcomes, aiming to provide valuable insights into the tangible benefits of integrated people-and-goods transportation. The critical planning problems involved in the innovative solutions that this thesis proposes are optimization problems. By solving these optimization problems, this thesis gains insights into how the proposed integrated people-and-goods transportation systems compare to traditional separated transportation systems. The key performance indicators considered in this thesis are total operation costs, the number of used vehicles, and the vehicle kilometers traveled. Comparing these indicators in the proposed systems with those in separated people and goods transportation systems, the benefits of the proposed solutions in this thesis are quantified. There are two types of methods for solving optimization problems: exact methods and heuristics/metaheuristics. Exact methods are acknowledged for their ability to provide global optimal solutions, but they are also recognized for their limitations in solving large instances. In contrast, heuristics/metaheuristics are highlighted for their computational efficiency and capacity to solve large instances, but they do not guarantee the global optimality of their solutions.

1.3 Overview of the thesis

The remainder of this thesis comprises four papers that address the aforementioned three research questions and a concluding chapter. Chapter 2 is a review paper on integrated people-and-goods transportation systems that addresses research question Q1. Chapters 3 and 4 focus on the first proposed solution: passenger and parcel share-a-ride problem with drones (SARP-D), which uses demand-responsive buses (DRBs) and drones to combine passenger and parcel transportation. In this concept, DRBs could serve both passenger and parcel requests, while drones perform only parcel delivery. These chapters present different solution methods and address research questions Q2 and Q3. Chapter 5 focuses on the second proposed solution: public transport (PT)-based crowdshipping, where PT passengers act as crowdshippers, transporting parcels between parcel lockers positioned at their origin and destination PT stations. This chapter tackles research questions Q2 and Q3. Finally, Chapter 6 concludes this thesis by responding to the three research questions, summarizing contributions, and providing future research directions. Figure 1.1 presents the overview of this thesis.

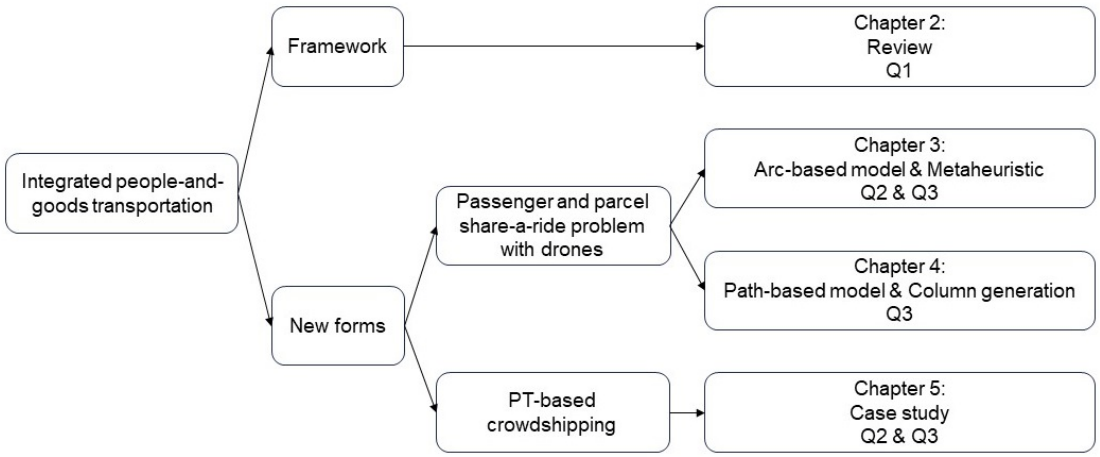

Figure 1.1: Overview of the thesis

Chapter 2 begins with categorizing three distinctive forms of integrating people and goods transportation: people and goods share-a-ride, freight on transit, and crowdshipping. Subsequently, this chapter delves into real-world applications of these integration forms and points out the main challenges for implementing the integrated transportation system. The challenges encompass various dimensions: policy, economics, society, organization, and technology. Given that technical challenges are more tractable and solving technical problems contributes to mitigating other problems, this chapter embarks on an examination of technical problems and corresponding solutions that have been explored in existing literature for each integration form. Drawing from this extensive review, this chapter proposes a framework designed for planning and operating an integrated people-and-goods transportation system. By mapping the technical problems studied within existing integration forms onto the proposed general framework, two key research opportunities are identified: to enhance or expand existing research and to conduct pioneering research to fill the blanks in the framework.

Chapter 3 elaborates on the SARP-D and formulates it as an arc-based mixed integer non-linear programming model. The objective is to minimize the total costs, including transportation costs of DRBs and drones and the delay penalty cost at each node. A linearization method is presented to make the model solvable by a commercial solver (CPLEX) for small instances with up to 12 nodes. An adaptive large neighborhood search (ALNS) metaheuristic is devised to solve large instances. Two works are conducted to evaluate the effectiveness of the ALNS algorithm. First, this chapter compares the results given by ALNS and CPLEX on small instances of SARP-D instances. The results reveal that our ALNS could produce the optimal solutions as CPLEX does but takes much less time. Second, this chapter applies the proposed ALNS to solve instances of vehicle routing problems with drones (VRP-D) provided by Sacramento et al. (2019). The comparison results demonstrate that although the proposed ALNS is not explicitly designed for the VRP-D, it can effectively solve the VRP-D, yielding results very close to a specialized algorithm for the VRP-D proposed by Sacramento et al. (2019). Then, this chapter uses ALNS to solve large SARP-D instances with up to 200 nodes and conducts sensitivity analysis on some key parameters in the SARP-D to provide valuable managerial insights to SARP-D operators. The computation results show that integrating passenger and parcel transportation reduces the total operation costs, the number of used vehicles, and total DRB-traveled miles.

Chapter 4 is a follow-up study of Chapter 3. Chapter 4 focuses on the same problem as Chapter 3, but employs a different solution methodology, which can be used to evaluate the ALNS presented in Chapter 3. Specifically, Chapter 4 formulates a path-based model for the SARP-D and uses the column generation (CG) approach to solve it. The pricing problem of the CG is an elementary shortest path problem with resource constraints, which is solved by a tailored labeling algorithm. To speed up the procedure of CG, this chapter devises a heuristic to find paths with negative reduced costs and proposes two propositions to reduce the number of generated labels in the labeling algorithm, hereby reducing the computation time of the labeling algorithm. Extensive experiments are conducted to test the efficiency of the CG. The results prove that the CG is able to solve not only the SARP-D efficiently for instances comprising up to 50 nodes, but also two variations of the SARP-D, i.e., VRP-D and one-to-one pickup and delivery problem (PDP). Moreover, this chapter conducts sensitivity analysis on key parameters of the SARP-D, e.g., the distribution area of the network, the maximum number of intermediate stops between one passenger request, the maximum drone flying time, and the time window. The results are consistent with what has been found in Chapter 3.

Chapter 5 focuses on the second solution: PT-based crowdshipping. This chapter aims to assess the potential benefits of PT-based crowdshipping. PT-based crowdshipping involves two critical problems: the location problem for parcel lockers and the vehicle routing problem for delivery vans. For the former problem, a mixed integer programming model is formulated to determine in which PT stations to install parcel lockers for recipients picking up their parcels. The model can be solved by CPLEX. The routing problem of delivery vans is formulated as a capacitated vehicle routing problem with deadlines. A mixed integer programming model and an ALNS metaheuristic were developed to find vehicle routes with minimum operation costs. A case study in a central district in Copenhagen using real-world data is conducted to estimate the impacts of PT-based crowdshipping. The results reveal that compared with the traditional distribution mode, PT-based crowdshipping offers several key advantages, specifically, reductions in the total vehicle kilometers traveled, the number of used vehicles, and the total working time of drivers. The extent of these benefits depends on the proportion of parcels shifted from delivery vans to crowdshippers.

The chapters of this thesis are based on the following papers:

> Chapter 2 (Paper 1): Cheng, R., Jiang, Y., & Nielsen, O. A. (2023). Integrated people-and-goods transportation systems: from a literature review to a general framework for future research. Transport Reviews, 1-24. DOI: 10.1080/01441647.2023.2189322.
>
> Chapter 3 (Paper 2): Cheng, R., Jiang, Y., Nielsen, O. A., & Pisinger, D. (2023). An adaptive large neighborhood search metaheuristic for a passenger and parcel share-a-ride problem with drones. Transportation Research Part C: Emerging Technologies, 153, 104203. DOI: 10.1016/j.trc.2023.104203.
>
> Chapter 4 (Paper 3): Cheng, R., Jiang, Y., Nielsen, O. A., & Van Woensel, T. (2023). A passenger and parcel share-a-ride problem with drones: A column generation approach. Under review in Transportation Research Part B: Methodological.
>
> Chapter 5 (Paper 4): Cheng, R., Fessler A., Larsen, A., Nielsen, O. A. & Jiang, Y. Assessing the impacts of public transport-based crowdshipping: A case study in a central district in Copenhagen. To be submitted to Frontiers of Engineering Management.

References

Elbert, R., & Rentschler, J. (2022). Freight on urban public transportation: A systematic literature review. *Research in Transportation Business & Management*, *45*, 100679.

European Commission. (2007). Green paper, towards a new culture for urban mobility, Luxembourg: Publications Office of the European Union.

European Court of Auditors. (2019). *Urban mobility in the eu. european court of auditors*. https://www.eca.europa.eu/lists/ecadocuments/ap19_07/ap_urban_mobility_en.pdf

European Environment Agency. (2022). Transport and environment report 2022, Luxembourg: Publications Office of the European Union.

European Regulators Group for Postal Services. (2022). ERGP PL II (22) 12 ERGP report on core indicators 2021 for monitoring the European postal market.

Habitat, U. (2022). World cities report 2022: Envisaging the future of cities. *United Nations Human Settlements Programme: Nairobi, Kenya*, 41–44.

Le, T. V., Stathopoulos, A., Van Woensel, T., & Ukkusuri, S. V. (2019). Supply, demand, operations, and management of crowd-shipping services: A review and empirical evidence. *Transportation Research Part C: Emerging Technologies*, *103*, 83–103.

Li, B., Krushinsky, D., Reijers, H. A., & Van Woensel, T. (2014). The share-a-ride problem: People and parcels sharing taxis. *European Journal of Operational Research*, *238*(1), 31–40.

Sacramento, D., Pisinger, D., & Ropke, S. (2019). An adaptive large neighborhood search metaheuristic for the vehicle routing problem with drones. *Transportation Research Part C: Emerging Technologies*, *102*, 289–315.

Statista. (2022). *Worldwide retail e-commerce sales. statista*. https://www.statista.com/statistics/379046/worldwide-retail-e-commerce-sales/

Van Duin, R., Wiegmans, B., Tavasszy, L., Hendriks, B., & He, Y. (2019). Evaluating new participative city logistics concepts: The case of cargo hitching. *Transportation Research Procedia*, *39*, 565–575.

2 Integrated people-and-goods transportation systems: from a literature review to a general framework for future research

Cheng, R., Jiang, Y., & Nielsen, O. A. (2023). Integrated people-and-goods transportation systems: from a literature review to a general framework for future research. Transport Reviews, 1-24.

Abstract

The promotion of urban mobility by integrating people-and-goods transportation has attracted increasing attention in recent years. Within this framework, diversified forms such as co-modality, freight on transit, and crowdshipping have been proposed, piloted or implemented. The success of the implementation and market penetration depends on not only the novelties of the concept but also the planning and operational efficiency. Thus, a comprehensive review focusing on the operation of integrated people-and-goods transportation systems and associated critical decisions and subproblems is performed. Different practical forms in which people and goods are transported in an integrated manner are identified. The critical decisions associated with each form and subproblem are discussed, along with corresponding models and solution approaches. Notably, because integrated transportation systems are in the early exploration stage at present, new forms are expected to emerge. Therefore, this paper proposes a general framework to realise the planning and operation of new forms in the future. The decisions and subproblems identified from existing forms are fed to the proposed general framework to identify two key research opportunities: to improve or extend existing research and to conduct pioneering research to fill the gaps in the frameworks for operating potential forms of integrated people-and-goods transportation.

Keywords: Integrated people-and-goods transportation; shared mobility; share-a-ride; freight on transit; crowdshipping

2.1 Introduction

Urban mobility faces increasing challenges with population growth, urbanisation, e-commerce and varying land-use patterns. Many daily tasks require transporting people or goods. While transport services enhance the convenience of daily life, they also have adverse effects, such as greenhouse gas emissions, local air pollution, traffic accidents, and congestion (European Commission, 2019). These negative externalities can be mitigated by establishing shared and integrated transportation systems (Mourad et al., 2019). Although moving people and goods together has been successfully implemented in long-haul transportation modes such as aircraft and ferries, passenger and goods movements in urban transport systems are typically planned and performed separately. Since the transportation of people and goods is mutually affected by sharing and competition for road space and infrastructures, a separate implementation may underutilise the existing infrastructure and vehicle capacity. Thus, a promising solution, integrating people-and-goods transportation systems, has attracted increasing attention in recent years.

The idea of transporting people and goods together in an urban transportation context was highlighted by the European Commission, stating that "Local authorities need to consider all urban logistics related to passenger and freight transport together as a single logistics system" (European Commission, 2007). Since then, several researchers have focused on integrated people-and-goods transportation systems (hereinafter referred to as integrated transportation systems). Diverse novel terms such as co-modality, freight on transit (FOT), crowdshipping, cohabitation of passengers and goods, and cargo hitching have been proposed, coupled with various methodological developments.

There have been several remarkable reviews focusing on particular forms of integrated transportation systems, like crowdshipping and FOT (Alnaggar et al., 2021; Elbert & Rentschler, 2022; Le et al., 2019), discussing it within broader topics such as shared mobility (Mourad et al., 2019), collaborative urban transportation (Cleophas et al., 2019), and city logistics (Savelsbergh & Van Woensel, 2016), or conducting bibliometric analysis (Cavallaro & Nocera, 2022). This paper offers a systematic review to complement existing reviews with the following objectives: (1) categorising different forms of integrated transportation systems; (2) identifying the key issues for different forms and discussing corresponding solutions; (3) proposing a general framework to describe the operation of integrated transportation systems; and (4) giving recommendations for future development and research.

The remaining paper is organised as follows. Section 2.2 describes different forms of integrated transportation systems. Section 2.3 specifies the research problems in existing studies. These problems are incorporated in a general framework proposed in Section 2.4. Section 2.5 highlights the research gaps and future research directions.

2.2 Forms of integrated people-and-goods transportation

We define an integrated people-and-goods transportation system as a system in which the resources for transporting people and goods are jointly utilised such that people and goods are transported in the same vehicle, either private or public, or share the same infrastructure, such as railways, stations, and platforms. We then categorise three forms: people and goods share-a-ride (SAR), FOT, and crowdshipping. In what follows, we will first introduce the definition and characteristics of each form (see Table 2.1), then comment on real-world applications.

2.2.1 Definition

(1) People and goods share-a-ride

Table 2.1: Forms of integrated transportation systems in the literature

Integration form	Transportation means	Shared resource		Goods operators			Practical application
		Vehicles	Infrastructure	Dedicated workers*	Crowd-shippers**	Senders and receivers	
Share-a-ride	Taxis	√				√	
	SAVs	√				√	
Freight on transit	Buses	√		√			√
	Metros	√	√	√			√
	Trains	√	√	√			√
	Trams		√	√			√
	Personal rapid transit	√	√	√			
	Drones	√		√			
	Robots	√		√			
Crowdshipping	Private cars/bikes/ cargo bikes	√			√		√
	Public transport	√			√		√

*Dedicated workers: Staff at stations or distribution centres are in charge of loading and unloading goods.
**Crowdshippers: Ordinary people assist in picking up and delivering goods.

In this form, a shared vehicle, e.g., a taxi or shared autonomous vehicle (SAV), provides door-to-door service for both passengers and goods. The vehicle with passengers can simultaneously transport small parcels such as mail, documents, and takeaway meals. The primary research problem involved is the routing problem, known as the people and parcel SAR problem (SARP, Li et al., 2014).

(2) Freight on transit

Elbert and Rentschler (2022) defined FOT as "the integrated and organised transportation of passengers and goods within urban areas using a system of vehicles such as buses and trains that operate at regular times on fixed routes and are used by the public." We hereby extend this definition by considering (1) emerging flexible public transport, particularly, demand-responsive services such as personal rapid transit and freight rapid transit; (2) urban-suburban and urban-rural transit. Depending on the public transport vehicles used, goods and passengers could share three resources in FOT: carriage, vehicle, and tracks.

(3) Crowdshipping

Buldeo Rai et al. (2017) defined crowdshipping as "an information connectivity enabled marketplace concept that matches supply and demand for logistics services with an undefined and external crowd that has free capacity with regards to time and/or space, participates on a voluntary basis and is compensated accordingly". Crowdshippers are categorised into dedicated and ad-hoc crowdshippers. Dedicated crowdshippers devoted their available time to perform deliveries using dedicated trips. In contrast, ad-hoc crowdshippers utilise their already planned trips with extra capacities. The two modes of crowdshipping have their own advantages and disadvantages. For example, crowdshipping with dedicated crowdshippers usually provides more efficient crowd logistics than ad-hoc crowdshippers, but it leads to much longer travel distances than crowdshipping with ad-hoc drivers (Buldeo Rai et al., 2018). Both types of crowdshipping are likely to be functional in the future. Nonetheless, in this study, we do not consider dedicated crowdshippers because, although people and goods move simultaneously, they do not integrate peoples' existing travel demands but induce new ones. Without further specification, the crowdshippers in the rest of this paper refer to as ad-hoc crowdshippers. Primarily, crowdshippers perform crowdsourced delivery through a single transportation mode, e.g., taxis, public transit, or their vehicles. With the emerging concept of mobility as a service (MaaS), He and Csiszár (2021) and Le Pira et al. (2021) proposed utilising multiple transportation modes.

2.2.2 Applications and barriers

2.2.2.1 Applications

Table 2.2 lists the applications of different forms. To the best of the authors' knowledge, there are no real-world applications of people-and-goods SAR yet. Hence, we only present FOT and crowdshipping.

Table 2.2: Application of integrated people-and-goods transportation

Integration form	Transportation means	Projects	Status	Comment / Failure reason
Freight on transit	Bus	Bussgods (Sweden)	On going	
		Matkahuolto (Finland)	On going	
		Greyhound Freight (Australia)	On going	
		Maritime Bus (Canada)	On going	
		Greyhound Package Express (US)	Closed in September 2022	Concentrate on passenger services
	Metro	Subway-integrated city logistics system (Japan)	September 2–15, 2010	Lack of money
	Train	Dabbawalas (India)	On going	
		CarGo Tram of Volkswagen (Dresden)	November 2000 – December 2020	End of producing
		Cargo-Trams/E-Trams (Zurich)	On going	
	Tram	Recycling Tram (Iasi)	On going	
		GuterBim (Vienna)	May 2005 – June 2007	Lack of customer interest
		City Cargo (Amsterdam)	March 2007 – April 2007	Lack of money
		TramFret (Saint-Etienne)	June 2017 – July 2017	Lack of customer interest
Crowdshipping	Private vehicles	DHL Myways (Stockholm)	September 2013 – Unknown	Unknown
		Hitch (US)	Unknown	Unknown
		Nimber (London, Athens, Oslo)	On going	
		Roadie (US)	On going	
	Public transport	Crowd ship (Denmark)	September – October 2020	
		Öffi-Packerl (Austria)	Planning	

Sources:
Alnaggar et al., 2021; Arvidsson et al., 2016; Arvidsson and Browne, 2013; Cochrane et al., 2017; Fessler et al., 2022; Kikuta et al., 2012; Qu et al., 2022;
https://www.railjournal.com/passenger/metros/tokyo-metro-to-test-parcel-operation/;
https://en.wikipedia.org/wiki/CarGoTram;
https://industriemagazin.at/artikel/die-wiener-gueterbim-das-kurze-gastspiel-der-transport-strassenbahn/;
http://www.tautonline.com/zurichs-cargo-tram/;
https://aqtr.com/association/actualites/freight-transit-new-concept-city-logistics;
https://brutkasten.com/oeffi-packerl-entwicklung-startet/.

(1) FOT

(a) Bus-based FOT. This is the most widely implemented FOT system worldwide, e.g., Bussgods in Sweden, Matkahuolto in Finland, Greyhound Freight in Australia, Maritime Bus in Canada, and Greyhound Package Express US. It usually operates on existing long-distance transit routes connecting regional centres and rural areas. Goods utilise the available space on passenger vehicles, e.g., the luggage compartment or a dedicated goods compartment of a bus. Most above-mentioned systems are still in operation, except Greyhound Package Express US, which ends on September 30, 2022, for concentrating on passenger services.

(b) Tram-based FOT. Most of the tram-based FOT are implemented in Europe in the form that dedicated freight trams share tracks with passenger trams connecting urban and suburban areas. Three projects (CarGo Tram of Volkswagen, Cargo-Trams/E-Trams in Zurich, and Recycling Trams in Iasi) succeed under specific conditions. The success of the first one is attributed to its low cost of building additional connection tracks, as the factory is only about three miles away from the logistics centre. The other two are provided as public service and avoid additional infrastructure investment and interference with passenger traffic by carefully selecting stop stations. Three projects are short-lived. City Cargo in Amsterdam was abandoned because it failed to acquire adequate finance for investments in trams, electric last-mile delivery vehicles, new tracks, and distribution centres, and there were conflicting objectives among stakeholders (Arvidsson & Browne, 2013). The other two projects, GüterBim in Vienna and TramFret in Saint-Etienne were discontinued due to a lack of customer interest.

(c) Train-based FOT. One successful example of the train-based FOT is the Dabbawala food delivery system in Mumbai. It links kitchens in local villages to people working in metropolitan areas using a hub-and-spoke transport system with passenger trains and bicycles.

(d) Metro-based FOT. We only found one trial in Sapporo that tested using the metro to transport parcels from the suburbs to the city centre. The trial was successful, but the project ceased due to poor demand and the high cost of retrofitting metro stations to handle goods.

(2) Crowdshipping

Alnaggar et al. (2021) reviewed crowdsourced delivery platforms operated by E-retailers (e.g., Amazon Flex) and couriers (e.g., DHL), among which four are with ad-hoc crowdshippers, i.e., DHL Myways, Hitch, Nimber, and Roadie. Hitch mainly supports local deliveries, while others allow for both local and long-haul deliveries. Notably, public transport-based crowdshipping has emerged in recent years. It allows passengers to bring a parcel from a parcel locker located in a public transport station to another along their ride. A "Crowd ship" trial was conducted in the Greater Copenhagen Area in 2020 to analyse people's preference for public transport-based crowdshipping. A similar project, "Öffi-Packerl" in Vienna, is expected to make the first test in Vienne in 2024.

2.2.2.2 Barriers

We summarise the main challenges for deploying the integrated system from five aspects, policy, economics, society, organisation, and technology.

First, passengers and goods transportation are usually regulated by different authorities with separate rules and policies (Bruzzone et al., 2021). Passengers can carry goods on their trip, but taxi drivers and privately hired vehicles are forbidden to be couriers if no passenger is on board. This could explain why taxi companies or technology companies (e.g., Uber, Grab, etc.) do not offer integrated people and goods transportation services. However, in practice, there is a grey area where a passenger hires a taxi while the "real passenger" is a package. The good news is that the Land Transport Authority of Singapore is monitoring recent trends to see if these regulations need to be reviewed, and a temporary relaxation of this rule was extended for a third time [1].

Secondly, economic viability is important for the success of a project. Many FOT projects were terminated due to a lack of money or customer interests and conflicting objectives among stakeholders. These issues could be partially avoided by carefully identifying suitable markets and optimising the organisation/operation/revenue allocation of the integrated transport service.

Thirdly, people may have psychological barriers. For example, passengers may feel unsafe or reluctant to share a ride with goods; the conflicts between freight operators and passengers at transit stations may increase passengers' discomfort level; crowdshippers may be concerned about privacy. These problems could be mitigated by regulating the type of goods, proper planning of integrated transportation services, and tightening regulations on privacy and data security.

Fourthly, organisational challenges include finding initial capital investment, coordinating various stakeholders and entities, dealing with resistance from passengers, transit

[1] https://tnp.straitstimes.com/news/singapore/cabbies-private-hire-drivers-can-make-deliveries-until-march

agencies, workers from logistics service providers, ensuring the safety of passengers and goods, etc (Cochrane et al., 2017).

Lastly, technical challenges include searching underutilised capacity, designing the routes and schedules of shared vehicles, selecting routes for FOT, integrating freight delivery and passenger schedules, coordinating last-mile delivery with FOT, matching crowdshippers with parcels, designing an optimal price for the integrated transportation systems, etc.

Overall, the technical challenges are easier to overcome than the challenges on other dimensions. Besides, solving technical challenges could contribute to resolving other challenges. For example, deploying advanced techniques aiming at operating integrated transportation systems cost-effectively could enhance the economic viability of the integrated system, which contributes to attracting investors; well-planned freight hub location, route and schedules of freight vehicles could reduce unnecessary conflicts between passengers and goods or inconvenience to passengers.

2.3 Literature review

As discussed in the previous section, solving technical problems contributes to mitigating the barriers to implementing integrated transportation systems. This section reviews the technical problems examined in the existing studies for each form listed in Table 2.1 (see Figure 2.1).

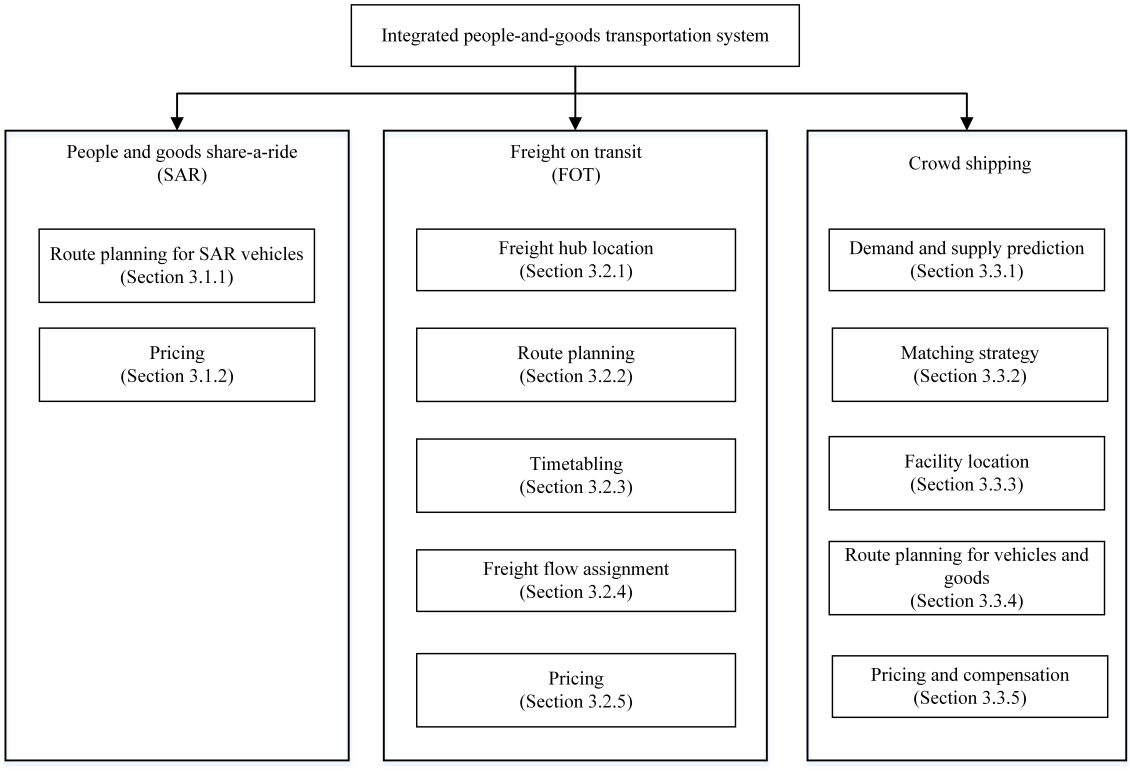

Figure 2.1: Technical problems that have been studied for different integration forms

2.3.1 People-and-goods share-a-ride

2.3.1.1 Route planning for share-a-ride vehicles

Li et al. (2014) first defined the routing problem for integrated transportation using taxis as SARP. Several regulations were introduced to ensure high-quality services: (R1) Passengers must have a maximum ride time. (R2) An upper limit exists on the number of parcels served during one passenger service. (R3) Two passengers cannot be served

simultaneously by one taxi. R1 and R2 aim to decrease the influence of parcel delivery on passenger services, and R3 aims to ensure personal security and convenience (e.g., gender or smoking preferences). These regulations were gradually relaxed to present a more general SARP, leading to more profits. Beirigo et al. (2018) and Tholen et al. (2021) eliminated R2 and R3. Yu et al. (2018, 2023) relaxed all these regulations.

Many features have been added to the original SARP to accommodate various application scenarios. Yu et al. (2021a) allowed passenger compartments to store parcels, which utilises the total vehicle capacity more flexibly and efficiently. Yu et al. (2023) extended a single depot to multiple depots, given that it is challenging to serve scattered transportation demands from one depot. To make the models closer to real life, Li et al. (2016b) took stochastic travel times and delivery locations into account. Ren et al. (2021) described the dynamics in SAR by updating parcel delivery information and reoptimizing routes when vehicles arrive at distribution centres (the origins of parcels). Considering the trends of electrification and automation in transportation, Lu et al. (2022) investigated a system with a mixed fleet of electric and gasoline taxis, while Beirigo et al. (2018), Tholen et al. (2021), and Zhang et al. (2022) envisioned a system with SAVs.

To solve these problems, scholars have developed different models and solution approaches. MIP models and two-stage stochastic programming models are commonly used for deterministic problems and problems with uncertainty, respectively. Regarding solution approaches, commercial solvers such as CPLEX and Gurobi can solve small instances (Beirigo et al., 2018; Li et al., 2014; Tholen et al., 2021). Metaheuristics, e.g., genetic algorithm (Ren et al., 2021), adaptive large neighbourhood search (ALNS) (Li et al., 2016a, 2016b), simulated annealing (Yu et al., 2021a; Yu et al., 2018; Yu et al., 2023), are widely applied to solve large-scale instances since SARP is an NP-hard problem. Other solution methods include the Lagrangian dual decomposition method (Zhang et al., 2022), math-heuristic (Lu et al., 2022), and model-free deep reinforcement learning (Manchella et al., 2021a; Manchella et al., 2021b).

2.3.1.2 Pricing

The above-mentioned studies were based on a given pricing strategy. Specifically, the initial price for each passenger and parcel was considered to remain unchanged or increase based on travel distance. However, a passenger may obtain a discount depending on the degree of deviation from his/her direct route (Li et al., 2014; Ren et al., 2021; Yu et al., 2021a). A more interesting strategy developed by Manchella et al. (2021a) allows drivers and passengers to negotiate for the best price.

2.3.2 Freight on transit

2.3.2.1 Freight hub location

The freight hub location problem aims to choose among existing passenger public transport stations as distribution centres for delivering or transhipping goods. Most papers on this topic rely on the metro system as the backbone, indicating that researchers are optimistic that freight can be successfully integrated with the metro system. We divide these studies into two groups based on whether all selected freight hubs have the function of connecting underground and ground networks. In the first group, goods can enter the metro system from the ground and leave from the metro system to the ground at any selected freight hubs (Ji et al., 2020; Kızıl & Yıldız, 2023; Zhao et al., 2018). The decision variables are the locations of freight hubs. In the second group, there are two types of freight hubs (Dong et al., 2018; Sun et al., 2022). Freight hubs of the first type are similar to the freight hubs in the first group, where goods have access and egress to the underground and ground networks. Freight hubs of the second type can only be used for

transhipping freight between different metro lines, not connected to the ground network. In addition to deciding the locations of freight hubs, their functions are decided as well.

Azcuy et al. (2021) considered a more general urban delivery system using public transport where the public transport could be the bus, metro, tram, etc. Freight can be transferred from public transport to last-mile delivery vehicles at any selected station.

2.3.2.2 Route planning

(1) Route planning for public transport vehicles

Two types of public transport services have been studied in FOT, scheduled public transport (with fixed lines and schedules) and demand-responsive public transport (with flexible routes and schedules). When scheduled public transport is used in FOT, it is usually assumed that the capacity of the public transport system is underutilised, and the existing routes and schedules of public transport vehicles are treated as exogenous model parameters. Only Li et al. (2021) designed the stations where added freight trains should stop, categorised as a route planning problem.

When FOT is based on demand-responsive public transport, passengers and freight could be on a shared network or in the same vehicle. For the former scenario, Fatnassi et al. (2015) devised two routing strategies: a reactive dynamic matching strategy and a proactive one for passenger rapid transit (PRT) and freight rapid transit (FRT). For the latter, Chebbi and Chaouachi (2016) studied an empty vehicle redistribution problem that minimizes the empty movement and the number of used vehicles while reducing the wasted capacity of PRT. Peng et al. (2021) explored a bus-pooling service at a railway station, where demand-responsive buses pick up passengers and parcels and deliver them to their destinations. Parcels with similar itineraries and departure times to passengers were matched and inserted into bus routes following the shortest road route.

(2) Route planning for supportive vehicles

As conventional public transport modes with fixed routes cannot provide door-to-door services, support vehicles (e.g., small trucks or electric vehicles run by logistic companies) are typically used to realise the first/last-mile transportation.

Route planning for supportive vehicles is usually formulated as variants of pickup and delivery problem (PDP) to accommodate operation modes. Masson et al. (2017) modelled a PDP with transfers in a setting where all goods originate from warehouses known as consolidation and distribution centres (CDCs). Buses start from a CDC and travel to bus stops where goods are unloaded and transhipped to support vehicles for the last-mile delivery. Similar work was performed by Ye et al. (2021) for a metro-based FOT. The difference is that the supportive vehicles also perform the first-mile delivery from the CDC to metro stations.

Another variant is the PDP with scheduled lines (PDP-SL). Different from the PDP with transfers where goods must take public transport, the PDP-SL allows goods to be either delivered directly to customers by support vehicles or first collected by a support vehicle, transported via scheduled lines (SLs) such as bus, train, metro, etc., and then delivered to customers by another support vehicle (Ghilas et al., 2016b). Ghilas et al. (2016c) extended the deterministic PDP-SL problem proposed by Ghilas et al. (2016b) into a stochastic PDP-SL problem by considering uncertain freight demand. People and parcels only share public transport vehicles in the two studies, whereas they share supportive vehicles in Ghilas et al. (2013). All three studies assume that the freight capacity is fixed and not influenced by passenger flows. This

assumption is relaxed by Mourad et al. (2021), in which robots function as support vehicles. When the delivery robots travel on a bus, they share the same bus capacity with passengers but have a lower priority. In other words, at some stations, the robots may be unable to board a bus or be required to deboard to make space for passengers.

As an alternative to using ground vehicles as support vehicles, Huang et al. (2020) introduced an innovative integrated transportation system that involves trains with given routes and timetables for passenger transportation and drones for parcel delivery.

In terms of the solution approaches, most studies apply metaheuristics to solve large-scale instances, e.g., ALNS (Ghilas et al., 2016a, 2016c; Masson et al., 2017; Mourad et al., 2021) and variable neighbourhood search (Ye et al., 2021). Ghilas et al. (2018) developed a branch-and-price algorithm to solve medium-sized instances.

2.3.2.3 Timetabling

The design of timetables for scheduled public transport vehicles in the context of FOT has been considered only in rail-based FOT, i.e., trams and trains. When people and freight share the vehicles/carriage, the timetables of passenger vehicles were designed from scratch, aiming to transport more freight in less time without influencing passenger transport (Li et al., 2022). When people and freight share the rail infrastructure, two strategies are found to design timetables for added dedicated freight trains: 1) Timetables for freight trains are created while the timetables of passenger trains remain unchanged (Ozturk & Patrick, 2018); 2) Schedules for both passenger and freight trains are constructed from scratch (Hörsting & Cleophas, 2023; Li et al., 2021). Hörsting and Cleophas (2023) compared the two transportation modes and concluded that sharing vehicles/carriages is more robust towards fluctuating demand while sharing infrastructures allows higher dwell time for dedicated freight trains/trams.

2.3.2.4 Freight flow assignment

The freight flow assignment problem determines where, when, and on which vehicle a request takes a public transport ride. The flow assignment can be obtained either as key decision variables in a model that exclusively determines the flow given public transport routes and schedules of vehicles that can be used for freight transportation or as auxiliary variables in a model that designs the hub location, route, and timetable (Ji et al., 2020; Li et al., 2021; Ozturk & Patrick, 2018). This section focuses on the former case.

For bus-based FOT, Pimentel and Alvelos (2018) developed an MIP model to determine the freight flow that minimises the delivery time. Their system allows goods to be unloaded at any stop but only loaded at specific bus stops. This situation was relaxed by Cheng et al. (2018) by permitting goods to be loaded and unloaded at any stop. If the goods capacity on the part of the selected route is not adequate, the goods are unloaded at intermediate stops and wait for the next vehicle along the same route.

For rail-based FOT, Behiri et al. (2018) hypothesised that physical components of a rail network, i.e., stations, railways, and trains, are shared by participants, and freights can be loaded and unloaded at any station. The objective of their model is to minimise the total waiting time of each demand, defined as the difference between the time at which demand is loaded into the train and that at which it arrives at the departure station. In this manner, the turnover of goods in stations can be maximised. Sahli et al. (2022) simplified the model and improved the heuristic solution algorithm proposed by Behiri et al. (2018). Di et al. (2022) considered a system where freight and passengers are allowed to share each service train. In addition to optimising the flow assignment, they also optimised the

carriage arrangement.

2.3.2.5 Pricing

Most studies on FOT focus on solving operation management problems to reduce operation costs and total delivery time. Only a few consider the price charged to customers and the profits operators gain. We only found two papers mentioning the price. The first one is Li et al. (2021), which set a parameter representing the price of transporting a container. The other is Ma et al. (2022), which jointly optimised a logistic company's modal split strategy and a metro company's pricing strategy based on non-cooperative and cooperative game theoretical models. The results showed that metro-based FOT could generate Pareto-improving outcomes for the metro and logistics companies.

2.3.3 Crowdshipping

2.3.3.1 Demand and supply prediction

Two approaches can be used to predict the demand and supply in crowdshipping. The first one is to use historical data (Shen & Lin, 2020), while the second one is to identify the factors that influence the demand and supply through a survey (Ermagun et al., 2020; Gatta et al., 2019; Le et al., 2019; Le & Ukkusuri, 2019; Rechavi & Toch, 2022). As crowdshipping is a new service, only a limited amount of historical data is available. Thus, most are based on the second approach. The key factors influencing the demand and supply of crowdshipping are listed as follows.

(1) Demand: Dry cleaning, groceries, and home-delivered foods are favoured categories of goods in crowdshipping. Factors influencing people's acceptance rate of crowdshipping include personal attributes (including socio-demographic characteristics), built environments, crowd types, and driver performance. Specifically, younger people, online shoppers, and people with a strong sense of community and environmental concern are more likely to accept crowdshipping; areas with high population density but low job accessibility are suitable for crowdshipping development (Buldeo Rai et al., 2021; Le et al., 2019).

(2) Supply: Young individuals and students are more likely to work as crowdshippers. The supply of crowdshipping is enhanced by lower additional travel time spent on crowdsourced tasks, higher remuneration, and higher levels of crowdshipping experience (Ermagun et al., 2020; Fessler et al., 2022; Gatta et al., 2019; Le & Ukkusuri, 2019; Rechavi & Toch, 2022).

2.3.3.2 Matching strategy

As defined in Section 2.2.1, in this review, we focus on the case in which crowdshippers are matched with delivery requests on their way to a pre-planned trip, known as en route matching (Alnaggar et al., 2021).

The key component in the en route matching problem is the criteria for an acceptable matching. Most studies set a maximum percentage by which crowdshippers can deviate from their normal trip in terms of the distance or travel time (Al Hla et al., 2019; Archetti et al., 2016; Martín-Santamaría et al., 2021; Zehtabian et al., 2022). Additionally, the crowdshipper's earliest departure time at his/her origin and latest arrival time at the destination can be confined (Arslan et al., 2019; Chen et al., 2018; Macrina et al., 2020). Other than time-specified criteria, the maximum number of parcels or stops that crowdshippers accept are used by Arslan et al. (2019), Voigt and Kuhn (2022), Wang et al. (2016), and Zehtabian et al. (2022). Instead of a single match, Ausseil et al. (2022) and Mancini and Gansterer (2022) provided several options for a crowdshipper to choose from.

2.3.3.3 Facility location

Most studies on crowdshipping have focused on operational-level decisions and considered point-to-point deliveries in which the origin-destination pairs of crowdshippers are close to those of the parcels to be delivered. This may cause a lower success delivery rate compared with crowdshipping allowing relays. To overcome this challenge, facilities such as parcel lockers could be established to connect multiple crowdshippers for the same task, leading to a facility location problem. Ghaderi et al. (2022) developed a two-phase algorithm to locate the parcel lockers to maximise total profits and delivery rate. Considering the stochastic crowd capacity and demands, Nieto-Isaza et al. (2022) developed a two-stage stochastic programming model to determine the locations of mini depots to minimise total expected installation and transportation costs.

2.3.3.4 Route planning for vehicles and goods

The route planning problem includes routing for a fleet owned by an operator and occasional drivers. Archetti et al. (2016) initially modelled this problem as a VRP with occasional drivers (VRPOD). This framework involves a single depot from where goods, dedicated vehicles, and occasional drivers start. Many variants of this simple setting have been studied. For example, Al Hla et al. (2019) considered the behaviours of both regular and occasional drivers. Triki (2021) allowed occasional drivers to bid for delivery tasks. Macrina et al. (2017) considered the time windows of customers. Lan et al. (2022), Macrina et al. (2020), and Yu et al. (2021b), Yu et al. (2022) introduced transhipment nodes. Besides, the stochasticity and dynamics of the crowdshipping system have been addressed by Archetti et al. (2021), Dahle et al. (2017), Dayarian and Savelsbergh (2020), Mousavi et al. (2022), Santini et al. (2022), and Silva and Pedroso (2022).

In the above-mentioned VRPOD framework, all parcels originate from the depot, and a single crowdshipper fulfils the crowdsourced delivery. This overlooks the possibility that relaying crowdsourced tasks between crowdshippers could attract more participants to work as crowdshippers and increase the delivery success rate, addressed by Chen et al. (2018) and Voigt and Kuhn (2022). They extended the VRPOD to a pickup and delivery problem with occasional drivers, where each parcel has a different origin, vehicles not only deliver parcels but also collect parcels, and relays between crowdshippers are allowed.

Unlike the VRPOD that determines the operator-scheduled vehicle routes, Yıldız (2021a, 2021b) explored the express package routing problem to determine the combinations of self-scheduled trips of crowdshippers to fulfil transportation requests. They designed a system involving service points at which pickup and drop-off operations occur. Senders drop off goods at their selected service points, and receivers pick up goods from other service points. Crowdshippers are responsible for transferring goods between the selected service points. Each crowdshipper only performs one single trip between service points, but one task may have multi-leg trips.

Crowdshippers are typically ordinary people. In addition, taxi drivers can serve as crowdshippers to transport parcels without influencing the passenger service (Chen et al., 2017; Chen et al., 2016; Cheng et al., 2022). Elsewhere, Boysen et al. (2022) considered voluntary employees of distribution centres as crowdshippers and optimised the delivery routes for these employees to maximise the number of parcels assigned to them.

2.3.3.5 Pricing and compensation

Crowdshippers usually receive compensation from retailers such as Walmart and logistics companies. Five compensation schemes have been proposed in the literature: 1) Customer-dependent compensation: The compensation for crowdshippers depends on the customer's location. A larger distance between the customer and depot corresponds

to a higher compensation for crowdshippers (Archetti et al., 2021; Archetti et al., 2016; Dahle et al., 2019; Macrina et al., 2017); 2) Crowdshipper dependent compensation: The compensation for crowdshippers depends on the amount of additional distance travelled or additional time spent compared with normal travel (Dahle et al., 2019; Yu et al., 2021b; Yu et al., 2022); 3) Fixed compensation for each delivery: The compensation for crowdshippers depends on the number of deliveries performed (Boysen et al., 2022; Dahle et al., 2019; Lan et al., 2022; Santini et al., 2022; Yıldız, 2021a, 2021b); 4) Combined compensation: The compensation for crowdshippers consists of two elements. Specifically, a fixed compensation is provided when the crowdshippers fulfil at least one delivery, and variable compensation is provided depending on additional efforts (extra travel distance or travel time) made for crowdsourced deliveries (Dahle et al., 2019; Dayarian & Savelsbergh, 2020; Mousavi et al., 2022); 5) Auction-based compensation: Crowdshippers bid for crowdsourced tasks and are paid their bidding price if they win (Triki, 2021).

In terms of optimising the compensation provided to crowdshippers and the price charged for requesters, we found three studies in which a third-party platform controls the crowdshipping service. Le et al. (2021) optimised the price and compensation from the platform's perspective, aiming to maximise the platform's profits. Zhou et al. (2021) proposed a pricing strategy considering the varying package–driver ratio in a local region to maximise the number of stable matches such that both the requester and crowdshipper have strong incentives to be matched. These two studies neglect attributes associated with the parcel, e.g., weight and size, which may influence the behaviours of the receivers and crowdshippers. This aspect is addressed by Xiao et al. (2021), wherein a multi-unit multi-attribute auction for crowdsourced delivery to maximise social welfare is designed.

2.4 General framework

Based on the above review of the existing forms of integrated transportation systems, we propose a general framework for planning and operating such systems, as shown in Figure 2.2.

First, we divide an integrated transportation system into three core components, each comprising various elements worthy of investigation.

(1) Passenger and goods demand. Demand is generated by the requirement of people to move from origins to destinations for a certain purpose, such as work, while goods must be delivered from senders to recipients to fulfil customers' requirements.

(2) Transport supply. Integrated people-and-goods transportation operators may be public transport operators (e.g., bus, metro, and train companies), private transportation companies, retailers with their own fleets and dedicated drivers, or third-party companies that employ occasional drivers who use their vehicles to perform tasks.

(3) Infrastructure and technology. The infrastructure includes all materials that support the integrated transportation of people and goods, e.g., roads, railways, and information and communications technology.

In this context, each operator must address the following three main problems, which contain two or three subproblems.

(1) Demand management. This problem includes i) demand prediction to understand how travellers and senders make transportation decisions; ii) pricing strategies to control the spatiotemporal distribution of transportation demand.

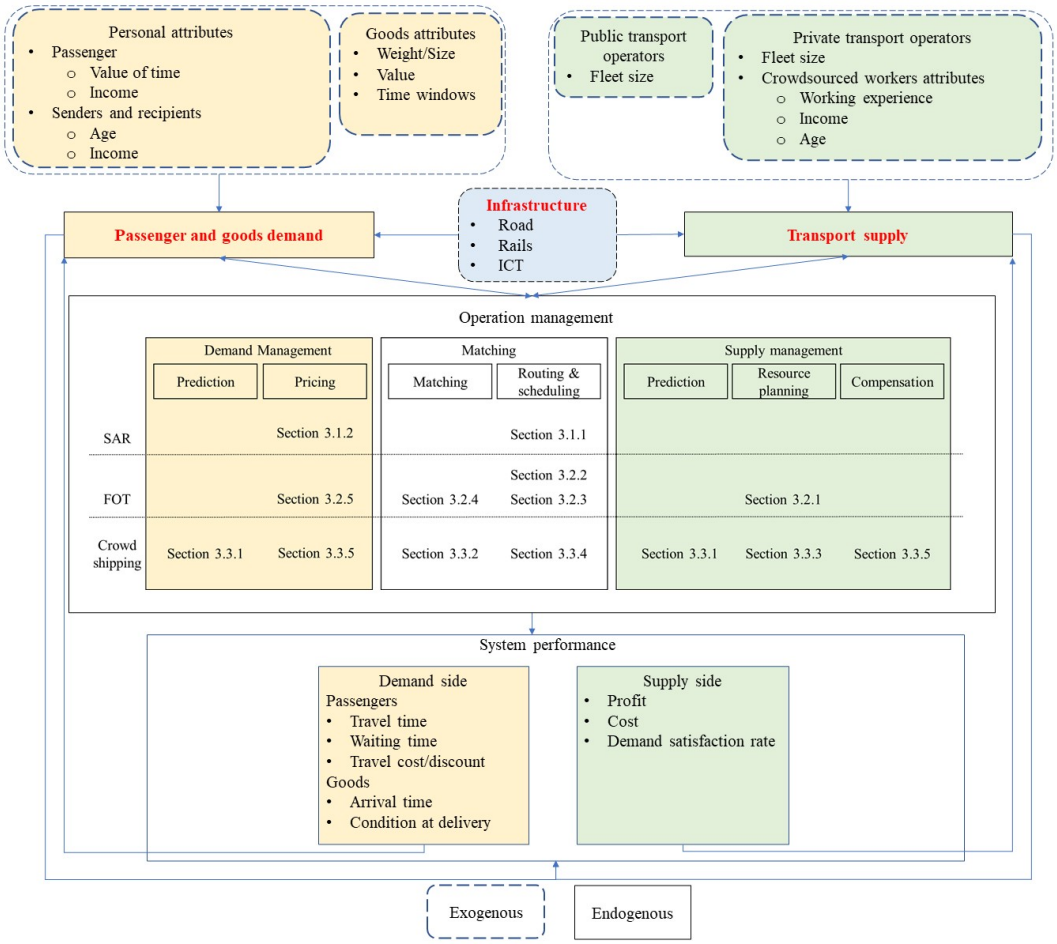

Figure 2.2: A general framework for integrated people-and-goods transportation systems

(2) Supply management. This problem includes predicting and planning the capacity that can be used to fulfil the transportation demand and designing compensation strategies to control the supply.

(3) Demand and supply matching. This problem aims at matching a specific request with a vehicle, which typically involves the design of the routes and schedules of vehicles or the assignment of requests to a vehicle, depending on the integration form.

Figure 2.2 also shows the subproblems examined in the existing studies. Several gaps remain, considered promising research directions, as described in Section 2.5.

The performance of the integrated transportation system could be evaluated from different perspectives. On the demand side, passengers care mostly about the travel time, waiting time, and travel cost, while shippers are more concerned with the transportation costs and whether the goods are delivered in a satisfactory condition and timely manner. On the supply side, operators focus mostly on profit, operation cost, and demand satisfaction

rate. Solving the operation management problems will directly influence the indicators on the two sides, which will further influence the demand and supply. The demand and supply, in turn, influence the operational strategies and decisions and the resulting efficiency of the integrated people-and-goods transportation system. The application of integrated people-and-goods transportation will inevitably impact various aspects of sustainability, like environmental (e.g., air pollutants) and social (e.g., employment, equity). Nevertheless, they are well beyond the scope of this review and are left for future work.

2.5 Research gaps and future directions

Based on the framework proposed in Section 2.4, we specify future research directions from three aspects. For each aspect, we categorise two types of future research aimed at, respectively, filling the research gap and enhancing the existing research. Notably, research gaps may exist owing to the different implementation methods of different forms in practice. Then, we presented some research opportunities in the era of technology.

2.5.1 Demand management

2.5.1.1 Pioneering research

As shown in Figure 2.2, demand prediction for SAR and FOT has not been extensively studied, despite its importance for service operators in providing supply that matches the demand. Currently, both SAR and FOT are in the early implementation stage, and the amount of historical data is inadequate. In this context, the demand can be predicted by identifying the factors influencing people's choices. To this end, unique features/phenomena associated with the system must be understood. For example, in terms of passenger demand, some passengers may transfer from separated to integrated modes due to decreased travel costs. In contrast, passengers with a high value of time are less likely to accept a detour for the delivery of goods even if a discount is available. Moreover, some passengers may refuse to be transported with goods owing to safety and comfort concerns when the goods are placed in the same vehicle (or carriage). In terms of goods demands, the incomes of senders and recipients, environmental conscientiousness, and requirement for time windows determine whether the senders and recipients choose an SAR vehicle or public transport for delivery. Additionally, the goods' attributes (type, size, weight, volume, value, etc.) determine whether they can be transported with people and the mode suitable for transporting them. For example, dangerous goods cannot be transported with passengers, while groceries, which typically involve a large volume and number of goods, can be transported by trains or metros instead of taxis. In the future, with the development of SAR and FOT and the availability of adequate data, historical data may be used to predict the spatiotemporal transportation demand distribution.

2.5.1.2 Research for improvement

Most studies have considered the price charged to customers as a parameter under different pricing schemes. Because the influence of pricing on demand and supply is complex, the pricing can instead be considered a decision variable and determined using an optimization model.

2.5.2 Supply management

2.5.2.1 Pioneering research

Supply management in SAR frameworks has not been extensively investigated. This is probably because SAR can be implemented in multiple ways, and a common supply management strategy cannot be applied to all methods. In practice, the supply management subproblem to be addressed depends on the type of operator. Operators are classified in terms of the possession of the fleet and drivers. The supply management subproblem for operators with their own fleet and drivers is focused on resource planning because

the supply is determined by the fleet size, the dedicated drivers must follow the routes designed by the operators to service customers, and the drivers are paid salaries by the operators. In this framework, the supply distribution does not need to be predicted, and no compensation exists. The supply management subproblem for operators without their own fleet and drivers is focused on supply prediction and compensation because the supply of drivers is affected by various factors such as age, income, and compensation for each request.

The supply prediction for FOT has not been extensively studied. Compensation for drivers might not be considered a problem that needs to be practically addressed, as drivers of public transport vehicles typically receive a regular monthly salary. For public transport operators, supply prediction is focused on predicting the available capacity that can be used for transporting passengers and goods. This supply decides whether goods and passengers can be transported simultaneously in specific periods. This aspect can be considered a counterpart to predicting the passengers' route choice behaviour given the transit capacities. In the case of underused capacity, companies can enter the integrated people-and-goods transport market. Otherwise, the companies can simply serve passengers as usual.

2.5.2.2 Research for improvement

Scheduled-public-transport-based FOT consists of two parts: a public transport mode for backbone transportation and support vehicles for first/last-mile transportation. Although several researchers have studied FOT based on various transportation means, the backbone transportation consisted of a single public transport mode. In practice, each public transport mode has its advantages and disadvantages. For example, metros and trains are faster and more punctual than buses, while buses have a wider service area. Different public transportation modes can be combined to fully exploit the advantages of all parties to provide a more time-efficient or cost-efficient service. Because hubs for transferring passengers from one public transport mode to another already exist, goods can also be transhipped at these nodes. In addition, as described in Section 2.3.2.1, most studies on freight hub selection have focused on metro-based FOT. For bus-based FOT, it is typically assumed that all bus stations can be used to handle and tranship goods. However, considering the goods transportation demand and cost of reforming a passenger platform to an enhanced platform suitable for goods storage and transhipment, it is not reasonable to set all passenger boarding/alighting points as goods loading/unloading points. Therefore, the hub location problem must also be addressed in bus-based FOT. In addition, the fleet size of scheduled and demand-responsive public transport vehicles considerably influences the supply and must be further investigated.

For crowdshipping, research can be performed to understand peoples' attitudes toward public-transport-based crowdshipping. Moreover, as in the case of the pricing problem in demand management, the compensation provided to crowdshippers affects the supply of crowdshippers. Therefore, the compensation of crowdshippers must be optimised. In addition, researchers can optimise the location and capacity of the support infrastructure. In this way, similar origin-destination pairs between crowdshippers and parcels do not need to be identified, making the system more flexible and efficient.

2.5.3 Matching

2.5.3.1 Pioneering research

The matching problem for SAR has not been studied, probably because the existing studies have assumed that the SAR operators belong to the first type of operator, as described in Section 2.5.2.1. In this scenario, the dedicated drivers working for the operator cannot

reject requests assigned to them. If the operators belong to the second type, the occasional drivers can reject requests assigned to them. In this scenario, an optimal matching problem must be solved to increase the successful matching rate. Different matching strategies can be explored, e.g., en route matching and negotiation between occasional drivers and requesters.

2.5.3.2 Research for improvement

The following research directions can be considered for improving research on matching transportation demands with supply.

First, for SAR with the second type of operators, occasional drivers can be guided to reposition their vehicles after finishing their tasks to increase their chance of accepting another task when they do not have a personal trip planned after the delivery.

Second, for scheduled-public-transport-based FOT, matching between goods requests with a specific public transport vehicle can be examined in the context of multimodal urban transport so that a goods request can be matched to a multimodal trip chain of public transport services.

Third, we recommend developing models to solve the matching problem in public-transport-based crowdshipping. This matching is different from that in private-vehicle-based crowdshipping because a parcel request suitable for a private-vehicle-based crowdshipper might not be accepted by a public-transport-based crowdshipper.

Fourth, researchers can attempt to solve the subproblems associated with all three forms of integrated systems in a stochastic and dynamic setting, as this is more realistic and research in this domain is limited.

2.5.4 Opportunities in the era of technology

Rapid developments of new technologies, e.g., 5G technology, artificial intelligence (AI), Internet of things (IoT), autonomous vehicles (AVs), digital twins, etc., will revolutionize the transportation industry, which brings opportunities for the development of integrated transportation system. First, the potential deployment of AVs, drones, and robots and their impacts on integrated transportation systems should be studied before they are widely applied. Second, technologies such as ICT and intelligent transportation systems enable the synchromodality, which aims to provide efficient, reliable, and flexible transportation services using real-time information. This strengthens the need for fast online algorithms to support real-time re-optimisation. Third, driven by AI, IoT, etc., digital twins could be used to simulate different activities in the integrated transportation system, which enables planners to manage transportation dynamically, react to unexpected events appropriately, etc. Moreover, digital twins could be used to analyse the potential impacts of new concepts before real implementations. As Arvidsson and Browne (2013) recommended, it is better to try a new concept in a small-scale fashion and gradually scale up, especially for big projects requiring high investment or new infrastructure. This could be achieved by digital twins in a time and cost-efficient way to explore the economic viability and scalability to meet the exploding delivery demand and the need for infrastructure and equipment investment for the integrated transportation system before real application. We recommend that researchers apply more advanced methods, e.g., digital twins, in the era of technologies to assess the feasibility of an integrated system, in addition to using traditional methods such as simulation.

References

Al Hla, Y. A., Othman, M., & Saleh, Y. (2019). Optimising an eco-friendly vehicle routing problem model using regular and occasional drivers integrated with driver behaviour control. *Journal of Cleaner Production*, *234*, 984–1001.

Alnaggar, A., Gzara, F., & Bookbinder, J. H. (2021). Crowdsourced delivery: A review of platforms and academic literature. *Omega*, *98*, 102139.

Archetti, C., Guerriero, F., & Macrina, G. (2021). The online vehicle routing problem with occasional drivers. *Computers & Operations Research*, *127*, 105144.

Archetti, C., Savelsbergh, M., & Speranza, M. G. (2016). The vehicle routing problem with occasional drivers. *European Journal of Operational Research*, *254*(2), 472–480.

Arslan, A. M., Agatz, N., Kroon, L., & Zuidwijk, R. (2019). Crowdsourced delivery—a dynamic pickup and delivery problem with ad hoc drivers. *Transportation Science*, *53*(1), 222–235.

Arvidsson, N., & Browne, M. (2013). A review of the success and failure of tram systems to carry urban freight: The implications for a low emission intermodal solution using electric vehicles on trams.

Arvidsson, N., Givoni, M., & Woxenius, J. (2016). Exploring last mile synergies in passenger and freight transport. *Built Environment*, *42*(4), 523–538.

Ausseil, R., Pazour, J. A., & Ulmer, M. W. (2022). Supplier menus for dynamic matching in peer-to-peer transportation platforms. *Transportation Science*, *56*(5), 1304–1326.

Azcuy, I., Agatz, N., & Giesen, R. (2021). Designing integrated urban delivery systems using public transport. *Transportation Research Part E: Logistics and Transportation Review*, *156*, 102525.

Behiri, W., Belmokhtar-Berraf, S., & Chu, C. (2018). Urban freight transport using passenger rail network: Scientific issues and quantitative analysis. *Transportation Research Part E: Logistics and Transportation Review*, *115*, 227–245.

Beirigo, B. A., Schulte, F., & Negenborn, R. R. (2018). Integrating people and freight transportation using shared autonomous vehicles with compartments. *IFAC-PapersOnLine*, *51*(9), 392–397.

Boysen, N., Emde, S., & Schwerdfeger, S. (2022). Crowdshipping by employees of distribution centers: Optimization approaches for matching supply and demand. *European Journal of Operational Research*, *296*(2), 539–556.

Bruzzone, F., Cavallaro, F., & Nocera, S. (2021). The integration of passenger and freight transport for first-last mile operations. *Transport policy*, *100*, 31–48.

Buldeo Rai, H., Verlinde, S., & Macharis, C. (2018). Shipping outside the box. environmental impact and stakeholder analysis of a crowd logistics platform in belgium. *Journal of Cleaner Production*, *202*, 806–816.

Buldeo Rai, H., Verlinde, S., & Macharis, C. (2021). Who is interested in a crowdsourced last mile? a segmentation of attitudinal profiles. *Travel Behaviour and Society*, *22*, 22–31.

Buldeo Rai, H., Verlinde, S., Merckx, J., & Macharis, C. (2017). Crowd logistics: An opportunity for more sustainable urban freight transport? *European Transport Research Review*, *9*, 1–13.

Cavallaro, F., & Nocera, S. (2022). Integration of passenger and freight transport: A concept-centric literature review. *Research in Transportation Business & Management*, *43*, 100718.

Chebbi, O., & Chaouachi, J. (2016). Reducing the wasted transportation capacity of personal rapid transit systems: An integrated model and multi-objective optimization approach. *Transportation research part E: logistics and transportation review*, *89*, 236–258.

Chen, C., Pan, S., Wang, Z., & Zhong, R. Y. (2017). Using taxis to collect citywide e-commerce reverse flows: A crowdsourcing solution. *International Journal of Production Research*, *55*(7), 1833–1844.

Chen, C., Zhang, D., Ma, X., Guo, B., Wang, L., Wang, Y., & Sha, E. (2016). Crowddeliver: Planning city-wide package delivery paths leveraging the crowd of taxis. *IEEE Transactions on Intelligent Transportation Systems*, *18*(6), 1478–1496.

Chen, W., Mes, M., & Schutten, M. (2018). Multi-hop driver-parcel matching problem with time windows. *Flexible services and manufacturing journal*, *30*, 517–553.

Cheng, G., Guo, D., Shi, J., & Qin, Y. (2018). When packages ride a bus: Towards efficient city-wide package distribution. *2018 IEEE 24th international conference on parallel and distributed systems (ICPADS)*, 259–266.

Cheng, S., Chen, C., Pan, S., Huang, H., Zhang, W., & Feng, Y. (2022). Citywide package deliveries via crowdshipping: Minimizing the efforts from crowdsourcers. *Frontiers of Computer Science*, *16*, 1–13.

Cleophas, C., Cottrill, C., Ehmke, J. F., & Tierney, K. (2019). Collaborative urban transportation: Recent advances in theory and practice. *European Journal of Operational Research*, *273*(3), 801–816.

Cochrane, K., Saxe, S., Roorda, M. J., & Shalaby, A. (2017). Moving freight on public transit: Best practices, challenges, and opportunities. *International Journal of Sustainable Transportation*, *11*(2), 120–132.

Dahle, L., Andersson, H., & Christiansen, M. (2017). The vehicle routing problem with dynamic occasional drivers. *Computational Logistics: 8th International Conference, ICCL 2017, Southampton, UK, October 18-20, 2017, Proceedings 8*, 49–63.

Dahle, L., Andersson, H., Christiansen, M., & Speranza, M. G. (2019). The pickup and delivery problem with time windows and occasional drivers. *Computers & Operations Research*, *109*, 122–133.

Dayarian, I., & Savelsbergh, M. (2020). Crowdshipping and same-day delivery: Employing in-store customers to deliver online orders. *Production and Operations Management*, *29*(9), 2153–2174.

Di, Z., Yang, L., Shi, J., Zhou, H., Yang, K., & Gao, Z. (2022). Joint optimization of carriage arrangement and flow control in a metro-based underground logistics system. *Transportation Research Part B: Methodological*, *159*, 1–23.

Dong, J., Hu, W., Yan, S., Ren, R., & Zhao, X. (2018). Network planning method for capacitated metro-based underground logistics system. *Advances in civil engineering*, *2018*.

Elbert, R., & Rentschler, J. (2022). Freight on urban public transportation: A systematic literature review. *Research in Transportation Business & Management*, *45*, 100679.

Ermagun, A., Punel, A., & Stathopoulos, A. (2020). Shipment status prediction in online crowd-sourced shipping platforms. *Sustainable Cities and Society*, *53*, 101950.

European Commission. (2007). Green paper, towards a new culture for urban mobility, Luxembourg: Publications Office of the European Union.

European Commission. (2019). *Transport in the European union – current trends and issues*. https://ec.europa.eu/transport/sites/transport/files/2019-transport-in-theeu-current-trends-and-issues.pdf.

Fatnassi, E., Chaouachi, J., & Klibi, W. (2015). Planning and operating a shared goods and passengers on-demand rapid transit system for sustainable city-logistics. *Transportation Research Part B: Methodological*, *81*, 440–460.

Fessler, A., Thorhauge, M., Mabit, S., & Haustein, S. (2022). A public transport-based crowdshipping concept as a sustainable last-mile solution: Assessing user preferences with a stated choice experiment. *Transportation Research Part A: Policy and Practice*, *158*, 210–223.

Gatta, V., Marcucci, E., Nigro, M., & Serafini, S. (2019). Sustainable urban freight transport adopting public transport-based crowdshipping for b2c deliveries. *European Transport Research Review*, *11*(1), 1–14.

Ghaderi, H., Zhang, L., Tsai, P.-W., & Woo, J. (2022). Crowdsourced last-mile delivery with parcel lockers. *International Journal of Production Economics*, *251*, 108549.

Ghilas, V., Cordeau, J.-F., Demir, E., & Woensel, T. V. (2018). Branch-and-price for the pickup and delivery problem with time windows and scheduled lines. *Transportation Science*, *52*(5), 1191–1210.

Ghilas, V., Demir, E., & Van Woensel, T. (2013). Integrating passenger and freight transportation: Model formulation and insights.

Ghilas, V., Demir, E., & Van Woensel, T. (2016a). An adaptive large neighborhood search heuristic for the pickup and delivery problem with time windows and scheduled lines. *Computers & Operations Research*, *72*, 12–30.

Ghilas, V., Demir, E., & Van Woensel, T. (2016b). The pickup and delivery problem with time windows and scheduled lines. *INFOR: Information Systems and Operational Research*, *54*(2), 147–167.

Ghilas, V., Demir, E., & Van Woensel, T. (2016c). A scenario-based planning for the pickup and delivery problem with time windows, scheduled lines and stochastic demands. *Transportation Research Part B: Methodological*, *91*, 34–51.

He, Y., & Csiszár, C. (2021). Model for crowdsourced parcel delivery embedded into mobility as a service based on autonomous electric vehicles. *Energies*, *14*(11), 3042.

Hörsting, L., & Cleophas, C. (2023). Scheduling shared passenger and freight transport on a fixed infrastructure. *European Journal of Operational Research*, *306*(3), 1158–1169.

Huang, H., Savkin, A. V., & Huang, C. (2020). A new parcel delivery system with drones and a public train. *Journal of Intelligent & Robotic Systems*, *100*, 1341–1354.

Ji, Y., Zheng, Y., Zhao, J., Shen, Y., & Du, Y. (2020). A multimodal passenger-and-package sharing network for urban logistics. *Journal of Advanced Transportation*, *2020*, 1–16.

Kikuta, J., Ito, T., Tomiyama, I., Yamamoto, S., & Yamada, T. (2012). New subway-integrated city logistics szystem. *Procedia-Social and Behavioral Sciences*, *39*, 476–489.

Kızıl, K. U., & Yıldız, B. (2023). Public transport-based crowd-shipping with backup transfers. *Transportation Science*, *57*(1), 174–196.

Lan, Y.-L., Liu, F., Ng, W. W., Gui, M., & Lai, C. (2022). Multi-objective two-echelon city dispatching problem with mobile satellites and crowd-shipping. *IEEE Transactions on Intelligent Transportation Systems*, *23*(9), 15340–15353.

Le, T. V., Stathopoulos, A., Van Woensel, T., & Ukkusuri, S. V. (2019). Supply, demand, operations, and management of crowd-shipping services: A review and empirical evidence. *Transportation Research Part C: Emerging Technologies*, *103*, 83–103.

Le, T. V., & Ukkusuri, S. V. (2019). Modeling the willingness to work as crowd-shippers and travel time tolerance in emerging logistics services. *Travel Behaviour and Society*, *15*, 123–132.

Le, T. V., Ukkusuri, S. V., Xue, J., & Van Woensel, T. (2021). Designing pricing and compensation schemes by integrating matching and routing models for crowd-shipping systems. *Transportation Research Part E: Logistics and Transportation Review*, *149*, 102209.

Le Pira, M., Tavasszy, L. A., de Almeida Correia, G. H., Ignaccolo, M., & Inturri, G. (2021). Opportunities for integration between mobility as a service (maas) and freight transport: A conceptual model. *Sustainable Cities and Society*, *74*, 103212.

Li, B., Krushinsky, D., Reijers, H. A., & Van Woensel, T. (2014). The share-a-ride problem: People and parcels sharing taxis. *European Journal of Operational Research*, *238*(1), 31–40.

Li, B., Krushinsky, D., Van Woensel, T., & Reijers, H. A. (2016a). An adaptive large neighborhood search heuristic for the share-a-ride problem. *Computers & Operations Research*, *66*, 170–180.

Li, B., Krushinsky, D., Van Woensel, T., & Reijers, H. A. (2016b). The share-a-ride problem with stochastic travel times and stochastic delivery locations. *Transportation Research Part C: Emerging Technologies*, *67*, 95–108.

Li, F., Guo, X., Zhou, L., Wu, J., & Li, T. (2022). A capacity matching model in a collaborative urban public transport system: Integrating passenger and freight transportation. *International Journal of Production Research*, *60*(20), 6303–6328.

Li, Z., Shalaby, A., Roorda, M. J., & Mao, B. (2021). Urban rail service design for collaborative passenger and freight transport. *Transportation Research Part E: Logistics and Transportation Review*, *147*, 102205.

Lu, C.-C., Diabat, A., Li, Y.-T., & Yang, Y.-M. (2022). Combined passenger and parcel transportation using a mixed fleet of electric and gasoline vehicles. *Transportation Research Part E: Logistics and Transportation Review*, *157*, 102546.

Ma, M., Zhang, F., Liu, W., & Dixit, V. (2022). A game theoretical analysis of metro-integrated city logistics systems. *Transportation Research Part B: Methodological*, *156*, 14–27.

Macrina, G., Di Puglia Pugliese, L., Guerriero, F., & Laganà, D. (2017). The vehicle routing problem with occasional drivers and time windows. *Optimization and Decision Science: Methodologies and Applications: ODS, Sorrento, Italy, September 4-7, 2017 47*, 577–587.

Macrina, G., Di Puglia Pugliese, L., Guerriero, F., & Laporte, G. (2020). Crowd-shipping with time windows and transshipment nodes. *Computers & Operations Research*, *113*, 104806.

Manchella, K., Haliem, M., Aggarwal, V., & Bhargava, B. (2021a). Passgoodpool: Joint passengers and goods fleet management with reinforcement learning aided pricing, matching, and route planning. *IEEE Transactions on Intelligent Transportation Systems*, *23*(4), 3866–3877.

Manchella, K., Umrawal, A. K., & Aggarwal, V. (2021b). Flexpool: A distributed model-free deep reinforcement learning algorithm for joint passengers and goods transportation. *IEEE Transactions on Intelligent Transportation Systems*, *22*(4), 2035–2047.

Mancini, S., & Gansterer, M. (2022). Bundle generation for last-mile delivery with occasional drivers. *Omega*, *108*, 102582.

Martín-Santamaría, R., López-Sánchez, A. D., Delgado-Jalón, M. L., & Colmenar, J. M. (2021). An efficient algorithm for crowd logistics optimization. *Mathematics*, *9*(5), 509.

Masson, R., Trentini, A., Lehuédé, F., Malhéné, N., Péton, O., & Tlahig, H. (2017). Optimization of a city logistics transportation system with mixed passengers and goods. *EURO Journal on Transportation and Logistics*, *6*(1), 81–109.

Mourad, A., Puchinger, J., & Chu, C. (2019). A survey of models and algorithms for optimizing shared mobility. *Transportation Research Part B: Methodological*, *123*, 323–346.

Mourad, A., Puchinger, J., & Van Woensel, T. (2021). Integrating autonomous delivery service into a passenger transportation system. *International Journal of Production Research*, *59*(7), 2116–2139.

Mousavi, K., Bodur, M., & Roorda, M. J. (2022). Stochastic last-mile delivery with crowdshipping and mobile depots. *Transportation Science*, *56*(3), 612–630.

Nieto-Isaza, S., Fontaine, P., & Minner, S. (2022). The value of stochastic crowd resources and strategic location of mini-depots for last-mile delivery: A benders decomposition approach. *Transportation Research Part B: Methodological*, *157*, 62–79.

Ozturk, O., & Patrick, J. (2018). An optimization model for freight transport using urban rail transit. *European Journal of Operational Research*, *267*(3), 1110–1121.

Peng, Z., Feng, R., Wang, C., Jiang, Y., & Yao, B. (2021). Online bus-pooling service at the railway station for passengers and parcels sharing buses: A case in dalian. *Expert Systems with Applications*, *169*, 114354.

Pimentel, C., & Alvelos, F. (2018). Integrated urban freight logistics combining passenger and freight flows–mathematical model proposal. *Transportation research procedia*, *30*, 80–89.

Qu, X., Wang, S., & Niemeier, D. (2022). On the urban-rural bus transit system with passenger-freight mixed flow. *Communications in Transportation Research*, *2*(1), 100054.

Rechavi, A., & Toch, E. (2022). Crowd logistics: Understanding auction-based pricing and couriers' strategies in crowdsourcing package delivery. *Journal of Intelligent Transportation Systems*, *26*(2), 129–144.

Ren, T., Jiang, Z., Cai, X., Yu, Y., Xing, L., Zhuang, Y., & Li, Z. (2021). A dynamic routing optimization problem considering joint delivery of passengers and parcels. *Neural Computing and Applications*, *33*, 10323–10334.

Sahli, A., Behiri, W., Belmokhtar-Berraf, S., & Chu, C. (2022). An effective and robust genetic algorithm for urban freight transport scheduling using passenger rail network. *Computers & Industrial Engineering*, *173*, 108645.

Santini, A., Viana, A., Klimentova, X., & Pedroso, J. P. (2022). The probabilistic travelling salesman problem with crowdsourcing. *Computers & Operations Research*, *142*, 105722.

Savelsbergh, M., & Van Woensel, T. (2016). 50th anniversary invited article—city logistics: Challenges and opportunities. *Transportation science*, *50*(2), 579–590.

Shen, H., & Lin, J. (2020). Investigation of crowdshipping delivery trip production with real-world data. *Transportation Research Part E: Logistics and Transportation Review*, *143*, 102106.

Silva, M., & Pedroso, J. P. (2022). Deep reinforcement learning for crowdshipping last-mile delivery with endogenous uncertainty. *Mathematics*, *10*(20), 3902.

Sun, X., Hu, W., Xue, X., & Dong, J. (2022). Multi-objective optimization model for planning metro-based underground logistics system network: Nanjing case study. *Journal of Industrial and Management Optimization*, *19*(1), 170–196.

Tholen, M. v. d., Beirigo, B. A., Jovanova, J., & Schulte, F. (2021). The share-a-ride problem with integrated routing and design decisions: The case of mixed-purpose shared autonomous vehicles. *Computational Logistics: 12th International Conference, ICCL 2021, Enschede, The Netherlands, September 27–29, 2021, Proceedings 12*, 347–361.

Triki, C. (2021). Using combinatorial auctions for the procurement of occasional drivers in the freight transportation: A case-study. *Journal of Cleaner Production*, *304*, 127057.

Voigt, S., & Kuhn, H. (2022). Crowdsourced logistics: The pickup and delivery problem with transshipments and occasional drivers. *Networks*, *79*(3), 403–426.

Wang, Y., Zhang, D., Liu, Q., Shen, F., & Lee, L. H. (2016). Towards enhancing the last-mile delivery: An effective crowd-tasking model with scalable solutions. *Transportation Research Part E: Logistics and Transportation Review*, *93*, 279–293.

Xiao, F., Wang, H., Guo, S., Guan, X., & Liu, B. (2021). Efficient and truthful multi-attribute auctions for crowdsourced delivery. *International Journal of Production Economics*, *240*, 108233.

Ye, Y., Guo, J., & Yan, L. (2021). A mixed decision strategy for freight and passenger transportation in metro systems. *Computational intelligence and neuroscience*, *2021*, 1–22.

Yıldız, B. (2021a). Express package routing problem with occasional couriers. *Transportation Research Part C: Emerging Technologies*, *123*, 102994.

Yıldız, B. (2021b). Package routing problem with registered couriers and stochastic demand. *Transportation Research Part E: Logistics and Transportation Review*, *147*, 102248.

Yu, V. F., Indrakarna, P. A., Redi, A. A. N. P., & Lin, S.-W. (2021a). Simulated annealing with mutation strategy for the share-a-ride problem with flexible compartments. *Mathematics*, *9*(18), 2320.

Yu, V. F., Jodiawan, P., Hou, M.-L., & Gunawan, A. (2021b). Design of a two-echelon freight distribution system in last-mile logistics considering covering locations and occasional drivers. *Transportation Research Part E: Logistics and Transportation Review*, *154*, 102461.

Yu, V. F., Jodiawan, P., & Redi, A. P. (2022). Crowd-shipping problem with time windows, transshipment nodes, and delivery options. *Transportation Research Part E: Logistics and Transportation Review*, *157*, 102545.

Yu, V. F., Purwanti, S. S., Redi, A. P., Lu, C.-C., Suprayogi, S., & Jewpanya, P. (2018). Simulated annealing heuristic for the general share-a-ride problem. *Engineering Optimization*, *50*(7), 1178–1197.

Yu, V. F., Zegeye, M. M., Gebeyehu, S. G., Indrakarna, P. A., & Jodiawan, P. (2023). The multi-depot general share-a-ride problem. *Expert Systems with Applications*, *213*, 119044.

Zehtabian, S., Larsen, C., & Wøhlk, S. (2022). Estimation of the arrival time of deliveries by occasional drivers in a crowd-shipping setting. *European Journal of Operational Research*, *303*(2), 616–632.

Zhang, S., Markos, C., & James, J. (2022). Autonomous vehicle intelligent system: Joint ride-sharing and parcel delivery strategy. *IEEE Transactions on Intelligent Transportation Systems*, *23*(10), 18466–18477.

Zhao, L., Li, H., Li, M., Sun, Y., Hu, Q., Mao, S., Li, J., & Xue, J. (2018). Location selection of intra-city distribution hubs in the metro-integrated logistics system. *Tunnelling and Underground Space Technology*, *80*, 246–256.

Zhou, Z., Chen, R., & Guo, S. (2021). A domain-of-influence based pricing strategy for task assignment in crowdsourcing package delivery. *IET Intelligent Transport Systems*, *15*(6), 808–823.

3 An adaptive large neighborhood search metaheuristic for a passenger and parcel share-a-ride problem with drones

Cheng, R., Jiang, Y., Nielsen, O. A., & Pisinger, D. (2023). An adaptive large neighborhood search metaheuristic for a passenger and parcel share-a-ride problem with drones. Transportation Research Part C: Emerging Technologies, 153, 104203.

Abstract

With the increasing concerns about traffic congestion and climate change, much effort has been made to enhance sustainable urban mobility for passengers and goods. One emerging promising strategy is to transport passengers and goods in an integrated manner, as it could reduce the number of vehicles on the road compared with the separate transportation of passengers and goods. This study proposes the simultaneous transportation of passengers and goods using demand-responsive buses and drones. Compared with the prevalent strategies that rely only on ground vehicles to integrate passenger and parcel transportation, we propose the joint usage of ground vehicles and drones to transport passengers and deliver parcels. The ground vehicles for passenger and parcel delivery are on-demand buses, which combine the advantages of the flexibility of taxis and the large capacity of public transport modes. The drones automatically take off from and land on the on-demand buses' rooftops and are only for parcel delivery. A new optimization problem that designs the routes for both demand-responsive buses and drones is proposed and denoted as the passenger and parcel share-a-ride problem with drones (SARP-D). A mixed-integer nonlinear programming model is devised; the nonlinearity exists because drone launch/recovery can occur simultaneously with request servicing by a bus at the same node. To solve the model for large-scale instances, we develop an adaptive large neighborhood search metaheuristic. Numerical experiments are conducted to validate the correctness of the model and evaluate the efficiency of the metaheuristic. Moreover, sensitivity analyses are performed to explore the influences of the maximum number of intermediate stops during one passenger request service, the drone flight endurance, and the unit delay penalty on the total cost, which comprises the transportation and delay costs.

Keywords: Urban logistics; On-demand transit; Adaptive large neighborhood search; Integrated passenger-and-goods transportation; Share-a-ride problem with drones; Vehicle routing problem with drones

3.1 Introduction

Rapid urbanization and the boom in E-commerce have increased the demands for passenger and goods transportation. Traditionally, the demands for passenger and goods transportation are separately managed. In 2007, the European Commission (2007) stated that "local authorities need to consider all urban logistics related to passenger and freight transport as a single logistics system." Integrating passengers and goods transportation has emerged as a new research topic to achieve sustainable urban mobility because of its great potential to reduce the number of road vehicles serving the transportation demand (Cavallaro & Nocera, 2022; Cheng et al., 2023; Li et al., 2014).

Recently, Elbert and Rentschler (2022) summarized the literature on integrating passengers and parcels using public transport modes, such as buses and light rail. These conventional public transport modes are operated according to predefined routes and timetables and can hardly provide door-to-door services, as public transport stations are seldom the final destinations of passengers and goods. Thus, feeder vehicles must be used for last-mile delivery, which can cause additional traffic congestion and cost. Li et al. (2014) suggested that taxis, which are flexible and can deliver door-to-door services, are a better alternative to public transport for the integrated transport of passengers and goods. However, a taxi is characterized by limited capacity and availability and high costs. Considering the limitations associated with conventional public transport and taxis, this study proposes the use of on-demand transit, which can allow for the provision of door-to-door demand-responsive services with a larger capacity. Although on-demand transit has been extensively studied (e.g., Vansteenwegen et al., 2022), to the best of our knowledge, only Peng et al. (2021) considered it a means of integrating passengers and parcels transportation.

Another trend in urban mobility is the exploration and exploitation of autonomous technologies. Autonomous vehicle (AV) technology offers the possibility of relieving passenger transport-related congestion in various ways, such as improving coordination between vehicles and reducing accidents (Anderson et al., 2014), reducing parking demand and the congestion caused by the search for parking space (Othman, 2022), and reducing the time gap and thereby increasing the road capacity and mitigating congestion (Milanés & Shladover, 2014). Integrating shared autonomous vehicles (SAVs) with ridesharing services could further reduce congestion through traveler trip combination and SAV fleet size reduction (Golbabaei et al., 2021; Levin et al., 2017). Although accurately evaluating the influence of AVs on the environment is difficult, the potential positive environmental benefits of electrifying AVs have been generally acknowledged (Anderson et al., 2014; Golbabaei et al., 2021; Williams et al., 2020).

For goods transportation, drone delivery has attracted increasing attention in smart city logistics (Büyüközkan & Ilıcak, 2022), particularly in last-mile delivery (Boysen et al., 2021; Lemardelé et al., 2021). Recently, Amazon and Walmart have launched drone delivery services in some areas [1]. Drones have also been used to transport nucleic acid samples in Hangzhou, China [2]. Compared with traditional delivery vehicles, such as trucks and vans, drones are faster, do not occupy road space, and do not use fossil fuels. Therefore, drone usage has the potential of providing faster delivery and reducing urban congestion and greenhouse gas emissions (Agatz et al., 2018; Chiang et al., 2019; Moshref-Javadi et al., 2020b). However, drones have a limited service range owing to their battery capacity con-

[1] (1)https://www.aboutamazon.com/news/transportation/amazons-drone-delivery-is-coming-to-texas; (2)https://corporate.walmart.com/newsroom/2022/05/24/were-bringing-the-convenience-of-drone-delivery-to-4-million-u-s-households-in-partnership-with-droneup

[2] http://www.caacnews.com.cn/1/6/202211/t20221106_1356856.html

straint. To tackle this challenge, a truck–drone hybrid delivery system has been proposed. In this system, ground vehicles (typically vans or trucks) carry drones to a site near the customer's location and are responsible for launching and recovering the drones. More recently, scholars have investigated the potential of drone hitchhiking on public transit with fixed routes and timetables (Choudhury et al., 2021; Huang et al., 2020). The benefit of the hybrid system is that the drones utilize vehicles operating on fixed schedules.

Considering the two trends discussed above, this study explores a novel transportation system in which passengers and goods are simultaneously transported via demand-responsive buses (DRBs) and drones. In this system, a DRB contains separated passenger and parcel compartments and is equipped with a drone for goods delivery. A robotic shelving system is installed in the parcel compartment; the system automatically locates and prepares the parcel for the drone and customers, thereby relieving the driver of the task of placing the parcel on the drone and directly delivering the parcel to the customers. A DRB departs from the terminal, where it loads drones and parcels. The route of one DRB trip is determined by both passengers' requests and parcel delivery requests. The bus does not need to stop and visit every parcel delivery location; drones can be launched from the bus to undertake the delivery task and return to the bus. The launch and recovery of the drone are automatic. A more detailed problem description is provided in Section 3.3.1.

The envisioned system is inspired by the Mercedes-Benz vision van [3]. Most of the components of the proposed system have been implemented or are under piloting experiments for verification of their feasibility and attractiveness to the industry. For example, KT Corp, a telephone company in South Korea, demonstrated the practicability of a drone stored on the top of an autonomous bus delivering parcels to a designated pick-up point [4]. Transport for London ran two demand-responsive bus trials and found that 60% of users were willing to reduce car usage in favor of DRBs [5]. The Netherlands launched a project named Cargo Hitching to prove the viability of using the unused capacity of buses for parcel transport (Van Duin et al., 2019).

Operating the proposed system requires planning routes for both DRBs and drones. The corresponding optimization problem is denoted as the *passenger and parcel share-a-ride problem with drones* (SARP-D). This study devises a mixed-integer nonlinear programming (MINP) model for SARP-D to minimize the total operation costs, which comprise the transportation costs of DRBs and drones and delay penalties, considering both supply and demand constraints. Regarding supply, we consider the capacity constraints for passengers and parcels, the maximum operation time of a DRB, and the maximum battery endurance of drones. Regarding demand, we consider the time windows for both passenger and parcel requests. To reduce the inconvenience to passengers caused by extra stops to deliver parcels and pick up or drop off passengers, we restrict the maximum number of intermediate stops during the service for one passenger request.

We present an adaptive large neighborhood search (ALNS) algorithm that solves the proposed model for large-scale applications, given the high performance of the ALNS for a large variant of vehicle routing problems (Ghilas et al., 2016a, 2016b; Li et al., 2016a; Mourad et al., 2021; Ropke & Pisinger, 2006; Sacramento et al., 2019).

The remainder of this paper is organized as follows. Section 3.2 presents a literature review and summarizes our main contributions. Section 3.3 introduces the MINP model for

[3] https://www.youtube.com/watch?v=rnnSiK5mayY
[4] https://www.ajudaily.com/view/20170314142937637
[5] https://content.tfl.gov.uk/drb-research-report-july-2021.pdf

SARP-D, inspired by Li et al. (2014) and Sacramento et al. (2019). Section 3.4 describes the ALNS metaheuristic tailored to solve the proposed problem. Section 3.5 presents the numerical experiments conducted to validate the developed model, the analysis of operator performance in ALNS, and the algorithm performance under different instances. Section 3.6 provides some management insights. Finally, Section 3.7 concludes this paper and provides various directions for future research.

3.2 Passenger and parcel share-a-ride problem and the truck–drone routing problem

Our literature review focuses on two problems closely related to the proposed model: the passenger and parcel share-a-ride problem (SARP) and the truck–drone routing problem.

3.2.1 Passenger and parcel SARP

The SARP was first established by Li et al. (2014). It aims to determine a set of routes for taxis to serve both passenger and parcel requests and maximize profit for taxi companies, considering the time windows at both the origins and destinations of requests. Not all parcel requests can be served by taxis; hence, rejected parcels are served by a logistics company. Li et al. (2014) imposed three assumptions to ensure that passengers are assigned a higher priority than parcels: A1) Passengers have a maximum ride time; A2) a maximum number of parcels can be inserted within one passenger service; and A3) multiple passenger requests cannot be simultaneously served by one taxi. The authors developed a mixed-integer programming (MIP) model and solved instances with up to 12 requests (24 nodes) using Gurobi. Li et al. (2016a) solved large-scale instances with up to 300 requests using the ALNS metaheuristic.

Unlike in Li et al. (2014, 2016a, 2016b), in which passenger and parcel shared the same taxi capacity, Yu et al. (2018) set the vehicle capacity for each request type. They generalized the SARP by relaxing the three assumptions in Li et al. (2014). Moreover, the authors developed a simulated annealing heuristic to solve the general SARP with up to 288 requests. Later, following the assumptions of Li et al. (2014),Yu et al. (2021) studied an SARP with flexible compartments, in which passengers' capacity is considered in parcel storage, and the total capacities for passengers and parcels are fixed. They developed an MIP model and designed a mutation-based simulated annealing algorithm to solve the proposed problem. Beirigo et al. (2018) investigated an SARP model, focusing on SAVs with passenger and freight compartments, where each compartment has a fixed capacity. They relaxed assumptions A2 and A3 in Li et al. (2014) and devised an MIP model. Tholen et al. (2021) extended the model in Beirigo et al. (2018) by taking passenger and parcel capacities as decision variables. Unlike the aforementioned studies that aimed to maximize the profits of integrated passenger and parcel transportation, the authors aimed to minimize the total transportation cost, which depends on travel distance and vehicle capacity for each request type. Both Beirigo et al. (2018) and Tholen et al. (2021) solved only small instances with Gurobi.

3.2.2 Truck–drone routing problem

In a truck–drone delivery system, trucks can 1) perform deliveries in the same manner as drones and 2) serve as mobile carriers of drones, without performing the delivery themselves. Chung et al. (2020), Li et al. (2021), Macrina et al. (2020), and Otto et al. (2018) have provided a comprehensive review of truck–drone routing problems. This section focuses on the literature on the former scenario, in which trucks perform deliveries in the same manner as drones. The corresponding routing problem is classified into the traveling salesman problem with drones (TSP-D) and the vehicle routing problem with drones

(VRP-D), according to the number of trucks in the delivery system (Macrina et al., 2020). TSP-D involves only one truck, while VRP-D involves multiple trucks. The main characteristics of TSP-D and VRP-D are summarized in Table 3.1.

Table 3.1: Characteristics of TSP-D and VRP-D

		Number of trucks	Cooperation*		Synchronization	
			Y	N	Y	N
TSP-D	FSTSP	One	Drones take off from and land on the truck.		At customer locations or depot	
	PDSTSP	One		√		√
VRP-D	FSVRP	Multiple	Option 1: Drones take off from and land on the same truck. Option 2: Drones take off from a truck and land on a docking hub to travel with another truck.		At customer locations or depot	√
	PDSVRP	Multiple		√		√

* Remark
Most papers do not mention how drones take off and land. Generally, a human is needed to perform setup operations for drone launch and recovery (Otto et al., 2018).

Macrina et al. (2020) further classified TSP-D into the flying sidekick TSP (FSTSP) and the parallel drone scheduling TSP (PDSTSP). In FSTSP, the truck and the drones coordinate with other as the drones take off from and land on the truck. Truck–drone synchronization at a customer location or the depot is required. In contrast, in PDSTSP, the truck and the drone work independently, and no synchronization is required. VRP-D can be further classified into the flying sidekick VRP (FSVRP), which is a VRP-D in which trucks and drones cooperate, and the parallel drone scheduling VRP (PDSVRP), which is a VRP-D in which trucks and drones work individually. FSVRP and FSTSP differ in two aspects: cooperation and synchronization. For the first aspect, drones must return to the truck from where they took off in FSTSP, while some FSVRPs allow drones to take off from trucks but land on docking hubs serving as transfer locations for drones (Wang & Sheu, 2019) instead of at trucks. For the second aspect, FSTSP requires that the truck and drones are synchronized at customer locations or the depot, while some FSVRPs do not require synchronization in cases with docking hubs (Wang & Sheu, 2019) or allow en-route launch and rendezvous operations (Marinelli et al., 2018). Most papers do not mention how drones take off and land (i.e., autonomously or manually). Generally, a human is needed to perform setup operations for drone launch and recovery (Otto et al., 2018).

Murray and Chu (2015) first developed an MIP model to formulate an FSTSP. In their model, a single truck and a single drone cooperatively deliver parcels to customers. The drone can only take off and land at the depot or a customer location when the truck is stationary. The two vehicles wait for each other at rendezvous points. The objective of their model is to minimize the time required for both vehicles to return to the depot. The authors developed a heuristic with the idea of “truck-first, drone-second” to solve instances with 10 customers. Inspired by the work of Murray and Chu (2015), various studies emerged to study TSP-D (Agatz et al., 2018; Moshref-Javadi et al., 2020a) and VRP-D (Chiang et al., 2019; Kitjacharoenchai et al., 2020; Wang et al., 2017), considering different constraints and objective functions.

Because the problem proposed in the present study belongs to FSVRP and considers time windows, we focus on the works on FSTSP and FSVRP. Although there are numerous studies on FSTSP and FSVRP, only a few consider time windows. Table 3.2 summarizes related works on FSTSP and FSVRP with time windows. All of them require truck–drone synchronization.

In their studies on FSTSP and FSVRP considering time windows, Di Puglia Pugliese and Guerriero (2017) assumed that the time for preparing a drone for a new delivery is negligible, while the service time at each customer location is not. An MIP model was proposed, and instances with 5 and 10 nodes were solved using CPLEX. Di Puglia Pugliese et al. (2020) further compared three transportation systems for parcel delivery: truck delivery,

Table 3.2: Related works on FSTSP and FSVRP considering time windows

Reference	Variant	Launch/ recovery time	Service time	Flight range	Objective	Solution approach	Maximum no. of nodes
Di Puglia Pugliese and Guerriero (2017)	FSVRP	N	Y	Distance	Cost	CPLEX	10
Di Puglia Pugliese et al. (2020)	FSVRP	N	Y	Distance	Cost	CPLEX	15
Di Puglia Pugliese et al. (2021a)	FSVRP	Y	Y	Energy-related	Cost	Benders decomposition	15
Di Puglia Pugliese et al. (2021b)	FSVRP	N	Y	Distance	Cost	Heuristic	100
Kuo et al. (2022)	FSVRP	Y	Y	Endurance	Cost	Metaheuristic	50
Coindreau et al. (2021)	FSVRP	N	Y	Endurance	Cost	Metaheuristic	100
Luo et al. (2021)	FSTSP	Y	Y	Endurance	Cost & customer satisfaction	Metaheuristic	80
Wang et al. (2022)	FSVRP	Y	Y	Distance	Cost	Metaheuristic	200

drone delivery, and truck–drone delivery systems. The results of instances with up to 15 nodes solved by CPLEX indicated that the drone delivery system could reduce CO2 emissions by a factor of 144 compared with the truck delivery system; however, 44% of customers were not catered for. The truck–drone delivery system leveraged the advantages of drone delivery while overcoming its drawbacks. Specifically, the truck–drone delivery system could serve all customers and reduce transportation costs and CO2 emissions by 39% and 48%, respectively, compared with the truck delivery system. In addition to the service time at each customer location, Di Puglia Pugliese et al. (2021a) also considered the drone take-off and landing times. They proposed a Benders decomposition approach to solve instances with 5, 10, and 15 customers.

The previous studies developed exact methods to solve the truck–drone routing problem with time windows. Owing to computational complexity, the methods can only solve small instances. Several heuristic/metaheuristic algorithms have been proposed to solve large-scale instances. Di Puglia Pugliese et al. (2021b) extended Di Puglia Pugliese and Guerriero (2017) work by providing a two-phase heuristic embedded in a multi-start framework that can solve instances with up to 100 nodes. Kuo et al. (2022) devised a variable neighborhood search algorithm to solve the VRP-D considering time windows (VRP-DTW) with 50 customers, considering both customer service time and drone launch and recollection times. Coindreau et al. (2021) presented an ALNS algorithm for a VRP-DTW considering customer service time while neglecting drone launch and recollection times. They introduced a speed-up procedure to reduce the time consumed for each insertion process in the ALNS. Their proposed algorithm could solve instances with up to 100 customers. Wang et al. (2022) included the drone launch and recovery times into the service time and devised an iterative local search algorithm to solve VRP-DTW instances with up to 200 customers. The aforementioned studies aimed to minimize the total monetary costs of truck and drone operations. Luo et al. (2021) considered two objectives: minimizing transportation costs related to the travel distance and maximizing overall customer satisfaction related to the arrival time at each customer location. They designed a hybrid multi-objective genetic optimization approach combined with a Pareto local search algorithm, and the largest instance solved involved 80 customers.

Considering the limited drone battery capacity, Di Puglia Pugliese and Guerriero (2017), Di Puglia Pugliese et al. (2020, 2021b), and Wang et al. (2022) set a maximum distance that a drone can travel for one delivery. Di Puglia Pugliese et al. (2021a) embedded an energy consumption model into a VRP-DTW model. Coindreau et al. (2021), Kuo et al. (2022), and Luo et al. (2021) set a maximum flight endurance for drones. All of the above studies neglected the drone recharge time or assumed that the drones could be fully recharged instantly.

3.2.3 Paper contributions

The model developed in our study shares similarities with the SARP model in Li et al. (2014) and the VRP-D model in Sacramento et al. (2019). Nonetheless, our study has

several novelties, as described below.

(1) Compared with SARP, we introduce drones to cooperate with ground vehicles. This will lead to efficiency gains but also considerably increase the SARP model complexity.

(2) This study differs from the studies on VRP-D in five aspects.

   (i) In the existing VRP-D studies, the ground vehicles collect goods and originate from the depot. They only perform delivery. In our study, ground vehicles not only deliver goods from the depot to customers but also pick up and deliver passengers. Each passenger request is characterized by a pair of origin and destination nodes and time windows at these nodes.

   (ii) We introduce time window constraints into VRP-D because passengers usually have their preferred departure and arrival times, and customers can usually pick up the parcels at a specific time only.

   (iii) We assume that a drone can automatically take off from and land on DRBs. Meanwhile, the goods compartment of DRBs houses a robotic shelving system that can automatically locate and prepare goods for drone delivery and customer pick-up; this means that drone launch/recovery and DRBs' serving of a request can occur simultaneously. In contrast, existing models require the drivers to launch/recover the drone and deliver the parcel to the customers in person, and the two processes cannot happen simultaneously.

   (iv) In contrast to the literature on VRP-DTW, we consider soft time windows instead of hard time windows asssociated with each request. If a vehicle arrives at a node before its service time window, it is required to wait until the start time; otherwise, a penalty is imposed.

   (v) Most existing models can only solve large-scale instances with up to 100 nodes. In our study, the largest instance contains 200 nodes.

In conclusion, the contributions of this paper are summarized as follows:

(1) We propose a new transport system that utilizes drones and on-demand transit for the simultaneous transportation of passengers and goods.

(2) We introduce a new problem termed the passenger and parcel SARP-D, which enriches the existing studies on SARP, VRP-D, and VRP-DTW.

(3) We devise an MINP model for SARP-D. The nonlinearity originates from the possibility of the drone to take off from or land on the DRBs at a node while passengers are getting on/off or customers are picking up parcels at the same node. This leads to a nonlinear formula for computing the arrival times of DRBs and drones at each node. The MINP is then linearized to make it solvable by CPLEX for small instances.

(4) We develop an ALNS algorithm to solve the proposed problem and conduct numerical experiments to demonstrate the model properties and examine the ALNS efficiency. The largest instance solved in this study has 200 nodes.

3.3 Model formulation

3.3.1 Problem description

We consider a set of homogeneous DRBs, each containing separated and capacitated compartments for passengers and goods and equipped with a drone for goods delivery.

Owing to capacity and battery constraints, the drone only visits one customer during each flight. We assume that enough backup DRBs and drones are present at the depot so that each request can be served by one vehicle following the "depot–request location–depot" route. This is a reasonable assumption because transportation companies usually purchase sufficient vehicles to fulfill customer demands (Wang & Sheu, 2019). The task of the DRBs is to deliver goods to customers and fulfill travel requests from passengers. Each route is restricted by a maximum travel time. All goods requests have the same origin (i.e., a single depot). The parcel for each goods request is placed in a single position on the shelf inside the goods compartment of the DRBs. Considering the attributes of goods, such as weight and the suitability of the delivery location for drone landing, some goods can only be served by the DRBs, while others can be served by either a DRB or a drone. Each passenger's travel request includes origin and destination nodes and time windows at the corresponding nodes. If more than one passenger travels between the same origin and destination nodes within the same time interval, these passenger requests are combined into one, with an additional attribute indicating the number of passengers.

Both request types have a soft time window. If a vehicle arrives at a node before its earliest service time, it is required to wait until its start time. If a vehicle or drone arrives at a node after its latest service time, there is a penalty cost.

Both DRBs and drones must depart from and return to the depot at most once, either in tandem or independently. When the drone is not in service, it is transported by a DRB. The drone can be launched and retrieved at the depot or request locations when the DRB is stationary. It can be launched and recovered multiple times during a DRB route, but the launch and recovery points for a sortie (i.e., drone flight) cannot be the same. There is a setup time required to launch and retrieve a drone at the launch and recovery nodes. There is also a constant service time for each stop visited by the DRB, during which customers can pick up goods from the goods compartment and passengers can get on and off the passenger coach. As mentioned in Section 3.2.3, drone launch and recovery can occur while customers are picking up parcels or passengers are getting on/off the bus, owing to the robotic shelving system installed in the goods compartment.

We categorize all stops into five types according to the drone activities at the node, and designate the corresponding nodes as follows: (i) Stops in which no drone-related activity occurs belong to the "*common node*"; (ii) stops in which a drone is taking off belong to the "*launch node*"; (iii) stops in which a node is served by the drone belong to the "*drone service node*"; (iv) stops in which a drone is landing belong to the "*recovery node*"; and (v) stops in which a drone first lands and then takes off belong to the "*recovery–launch node*". At each node, the activities of customers/passengers and drone launch and recovery operations do not influence each other, meaning that the activities can be completed simultaneously.

To save the drone's battery, we assume that the drone can start landing immediately when the DRB arrives at the node, while the drone can start taking off immediately when or after the DRB starts catering to the service requests at the node. The launch and recovery times are longer than the service time at a node.

SARP-D aims to determine the DRB and drone routes according to the above description. The objective is to minimize the total transportation cost and penalty cost associated with the violation of time windows for serving all customers and passengers.

3.3.2 Notation

Sets

K	Set of homogeneous DRBs, $K = \{1, 2, ..., \|K\|\}$, where $\|K\|$ is the number of vehicles.
S_p^o	Set of origins of passenger requests, $S_p^o = \{1, 2, ..., \|P\|\}$, where $\|P\|$ is the number of passenger requests.
S_p^d	Set of destinations of passenger requests, $S_p^d = \{\|P\| + 1, \|P\| + 2, ..., 2\|P\|\}$.
S_p	Set of passenger stops, $S_p = S_p^o \cup S_p^d$.
S_g	Set of goods stops (destinations), $S_g = \{2\|P\| + 1, 2\|P\| + 2, ..., 2\|P\| + \|G\|\}$, where $\|G\|$ is the number of parcel requests.
$S_g{}'$	$S_g{}' \subseteq S_g$, set of parcel requests that can be delivered by a drone.
S	Set of passenger and goods stops, $S = S_p \cup S_g$.
N	Set of all nodes, $N = S_p \cup S_g \cup \{0, 2\|P\| + \|G\| + 1\}$, where 0 and $2\|P\|+\|G\|+1$ are the depot nodes indicating the start and end nodes of a route.
N_0	Set of nodes from which a DRB may depart, $N_0 = \{0, 1, ..., 2\|P\| + \|G\|\}$.
N_+	Set of nodes to which a DRB may arrive, $N_+ = \{1, 2, ..., 2\|P\| + \|G\| + 1\}$.
$\Delta^+(i)$	Set of nodes reachable from node $i \in N_0$, $\Delta^+(i) = N_+ \setminus \{i\}$.
$\Delta^-(i)$	Set of nodes that can be used to reach node $i \in N_+$, $\Delta^-(i) = N_0 \setminus \{i\}$.

Parameters

Cap^P	Capacity of the passenger compartment of a DRB.
Cap^G	Capacity of the goods compartment of a DRB.
T_{ij}^V	Time required for a DRB to travel from node $i \in N_0$ to node $j \in N_+$.
T_{ij}^D	Time required for a drone to travel from node $i \in N_0$ to node $j \in N_+$.
E	Maximum flight duration of a drone.
ST_i^V	Service time for a DRB at node $i \in S$.
ST_i^D	Service time for a drone at node $i \in S_g{}'$.
Q_i	Number of passengers boarding a DRB at node $i \in S$. $Q_{i+\|P\|} = -Q_i, \forall i \in S_p^o$ and $Q_i = 0, \forall i \in S_g$.
$T_{\max}$	Maximum travel time on a DRB route.
C_{ij}^V	Transportation cost for a DRB traveling from node $i \in N_0$ to node $j \in N_+$.
C_{ij}^D	Transportation cost for a drone flying from node $i \in N_0$ to node $j \in N_+$.
$[E_i, L_i]$	The earliest and latest service start times at node $i \in S$.
SL	Setup time required to launch a drone.
SR	Setup time required to retrieve a drone.
α_i	Unit delay penalty at node $i \in S$.
η	Maximum intermediate stops between the origin and destination of a passenger request.

Decision Variables

x_{ij}^k	$x_{ij}^k = 1$ if DRB $k \in K$ travels from node $i \in N_0$ to node $j \in N_+$; otherwise, $x_{ij}^k = 0$.
y_{ajb}^k	$y_{ajb}^k = 1$ if sortie $< a, j, b >$ is used in the route of DRB $k \in K$, where $a \in N_0$ represents the launch node of the drone, $j \in S_g{}'$ represents the goods request served by the drone, $b \in N_+$ represents the rendezvous node of the drone; otherwise, $y_{ajb}^k = 0$.
w_i^k	Load of the passenger compartment of DRB $k \in K$ after the visitation of node $i \in S$.

t_j^k	If node $j \in N_+$ is a recovery node or recovery-launch node, t_j^k is the time point at which the drone is recovered by DRB $k \in K$ at node $j \in N_+$; otherwise, t_j^k is the arrival time of DRB $k \in K$ at node $j \in N$ or the arrival time of drone $k \in K$ at node $j \in {S_g}'$.
${t'}_j^k$	If node $j \in S$ is a recovery node, ${t'}_j^k$ is the time point at which DRB $k \in K$ leaves node $j \in S$; if node $j \in S$ is a launch node or recovery-launch node, ${t'}_j^k$ is the time point at which drone $k \in K$ starts taking off; otherwise, ${t'}_j^k$ is the time point at which DRB $k \in K$ starts service at node $j \in S$ or drone $k \in K$ starts service at node $j \in {S_g}'$.
u_i^k	A continuous variable indicating the position of node $i \in N$ in the route of DRB $k \in K$.
p_{ij}^k	$p_{ij}^k = 1$ if node $j \in S$ is visited after node $i \in N_0$ in the route of DRB $k \in K$.
v_a^k	Binary auxiliary variable for linearization.
λ_a^k	Delay of DRB/drone $k \in K$ at node $a \in S$.

3.3.3 Formulation

In this section, SARP-D is modeled as an MINP model and then linearized. The constraints are categorized into three groups:

(i) routing and flow constraints (constraints 3.2–3.16 and 3.29–3.36);

(ii) scheduling and synchronization constraints (constraints 3.17–3.28);

(iii) decision variable domain constraints (constraints 3.37–3.40).

$$\min \sum_{k \in K} \left[\sum_{i \in N_0} \sum_{j \in \Delta^+(i)} C_{ij}^V x_{ij}^k + \sum_{c \in {S_g}'} \sum_{a \in \Delta^-(c)} \sum_{b \in \Delta^+(c), b \neq a} \left(C_{ac}^D + C_{cb}^D \right) y_{acb}^k + \sum_{m \in S} \alpha_m \lambda_m^k \right] \tag{3.1}$$

s.t.

$$\sum_{i \in \Delta^-(j)} \sum_{k \in K} x_{ij}^k = 1, \forall j \in S_p^o \cup \left(S_g \backslash {S_g}' \right) \tag{3.2}$$

$$\sum_{i \in \Delta^-(j)} x_{ij}^k = \sum_{i \in \Delta^-(j+|P|)} x_{i,j+|P|}^k, \forall j \in S_p^o, k \in K \tag{3.3}$$

$$\sum_{i \in \Delta^-(j)} \sum_{k \in K} x_{ij}^k + \sum_{a \in \Delta^-(j)} \sum_{b \in \Delta^+(j), b \neq a} \sum_{k \in K} y_{ajb}^k = 1, \forall j \in {S_g}' \tag{3.4}$$

$$\sum_{j \in N_+} x_{0j}^k \leq 1, \forall k \in K \tag{3.5}$$

$$\sum_{j \in N_0} x_{j,2|P|+|G|+1}^k \leq 1, \forall k \in K \tag{3.6}$$

$$x_{0,2|P|+|G|+1}^k = 0, \forall k \in K \tag{3.7}$$

$$\sum_{i \in \Delta^-(j)} x_{ij}^k = \sum_{i \in \Delta^+(j)} x_{ji}^k, \forall j \in S, k \in K \tag{3.8}$$

$$w_0^k = 0, \forall k \in K \tag{3.9}$$

$$w_j^k \geq w_i^k + Q_j - \left(1 - x_{ij}^k\right) M, \forall i \in N_0, j \in S \backslash \{i\}, k \in K \tag{3.10}$$

$$\max\{0, Q_i\} \leq w_i^k \leq \min\left\{Cap^P, Cap^P + Q_i\right\}, \forall i \in S, k \in K \tag{3.11}$$

$$\sum_{i \in N_0} \sum_{j \in S_g, j \neq i} x_{ij}^k + \sum_{c \in S_g{}'} \sum_{a \in \Delta^-(c)} \sum_{b \in \Delta^+(c), b \neq a} y_{acb}^k \leq Cap^G, \forall k \in K \tag{3.12}$$

$$\sum_{j \in S_g{}', j \neq a} \sum_{b \in \Delta^+(j), b \neq a} y_{ajb}^k \leq 1, \forall a \in N_0, k \in K \tag{3.13}$$

$$\sum_{j \in S_g{}', j \neq b} \sum_{a \in \Delta^-(j), a \neq b} y_{ajb}^k \leq 1, \forall b \in N_+, k \in K \tag{3.14}$$

$$2y_{ajb}^k \leq \sum_{h \in \Delta^+(a)} x_{ah}^k + \sum_{l \in \Delta^-(b)} x_{lb}^k, \forall a \in N_0, j \in \left\{S_g{}' : j \neq a\right\}, b \in \left\{\Delta^+(j) : b \neq a\right\}, k \in K \tag{3.15}$$

$$y_{0,j,2|P|+|G|+1}^k = 0, \forall j \in S_g{}', k \in K \tag{3.16}$$

$$t_0^k = 0, \forall k \in K \tag{3.17}$$

$$t_{2|P|+|G|+1}^k \leq T_{\max} \sum_{i \in N_0} x_{i,2|P|+|G|+1}^k, \forall k \in K \tag{3.18}$$

$$t'^k_a \geq t_a^k, a \in N, k \in K \tag{3.19}$$

$$t'^k_0 + T_{0b}^V + SL \sum_{h \in S_g{}'} \sum_{l \in \Delta^+(h)} y_{0hl}^k + SR \sum_{g \in S_g{}', g \neq b} \sum_{f \in \Delta^-(g), f \neq b} y_{fgb}^k \leq t_b^k + T_{\max}\left(1 - x_{0b}^k\right), \forall b \in N_+, k \in K \tag{3.20}$$

$$t'^k_a + T_{ab}^V + \max\left(1 - \sum_{\substack{h \in S_g{}' \\ h \neq a}} \sum_{\substack{l \in \Delta^+(h) \\ l \neq a}} y_{ahl}^k - \sum_{\substack{n \in S_g{}' \\ n \neq a}} \sum_{\substack{m \in \Delta^-(n) \\ m \neq a}} y_{mna}^k, 0\right) ST_a^V + SL \sum_{\substack{h \in S_g{}' \\ h \neq a}} \sum_{\substack{l \in \Delta^+(h) \\ l \neq a}} y_{ahl}^k + SR \sum_{\substack{g \in S_g{}' \\ g \neq b}} \sum_{\substack{f \in \Delta^-(g) \\ f \neq b}} y_{fgb}^k \leq t_b^k + T_{\max}\left(1 - x_{ab}^k\right), \forall a \in S, b \in \Delta^+(a), k \in K \tag{3.21}$$

$$t'^k_i + T_{ij}^D + SL - T_{\max}\left(1 - \sum_{b \in \Delta^+(j), b \neq i} y_{ijb}^k\right) \leq t_j^k, \forall j \in S_g{}', i \in \Delta^-(j), k \in K \tag{3.22}$$

$$t'^k_j + T_{jb}^D + ST_j^D + SR - T_{\max}\left(1 - \sum_{a \in \Delta^-(j), a \neq b} y_{ajb}^k\right) \leq t_b^k, \forall j \in S_g{}', b \in \Delta^+(j), k \in K \tag{3.23}$$

$$\lambda_b^k \geq \left(t'^k_0 + T_{0b}^V + SL \sum_{h \in S_g{}'} \sum_{l \in \Delta^+(h)} y_{0hl}^k - T_{\max}\left(1 - x_{0b}^k\right) - L_b\right)^+, \forall b \in S, k \in K \tag{3.24}$$

$$\lambda_b^k \geq \left(\begin{array}{l} t'^k_a + T_{ab}^V + \max\left(1 - \sum_{\substack{h \in S_g{}' \\ h \neq a}} \sum_{\substack{l \in \Delta^+(h) \\ l \neq a}} y_{ahl}^k - \sum_{\substack{n \in S_g{}' \\ n \neq a}} \sum_{\substack{m \in \Delta^-(n) \\ m \neq a}} y_{mna}^k, 0\right) ST_a^V \\ + SL \sum_{\substack{h \in S_g{}' \\ h \neq a}} \sum_{\substack{l \in \Delta^+(h) \\ l \neq a}} y_{ahl}^k - T_{\max}\left(1 - x_{ab}^k\right) - L_b \end{array}\right)^+, \tag{3.25}$$

$$\forall a \in S, b \in \Delta^+(a), k \in K$$

$$\lambda_j^k \geq \left({t'}_i^k + T_{ij}^D + SL - T_{\max} \left(1 - \sum_{b \in \Delta^+(j), b \neq i} y_{ijb}^k \right) - L_j \right)^+, \forall j \in {S_g}', i \in \Delta^-(j), k \in K \tag{3.26}$$

$$t'^k_a - ST_a^V \sum_{n \in {S_g}', n \neq a} \sum_{m \in \Delta^-(n), m \neq a} y_{mna}^k \geq E_a, \forall a \in S, k \in K \tag{3.27}$$

$$t_b^k - {t'}_a^k \leq E + T_{\max} \left(1 - \sum_{j \in {S_g}', j \neq a, j \neq b} y_{ajb}^k \right), \forall a \in N_0, b \in \Delta^+(a), k \in K \tag{3.28}$$

$$1 - M\left(1 - x_{ij}^k\right) \leq u_j^k - u_i^k, \forall i \in N_0, j \in \Delta^+(i), k \in K \tag{3.29}$$

$$u_j^k - u_i^k \leq 1 - M\left(x_{ij}^k - 1\right), \forall i \in N_0, j \in \Delta^+(i), k \in K \tag{3.30}$$

$$u_j^k \leq M \sum_{i \in \Delta^-(j)} x_{ij}^k, \forall j \in N_+, k \in K \tag{3.31}$$

$$u_j^k - u_i^k \leq M p_{ij}^k, \forall i \in N_0, j \in S \backslash \{i\}, k \in K \tag{3.32}$$

$$u_j^k - u_i^k \geq M(p_{ij}^k - 1) + 1, \forall i \in N_0, j \in S \backslash \{i\}, k \in K \tag{3.33}$$

$$t_b^k - T_{\max} \left(3 - \sum_{j \in {S_g}'} y_{ajb}^k - \sum_{\substack{m \in {S_g}', m \neq l \\ m \neq a, m \neq b}} \sum_{\substack{n \in \Delta^+(m) \\ n \neq a, n \neq b}} y_{lmn}^k - p_{al}^k \right) \leq t_l^k, \tag{3.34}$$
$$\forall k \in K, a \in N_0, b \in N_+, l \in S \backslash \{a, b\}$$

$$u_{i+|P|}^k - u_i^k \geq 0, \forall i \in S_p^o, k \in K \tag{3.35}$$

$$u_{i+|P|}^k - u_i^k - 1 \leq \eta, \forall i \in S_p^o, k \in K \tag{3.36}$$

$$x_{ij}^k \in \{0, 1\}, \forall i \in N_0, j \in \Delta^+(i), k \in K \tag{3.37}$$

$$y_{ajb}^k \in \{0, 1\}, \forall k \in K, a \in N_0, j \in \left\{ {S_g}' : j \neq a \right\}, b \in \left\{ \Delta^+(j) : b \neq a \right\} \tag{3.38}$$

$$u_i^k, t_i^k, {t'}_i^k \geq 0, \forall i \in N, k \in K \tag{3.39}$$

$$p_{ij}^k \in \{0, 1\}, \forall i \in N_0, j \in S \backslash \{i\}, k \in K \tag{3.40}$$

Objective function (3.1) minimizes the sum of transportation costs and the penalty cost of time window violation for serving all passenger and goods requests.

Constraints (3.2) ensure that each pick-up point of passengers and each goods delivery point that can only be served by DRBs (i.e.,$S_g \backslash S_g'$) are visited by DRBs exactly once. Constraints (3.3) ensure that whenever the pick-up point of a passenger is visited, the corresponding drop-off point is also visited. The constraints also ensure that the pick-up and delivery points of a passenger request are served by the same DRB. Constraints

(3.4) ensure that the delivery points of goods that can be served by drones are visited exactly once, either by a DRB or a drone. Constraints (3.5) ensure that all DRBs depart from the depot at most once, and constraints (3.6) ensure that all DRBs return to the depot at most once. Constraints (3.7) prohibit travel between depots. Constraints (3.8) ensure flow conservation. Constraints (3.9) ensure that the DRB leaves the depot with no passengers. Constraints (3.10) update the passenger load of the DRB, and constraints (3.11) ensure that the DRB load does not exceed the passenger capacity. Constraints (3.12) ensure that for one DRB route, the amount of goods served by the DRB or the drone carried by the DRB does not exceed the capacity of the DRB's goods compartment. Constraints (3.13) ensure that the drone can be launched at most once in each location. Constraints (3.14) ensure that the drone can be recovered at most once in each location. Constraints (3.15) ensure that if a drone carried by DRB $k \in K$ is launched from node $a \in N_0$, visits node $j \in \{S_g{}' : j \neq a\}$, and is recovered at node $b \in \{\Delta^+(j) : b \neq a\}$, the DRB must visit both nodes a and b. Constraints (3.16) prohibit the drone from launching from the depot, serving a single customer, and returning to the depot because under this condition, no cooperation exists between the drone and a DRB, which is not within the scope of this study. Constraints (3.17) indicate that DRB $k \in K$ and its drone are ready at the depot at time 0. Constraints (3.18) limit the maximum travel time of a route. Constraints (3.19) regulate the relationship between t_j^k and t'^k_j. Given node b visited by a DRB and its preceding node a visited by the same DRB, if node b is designated for drone retrieval, constraints (3.20) and (3.21) ensure that the time point at which the drone is retrieved is later than the sum of the time point at which the corresponding vehicle finishes all tasks (including serving a passenger/goods request and launching and/or retrieving a drone) at node a, the time required for the vehicle to travel between nodes a and b, and the drone recovery duration. If node b does not have a recovery task, constraints (3.20) and (3.21) ensure that the arrival time of the vehicle at node b is later than the sum of the time point at which the corresponding vehicle finishes all tasks (including serving a passenger/goods request and launching and/or retrieving a drone) at node a and the travel time between nodes a and b. If node a is the depot, constraints (3.20) are applied; otherwise, constraints (3.21) are applied. Constraints (3.22) ensure that the arrival time of a drone at its service node is later than the sum of the time point at which the drone takes off at the launch node, the time required for launching, and the travel time between the launch and service nodes. Constraints (3.23) ensure that the time point at which a drone is retrieved at the recovery node is later than the sum of the time point at which the drone starts its service, the customer service duration, the travel time between the service and recovery nodes, and the drone recovery duration. Constraints (3.24) and (3.25) calculate the delay of the DRB at its first visited node and other nodes, respectively. Constraints (3.26) calculate the delay of drones at each drone service node. Constraints (3.27) ensure that the vehicle can only start service after the earliest service start time. Constraints (3.28) ensure the drone flight time does not exceed the battery's endurance time. Constraints (3.29) to (3.33) define the position of each node that DRB $k \in K$ visits and eliminate the sub-tours of DRBs. Constraints (3.34) prohibit new launches while the drone is already performing a delivery task. Constraints (3.35) ensure that a DRB visits the origin of passenger request i before its destination. Constraints (3.36) state that the DRB can stop at most η times during a passenger request service. Constraints (3.37) to (3.40) are the definitional constraints for the decision variables. Constraints (3.21) and (3.25) are nonlinear. To linearize them, we introduce a binary auxiliary variable υ_a^k. Constraints (3.41) to (3.44) are introduced to replace constraints (3.21). Constraints (3.42) to (3.46) are introduced to replace constraints (3.25).

$$t_a^k + T_{ab}^V + \upsilon_a^k ST_a^V + SL \sum_{\substack{h \in S_g{}' \\ h \neq a}} \sum_{\substack{l \in \Delta^+(h) \\ l \neq a}} y_{ahl}^k + SR \sum_{\substack{g \in S_g{}' \\ g \neq b}} \sum_{\substack{f \in \Delta^-(g) \\ f \neq b}} y_{fgb}^k \leq t_b^k + T_{\mathsf{max}}(1 - x_{ab}^k), \forall a \in S, b \in \Delta^+(a), k \in K \tag{3.41}$$

$$\upsilon_a^k \geq 1 - \sum_{\substack{h \in S_g{}' \\ h \neq a}} \sum_{\substack{l \in \Delta^+(h) \\ l \neq a}} y_{ahl}^k - \sum_{\substack{n \in S_g{}' \\ n \neq a}} \sum_{\substack{m \in \Delta^-(n) \\ m \neq a}} y_{mna}^k, \forall a \in S, k \in K \tag{3.42}$$

$$\upsilon_a^k \leq 1 - \frac{1}{2} \left(\sum_{\substack{h \in S_g{}' \\ h \neq a}} \sum_{\substack{l \in \Delta^+(h) \\ l \neq a}} y_{ahl}^k + \sum_{\substack{n \in S_g{}' \\ n \neq a}} \sum_{\substack{m \in \Delta^-(n) \\ m \neq a}} y_{mna}^k \right), \forall a \in S, k \in K \tag{3.43}$$

$$\upsilon_a^k \in \{0, 1\}, \forall a \in S, k \in K \tag{3.44}$$

$$\lambda_b^k \geq t'^k_a + T_{ab}^V + \upsilon_a^k ST_a^V + SL \sum_{\substack{h \in S_g{}' \\ h \neq a}} \sum_{\substack{l \in \Delta^+(h) \\ l \neq a}} y_{ahl}^k - T_{\mathsf{max}}(1 - x_{ab}^k) - L_b, \forall a \in S, b \in \Delta^+(a), k \in K \tag{3.45}$$

$$\lambda_b^k \geq 0, \forall b \in S, k \in K \tag{3.46}$$

3.4 ALNS

To solve SARP-D, an ALNS metaheuristic is proposed. The ALNS was first introduced by Ropke and Pisinger (2006). It has been widely used and has shown high performance in various VRP variants. In this section, we present the ALNS framework and introduce the destroy and repair methods and the proposed time slack strategy.

3.4.1 The ALNS framework

Let s and s^* denote the current and best solutions, respectively. s is initialized via the repair method R0 described in Section 3.4.3 (Line 1) and set as the current best solution (Line 2). The ALNS improves the best solution s^* by repeatedly generating a new solution s' by destroying and repairing the current solution (Lines 8–29). Let Ω^- and Ω^+ respectively denote the sets of destroy methods, which eliminate part of the current solution, and repair methods, which rebuild the partial solution to a feasible solution. In each iteration, one destroy method $d \in \Omega^-$ and one repair method $r \in \Omega^+$ are selected (Line 9) via the roulette wheel selection method. Let ϖ_d^- (ϖ_r^+) denote the weights of the destroy (repair) method $d \in \Omega^-$ ($r \in \Omega^+$). The probabilities of selecting a destroy and a repair method are calculated as (3.47) and (3.48), respectively.

$$prob_d = \frac{\varpi_d^-}{\sum_{a \in \Omega^-} \varpi_a^-}, \forall d \in \Omega^- \tag{3.47}$$

Algorithm 1 ALNS

Input: Initial temperature T_0; score σ; cooling parameter β; reaction factor ρ; maximum non-improvement iterations to set the best solution as the current solution: $s \leftarrow s^* : noImp^{\max}$.

1 Current solution $s \leftarrow InitialSolution()$.
2 Best solution $s^* \leftarrow s$.
3 The number of non-improvement iterations $noImp \leftarrow 0$.
4 Current temperature $T \leftarrow T_0$.
5 $\varpi^-, \varpi^+ \leftarrow InitialWeights()$.
6 $o^-, o^+ \leftarrow InitialOperationTimes()$.
7 $\xi^-, \xi^+ \leftarrow InitialScores()$.
8 **While the** *stop criteria are not met*, **do**
9 Choose a destroy method d and a repair method r from the destroy method set Ω^- and the repair method set Ω^+ according to $\varpi^- = \{\varpi_d^-\}_{d\in\Omega^-}$ and $\varpi^+ = \{\varpi_r^+\}_{r\in\Omega^+}$, respectively.
10 Generate the new solution $s' \leftarrow r(d(s))$
11 **If** $f(s') < f(s^*)$, **then**
12 $s^* \leftarrow s'$
13 $s \leftarrow s'$
14 $noImp \leftarrow 0$
15 **Else**
16 $noImp \leftarrow noImp + 1$
17 **If** $noImp \le noImp^{\max}$, **then**
18 **If** $Random(0,1) < \exp\left(\left(f(s) - f(s')\right)/T\right)$, **then**
19 $s \leftarrow s'$
20 **Else**
21 $s \leftarrow s^*$
22 $o^- \leftarrow UpdateOperationTimes(d)$; $o^+ \leftarrow UpdateOperationTimes(r)$
23 $\xi^- \leftarrow UpdateScores(\sigma, d)$; $\xi^+ \leftarrow UpdateScores(\sigma, r)$
24 $T \leftarrow \beta T$
25 **If** the *update criterion is met*, **then**
26 $\varpi^- \leftarrow UpdateWeights(\xi^-, o^-, \rho)$; $\varpi^+ \leftarrow UpdateWeights(\xi^+, o^+, \rho)$
27 $o^-, o^+ \leftarrow ResetOperationTimes()$
28 $\xi^-, \xi^+ \leftarrow ResetScores()$
29 **Return** s^*

$$prob_r = \frac{\varpi_r^+}{\sum_{a\in\Omega^+} \varpi_a^+}, \forall r \in \Omega^+ \tag{3.48}$$

At the start of the metaheuristic, the weights of each destroy method and repair method are initialized to 1 (Line 5). When the update criterion is met, the values of the weights will

be updated according to $o^- = \{o_d^-\}_{d\in\Omega^-}$ and $o^+ = \{o_r^+\}_{r\in\Omega^+}$, which represents the sets of the number of times that the destroy and repair methods are selected, and $\xi^- = \{\xi_d^-\}_{d\in\Omega^-}$ and $\xi^+ = \{\xi_r^+\}_{r\in\Omega^+}$, which denote the sets of accumulated scores of destroy and repair methods. Each element in the above four sets is initialized to 0 (Lines 6–7) and updated after each iteration.

Specifically, after each iteration, the usage frequencies of the destroy method $o_d^-, \forall d \in \Omega^-$ and the repair method $o_r^+, \forall r \in \Omega^+$ are increased by 1 (Line 22). The accumulated scores of the selected destroy method $\xi_d^-, \forall d \in \Omega^-$ and repair method $\xi_r^+, \forall r \in \Omega^+$ are increased by the same score σ (Line 23). In each iteration, there are four preset values for σ to be chosen from: σ_1, σ_2, σ_3, and σ_4, depending on the quality of the newly generated solution for the iteration under consideration. We explain how to choose the σ value later.

The selected destroy and repair methods are sequentially applied to the current solution to generate a new solution s' (Line 10); however, the newly generated solution may not always be accepted. The simulated annealing acceptance criterion is adopted to avoid being stuck in a local optimum. Specifically, when the number of non-improvement iterations is less than or equal to a predefined number $noImp^{\max}$(Lines 11–19), we accept the new solution s' and set it as the current solution s with a probability $p(s', s)$ computed as

$$p(s', s) = \min\left\{1, \exp\left(\frac{(f(s) - f(s'))}{T}\right)\right\} \tag{3.49}$$

where T is the current temperature, which starts at T_0 and decreases after each iteration according to the expression $T = \beta T$, where $\beta \in (0, 1)$ is a cooling parameter (Line 24). If the number of non-improvement iterations is greater than $noImp^{\max}$, we set the best solution at hand s^* as the current solution s (Lines 20–21). The σ value is selected according to the quality of the newly generated solution s'. If s' results in a global best solution, then $\sigma = \sigma_1$. Otherwise, if s' is accepted and better than the current solution s, then $\sigma = \sigma_2$; if s' is accepted but worse than the current solution s, then $\sigma = \sigma_3$; if s' is rejected, then $\sigma = \sigma_4$. The four values, i.e., $\sigma_1, \sigma_2, \sigma_3$, and σ_4, can be tuned in the metaheuristic. In Ropke and Pisinger (2006), the default setting was $\sigma_1 = 33$, $\sigma_2 = 9$, $\sigma_3 = 13$, and $\sigma_4 = 0$.

The entire search is divided into several segments, where a segment is a certain number of iterations $iter^{seg}$. At the end of each segment, the weights of the destroy and repair methods are updated according to equations (3.50) and (3.51).

$$\varpi_d^- \leftarrow \rho\varpi_d^- + (1-\rho)\frac{\xi_d^-}{o_d^-}, \forall d \in \Omega^- \tag{3.50}$$

$$\varpi_r^+ \leftarrow \rho\varpi_r^+ + (1-\rho)\frac{\xi_r^+}{o_r^+}, \forall r \in \Omega^+ \tag{3.51}$$

where $\rho \in [0, 1]$ is a reaction factor controlling the degree of change in weights. The accumulated scores and the number of times each destroy or repair operator is selected are reset to 0 (Lines 25–28).

The two termination criteria for the ALNS metaheuristic are as follows: the maximum number of iterations $iter^{stop}$ is reached and the maximum number of iterations in which the best solution is not improved $noImp^{stop}$ is reached. The algorithm stops and outputs the best solution when either criterion is met.

3.4.2 Destroy methods

In each iteration, the selected destroy method removes a certain number of requests δ from the current solution. The number is set as

$$\delta \in \{\min(r_{\min}, \max(1, r_{low}(|P| + |G|))), \min(r_{\max}, \max(1, r_{up}(|P| + |G|)))\}.$$

r_{low} and r_{up} are the lowest and highest ratios to control the percentage of requests to be removed, respectively. $r_{\min}$ and $r_{\max}$ are the absolute upper bounds of the minimum and maximum numbers of requests that can be removed, respectively; these parameters ensure that the number of removed requests δ is reasonable for very large instances (Sacramento et al., 2019). The absolute lower bounds on the minimum and maximum numbers of removed requests are set to 1 in the case of very small instances.

We propose four removal operators. For ease of explanation, the following notation is used in this subsection. Given a request req, let $O(req)$ and $D(req)$ denote the origin and destination of req. If req is a goods request, $O(req)$ is the depot. d_{ij} is the DRB travel distance between nodes i and j. For all removal methods, the actual number of removed requests when removing a selected request req could be more than one, such as between two and five, depending on the type of selected request and the nature of the stop(s) of the selected request. If request req is a goods request, we only need to check the type of node $D(req)$. If $D(req)$ has launch or recovery tasks, the corresponding goods request served by the drone should be removed. If request req is a passenger request, the type of its origin node $O(req)$ and destination node $D(req)$ should be checked. Similarly, if $O(req)$ or $D(req)$ is associated with a launch or recovery task, the corresponding goods request served by the drone should also be removed.

D0) **Random removal**

This method randomly removes requests from the current solution until δ requests are removed.

D1) **Worst removal**

Given a request req in a current solution s, the insertion cost of request req is defined as $InsCost\left(req, s\right) = f\left(s\right) - f_{-req}\left(s\right)$, where $f_{-req}(s)$ is the objective value of solution s without request req. The worst removal method repeatedly removes the request with the largest insertion cost $InsCost\left(req, s\right)$ until δ requests are removed.

D2) **Shaw removal**

This method was proposed by Shaw (1998). The idea is to remove requests that are similar in certain aspects. The similarity between requests req and req', denoted as $R\left(req, req'\right)$, is measured according to the following equation:

$$R\left(req, req'\right) = \varphi_1\left(d_{O(req),O(req')} + d_{D(req),D(req')}\right) + \varphi_2\left(|T_{O(req)} - T_{O(req')}| + |T_{D(req)} - T_{D(req')}|\right) + \varphi_3\left(|W_{req} - W_{req'}|\right) + \varphi_4 k_{req,req'} \tag{3.52}$$

where T_i is the service start time of the vehicle at node i; W_{req} is the number of passengers/goods included in request req; and $k_{req,req'} = -1$ if requests req and req' are in the same route; otherwise, $k_{req,req'} = 1$; φ_1, φ_2, φ_3, and φ_4 are weights associated with the four terms. d_{ij}, T_i, and W_{req} are normalized. The smaller the $R\left(req, req'\right)$ value, the higher the similarity between requests req and req'. The Shaw removal method first randomly chooses a request req from the current solution s and then selects the request $req^* = \arg\min_{req' \in \overline{Req}}\{R\left(req, req'\right)\}$ to remove, where $\overline{Req}$ denotes the requests in the current solution s. The two steps are repeated until δ requests are removed.

D3) **Nearest removal**

In this method, the request req to be removed is randomly selected. If request req is a goods request, the node $i^* = \arg\min_{i \in \overline{N}} \{d_{D(req),i}\}$ is determined, where $\overline{N}$ denotes the nodes in the current solution s. Then, the req's nearest request req' whose origin or destination node is i^* is removed. If request req is a passenger request, nodes $i_1^* = \arg\min_{i \in \overline{N}} \{d_{O(req),i}\}$ and $i_2^* = \arg\min_{i \in \overline{N}} \{d_{D(req),i}\}$ are determined. If $d_{O(req),i_1^*} \leq d_{D(req),i_2^*}$, the req's nearest request req' whose origin or destination node is i_1^* is removed. Otherwise, the req's nearest request req' whose origin or destination node is i_2^* is removed. The two steps are repeated until δ requests are removed.

3.4.3 Repair methods

The repair methods rebuild a solution by inserting removed requests into the current partial solution. Five customized repair methods are developed. Not all repair methods ensure a feasible solution. We explain which repair methods may produce an infeasible solution and how to deal with the infeasible solution after the introduction of all of the repair methods.

The following notations are used in this section. Given a request req, the cost of inserting request req into solution s in route rt at position pos is defined as $InsCost\,(req, s, rt, pos) = f\,(req, s, rt, pos) - f\,(req, s)$, where $f\,(req, s, rt, pos)$ is the objective value of solution s with request req in route rt at position pos, and $f\,(req, s)$ is the objective value of solution s with request req in its current position[6]. If req is not in solution s, $f\,(req, s)$ is the objective value of solution s without request req. Route rt refers to a DRB route. If request req is a passenger request, pos represents the combination of the positions of both the origin and destination nodes of req, and it can only be in a DRB route; if request req is a goods request, pos could be the position of the delivery point of req in a DRB route or in a drone sortie described by a tuple <launch node, delivery point of req, recovery node>. $RemovedSet$ is the set containing all removed requests in the previous destroy step. $RouteSet$ is the set containing all routes in solution s. $DRBPositionSet$ is the set containing all positions in the DRB route in route rt. $DinRSet$ is the set containing goods requests that can be served by drones but is now assigned to a DRB route. $SortieSet$ is the set containing all possible sorties for request req in route rt. If req is a passenger request or goods request not eligible for drone service, the corresponding $SortieSet$ is empty.

R0) **Greedy DRB-first drone-second repair method**

This repair method consists of two phases.

In the first phase, request req^* is repeatedly inserted into route rt^* in solution s at position pos^*, where

$$(req^*, rt^*, pos^*) = \arg\min_{\substack{req \in RemovedSet, rt \in RouteSet, \\ pos \in DRBPositionSet}} \{InsCost\,(req, s, rt, pos)\}.$$

After the insertion of one request into the solution, $RemovedSet$, $RouteSet$,$DinRSet$, $DRBPositionSet$, $SortieSet$, and s are updated. This phase stops until all requests have been inserted into DRB routes.

[6] In the second phase of repair methods R0 and R1, a goods request eligible for drone service may be moved from its current position (in a DRB route) to a new position (a drone sortie). "Inserting" a request means either adding a request from the removed request set to a current solution or moving a request already existing in the current solution from its current position to a new position.

In the second phase, the minimum insertion cost of moving a goods request that drones can serve from its current position in a DRB route to a drone sortie is checked. If the cost is less than 0, then request $dreq^*$ will be inserted into a sortie $dpos^*$ in route drt^* in solution s, where

$$(dreq^*, drt^*, dpos^*) = \arg\min_{\substack{req \in DinRSet, rt \in RouteSet, \\ pos \in SortieSet}} \{InsCost\,(req, s, rt, pos)\}\,.$$

Subsequently, solution s and sets $RouteSet$,$DinRSet$, $DRBPositionSet$, and $SortieSet$ are updated. If the corresponding request at the launch or recovery node of request $dreq^*$ is eligible for drone service, the request(s) at the launch or recovery node will be removed from $DinRSet$. This procedure is repeated until $DinRSet$ is empty or

$$\min_{\substack{req \in DinRSet, rt \in RouteSet, \\ pos \in SortieSet}} \{InsCost\,(req, s, rt, pos)\} \geq 0.$$

Putting all requests in the removed request set $RemovedSet$, we use R0 to construct the initial solution.

R1) **Regret DRB-first drone-second repair method**

Repair method R1 involves two phases similar to R0. The difference is that in each phase of R1, we use the 2-regret criterion to select requests to operate. That is, we insert the request with the largest regret value at the best position in solution s. The regret value represents the difference in the costs associated with inserting a request into the best and second-best positions. Let $InsCost\,(req, s, rt^*, pos^*)$ and $InsCost\,(req, s, rt^{**}, pos^{**})$ denote the insertion cost of inserting req into the best and the second-best positions in solution s, respectively. The regret value of req in solution s is calculated as

$$reg\,(req, s) = InsCost\,(req, s, rt^*, pos^*) - InsCost\,(req, s, rt^{**}, pos^{**})\,.$$

R2) **Best insertion repair method**

This method involves the sequential insertion of request req from $RemovedSet$ into route rt^* in solution s at position pos^*, where

$$(rt^*, pos^*) = \arg\min_{\substack{rt \in RouteSet, \\ pos \in DRBPositionSet \cup SortieSet}} \{InsCost\,(req, s, rt, pos)\}\,.$$

Sets $RouteSet$, $DRBPositionSet$, $SortieSet$, and $RemovedSet$, and solution s are updated after each insertion.

R3) **Balanced best insertion repair method**

The balanced best insertion repair method aims to generate a relatively balanced solution in which each route has a similar objective value. This method involves the sequential insertion of request req from $RemovedSet$ into route $rt_{\min}$, a non-empty route with the minimum objective value, and the insertion position pos^* is determined as

$$pos^* = \arg\min_{pos \in DRBPositionSet \cup SortieSet} \{InsCost\,(req, s, rt_{\min}, pos)\}\,.$$

Sets $RouteSet$, $DRBPositionSet$, $SortieSet$, and $RemovedSet$, and solution s are updated after each insertion.

R4) **Nearest best insertion repair method**

The nearest best insertion repair method attempts to sequentially insert request req from $RemovedSet$ into the best position pos^* of route $rt_{nearest}$ in solution s, where

$$pos^* = \arg\min_{pos \in DRBPositionSet \cup SortieSet} \{InsCost\,(req, s, rt_{nearest}, pos)\}\,,$$

and route $rt_{nearest}$ is the route that contains req's nearest request req'. The concept of the nearest request is defined in destroy method D3. Sets $RouteSet$, $DRBPositionSet$, $SortieSet$, and $RemovedSet$, and solution s are updated after each insertion.

The five repair methods are categorized into two groups. R0 and R1 belong to the first group, G1. R2, R3, and R4 belong to the second group, G2. The basis for this classification is as follows: i) R0 and R1 are two-stage heuristics. In the first stage, all requests are inserted into a DRB route. In the second stage, requests that drones can serve may be moved from the DRB route into a drone sortie. In contrast, R2, R3, and R4 feature one stage. The costs of inserting a request eligible for drone service into a DRB route and a drone sortie are compared, and the better route is selected. ii) In G1, we evaluate the cost of inserting each candidate request into each position and choose the best request with the best position to perform operations. This means that the request to be inserted into the partial solution at each time is not known before the evaluation of all removed requests. In contrast, in G2, the request to be inserted at each time is known.

R0, R1, and R2 will always produce feasible solutions because 1) we assume that there are a sufficient number of vehicles (routes) ensuring that all requests can be served by the DRB and 2) the request can be inserted into any route, including the empty route. In contrast, R3 and R4 may produce infeasible solutions because a request can only be inserted into a specific non-empty route, which may cause a violation of vehicle capacity or the maximum travel time on a route. If an infeasible solution is generated, the repair method returns the solution obtained before executing the destroy and repair operations in the iteration.

3.4.4 Time slack strategy

The objective function minimizes the sum of the transportation and delay costs. Transportation costs can be reduced through the use of drones to deliver as many goods requests as possible because the operational cost of drones is much lower than that of DRBs. To mitigate the delay cost, DRBs and drones should leave a preceding node as soon as possible. If a preceding node is a launch node, leaving it too early may cause a long drone or DRB waiting time at the service node. This may result in an infeasible flight sortie because of the limited drone battery capacity. To address this, this study proposes a time slack strategy. DRBs and drones are allowed to wait at a node after completing the service task at the node. The time slack strategy will be adopted whenever the repair methods try to insert a drone sortie into a DRB route but the total flight time of the drone exceeds the maximum flight endurance. Through the implementation of this strategy, an infeasible flight sortie may be rendered feasible.

An illustrative example is presented in Figure 3.1. The numbers above the black and blue arrows represent the DRB and drone travel times between two nodes. The time window at each node is indicated in brackets below the node box. The launch, recovery, and service times at each node are set to 1 min. The maximum drone flight time is 30 min. Consider a scenario in which a DRB carrying a drone arrives at node 1 at time 5 and the earliest service time at node 1 is time 5. If the time slack strategy is not considered, at time 5, the DRB starts its service at node 1, and the drone starts taking off at the same

time. At time 6, the DRB leaves node 1 and proceeds to node 2, while the drone flies to node 4. The two vehicles wait at nodes 2 and 4 until the earliest time window at their service node is reached. Then, they travel to recovery node 3. Because the drone arrives at node 3 earlier than the DRB, it continues flying and waits for the DRB's arrival. Once the DRB arrives at node 3, the drone starts landing. The total flight time of the drone is 33 min. Because 33 is greater than 30, the solution is infeasible.

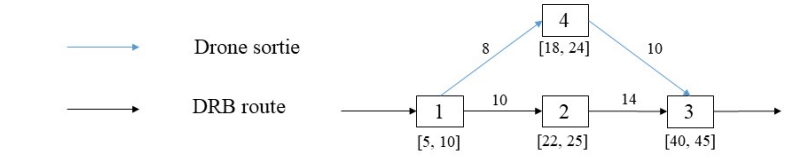

Without time slack

Node	1	2	4	3
DRB arrival time	5	16		37
DRB service start time	5	22		40
DRB departure time	6	23		
Drone arrival time			14	29
Drone service start time			18	
Drone launch start time	**5**			
Drone departure time	6		19	
Drone recovery time				38
Drone flight time	38 - 5 = **33** > 30			

With time slack

Node	1	2	4	3
DRB arrival time	5	19		37
DRB service start time	5	22		40
DRB departure time	9	23		
Drone arrival time			17	29
Drone service start time			18	
Drone launch start time	**8**			
Drone departure time	9		19	
Drone recovery time				38
Drone flight time	38 - 8 = **30**			

Infeasible solution → Feasible solution

Figure 3.1: Time slack strategy

Consider a time slack strategy in which the drone starts taking off at time 5 + (33 − 30) = 8. The drone flight time is recalculated as 30 min and is within the maximum flight time; therefore, the solution becomes feasible. The time slack strategy does not guarantee a better solution because postponing the departure time at a node may cause a delay at the subsequently visited nodes. The time slack strategy is applied only when an infeasible drone sortie occurs in the repair stage. The implementation of the strategy may render an infeasible solution feasible and better than the current best solution.

3.5 Numerical experiments

All numerical experiments were conducted on a Huawei XH620 V3 computer with an Intel Xeon Processor 2660v3 at 2.60 GHz. The CPLEX version was 12.9.0.0, and the ALNS was coded in C++. For each instance, we ran the ALNS 10 times and chose the best solution with the minimum objective value for our analysis.

3.5.1 Test instances and parameter tuning

The tested networks were generated according to the work by Sacramento et al. (2019). The coordinates of each node were the same as those in Sacramento et al. (2019). The coordinates were uniformly distributed on a grid of dimensions $2d \times 2d$ around the depot (0, 0). The distribution is expressed as $U(-d, d)$. The first $|P|$ nodes are the passenger request origins, and the following $|P|$ nodes represent the passenger request destinations. The rest of the nodes denote goods requests, some of which can be visited by drones. Each node is associated with a time window, and the interval between the latest and earliest service start time is 15 min. The instances are named as structure

$|S|\_|P|\_|G|\_|D|---Dim$. $|S|$ is the sum of the number of passenger stops and goods stops; $|D|$ is the number of goods requests that can be served by the drones; Dim represents the grid dimensions; $|S|$ and Dim are the same as in Sacramento et al. (2019), while for instances with the same size, we use the instances with the generic name "1" in Sacramento et al. (2019).

Here, we introduce the main setup of our experiments. The travel distances for a DRB and a drone between two nodes were equal to the Manhattan distance and Euclidean distance between the two nodes, respectively (Murray & Chu, 2015). The number of passengers for a passenger request was randomly selected from $\{1, 2, 3\}$. The maximum number of stops between the origin and destination of a passenger request service was 2. The DRB and drone service time at each node was 1 min. The delay penalty cost was 1 $ /min for passenger requests (Transport DTU, 2022) and 0.5 $ /min for goods requests[7]. The DRB speed was set to 35 miles/h, which is the same as the truck speed in Sacramento et al. (2019) and similar to the speed limit of buses, passenger cars, and vans in Denmark (https://trip.studentnews.eu/s/4086/77069-Buses-standard-speed-limits-in-Europe.htm). The transportation cost for a DRB was 0.2 $/mile (Litman, 2022), and the transportation cost for a drone was 10% of that for a ground vehicle (Sacramento et al., 2019). It was assumed that there were enough DRBs and drones. The capacities for passengers and goods were set to be the same, but they varied with the network settings. When the number of nodes was less than 50, the capacity was set as 6; when the number of nodes was 50 or 100, the capacity was 10; when the number of nodes was 150 or 200, the capacity was 20. The values of the other parameters were the same as those in Sacramento et al. (2019); that is, the speed of a drone was 50 miles/h; the maximum duration times of a DRB and a drone were set to 480 and 30 min, respectively; the launch and recovery times were 1 min.

We set the values of most of the parameters used in ALNS to those in Sacramento et al. (2019). We tuned two parameters: the lowest ratio of the number of removed requests r_{low} to the number of overall requests (0.01, 0.05, 0.1) and the highest ratio of the number of removed requests r_{up} to the number of overall requests (0.2, 0.3, 0.4). The instances used for parameter tuning were those with the largest dimensions for each instance with a different number of nodes. We ran ALNS 10 times for each instance. The parameter values with the best behavior (in terms of the average value of the minimum objective values for tuning instances) were selected. The final parameter values were set as follows: The initial temperature T_0 was calculated as 0.004 × 1.1 times the objective value of the initial solution for small instances and 0.004 times the objective value of the initial solution for large instances. The cooling parameter β was set as 0.9997. The absolute upper bounds on the minimum and maximum numbers of requests to be removed were set to $r_{\text{min}} = 20$ and $r_{\text{max}} = 40$. The lowest and highest ratios of the number of requests to be removed to the number of total requests were set to $r_{low} = 0.1$ and $r_{up} = 0.2$, respectively. The value of each weight used in the Shaw removal was set to 0.25. The reaction factor was set to $\rho = 0.9$. The scores of the methods were set to $\sigma_1 = 33$, $\sigma_2 = 9$, $\sigma_3 = 13$, and $\sigma_4 = 0$. The number of iterations in a segment was $iter^{seg} = 100$. The maximum number of non-improvement iterations for setting the best solution as the current solution was set to $noImp^{\text{max}} = 250$. The parameters defining the stopping criteria were set to $iter^{stop} = 25000$ and $noImp^{stop} = 7000$.

[7] In the numerical experiments, we used the same $\alpha_{i \in S_p}$ value (i.e., the unit delay penalty for passenger requests) for all passenger requests and the same $\alpha_{i \in S_g}$ value (i.e., the unit delay penalty for goods requests) for all goods requests. The value of the unit delay penalty for a passenger request was greater than that for a goods request.

3.5.2 Comparison with CPLEX

Table 3.3 compares the results given by CPLEX and the ALNS for the instances with 6, 10, and 12 nodes. For each instance, we ran the ALNS 10 times and obtained the minimum objective value ($z_{ALNS_{\text{min}}}$), the average objective value ($z_{ALNS_{\text{avg}}}$), the standard deviation (Std.), and the average computation time of the 10 runs. The gap was calculated as $\frac{z_{ALNS}-z_{CPLEX}}{z_{CPLEX}} \times 100\%$. CPLEX solved all instances to optimality. The computation time increased from 0.5 to 140.0 s with increasing instance size. In contrast, the proposed ALNS yielded the same solution as CPLEX within 1.5 s and had a stable performance, with a standard deviation of 0.0000.

Table 3.3: Results from CPLEX and ALNS for small SARP-D instances

η	Network	CPLEX		ALNS				Gap
		z_{CPLEX}	Time (s)	$z_{ALNS_{\text{min}}}$	$z_{ALNS_{\text{avg}}}$	Std.	Time (s)	
0	6_2_2_2—5	4.0834	1.0	4.0834	4.0834	0.0000	0.6	0.00%
	6_2_2_2—10	8.3111	0.9	8.3111	8.3111	0.0000	0.4	0.00%
	6_2_2_2—20	10.4419	0.6	10.4419	10.4419	0.0000	0.4	0.00%
	10_3_4_3—5	5.2563	38.7	5.2563	5.2563	0.0000	0.7	0.00%
	10_3_4_3—10	12.5398	5.2	12.5398	12.5398	0.0000	1.1	0.00%
	10_3_4_3—20	17.6415	6.6	17.6415	17.6415	0.0000	0.6	0.00%
	12_4_4_3—5	7.1948	140.0	7.1948	7.1948	0.0000	1.0	0.00%
	12_4_4_3—10	10.6261	25.4	10.6261	10.6261	0.0000	0.9	0.00%
	12_4_4_3—20	25.2007	10.8	25.2007	25.2007	0.0000	0.6	0.00%
1	6_2_2_2—5	3.3346	0.5	3.3346	3.3346	0.0000	0.6	0.00%
	6_2_2_2—10	8.3111	1.1	8.3111	8.3111	0.0000	0.5	0.00%
	6_2_2_2—20	10.4419	0.5	10.4419	10.4419	0.0000	0.4	0.00%
	10_3_4_3—5	4.5126	42.9	4.5126	4.5126	0.0000	0.8	0.00%
	10_3_4_3—10	10.7309	4.6	10.7309	10.7309	0.0000	1.2	0.00%
	10_3_4_3—20	17.5246	6.7	17.5246	17.5246	0.0000	0.8	0.00%
	12_4_4_3—5	6.6085	118.4	6.6085	6.6085	0.0000	1.0	0.00%
	12_4_4_3—10	10.5319	31.4	10.5319	10.5319	0.0000	1.0	0.00%
	12_4_4_3—20	25.2007	14.7	25.2007	25.2007	0.0000	0.7	0.00%
2	6_2_2_2—5	3.2699	0.5	3.2699	3.2699	0.0000	0.8	0.00%
	6_2_2_2—10	8.1790	1.1	8.1790	8.1790	0.0000	0.6	0.00%
	6_2_2_2—20	10.4419	0.7	10.4419	10.4419	0.0000	0.5	0.00%
	10_3_4_3—5	4.4476	35.8	4.4476	4.4476	0.0000	0.9	0.00%
	10_3_4_3—10	10.7309	4.3	10.7309	10.7309	0.0000	1.5	0.00%
	10_3_4_3—20	17.5246	6.5	17.5246	17.5246	0.0000	0.9	0.00%
	12_4_4_3—5	6.4138	109.3	6.4138	6.4138	0.0000	1.2	0.00%
	12_4_4_3—10	10.5319	31.3	10.5319	10.5319	0.0000	1.2	0.00%
	12_4_4_3—20	25.2007	13.4	25.2007	25.2007	0.0000	0.9	0.00%

3.5.3 Analysis of operators

In this section, the performance of ALNS operators is analyzed using instances from the tuning set.

3.5.3.1 Percentage of usage and scores of operators

Figure 3.2a presents the percentage of the total usage of operators. All destroy and repair methods were used, and the usage frequency of each operator differed in the test

instances. This suggests that the roulette wheel selection method can select appropriate destroy and repair methods for each instance. On average, all destroy methods were used with similar frequencies (Figure 3.2a, Average). Each of the repair methods R0, R1, and R2 accounted for about 30.0% of the iterations. In contrast, the percentages of the total usage of R3 and R4 were 6.5% and 4.8%, respectively (Figure 3.2a, Average).

Because we rewarded the new accepted solution according to the simulated annealing acceptance criterion, the most used operators were not necessarily those that improved the best-found or current solution the most times. Following the analysis method adopted by Sun et al. (2020), we present the percentages of the usage of operators that generated a solution that improved the best-found solution and the current solution in Figures 3.2b and 3.2c, respectively. These percentages can help identify which operators are likely to improve the best-found and current solutions. Compared with other destroy methods, D1 was less likely to improve the best-found and current solutions (Figures 3.2b and 3.2c, Average). Regarding the repair methods, R1 exhibited the best performance (46.0%) in improving the best-found solution, followed by R0 (26.4%) and R2 (23.4%), while R3 (4.2%) and R4 (0.0%) made minimal contributions (Figure 3.2b, Average). Similarly, R1 also exhibited the best performance (45.7%) in improving the current solution, followed by R0 (27.7%) and R2 (22.4%). R3 and R4 contributed almost equally (2.1%) to the improvement of the current solution (Figure 3.2c, Average). Figures 3.2b and 3.2c indicate that all destroy and repair methods contribute to the improvement of the best-found or current solution. Although R3 and R4 had limited impacts, they showed effectiveness in some instances (Figure 3.2c, instances 10_3_4_3—20 and 12_4_4_3—20). Moreover, as shown in Section 3.5.3.2, there were instances in which R3 and R4 were required to diversify the search and help improve the overall performance of ALNS. Similar observations have been reported by Chen et al. (2021), Ghilas et al. (2016a), Sun et al. (2020), and Zhao et al. (2022).

Figure 3.3 presents the percentage of the total scores of operators. A comparison of Figure 3.2a and Figure 3.3 reveals that the performances of each operator in terms of the total usage and total scores were almost the same, with only minor differences in their values.

3.5.3.2 Effects of operators and the time slack strategy

We examined the effects of the destroy and repair methods by removing one or more operators from ALNS operators and compared the corresponding results with those given by base-operators, which contain all operators introduced in Section 3.4. The objective function value gaps and computation time gaps of different combinations of operators and base-operators are presented in Tables 3.4 and 3.5, respectively. The column name indicates the operator combination. NoD0, NoD1, NoD2, NoD3, NoR0, NoR1, NoR2, NoR3, NoR4, NoR3R4, NoG1, and NoG2 represent the combination of operators without D0, D1, D2, D3, R0, R1, R2, R3, R4, R3 and R4, G1, and G2 from the base-operators, respectively. Moreover, the effects of the time slack strategy were examined, and the results are presented in the last column of the two tables.

Table 3.4 reveals that on average, removing operators degraded the solution's quality, with a maximum gap of 21.1%, which indicates that all elements in the ALNS contributed to ensuring the solution's quality. Although Figure 3.2 suggests that repair methods R3 and R4 seemed to make limited contributions to improving the solution, the optimal solution worsened without them in some instances (instances 150_55_40_30—40 and 200_60_80_60—40). The primary purpose of these operators was to enhance the diversity of the neighborhood search and improve the overall ALNS performance. Repair methods without G2 (R2, R3, and R4) resulted in a large gap for the small instances

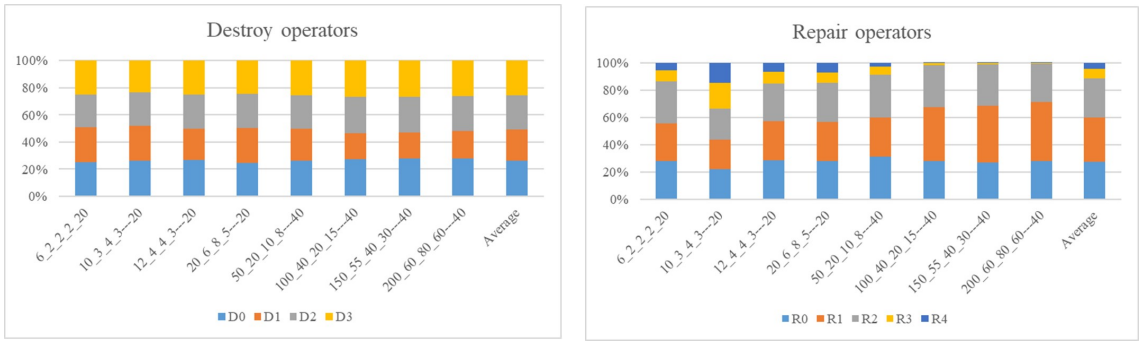

(a) Percentage of the total usage of operators

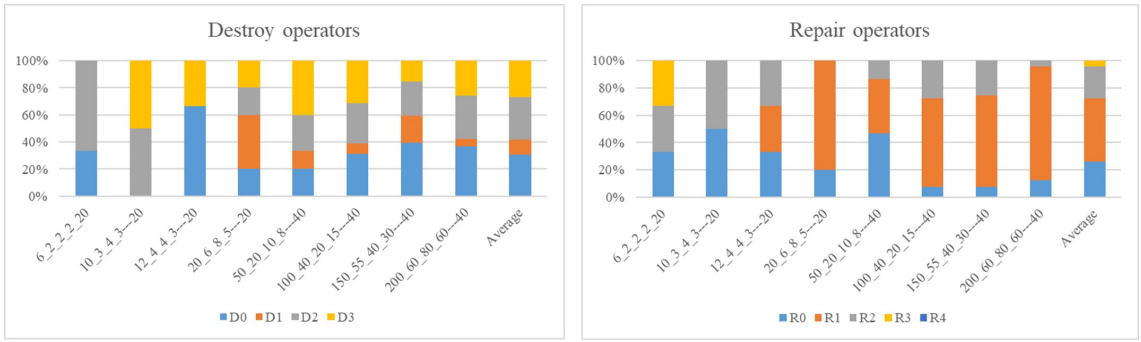

(b) Percentage of the usage of operators that generated a solution that improved the best-found solution

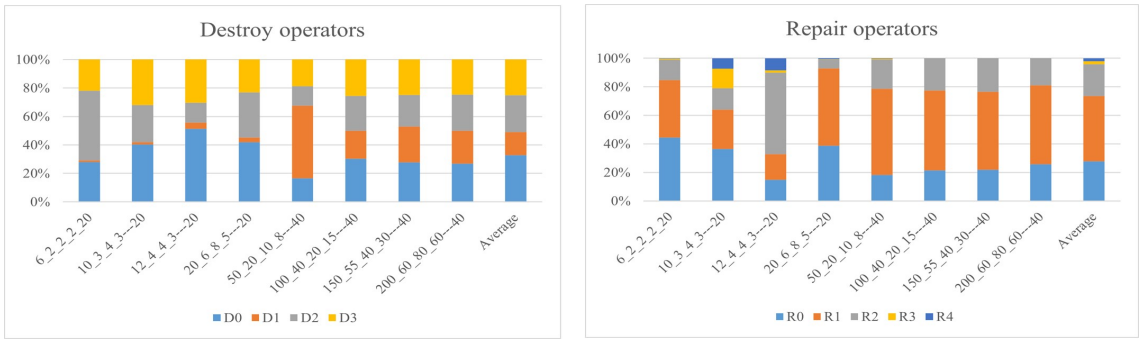

(c) Percentage of the usage of operators that generated a solution that improved the current solution

Figure 3.2: Percentage of the usage of operators

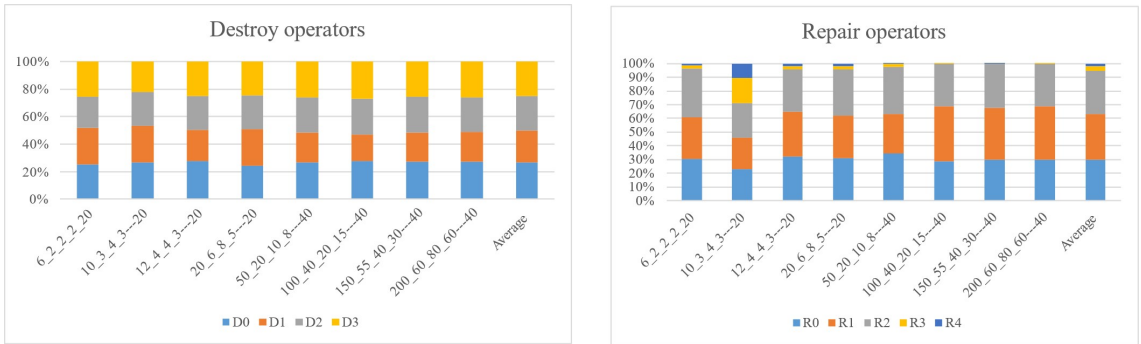

Figure 3.3: Percentage of the total scores of operators

6_2_2_2—20 with six nodes (21.1%) and 12_4_4_3—20 with 12 nodes (10.0%). Therefore, the best insertion-based repair methods (G2) played an essential role in the ALNS. The reason is explained in more detail as follows.

Table 3.4: Comparison of the objective function value yielded by different combinations of operators with that yielded by base-operators

Objective value gap	noD0	noD1	noD2	noD3	noR0	noR1	noR2	noR3	noR4	noG1	noG2	noR3R4	noSlack
6_2_2_2_20	0.0%	0.0%	0.0%	0.0%	0.0%	0.0%	0.0%	0.0%	0.0%	0.0%	21.1%	0.0%	0.0%
10_3_4_3—20	0.0%	0.0%	0.0%	0.0%	0.0%	0.0%	0.0%	0.0%	0.0%	0.0%	0.0%	0.0%	0.0%
12_4_4_3—20	0.0%	0.0%	0.0%	0.0%	0.0%	0.0%	0.0%	0.0%	0.0%	0.0%	10.0%	0.0%	0.3%
20_6_8_5—20	0.0%	0.0%	0.0%	0.0%	0.0%	0.0%	0.0%	0.0%	0.0%	0.0%	0.0%	0.0%	0.7%
50_20_10_8—40	0.0%	0.0%	0.0%	0.0%	0.0%	0.0%	0.0%	0.0%	0.0%	0.0%	0.0%	0.0%	3.0%
100_40_20_15—40	0.0%	0.0%	0.0%	0.0%	0.0%	0.0%	0.0%	0.0%	0.0%	0.1%	0.0%	0.0%	0.0%
150_55_40_30—40	0.4%	1.0%	1.1%	0.5%	0.8%	0.6%	0.6%	0.3%	0.6%	0.6%	0.6%	0.9%	1.3%
200_60_80_60—40	1.8%	1.3%	1.0%	1.7%	2.0%	3.1%	1.4%	0.5%	1.3%	2.1%	1.3%	1.8%	3.4%
Average	0.3%	0.3%	0.3%	0.3%	0.4%	0.5%	0.3%	0.1%	0.2%	0.4%	4.1%	0.3%	1.1%

In repair methods R0 and R1, not all nodes eligible for drone service could be inserted into a drone sortie, causing the loss of good solutions. This is explained by the example in Figure 3.4. We considered a scenario in which requests 3 and 4 were removed by a destroy method and both could be visited by a drone; the partial solution after the destroy procedure was a DRB route: 1 – 2 – 5. For R0 or R1, we first inserted requests 3 and 4 into the DRB route. If drone sortie <1,4,3> is good enough (that is, regardless of the sequence of the DRB route after the first stage, removing request 4 from the DRB route and inserting it into a drone sortie whose launch node is at request 1 and recovery node is at request 3 will always be the first operation in the second stage of R0 and R1), there is no opportunity for request 3 to be inserted into the drone sortie. This is because when a request from the DRB route is moved to a drone sortie, supposing the drone can serve the corresponding request(s) at its launch node or recovery node, the corresponding request(s) at the launch node or recovery node, together with the drone service request, will be deleted from the set of candidate requests that can be served by the drone. In this example, when we moved request 4 from the DRB route to a sortie, both requests 3 and 4 were deleted from the set of candidate requests that could be served by the drone, because request 3 was the recovery node of a sortie. If the optimal solution is DRB route 1 – 2 – 5 with drone sorties <1, 4, 2> and <2, 3, 5>, the ALNS with only repair methods R0 and R1 will not be able to find the optimal solution.

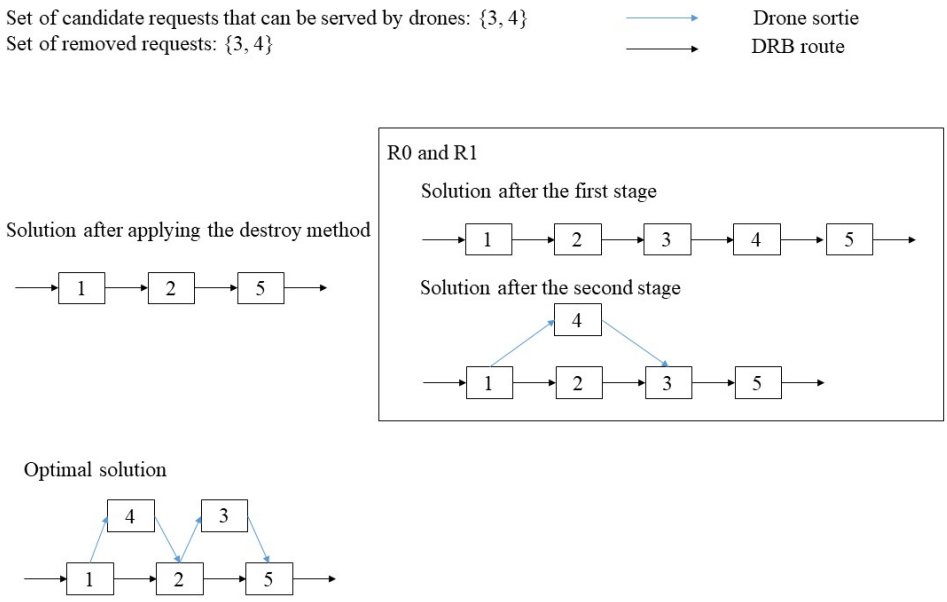

Figure 3.4: An example in which ALNS with only repair methods R0 and R1 cannot find the optimal solution

According to Table 3.4, removing the time slack strategy degraded the solution quality by up to 3.4%. Although the time slack strategy contributed to minimizing the total cost, it caused extra waiting time at some locations. Table 3.6 presents the total waiting time caused by the time slack strategy in different instances. In real life, DRBs may not be able to wait at every location, and idle DRBs may cause traffic obstructions. This problem could be solved by a model that considers different objectives, such as minimizing the total time span of serving all requests, regulating the locations where vehicles can wait, or setting the maximum waiting time at each location. Nevertheless, this problem is beyond the scope of this study, and we leave it for our future research.

As indicated by Table 3.5, removing destroy operators from base-operators reduced the computation time. Specifically, on average, the computation time was reduced by 14.2%, 15.2%, and 20.5% when repair methods D0, D1, and D3 were removed, respectively. Removing D2 reduced the computation time by only 1.8%. The influence of the removal of repair operators on computation time was complex. Removing repair operators R0, R1, R3, and R4 reduced the computation time by 10.3% to 21.8% on average. The computation time was considerably reduced (by 52.3%) when operators in group G1 were removed, which is logical considering the higher time complexities of R0 and R1. In contrast, operator combinations without repair method R2 (i.e., NoR2 and NoG2) led to a longer computation time. As presented in Figure 3.2, repair methods R0, R1, and R2 were the most frequently used operators in the ALNS. Compared with R0 and R1, R2 had a lower time complexity. When R2 was removed, the usage of R0 and R1 increased, leading to a longer computation time. Because R3 and R4 were seldom used, removing them did not significantly affect the computation time. Moreover, eliminating the time slack strategy reduced the computation time by 12.5% on average.

According to the results presented in Table 3.4 and Table 3.5, we recommend that decision makers use the operator combination NoG1 when they need to make a fast decision. This could significantly reduce the computation time without sacrificing too much solution quality. However, to better understand the proposed model's properties, we used the base-operators in our following experiments because they produced the best solutions among all operator combinations.

Table 3.5: Comparison of computation time used by different combinations of operators with that used by base-operators

CPU time gap	noD0	noD1	noD2	noD3	noR0	noR1	noR2	noR3	noR4	noG1	noG2	noR3R4	noSlack
6_2_2_2_20	-15.0%	-6.9%	2.8%	-25.9%	-8.5%	-9.1%	9.5%	-10.3%	-10.9%	-30.6%	-15.6%	4.9%	0.0%
10_3_4_3—20	-12.1%	-9.5%	5.2%	-23.2%	-19.4%	-16.2%	9.2%	8.6%	-2.2%	-50.1%	53.1%	37.6%	-14.0%
12_4_4_3—20	-9.6%	-11.7%	-2.7%	-22.1%	-11.3%	-13.9%	7.5%	-4.7%	-7.2%	-40.1%	13.3%	13.3%	-16.5%
20_6_8_5—20	-16.2%	-21.2%	0.7%	-20.8%	-15.3%	-13.8%	6.6%	-3.7%	-10.8%	-35.5%	12.4%	5.5%	1.0%
50_20_10_8—40	-19.2%	-24.9%	1.4%	-16.6%	-17.6%	-5.0%	14.9%	-19.6%	-8.9%	-43.1%	4.9%	-6.5%	-11.9%
100_40_20_15—40	-25.0%	-22.2%	-12.0%	-24.2%	-39.1%	-15.3%	27.7%	-21.5%	-15.3%	-70.5%	-4.7%	-14.1%	-9.1%
150_55_40_30—40	-18.2%	-19.0%	-14.6%	-24.2%	-31.0%	-15.9%	26.9%	-22.7%	-17.9%	-65.5%	7.9%	-12.5%	-20.3%
200_60_80_60—40	1.3%	-6.4%	4.8%	-6.8%	-32.0%	-22.6%	16.4%	-8.7%	-9.4%	-82.8%	18.2%	-8.4%	-28.9%
Average	-14.2%	-15.2%	-1.8%	-20.5%	-21.8%	-14.0%	14.9%	-10.3%	-10.3%	-52.3%	11.2%	2.5%	-12.5%

3.5.4 Results for VRP-D and SARP-D instances

Because this work is the first study of SARP-D, there are no benchmark instances in the published literature. We first applied our algorithm to a similar VRP-D to assess its performance and then used the proposed ALNS to solve SARP-D. As introduced in Section 3.2, SARP-D combines the features of both SARP and VRP-D. We tested our algorithm with VRP-D instead of SARP because SARP-D is much more similar to VRP-D. Table 3.7 summarizes the characteristics of SARP, VRP-D, and SARP-D. As seen in Table 3.7, SARP-D shares more similarities with VRP-D. Moreover, from the modeling viewpoint, if we set the number of passenger requests to 0, SARP-D is reduced to VRP-D. If we set the number of parcel requests to 0, SARP-D cannot be converted into SARP, and we

Table 3.6: Total waiting time yielded by time slack strategy (min)

	Total waiting time yielded by the time slack strategy (min)
6_2_2_2_20	0
10_3_4_3—20	0
12_4_4_3—20	20
20_6_8_5—20	31
50_20_10_8—40	51
100_40_20_15—40	32
150_55_40_30—40	146
200_60_80_60—40	402

automatically lose the characteristics of drones. If we assume that no goods requests can be served by drones, SARP-D cannot be transformed to SARP, because in SARP, for both passenger and goods requests, the vehicle is required to visit its origin before its destination, while in SARP-D, the vehicle is not required to visit a goods request's origin (i.e., the depot) before the destination.

Table 3.7: Summary of the characteristics of SARP, VRP-D, and SARP-D

	SARP	VRP-D	SARP-D
Passenger request described by <origin, destination>	√		√
Parcel request described by <delivery point>		√	√
Drone		√	√

3.5.4.1 VRP-D instances

Under the assumption that there are no passenger requests and that the time windows at each node are very wide, SARP-D is completely reduced to the VRP-D presented by Sacramento et al. (2019). In this subsection, "VRP-D" refers to the problem described by Sacramento et al. (2019). Table 3.8 reports the computation results of our proposed ALNS with base-operators on VRP-D instances used by Sacramento et al. (2019). Columns Min., Avg., and Std. present the minimum objective value, average objective value, and standard deviation of the 10 runs of our algorithm, respectively. The "Gap" column represents the gap between the minimum objective value found by our ALNS out of 10 runs and the minimum objective value found by Sacramento et al. (2019). For the first nine instances, Sacramento et al. (2019) presented the optimal solution given by CPLEX. Our algorithm generated the optimal solution, as in Sacramento et al. (2019). For the other instances for which Sacramento et al. (2019) only presented the best solution obtained using their proposed ALNS algorithm, our algorithm sometimes found better solutions. On average, the gap between the best solution found by our algorithm and that found by Sacramento et al. (2019) was 0.04%. The results show that although our algorithm is designed for a more general SARP-D instead of VRP-D, it can effectively solve VRP-D, similarly to a specialized algorithm for VRP-D proposed by Sacramento et al. (2019).

3.5.4.2 SARP-D instances

We conducted experiments on networks with 20, 50, 100, 150, and 200 nodes and three η values (i.e., 0, 1, and 2). The results are presented in Table 3.9. Columns Min., Avg., and Std. represent the minimum objective value, the average objective value, and the standard deviation of the 10 runs. Gap is calculated as $\frac{Avg.-Min.}{Min.} \times 100\%$. The proposed ALNS

Table 3.8: Results of our ALNS on VRP-D instances

Instance	Sacramento et al. (2019)	Min.	Avg.	Std.	Gap	CPU time (min)
6.5.1	1.09821	1.09821	1.09821	0.0000	0.00%	0.0
6.10.1	2.40611	2.40611	2.40611	0.0000	0.00%	0.0
6.20.1	2.67759	2.67759	2.67759	0.0000	0.00%	0.0
10.5.1	1.65563	1.65563	1.65563	0.0000	0.00%	0.1
10.10.1	2.32647	2.32647	2.34515	0.0394	0.00%	0.1
10.20.1	4.45240	4.45240	4.45240	0.0000	0.00%	0.1
12.5.1	1.37381	1.37381	1.37381	0.0000	0.00%	0.1
12.10.1	2.68103	2.68103	2.68937	0.0264	0.00%	0.1
12.20.1	5.77759	5.77759	5.78967	0.0382	0.00%	0.1
20.5.1	1.79347	1.79347	1.79380	0.0010	0.00%	0.2
20.10.1	3.25253	3.25253	3.35375	0.0698	0.00%	0.3
20.20.1	7.34453	7.32295	7.37756	0.0373	-0.29%	0.2
50.10.1	5.86134	5.86133	5.94868	0.1072	0.00%	4.7
50.20.1	10.45526	10.46399	10.62728	0.0578	0.08%	2.7
50.30.1	15.81788	15.77222	15.90068	0.1578	-0.29%	2.2
50.40.1	20.37508	20.09076	20.42130	0.4499	-1.40%	2.5
100.10.1	6.85741	6.86435	6.95659	0.0695	0.10%	32.3
100.20.1	13.60671	14.01043	14.08554	0.0532	2.97%	32.2
100.30.1	22.58818	21.97805	22.37424	0.2410	-2.70%	25.1
100.40.1	29.13966	29.04801	29.49945	0.4113	-0.31%	21.1
150.10.1	8.79027	8.71331	8.84395	0.1164	-0.88%	153.8
150.20.1	17.31938	17.65019	18.18175	0.4526	1.91%	127.4
150.30.1	25.98537	25.68835	26.64764	0.7296	-1.14%	106.1
150.40.1	34.01210	33.78728	35.05252	0.7552	-0.66%	92.6
200.10.1	10.09452	10.38412	10.67978	0.2022	2.87%	355.3
200.20.1	21.21505	21.23676	21.75325	0.4384	0.10%	316.0
200.30.1	30.36023	30.58005	31.02294	0.3528	0.72%	266.2
200.40.1	41.49802	41.51556	42.14891	0.4578	0.04%	257.7
Average	-	-	-	-	0.04%	64.2

exhibited a stable performance over the 57 instances. The gap and standard deviation are within 2% and 3, respectively, with a few exceptions.

Table 3.9: Performance of the proposed ALNS metaheuristic on large-scale SARP-D instances

η	Network	Min.	Avg.	Std.	Gap	CPU time (min)
	20_6_8_5—5	11.1375	11.1375	0.0000	0.00%	0.0
	20_6_8_5—10	21.4303	21.4318	0.0046	0.01%	0.0
	20_6_8_5—20	45.7637	45.8995	0.0477	0.30%	0.0
	50_20_10_8—10	55.6624	55.6908	0.0886	0.05%	0.7
	50_20_10_8—20	88.6438	88.6499	0.0192	0.01%	0.7
	50_20_10_8—30	159.7266	159.7273	0.0009	0.00%	0.4
	50_20_10_8—40	230.6791	230.6896	0.0169	0.00%	0.3
	100_40_20_15—10	99.6675	99.8171	0.1225	0.15%	8.3
	100_40_20_15—20	186.8728	187.4096	0.6067	0.29%	6.6
0	100_40_20_15—30	291.5774	291.8542	0.4793	0.10%	5.7
	100_40_20_15—40	388.0544	389.0056	0.5156	0.25%	3.5
	150_55_40_30—10	123.9080	124.4212	0.4775	0.41%	41.8
	150_55_40_30—20	248.8823	250.8753	0.8585	0.80%	38.5

	150_55_40_30—30	361.9345	363.8738	2.0932	0.54%	24.0
	150_55_40_30—40	532.1596	534.1503	1.6316	0.37%	19.5
	200_60_80_60—10	132.2916	133.3536	0.8808	0.80%	169.6
	200_60_80_60—20	276.6224	277.9824	1.1870	0.49%	93.4
	200_60_80_60—30	459.4269	462.9329	2.2421	0.76%	80.7
	200_60_80_60—40	537.2808	539.1963	1.8413	0.36%	76.1
	20_6_8_5—5	10.0928	10.0928	0.0000	0.00%	0.1
	20_6_8_5—10	19.7241	19.7242	0.0000	0.00%	0.1
	20_6_8_5—20	41.3300	41.3300	0.0000	0.00%	0.0
	50_20_10_8—10	45.0251	45.6618	0.5508	1.41%	0.8
	50_20_10_8—20	78.0259	78.1545	0.1660	0.16%	0.6
	50_20_10_8—30	136.1432	136.1432	0.0000	0.00%	0.5
	50_20_10_8—40	205.0499	205.0499	0.0000	0.00%	0.4
	100_40_20_15—10	81.0970	82.1286	0.6780	1.27%	10.7
	100_40_20_15—20	169.9069	170.7529	0.5037	0.50%	6.4
1	100_40_20_15—30	247.4877	249.2932	1.9043	0.73%	5.7
	100_40_20_15—40	353.2098	354.3277	1.4020	0.32%	4.6
	150_55_40_30—10	104.3026	105.6459	0.8814	1.29%	50.6
	150_55_40_30—20	215.7509	217.3335	1.4215	0.73%	42.1
	150_55_40_30—30	318.2711	320.0464	1.7279	0.56%	32.1
	150_55_40_30—40	448.1320	451.8578	3.2835	0.83%	25.3
	200_60_80_60—10	114.9565	116.6402	0.8800	1.46%	171.5
	200_60_80_60—20	229.8977	231.7293	1.7907	0.80%	132.1
	200_60_80_60—30	404.2448	408.9268	2.6839	1.16%	126.8
	200_60_80_60—40	492.5034	495.4947	2.5606	0.61%	103.3
	20_6_8_5—5	9.2524	9.2524	0.0000	0.00%	0.1
	20_6_8_5—10	19.6796	19.6796	0.0000	0.00%	0.1
	20_6_8_5—20	39.4754	39.4754	0.0000	0.00%	0.0
	50_20_10_8—10	40.3762	40.7470	0.5819	0.92%	0.9
	50_20_10_8—20	77.9900	78.1306	0.1496	0.30%	0.8
	50_20_10_8—30	130.9397	131.1947	0.4169	0.19%	0.6
	50_20_10_8—40	203.2683	203.3346	0.2097	0.03%	0.5
	100_40_20_15—10	77.0423	78.4299	0.7457	1.80%	13.3
	100_40_20_15—20	158.7958	159.9565	0.8639	0.73%	9.0
2	100_40_20_15—30	235.2368	236.6466	1.3188	0.60%	6.6
	100_40_20_15—40	343.5126	345.5041	1.5995	0.58%	7.3
	150_55_40_30—10	100.0475	100.9884	0.7961	0.94%	61.1
	150_55_40_30—20	205.9190	207.8299	1.2262	0.93%	50.5
	150_55_40_30—30	304.1630	305.9224	1.7162	0.58%	30.4
	150_55_40_30—40	422.9446	428.5706	3.8084	1.33%	32.3
	200_60_80_60—10	111.1394	114.0036	1.7025	2.58%	168.9
	200_60_80_60—20	223.1800	227.5098	2.6625	1.94%	160.7
	200_60_80_60—30	392.0947	394.0151	1.5241	0.49%	132.8
	200_60_80_60—40	461.2592	472.1302	5.2387	2.36%	107.1

3.6 Management insights

In this study, we conducted sensitivity analysis by changing the values of the maximum number of intermediate stops during one passenger request service, the maximum drone

flight time, and the unit delay penalty for passengers and parcels.

3.6.1 Effects of the maximum number of intermediate stops during one passenger request service

This study compared the system performances of 19 networks containing over 12 nodes with $\eta = 0, 1, 2$. At $\eta = 0$, no passenger request shared a ride with either other passenger requests or goods requests. The transportation system in this case can be regarded as a separate passenger and parcel system, although it is not precisely a traditional separated passenger and goods transportation system. Taking $\eta = 0$ as a base scenario for each network, we calculated the percentage changes in the total cost and the DRB-traveled miles for each network with $\eta = 1$ and $\eta = 2$.

As shown in Figure 3.5, the percentage changes in the total cost and DRB-traveled miles were negative, which indicates that sharing a passenger request with another passenger request or goods request caused a significant reduction in the total cost and DRB-traveled miles. With increasing η value, the reduction in the total cost and DRB-traveled miles increased in the 19 networks. On average, at $\eta = 1$ and $\eta = 2$, the total cost decreased by 12.80% and 16.53%, respectively. The average percentage reduction in DRB-traveled miles was comparable to the total cost reduction: 13.29% and 17.47% at $\eta = 1$ and $\eta = 2$, respectively.

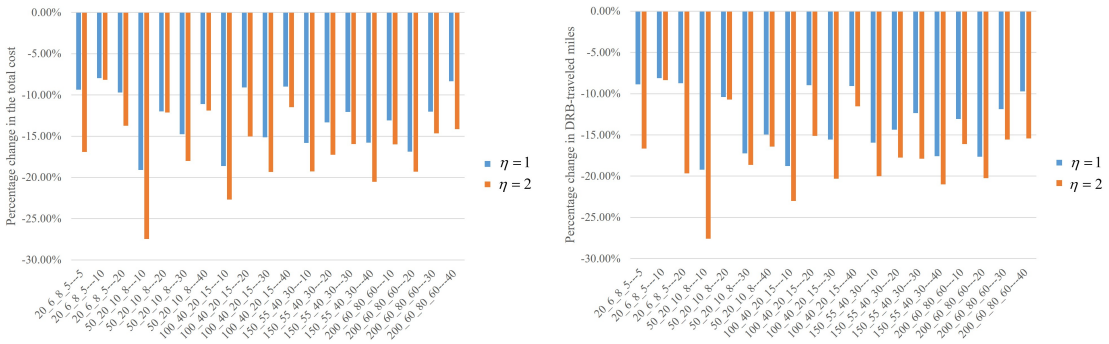

Figure 3.5: Percentage changes in the total cost (left) and the DRB-traveled miles (right) with different values of the maximum number of stops during one passenger request service

We examined the optimal solution for each instance. Although there were enough DRBs, sometimes postponing the service for some requests resulted in a lower total cost compared with using another DRB to serve the requests. This is reflected in the left plot of Figure 3.6, as a delay cost occurred in 26 instances. Moreover, the increase in the η value did not necessarily lead to a higher delay cost. On average, at $\eta = 0$, goods experienced more delays than passengers, whereas at $\eta = 1$ and $\eta = 2$, passengers experienced more delays than goods. The right side of Figure 3.6 shows that for all networks, fewer DRBs were used when a passenger request shared a ride with other requests. With increasing η value, the reduction in the number of used DRBs increased or was unchanged.

3.6.2 Effects of the endurance time of drones

This section compares the objective values under five drone battery endurance time settings: 5, 10, 20, 30, and 60 min at $\eta = 2$. Experiments were conducted on networks with 100, 150, and 200 nodes. The scenario with an endurance time of 5 min was the base scenario. Under this setting, the drones could fly for 2 min at most. Thus, few sorties could be performed. Figure 3.7 shows the percentage change in the total cost compared with the base scenario. The increase in the endurance of the drones magnified the reduction in the total cost, where the reduction degree depended on the degree of

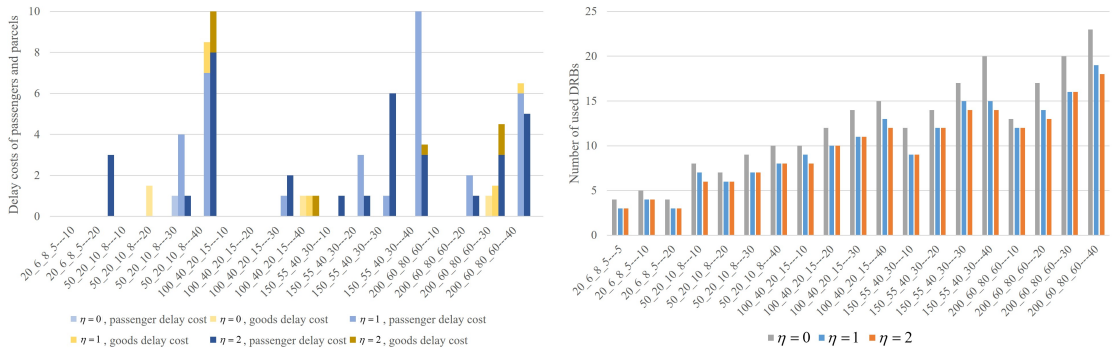

Figure 3.6: Delay cost (left) and the number of used DRBs (right) for each instance

the increase in endurance and the network dimensions. Increasing the endurance from 5 to 10 min saved more cost for smaller networks with dimensions of 10 and 20 than for networks with dimensions of 30 and 40. Increasing the endurance to 20 min significantly reduced cost (by 4.48% on average) for all networks. With the increase in endurance to 30 and 60 min, the total cost decreased by up to 10.39% and 10.58%, respectively. For some networks (100_40_20_15—10, 100_40_20_15—20, 200_60_80_60—10, and 200_60_80_60—20), the total costs under the two endurance settings did not largely differ. This indicates that an increase in endurance is not always attractive.

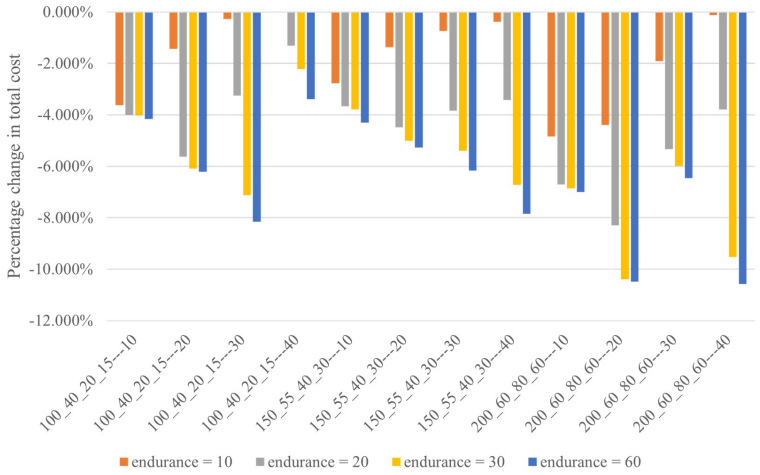

Figure 3.7: Percentage change in the total cost under different endurance levels

We present the percentage changes in DRB-traveled miles, drone flight miles, and the delay time in Figure 3.8. In most scenarios, with increasing battery endurance, the DRB-traveled miles decreased, and the drone flight miles increased. However, there were some exceptions, because although the increased endurance allowed for the long-distance traveling of drones, the long-distance traveling was time-consuming; therefore, fewer sorties were performed in a route, which may result in more DRB-traveled miles or fewer drone flight miles. There were no significant trends in delay time with increasing battery endurance. Overall, the increase in drone battery endurance ultimately reduced the total cost but possibly at the expense of increasing the total travel cost or the delay penalty.

3.6.3 Effects of unit delay penalty

The values of the unit delay penalty for passengers and goods can be used to control the service level measured by the delay time. We examined the SARP-D system performance

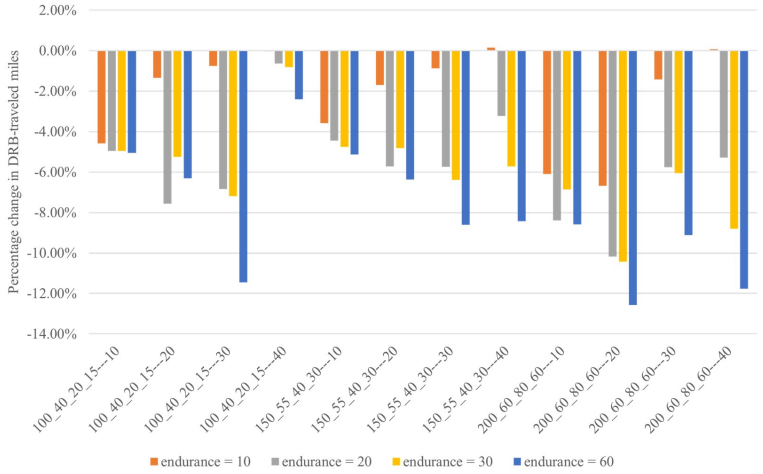

(a) Percentage change in DRB-traveled miles under different endurance levels

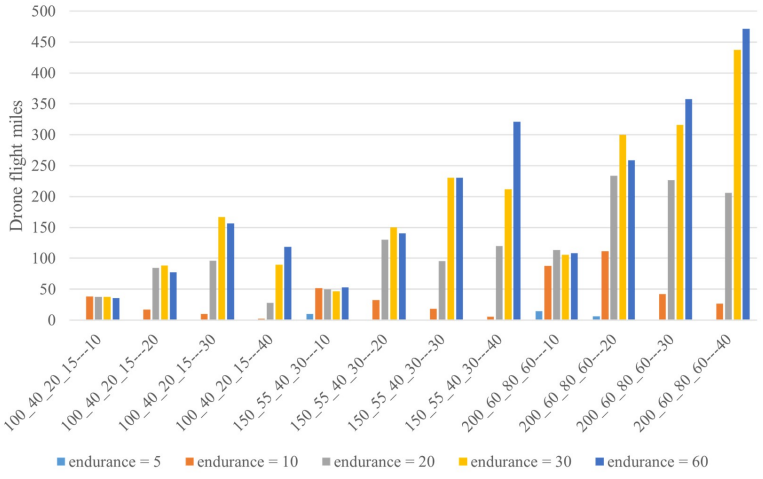

(b) Drone flight miles under different endurance levels

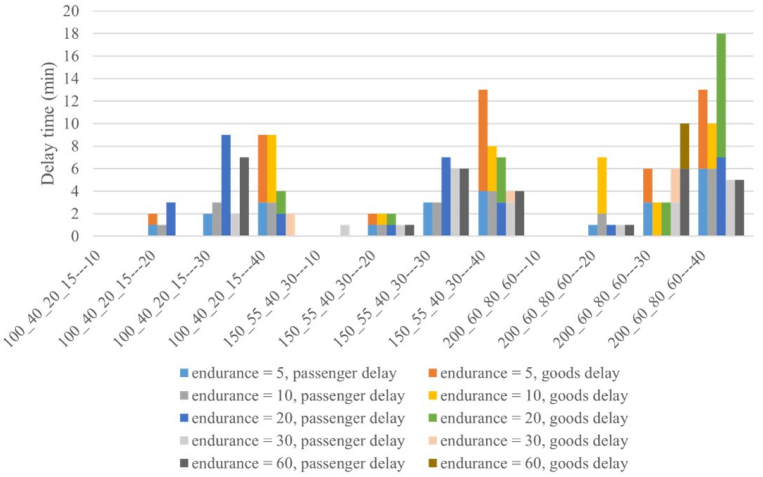

(c) Delay time under different endurance levels

Figure 3.8: Performance of DRB-traveled miles (a), drone flight miles (b), and delay time (c) under different endurance levels

with three unit delay penalty combinations: (0, 0), (1, 0.5), and (10, 5). The first number in the bracket is the unit delay penalty for passengers, and the second is for goods. We conducted experiments using the instances depicted in Section 3.6.2. Table 3.10 presents the total delay time for passengers and goods under different unit delay penalties. When the unit delay penalty is 0 for both passengers and goods, the time windows at each node are ignored during decision making, causing a huge total delay time for both passengers and goods. Increasing the values of the unit delay penalty can considerably reduce the total delay time. The larger the unit penalty value, the less the violation of the time window constraints.

Table 3.10: Total delay time under different unit delay penalties

	Total delay			Passenger delay			Goods delay		
	(0, 0)	(1, 0.5)	(10, 5)	(0, 0)	(1, 0.5)	(10, 5)	(0, 0)	(1, 0.5)	(10, 5)
100_40_20_15—10	5684	0	0	4594	0	0	1090	0	0
100_40_20_15—20	7832	0	0	6699	0	0	1133	0	0
100_40_20_15—30	7629	2	0	6644	2	0	985	0	0
100_40_20_15—40	5387	2	2	4915	0	0	472	2	2
150_55_40_30—10	12670	1	0	10326	1	0	2344	0	0
150_55_40_30—20	11794	1	0	10232	1	0	1562	0	0
150_55_40_30—30	12095	6	0	9839	6	0	2256	0	0
150_55_40_30—40	9382	4	0	7062	3	0	2320	1	0
200_60_80_60—10	13392	0	0	8981	0	0	4411	0	0
200_60_80_60—20	10658	1	0	7051	1	0	3607	0	0
200_60_80_60—30	10607	6	2	7697	3	0	2910	3	2
200_60_80_60—40	14625	5	0	9603	5	0	5022	0	0

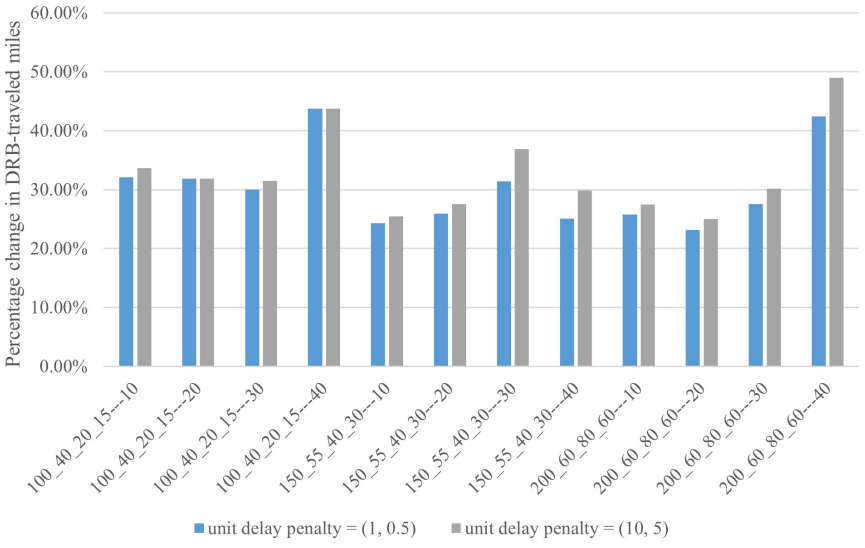

Figure 3.9: Percentage change in DRB-traveled miles under different unit delay penalties

Considering the unit delay penalty (0, 0) as the base scenario, Figure 3.9 presents the percentage change in DRB-traveled miles. Figure 3.10 shows the number of used DRBs. The two figures show that more DRBs were used, and more miles were traveled to reduce the time window violation and improve the service level.

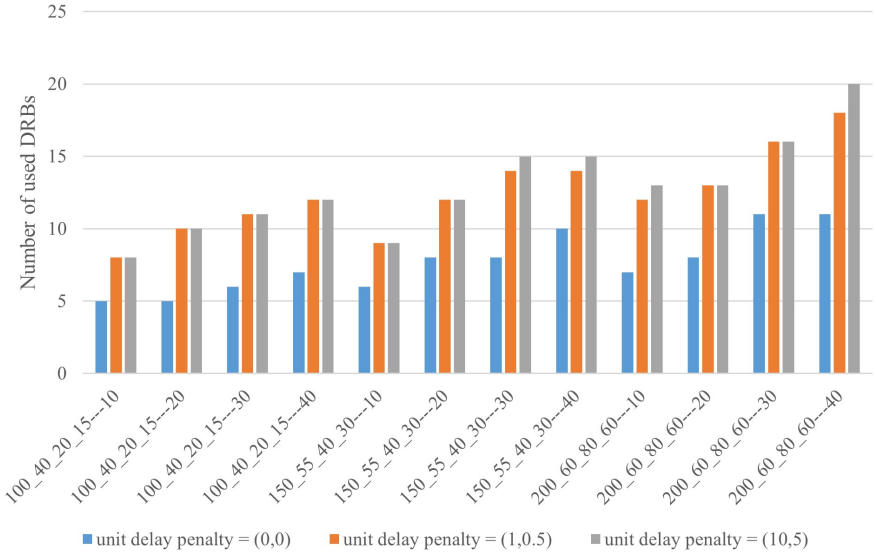

Figure 3.10: Number of used DRBs under different unit delay penalties

3.7 Conclusion

This paper introduces a new system that integrates passenger and goods transportation using demand-responsive vehicles (DRBs) and drones. The problem combines the features of both passenger and parcel SARP and VRP-D. The novelties of the proposed passenger and parcel SARP-D are as follows: First, compared with SARP, in which parcels are delivered using only ground vehicles, the proposed SARP-D incorporates drones to also perform parcel deliveries. Second, compared with VRP-D, in which ground vehicles undertake only delivery tasks, the ground vehicles in SARP-D undertake both pick-up and delivery tasks.

We developed an MINP model for SARP-D to determine the DRB and drone routes to minimize the total transportation cost of vehicles and the delay cost. The MINP was then linearized. Small instances with up to 12 nodes could be solved to optimality using CPLEX. To solve large instances with up to 200 nodes, we developed an ALNS metaheuristic. Numerical experiments showed that the proposed ALNS could find optimal solutions equivalent to those of CPLEX for small networks and demonstrated the stable and high-quality performance of the ALNS on large networks. The results showed that on average, sharing a passenger request with other passenger or parcel requests could significantly reduce the total cost and the miles traveled by ground vehicles by more than 10%. Allowing more stops during a passenger request service increased cost savings. Moreover, we revealed that extending the drone flight time reduced the total cost by up to 10.58% but did not always guarantee a reduction in ground vehicle-traveled miles.

Future studies could extend the model by introducing multiple objectives, such as minimizing the time span, maximizing the profit, and reducing carbon emissions. Moreover, researchers may be able to develop more efficient algorithms for SARP-D, for example, by exploring more efficient ways to identify better ALNS operator combinations and using reinforcement learning techniques. In addition, methods to optimize the DRB and drone routes in a stochastic and dynamic environment should be developed. Finally, researchers should consider replacing DRBs with more environmentally friendly vehicles such as electric vehicles and SAVs and develop corresponding models considering the features of electric vehicles.

Acknowledgment

The first author acknowledges financial support from the China Scholarship Council (No. 202107940012).

References

Agatz, N., Bouman, P., & Schmidt, M. (2018). Optimization approaches for the traveling salesman problem with drone. *Transportation Science*, *52*(4), 965–981.

Anderson, J. M., Nidhi, K., Stanley, K. D., Sorensen, P., Samaras, C., & Oluwatola, O. A. (2014). *Autonomous vehicle technology: A guide for policymakers*. Rand Corporation.

Beirigo, B. A., Schulte, F., & Negenborn, R. R. (2018). Integrating people and freight transportation using shared autonomous vehicles with compartments. *IFAC-PapersOnLine*, *51*(9), 392–397.

Boysen, N., Fedtke, S., & Schwerdfeger, S. (2021). Last-mile delivery concepts: A survey from an operational research perspective. *Or Spectrum*, *43*, 1–58.

Büyüközkan, G., & Ilıcak, Ö. (2022). Smart urban logistics: Literature review and future directions. *Socio-Economic Planning Sciences*, *81*, 101197.

Cavallaro, F., & Nocera, S. (2022). Integration of passenger and freight transport: A concept-centric literature review. *Research in Transportation Business & Management*, *43*, 100718.

Chen, C., Demir, E., & Huang, Y. (2021). An adaptive large neighborhood search heuristic for the vehicle routing problem with time windows and delivery robots. *European journal of operational research*, *294*(3), 1164–1180.

Cheng, R., Jiang, Y., & Nielsen, O. A. (2023). Integrated people-and-goods transportation systems: From a literature review to a general framework for future research. *Transport Reviews*, 1–24.

Chiang, W.-C., Li, Y., Shang, J., & Urban, T. L. (2019). Impact of drone delivery on sustainability and cost: Realizing the uav potential through vehicle routing optimization. *Applied energy*, *242*, 1164–1175.

Choudhury, S., Solovey, K., Kochenderfer, M. J., & Pavone, M. (2021). Efficient large-scale multi-drone delivery using transit networks. *Journal of Artificial Intelligence Research*, *70*, 757–788.

Chung, S. H., Sah, B., & Lee, J. (2020). Optimization for drone and drone-truck combined operations: A review of the state of the art and future directions. *Computers & Operations Research*, *123*, 105004.

Coindreau, M.-A., Gallay, O., & Zufferey, N. (2021). Parcel delivery cost minimization with time window constraints using trucks and drones. *Networks*, *78*(4), 400–420.

Di Puglia Pugliese, L., & Guerriero, F. (2017). Last-mile deliveries by using drones and classical vehicles. *Optimization and Decision Science: Methodologies and Applications: ODS, Sorrento, Italy, September 4-7, 2017 47*, 557–565.

Di Puglia Pugliese, L., Guerriero, F., & Macrina, G. (2020). Using drones for parcels delivery process. *Procedia Manufacturing*, *42*, 488–497.

Di Puglia Pugliese, L., Guerriero, F., & Scutellá, M. G. (2021a). The last-mile delivery process with trucks and drones under uncertain energy consumption. *Journal of Optimization Theory and Applications*, *191*(1), 31–67.

Di Puglia Pugliese, L., Macrina, G., & Guerriero, F. (2021b). Trucks and drones cooperation in the last-mile delivery process. *Networks*, *78*(4), 371–399.

Elbert, R., & Rentschler, J. (2022). Freight on urban public transportation: A systematic literature review. *Research in Transportation Business & Management*, *45*, 100679.

European Commission. (2007). Green paper, towards a new culture for urban mobility, Luxembourg: Publications Office of the European Union.

Ghilas, V., Demir, E., & Van Woensel, T. (2016a). An adaptive large neighborhood search heuristic for the pickup and delivery problem with time windows and scheduled lines. *Computers & Operations Research*, *72*, 12–30.

Ghilas, V., Demir, E., & Van Woensel, T. (2016b). A scenario-based planning for the pickup and delivery problem with time windows, scheduled lines and stochastic demands. *Transportation Research Part B: Methodological*, *91*, 34–51.

Golbabaei, F., Yigitcanlar, T., & Bunker, J. (2021). The role of shared autonomous vehicle systems in delivering smart urban mobility: A systematic review of the literature. *International Journal of Sustainable Transportation*, *15*(10), 731–748.

Huang, H., Savkin, A. V., & Huang, C. (2020). A new parcel delivery system with drones and a public train. *Journal of Intelligent & Robotic Systems*, *100*, 1341–1354.

Kitjacharoenchai, P., Min, B.-C., & Lee, S. (2020). Two echelon vehicle routing problem with drones in last mile delivery. *International Journal of Production Economics*, *225*, 107598.

Kuo, R., Lu, S.-H., Lai, P.-Y., & Mara, S. T. W. (2022). Vehicle routing problem with drones considering time windows. *Expert Systems with Applications*, *191*, 116264.

Lemardelé, C., Estrada, M., Pagès, L., & Bachofner, M. (2021). Potentialities of drones and ground autonomous delivery devices for last-mile logistics. *Transportation Research Part E: Logistics and Transportation Review*, *149*, 102325.

Levin, M. W., Kockelman, K. M., Boyles, S. D., & Li, T. (2017). A general framework for modeling shared autonomous vehicles with dynamic network-loading and dynamic ride-sharing application. *Computers, Environment and Urban Systems*, *64*, 373–383.

Li, B., Krushinsky, D., Reijers, H. A., & Van Woensel, T. (2014). The share-a-ride problem: People and parcels sharing taxis. *European Journal of Operational Research*, *238*(1), 31–40.

Li, B., Krushinsky, D., Van Woensel, T., & Reijers, H. A. (2016a). An adaptive large neighborhood search heuristic for the share-a-ride problem. *Computers & Operations Research*, *66*, 170–180.

Li, B., Krushinsky, D., Van Woensel, T., & Reijers, H. A. (2016b). The share-a-ride problem with stochastic travel times and stochastic delivery locations. *Transportation Research Part C: Emerging Technologies*, *67*, 95–108.

Li, H., Chen, J., Wang, F., & Bai, M. (2021). Ground-vehicle and unmanned-aerial-vehicle routing problems from two-echelon scheme perspective: A review. *European Journal of Operational Research*, *294*(3), 1078–1095.

Litman, T. (2022). *Autonomous vehicle implementation predictions: Implications for transport planning*. https://www.vtpi.org/avip.pdf

Luo, Q., Wu, G., Ji, B., Wang, L., & Suganthan, P. N. (2021). Hybrid multi-objective optimization approach with pareto local search for collaborative truck-drone routing problems considering flexible time windows. *IEEE Transactions on Intelligent Transportation Systems*, *23*(8), 13011–13025.

Macrina, G., Di Puglia Pugliese, L., Guerriero, F., & Laporte, G. (2020). Drone-aided routing: A literature review. *Transportation Research Part C: Emerging Technologies*, *120*, 102762.

Marinelli, M., Caggiani, L., Ottomanelli, M., & Dell'Orco, M. (2018). En route truck–drone parcel delivery for optimal vehicle routing strategies. *IET Intelligent Transport Systems*, *12*(4), 253–261.

Milanés, V., & Shladover, S. E. (2014). Modeling cooperative and autonomous adaptive cruise control dynamic responses using experimental data. *Transportation Research Part C: Emerging Technologies*, *48*, 285–300.

Moshref-Javadi, M., Hemmati, A., & Winkenbach, M. (2020a). A truck and drones model for last-mile delivery: A mathematical model and heuristic approach. *Applied Mathematical Modelling*, *80*, 290–318.

Moshref-Javadi, M., Lee, S., & Winkenbach, M. (2020b). Design and evaluation of a multi-trip delivery model with truck and drones. *Transportation Research Part E: Logistics and Transportation Review*, *136*, 101887.

Mourad, A., Puchinger, J., & Van Woensel, T. (2021). Integrating autonomous delivery service into a passenger transportation system. *International Journal of Production Research*, *59*(7), 2116–2139.

Murray, C. C., & Chu, A. G. (2015). The flying sidekick traveling salesman problem: Optimization of drone-assisted parcel delivery. *Transportation Research Part C: Emerging Technologies*, *54*, 86–109.

Othman, K. (2022). Exploring the implications of autonomous vehicles: A comprehensive review. *Innovative Infrastructure Solutions*, *7*(2), 165.

Otto, A., Agatz, N., Campbell, J., Golden, B., & Pesch, E. (2018). Optimization approaches for civil applications of unmanned aerial vehicles (uavs) or aerial drones: A survey. *Networks*, *72*(4), 411–458.

Peng, Z., Feng, R., Wang, C., Jiang, Y., & Yao, B. (2021). Online bus-pooling service at the railway station for passengers and parcels sharing buses: A case in dalian. *Expert Systems with Applications*, *169*, 114354.

Ropke, S., & Pisinger, D. (2006). An adaptive large neighborhood search heuristic for the pickup and delivery problem with time windows. *Transportation science*, *40*(4), 455–472.

Sacramento, D., Pisinger, D., & Ropke, S. (2019). An adaptive large neighborhood search metaheuristic for the vehicle routing problem with drones. *Transportation Research Part C: Emerging Technologies*, *102*, 289–315.

Shaw, P. (1998). Using constraint programming and local search methods to solve vehicle routing problems. *International conference on principles and practice of constraint programming*, 417–431.

Sun, P., Veelenturf, L. P., Hewitt, M., & Van Woensel, T. (2020). Adaptive large neighborhood search for the time-dependent profitable pickup and delivery problem with time windows. *Transportation Research Part E: Logistics and Transportation Review*, *138*, 101942.

Tholen, M. v. d., Beirigo, B. A., Jovanova, J., & Schulte, F. (2021). The share-a-ride problem with integrated routing and design decisions: The case of mixed-purpose shared autonomous vehicles. *Computational Logistics: 12th International Conference, ICCL 2021, Enschede, The Netherlands, September 27–29, 2021, Proceedings 12*, 347–361.

Transport DTU. (2022). *Transport economic unit prices v2.0*. https://www.cta.man.dtu.dk/modelbibliotek/teresa/transportoekonomiske-enhedspriser

Van Duin, R., Wiegmans, B., Tavasszy, L., Hendriks, B., & He, Y. (2019). Evaluating new participative city logistics concepts: The case of cargo hitching. *Transportation Research Procedia*, *39*, 565–575.

Vansteenwegen, P., Melis, L., Aktaş, D., Montenegro, B. D. G., Vieira, F. S., & Sörensen, K. (2022). A survey on demand-responsive public bus systems. *Transportation Research Part C: Emerging Technologies*, *137*, 103573.

Wang, X., Poikonen, S., & Golden, B. (2017). The vehicle routing problem with drones: Several worst-case results. *Optimization Letters*, *11*, 679–697.

Wang, Y., Wang, Z., Hu, X., Xue, G., & Guan, X. (2022). Truck–drone hybrid routing problem with time-dependent road travel time. *Transportation Research Part C: Emerging Technologies*, *144*, 103901.

Wang, Z., & Sheu, J.-B. (2019). Vehicle routing problem with drones. *Transportation research part B: methodological*, *122*, 350–364.

Williams, E., Das, V., & Fisher, A. (2020). Assessing the sustainability implications of autonomous vehicles: Recommendations for research community practice. *Sustainability*, *12*(5), 1902.

Yu, V. F., Indrakarna, P. A., Redi, A. A. N. P., & Lin, S.-W. (2021). Simulated annealing with mutation strategy for the share-a-ride problem with flexible compartments. *Mathematics*, *9*(18), 2320.

Yu, V. F., Purwanti, S. S., Redi, A. P., Lu, C.-C., Suprayogi, S., & Jewpanya, P. (2018). Simulated annealing heuristic for the general share-a-ride problem. *Engineering Optimization*, *50*(7), 1178–1197.

Zhao, J., Poon, M., Zhang, Z., & Gu, R. (2022). Adaptive large neighborhood search for the time-dependent profitable dial-a-ride problem. *Computers & Operations Research*, *147*, 105938.

4 A passenger and parcel share-a-ride problem with drones: A column generation approach

Cheng, R., Jiang, Y., Nielsen, O. A., & Van Woensel, T. (2023). A passenger and parcel share-a-ride problem with drones: A column generation approach. Under Review in Transportation Research Part B: Methodological

Abstract

The increasing worries regarding traffic congestion and environmental pollution necessitate innovative solutions to improve urban mobility for people and goods. An emerging and innovative concept involves the integration of passenger and parcel transportation using demand-responsive buses (DRBs) and drones. This integration aims to reduce the number of vehicles on the road by combining the movement of passengers and parcels. Each DRB is equipped with a drone in this concept and collaborates in its operations. While DRBs can serve passengers and parcels, drones are exclusively designated for parcel delivery. In this context, we introduce the induced route planning problem for DRBs and drones, termed the passenger and parcel Share-a-Ride Problem with Drones (SARP-D). We formulate a model based on paths to address this challenge and propose a column generation approach. We develop a specialized label correcting algorithm to tackle the pricing problem of column generation, which involves finding the best paths with limited resources. We conducted thorough numerical experiments to validate the effectiveness of our proposed methods. Our computational results demonstrate that the column generation approach offers notable advantages: firstly, it outperforms the CPLEX solver for smaller instances comprising up to 12 nodes; secondly, it achieves either optimal solutions or solutions very close to optimality within 3 hours for instances involving 50 nodes. Finally, we present several valuable insights for managerial considerations based on our findings.

Keywords: Urban logistics; On-demand transit; Integrated passenger and parcel transportation; Share-a-ride problem with drones; Vehicle routing problem with drones

4.1 Introduction

The transportation demands for people and goods increased significantly due to the rapid pace of urbanization and the E-commerce boom. Consequently, more and more vehicles move on the road to fulfill the growing transportation demands, aggravating traffic congestion and environmental pollution. Thereby, scholars and practitioners proposed several solutions to mitigate negative externalities of transportation.

One novel idea is integrating people and goods transportation because it can serve the same transportation demands with fewer vehicles. Traditionally, these two types of transportation are operated separately. Given that passenger and freight vehicles usually share and compete for road space and infrastructures, the European Commission (2007) pointed out that "local authorities need to consider all urban logistics related to passenger and freight transport as a single logistics system." In recent decades, multiple forms of integrating people and goods transportation, e.g., people and parcels sharing a taxi, freight on transit, have been explored in the literature (Ghilas et al., 2018; Ghilas et al., 2016; Li et al., 2014; Mourad et al., 2021) and successfully implemented in real-life (Cochrane et al., 2017). For example, Liftago, a taxi company in Prague, allows drivers to carry passengers and parcels simultaneously[1]; Cargo-Tram/E-tram transports waste via scheduled trams operated on existing public transport lines in Zurich[2]; buses with underutilized capacity are used to deliver parcels to rural areas in China[3]. For a comprehensive review of the integrated people and goods transportation, readers are referred to Cheng et al. (2023a).

Emerging technologies present another approach to alleviating the adverse impacts of transportation. For example, mobile and wireless communication technologies enable transportation companies to provide ride-hailing services, which could reduce traffic congestion (Yao & Bekhor, 2023). Autonomous vehicles could reduce passenger transport-related congestion by improving coordination between vehicles and reducing parking demand (Anderson et al., 2014; Othman, 2022). Although the impacts of autonomous vehicles on the environment vary depending on specific circumstances, there is a general recognition of the positive environmental benefits of electrifying AVs (Golbabaei et al., 2021). In city logistics, drones have been increasingly deployed for parcel delivery due to their advantages in speed and low greenhouse gas emissions (Agatz et al., 2018). For instance, Amazon and Walmart have provided drone delivery services to customers in some areas, e.g., Texas, Arizona, and Florida[4]. Drones usually have a limited service range, constrained by the limited battery capacity. To address this problem, a hybrid delivery system that involves trucks serving as mobile platforms for drones' takeoff, landing, and recharging has been proposed (Murray & Chu, 2015).

Inspired by the two ideas mentioned above, Cheng et al. (2023b) first proposed a novel integrated transportation system that combines the transportation of passengers and parcels using demand-responsive vehicles (DRBs) and drones to mitigate the negative impacts of increasing transportation demands in urban areas. In this integrated system, DRBs provide door-to-door service for passengers and parcels, while drones are only responsible

[1] https://www.prague-taxi.co.uk/taxi-drivers-to-become-couriers-and-carriers-liftago-will-be-delivering-packages-and-food/

[2] https://www.stadt-zuerich.ch/ted/de/index/entsorgung_recycling/publikationen_broschueren/fahrplan_cargo_tram_und_e_tram.html

[3] https://m-live.cctvnews.cctv.com/live/landscape.html?toc_style_id=feeds_only_back&liveRoomNumber=8265779572060234721&share_to=wechat&track_id=03E204C5-8EFA-4085-83AE-5673F19394FE_701442053332

[4] (1) https://www.aboutamazon.com/news/transportation/amazons-drone-delivery-is-coming-to-texas; (2) https://corporate.walmart.com/newsroom/2022/05/24/were-bringing-the-convenience-of-drone-delivery-to-4-million-u-s-households-in-partnership-with-droneup

for parcel delivery.

Figure 4.1 provides a schematic overview of the integrated passenger and parcel transportation system with DRBs and drones. This figure involves three passenger requests, four parcel requests, and two DRBs, each equipped with a drone. The origin-destination pairs for the three passenger requests are 1-4, 2-5, and 3-6. Parcel requests 8, 9, and 10 are eligible for drone service, while parcel request 7 can be served only by a DRB. Given that passenger vehicles and vans share the same urban environment, it makes sense to combine some passengers and parcels instead of utilizing dedicated passenger vehicles and vans, especially when the passenger stops and parcel stops are close. It is expected that the operation cost and the number of used vehicles will be reduced in the proposed system. The successful operation of such an integrated transportation system relies on planning the routes for DRBs and drones. The corresponding route planning problem is the passenger and parcel Share-a-Ride Problem with Drones (SARP-D). Section 4.3.1 presents a more detailed description of the SARP-D.

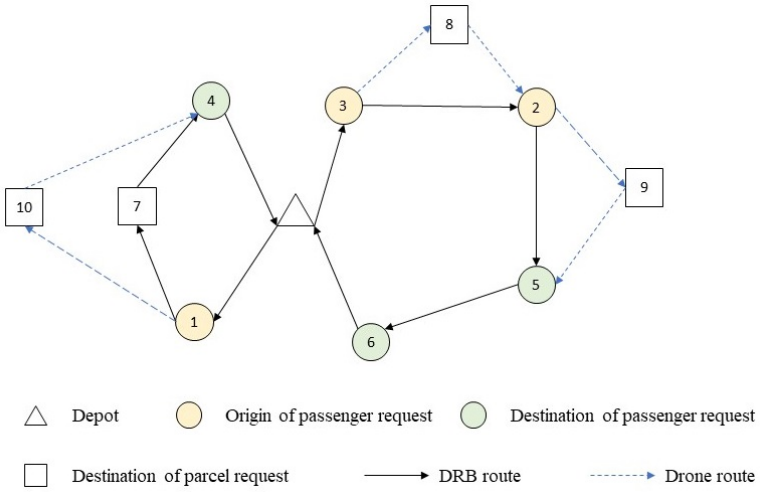

Figure 4.1: An illustrative example of the SARP-D

Since the SARP-D is a rather novel idea, little research has been conducted. To solve the SARP-D, Cheng et al. (2023b) developed a mixed integer non-linear programming model and an adaptive large neighborhood search (ALNS) metaheuristic for solving large-size instances. Nevertheless, as it is generally acknowledged that metaheuristics can hardly guarantee a global optimal solution, it is thus intriguing to evaluate the performance of a metaheuristic algorithm by knowing the gap to a potential optimal solution. To fill this niche, this study presents a column generation (CG) approach that provides a validated lower bound for the SARP-D. To the best of our knowledge, this is the first study that presents an approach for evaluating the algorithm performance for the SARP-D. Meanwhile, we conducted extensive numerical experiments to evaluate our proposed solution's performance and explore SARP-D's properties.

To sum up, this paper studies an integrated passenger and goods transportation system using DRBs and drones. It aims to reduce the number of vehicles on the road by combining passenger and goods flows. The integration is exemplified by cases where taxis carry passengers and parcels, and buses deliver packages to rural areas. It also considers the potential of emerging technologies, specifically drones, to alleviate transportation issues. The contributions of this paper are summarized as follows:

- We formulate a path-based model to address the passenger and parcel share-a-ride

problem with drones (SARP-D). This problem aims to optimize routes for DRBs and drones to efficiently serve passengers and deliver parcels.

- The paper proposes a column generation approach to solve the SARP-D efficiently. The column generation approach aims to find optimal or near-optimal solutions within a reasonable time frame. The results of the extensive numerical experiments demonstrate the advantages of the proposed column generation approach, particularly for smaller instances compared with the CPLEX solver and instances involving up to 50 nodes.
- The paper concludes by presenting insights that can be valuable for decision-makers and managers in urban logistics. These insights are drawn from the computational results and sensitivity analysis of critical parameters in the proposed transportation system.

The remainder of this paper is organized as follows. Section 4.2 reviews the related literature on SARP and VRP-D. Section 4.3 and Section 4.4 present the mathematical models and column generation approach for the proposed SARP-D, respectively. Section 4.5 conducts extensive numerical experiments to evaluate the performance of the CG. Section 4.6 conducts sensitivity analysis to explore the properties of the proposed transportation system. Section 4.7 concludes this paper and provides future directions.

4.2 Literature review

This section reviews the literature on passenger and parcel share-a-ride problem (SARP) and vehicle routing problem with drones (VRP-D), two problems closely related to the proposed SARP-D, and compares the differences between the SARP, VRP-D, and SARP-D.

4.2.1 SARP

Li et al. (2014) first proposed the SARP, a routing problem for integrating passenger and parcel transportation using taxis. Three assumptions are made in this pioneering work to prioritize passengers to parcels: A1) Passengers' rides are subject to a maximum time limit; A2) When serving one passenger request, the number of parcel stops that can be visited is no more than a maximum number; A3) Passengers only share a ride with parcels instead of other passengers. Yu et al. (2018) proposed a general SARP, which relaxes the three assumptions and leads to a higher profit. Additionally, numerous features have been added to the original SARP to cater to diverse application scenarios. For example, Li et al. (2016b) investigated the SARP with stochastic travel times and delivery locations; Yu et al. (2021) allowed passenger compartments to be used by parcels; Lu et al. (2022) explored the routing problem with a mixed fleet consisting of electric and gasoline vehicles.

Existing approaches to solving the SARP include ALNS (Li et al., 2016a, 2016b) and simulated annealing (Yu et al., 2021; Yu et al., 2018), math-heuristic (Lu et al., 2022; Yu et al., 2023), and Lagrangian dual decomposition (Zhang et al., 2022).

4.2.2 Truck-drone routing problem

Murray and Chu (2015) first introduced the traveling salesman problem with drones (TSP-D) for a single truck and a single drone delivery system. The drone has maximum flight endurance and can deliver only one parcel during one flight but can perform several flights along the truck route. It is restricted that the launch and recovery locations for a drone flight should be different. Murray and Chu (2015) defined a flying sidekick traveling salesman problem (FSTSP) and a parallel drone scheduling traveling salesman problem (PDSTSP).

In the former case, the truck and the drone work cooperatively, and they must be synchronized at some points, e.g., customer locations or the depot. In contrast, the truck and the drone work independently without synchronization in the latter case. The objectives of the FSTSP and PDSTSP in Murray and Chu (2015) are to minimize the latest time a truck or a drone returns to the depot. Subsequently, various variants of the TSP-D have been studied, e.g., allowing a drone to be retrieved at its launch point (Agatz et al., 2018), equipping one truck with multiple drones (Murray & Raj, 2020), allowing a drone to visit multiple nodes during one flight (Poikonen & Golden, 2020), minimizing the cost-related objectives (Ha et al., 2018), modeling the energy used by a drone (Jeong et al., 2019), and considering time windows (Luo et al., 2021).

Another important branch in the truck-drone routing problem is the vehicle routing problem with drones (VRP-D). Unlike the TSP-D, which involves only one truck, the VRP-D has multiple trucks. Similar to the TSP-D, there are lots of variants of the VRP-D in terms of the regulation of launch and recovery locations of drones, the number of drones associated with each truck, multiple visits during one flight, objective functions, drone energy modeling, time windows, etc. (Di Puglia Pugliese et al., 2021; Poikonen et al., 2017; Sacramento et al., 2019; Wang et al., 2017; Xia et al., 2023). Most of the literature on the VRP-D assumes that the drone should take off and land on the same truck. One interesting variant of the VRP-D is the introduction of docking hubs which serve as transfer locations for drones to land and travel with another truck (Wang & Sheu, 2019; Xia et al., 2023).

The solution approaches for the TSP-D and VRP-D are classified into heuristic / metaheuristic algorithms and exact methods. Because both the TSP-D and VRP-D are NP-hard and cannot be solved to optimality within a polynomial time for large instances, researchers have devised many heuristic/metaheuristics such as evolutionary-based heuristic algorithms (Jeong et al., 2019), hybrid heuristic algorithm (Luo et al., 2021; Salama & Srinivas, 2022), greedy randomized adaptive search procedure (Ha et al., 2018), ALNS (Sacramento et al., 2019). Although heuristics and metaheuristics could solve large-scale instances with 100 to 200 nodes, evaluating the algorithm performance regarding the solution quality is hard because these algorithms usually provide only the lower (upper) bounds of the instances. In comparison, the upper (lower) bounds are not known. Therefore, several exact methods such as branch-and-cut (Cavani et al., 2021; Tamke & Buscher, 2021; Tiniç et al., 2023), branch-and-price (Roberti & Ruthmair, 2021; Yang et al., 2023; Zhou et al., 2023), branch-and-price-and-cut (B-P-C) (Li & Wang, 2023; Xia et al., 2023; Yin et al., 2023a; Yin et al., 2023b; Zhen et al., 2023), dynamic programming (Bouman et al., 2018), have been proposed. These exact methods could solve instances with up to 20 to 50 nodes, depending on the attributes of the problems.

Since there are multiple ground vehicles, each equipped with a single drone in our proposed SARP-D, our reviews focus on the VRP-D variants, where there is at most one drone per truck (see Table 4.1). For a more comprehensive review of the truck-drone routing problem, readers are referred to Li et al. (2021) and Macrina et al. (2020).

Sacramento et al. (2019) developed a mixed integer programming model for a VRP-D in which each truck is paired with a drone. The drones have a limited flying time and serve one customer per flight. An ALNS metaheuristic was used to solve instances with up to 200 customers. Kuo et al. (2022) extended the model of Sacramento et al. (2019) by introducing time windows for each customer. They devised a variable neighborhood search (VNS) procedure to solve instances with 50 nodes. Coindreau et al. (2021) assumed each truck could carry at most one drone and set a limited number of used drones.

Table 4.1: A summary of related studies on the VRP-D

Reference	Time window	Multi-visits	Flight range	Objective	Solution method	Maximum instance size
Sacramento et al. (2019)	No	No	Endurance	Cost	ALNS	200
Kuo et al. (2022)	Hard	No	Endurance	Cost	VNS	50
Coindreau et al. (2021)	Hard	No	Endurance	Cost	ALNS	100
Wang et al. (2022)	Hard	No	Distance	Cost	Iterated local search	200
Yin et al. (2023a)	Hard	Yes	Endurance	Cost	B-P-C	45
Yin et al. (2023b)	Hard	Yes	Endurance	Cost	B-P-C	45
Zhen et al. (2023)	No	Yes	Endurance	Cost	B-P-C	14
This paper	Soft	No	Endurance	Cost	CG	50

Multi-visits: The drone visits more than one customer per flight.

They adopted an ALNS metaheuristic that could solve 100-node instances. Wang et al. (2022) investigated a VRP-D with time windows (VRP-DTW) considering time-dependent road travel time. Instances with 200 nodes were solved by an iterated local search heuristic. The four studies above do not allow a drone to serve more than one customer during each flight. This restriction is relaxed by Yin et al. (2023a, 2023b) and Zhen et al. (2023). Yin et al. (2023a) developed a B-P-C algorithm that could optimally solve most VRP-DTW instances with 45 customers. They further applied the B-P-C algorithm to a VRP-DTW with uncertain demands and road travel times (Yin et al., 2023b). Zhen et al. (2023) used the B-P-C algorithm to solve the VRP-D without considering time windows for customers, causing a larger solution space than the VRP-DTW. The largest instances they could solve to optimality contain 14 nodes. All literature presented in Table 4.1 optimizes the cost-related objectives. Most of them assumed the flight range of drones is constrained by endurance, except for Wang et al. (2022), which restricted the distance a drone can fly.

4.2.3 Position of SARP-D

Table 4.2 summarizes the characteristics of the SARP, VRP-D, and SARP-D. From Table 4.2 we can see that the SARP-D shares some similarities with the SARP and VRP-D. For example, both the SARP-D and SARP could serve passenger and parcel requests and provide one-to-one pickup and delivery (PDP) service for passengers. Both the SARP-D and VRP-D have two types of vehicles to serve parcel requests and the parcel requests only have delivery requirements. By setting the count of passenger requests in SARP-D to zero, the SARP-D is simplified to the VRP-D.

However, there are some attributes in the SARP-D, which make it more complicated than the SARP-D and VRP-D. Compared with the SARP, the SARP-D additionally includes drones and requires synchronization between the two types of vehicles. Even if we assume no parcel request can be served by drones, the SARP-D can not be reduced to the SARP. The SARP-D and SARP provide different services for parcels, i.e., delivery service in the SARP-D and one-to-one PDP service in the SARP. Compared with the VRP-D, the ground vehicles in the SARP-D perform one-to-one PDP tasks for passenger transportation and delivery tasks for parcel transportation. In contrast, the ground vehicles in the VRP-D only perform delivery tasks. The different attributes of requests, i.e., PDP or only delivery requirement, lead to a huge difference in modeling the transportation systems because one-to-one PDP has pairing and precedence constraints on requests' origins and destinations while the other does not.

Overall, the SARP-D, which incorporates aerial vehicles for parcel delivery, along with ground vehicles performing both one-to-one PDP and delivery services, is considerably more complex than the SARP and VRP-D, but has the potential to yield significant efficiency gains. However, little research has been conducted on the SARP-D, and the

prior work only developed a metaheuristic for it. This study enriches the research on the SARP-D by providing an approach that could produce high-quality solutions and can be used to evaluate the efficiency of metaheuristics. Meanwhile, this study enriches the existing studies on the SARP and VRP-D.

Table 4.2: Summary of characteristics of the SARP, VRP-D, and SARP-D

	Ground vehicle				Drone
	Passenger request		Parcel request		Parcel request
	Delivery	Pickup and Delivery	Delivery	Pickup and Delivery	Delivery
SARP		✓		✓	
VRP-D			✓		✓
SARP-D		✓	✓		✓

4.3 Problem description and model formulation

4.3.1 Problem description and solution characteristics

Let $|P|$ and $|G|$ denote the number of passenger and parcel requests. The SARP-D is defined on a complete undirected graph $Graph = (N, A)$, where $N = S_p \cup S_g \cup \{0, 2|P| + |G| + 1\}$. $S_p = S_p^o \cup S_p^d$, where S_p^o denote the origin stops of passenger requests and S_p^d denotes the destination stops of passenger requests. S_g denote the destination stops of parcel requests. Some parcel destinations, denoted by $S_g{}'$, could be visited by drones. 0 and $2|P| + |G| + 1$ are the origin and destination depots of DRBs. Each arc $(i, j) \in A$ is associated with a DRB travel cost C_{ij}^V, a drone travel cost C_{ij}^D. Let K denote the set of DRBs. Each DRB is equipped with a drone and can carry a limited number of passengers and parcels.

In the model development, we make the following assumptions: First, each passenger request is characterized by its origin, destination, and demand value. In contrast, all parcel requests stem from a central depot with diverse destinations, albeit with a uniform demand for each parcel. All service requests are fulfilled precisely once. An ample supply of both DRBs and drones is available to serve the requests. DRBs and drones have maximum travel and flying time, respectively. Drones are configured to visit a single customer per flight, with the flexibility to conduct multiple flights along a single route. Drones' take-off and recovery points vary in each flight, although they can share the same node for landing and take-off. Each node has a predefined service time for DRBs involving passenger boarding/alighting and for drones at customer locations. Notably, the time required to set up drone launch and recovery is no less than the DRB service time. The launch and recovery of drones can occur concurrently with passenger actions or recipient parcel pickups due to an integrated robotic shelving system. Drones are optimized to take off when a DRB commences customer service to conserve battery energy. Drones hover during waiting periods at recovery locations. Time windows are in place for each node, dictating when DRBs and drones can initiate service; delays within these windows incur penalties. Lastly, the travel time and cost matrices adhere to the triangle inequality, a property attainable by transforming arbitrary matrices (Ropke & Cordeau, 2009).

The SARP-D presented in this study aims to find the paths of DRBs and drones to serve all requests with the minimum operation costs, including the transportation costs of the two types of vehicles and delay penalties. To facilitate the presentation of our mathematical models in this section and solution method in Section 4.4, we introduce several concepts to characterize the solution of SARP-D and explain the solution shown in Figure 4.1 using these concepts.

Nodes

The stops of passengers and parcels are categorized into three types according to which type(s) of vehicles visit this node.

i) A *DRB node* is a node visited by a DRB alone.

ii) A *drone node* is a node visited by a drone alone.

iii) A *combined node* is a node visited by a DRB and a drone together.

We define four additional node types according to the activities performed at a node.

iv) A *common node* is a node without either launch or recovery activities. It could be a DRB node or a combined node.

v) A *launch node* is a combined node where a drone takes off.

vi) A *recovery node* is a combined node where a drone lands.

vii) A *recovery-launch node* is a combined node where a drone lands first and then takes off to perform another flight.

Arcs

i) A *DRB arc* is an arc traversed by a DRB alone, represented by $i \rightarrow j$.

ii) A *drone arc* is an arc traversed by a drone alone, represented by (i, j).

iii) A *combined arc* is an arc traversed by DRB and drone, represented by $i \Rightarrow j$.

Legs

i) A *DRB leg* is a series of DRB arcs between two consecutive combined nodes.

ii) A *drone leg* consists of two consecutive drone arcs between two combined nodes, represented by $< i, j, k >$, where i is the launch node, j is the drone node, and k is the recovery node.

iii) A *combined leg* is a sequence of consecutive combined arcs.

Operation

Finally, a DRB and drone legs between the same pair of combined nodes constitute an *operation* represented by "[]".

Path

A path is feasible only if the following constraints are satisfied: (i) It starts and ends at the depot; (ii) It visits a node once; (iii) The vehicle capacity constraint, the DRB maximum travel time constraint, the maximum number of intermediate stops between one passenger request service constraint, pairing and precedence constraints on passenger origins and destinations, and drone operation constraints (i.e., flying time, one customer per flight, different launch and recovery points in a flight) are satisfied.

A path can be considered concatenating combined legs and operations, and a SARP-D solution comprises one or multiple paths.

Example

Let 0 and 11 denote the start and end points of DRBs. We introduce the solution of Figure 4.1 using the previously defined concepts. The solution of Figure 4.1 has 1 DRB node

(7), 6 combined nodes (1, 4, 3, 2, 5, 6), 3 drone nodes (10, 8, 9), 2 launch nodes (1, 3), 2 recovery nodes (4, 5), 1 recovery-launch node (2), 2 common nodes (7, 6), 4 DRB arcs (1→7, 7→4, 3→2, 2→5), 6 drone arcs ((1,10), (10,4), (3,8), (8,2), (2,9), (9,5)), 5 combined arcs ($0 \Rightarrow 1$, $4 \Rightarrow 11$, $0 \Rightarrow 3$, $5 \Rightarrow 6$, $6 \Rightarrow 11$), 3 DRB legs (1→7→4, 3→2, 2→5), 3 drone legs (<1,10,4>, <3,8,2>, <2,9,5>), and 4 combined legs (0⇒1, 4⇒11, 0⇒3, 5⇒6⇒11). The solution of Figure 4.1 contains two paths. The first path is represented by a combination of 1 operation ([1→7→4, <1,10,4>]) and 2 combined legs ($0 \Rightarrow 1$, $4 \Rightarrow 11$). The second path is represented by a combination of 2 operations ([3→2, <3,8,2>], [2→5, <2,9,5>]) and 2 combined legs ($0 \Rightarrow 3$, $5 \Rightarrow 6 \Rightarrow 11$).

4.3.2 Notation

All notations used in Sections 4.3.3 and 4.3.4 are summarized in Table 4.3.

Table 4.3: Notations

Sets	
K	Set of homogeneous DRBs, $K = \{1, 2, ..., \|K\|\}$, where $\|K\|$ is the number of vehicles.
S_p^o	Set of origins of passenger requests, $S_p^o = \{1, 2, ..., \|P\|\}$, where $\|P\|$ is the number of passenger requests.
S_p^d	Set of destinations of passenger requests, $S_p^d = \{\|P\| + 1, \|P\| + 2, ..., 2\|P\|\}$.
S_p	Set of passenger stops, $S_p = S_p^o \cup S_p^d$.
S_g	Set of goods stops (destinations), $S_g = \{2\|P\| + 1, 2\|P\| + 2, ..., 2\|P\| + \|G\|\}$, where $\|G\|$ is the number of parcel requests.
$S_g{}'$	$S_g{}' \subseteq S_g$, set of parcel requests that a drone can deliver.
S	Set of passenger and goods stops, $S = S_p \cup S_g$.
N	Set of all nodes, $N = S_p \cup S_g \cup \{0, 2\|P\| + \|G\| + 1\}$, where 0 and $2\|P\|+\|G\|+1$ are the depot nodes indicating the start and end nodes of a route.
N_0	Set of nodes from which a DRB may depart, $N_0 = \{0, 1, ..., 2\|P\| + \|G\|\}$.
N_+	Set of nodes to which a DRB may arrive, $N_+ = \{1, 2, ..., 2\|P\| + \|G\| + 1\}$.
$\Delta^+(i)$	Set of nodes reachable from node $i \in N_0$, $\Delta^+(i) = N_+ \setminus \{i\}$.
$\Delta^-(i)$	Set of nodes that can be used to reach node $i \in N_+$, $\Delta^-(i) = N_0 \setminus \{i\}$.
R	Set of all feasible paths.
Parameters	
Cap^P	Capacity of the passenger compartment in each DRB.
Cap^G	Capacity of the goods compartment in each DRB.
T_{ij}^V	Time required for a DRB to travel from node $i \in N_0$ to node $j \in N_+$.
T_{ij}^D	Time required for a drone to travel from node $i \in N_0$ to node $j \in N_+$.
E	Maximum flight duration of a drone.
ST_i^V	Service time for a DRB at node $i \in S$.
ST_i^D	Service time for a drone at node $i \in S_g{}'$.
Q_i	Number of passengers boarding a DRB at node $i \in S$. $Q_{i+\|P\|} = -Q_i, \forall i \in S_p^o$ and $Q_i = 0, \forall i \in S_g$.
$T_{\max}$	Maximum travel time on a DRB route.
C_{ij}^V	Transportation cost for a DRB traveling from node $i \in N_0$ to node $j \in N_+$.
C_{ij}^D	Transportation cost for a drone flying from node $i \in N_0$ to node $j \in N_+$.
$[E_i, L_i]$	The earliest and latest service start times at node $i \in S$.
SL	Setup time required to launch a drone.
SR	Setup time required to retrieve a drone.
α_i	Unit delay penalty at node $i \in S$.

η	Maximum intermediate stops between the origin and destination of a passenger request.
c_r	Cost of a path $r \in R$.
a_{ir}	$a_{ir} = 1$ if path $r \in R$ visits node $i \in S_p \cup S_g$; otherwise $a_{ir} = 0$.
Decision Variables	
x_{ij}^k	$x_{ij}^k = 1$ if DRB $k \in K$ travels from node $i \in N_0$ to node $j \in N_+$; otherwise, $x_{ij}^k = 0$.
y_{ajb}^k	$y_{ajb}^k = 1$ if sortie $< a, j, b >$ is used in the route of DRB $k \in K$, where $a \in N_0$ represents the launch node of the drone, $j \in S_g{}'$ represents the goods request served by a drone, $b \in N_+$ represents the rendezvous node of the drone; otherwise, $y_{ajb}^k = 0$.
w_i^k	Load of the passenger compartment of DRB $k \in K$ after the visitation of node $i \in S$.
t_j^k	If node $j \in N_+$ is a recovery node or recovery-launch node, t_j^k is the time point at which the drone is recovered by DRB $k \in K$ at node $j \in N_+$; otherwise, t_j^k is the arrival time of DRB $k \in K$ at node $j \in N$ or the arrival time of drone $k \in K$ at node $j \in S_g{}'$.
t'^k_j	If node $j \in S$ is a recovery node, t'^k_j is the time point at which DRB $k \in K$ leaves node $j \in S$; if node $j \in S$ is a launch node or recovery-launch node, t'^k_j is the time point at which drone $k \in K$ starts taking off; otherwise, t'^k_j is the time point at which DRB $k \in K$ starts service at node $j \in S$ or drone $k \in K$ starts service at node $j \in S_g{}'$.
u_i^k	A continuous variable indicating the position of node $i \in N$ in the route of DRB $k \in K$.
p_{ij}^k	$p_{ij}^k = 1$ if node $j \in S$ is visited after node $i \in N_0$ in the route of DRB $k \in K$.
λ_a^k	Delay of DRB/drone $k \in K$ at node $a \in S$.
χ_r	$\chi_r = 1$ if path $r \in R$ is included in the solution; otherwise $\chi_r = 0$.

4.3.3 Arc-based formulation

Cheng et al. (2023b) first devised an arc-based formulation for the SARP-D. They further linearized the model to make it solvable by CPLEX for small instances. For the sake of completeness of the paper and readers' convenience, we copied their arc-based formulation and briefly explained the constraints in this section. A detailed explanation of each constraint and the linearization method can be found in Cheng et al. (2023b).

$$\min \sum_{k \in K} \left[\sum_{i \in N_0} \sum_{j \in \Delta^+(i)} C_{ij}^V x_{ij}^k + \sum_{c \in S_g{}'} \sum_{a \in \Delta^-(c)} \sum_{b \in \Delta^+(c), b \neq a} \left(C_{ac}^D + C_{cb}^D \right) y_{acb}^k + \sum_{m \in S} \alpha_m \lambda_m^k \right] \tag{4.1}$$

s.t.

$$\sum_{i \in \Delta^-(j)} \sum_{k \in K} x_{ij}^k = 1, \forall j \in S_p^o \cup \left(S_g \backslash S_g{}' \right) \tag{4.2}$$

$$\sum_{i \in \Delta^-(j)} x_{ij}^k = \sum_{i \in \Delta^-(j+|P|)} x_{i,j+|P|}^k, \forall j \in S_p^o, k \in K \tag{4.3}$$

$$\sum_{i \in \Delta^-(j)} \sum_{k \in K} x_{ij}^k + \sum_{a \in \Delta^-(j)} \sum_{b \in \Delta^+(j), b \neq a} \sum_{k \in K} y_{ajb}^k = 1, \forall j \in S_g{}' \tag{4.4}$$

$$\sum_{j \in N_+} x_{0j}^k \leq 1, \forall k \in K \tag{4.5}$$

$$\sum_{j \in N_0} x_{j,2|P|+|G|+1}^k \leq 1, \forall k \in K \tag{4.6}$$

$$x^k_{0,2|P|+|G|+1} = 0, \forall k \in K \tag{4.7}$$

$$\sum_{i \in \Delta^-(j)} x^k_{ij} = \sum_{i \in \Delta^+(j)} x^k_{ji}, \forall j \in S, k \in K \tag{4.8}$$

$$w^k_0 = 0, \forall k \in K \tag{4.9}$$

$$w^k_j \geq w^k_i + Q_j - \left(1 - x^k_{ij}\right) M, \forall i \in N_0, j \in S \backslash \{i\}, k \in K \tag{4.10}$$

$$\mathsf{max}\{0, Q_i\} \leq w^k_i \leq \mathsf{min}\left\{Cap^P, Cap^P + Q_i\right\}, \forall i \in S, k \in K \tag{4.11}$$

$$\sum_{i \in N_0} \sum_{j \in S_g{}', j \neq i} x^k_{ij} + \sum_{c \in S_g{}'} \sum_{a \in \Delta^-(c)} \sum_{b \in \Delta^+(c), b \neq a} y^k_{acb} \leq Cap^G, \forall k \in K \tag{4.12}$$

$$\sum_{j \in S_g{}', j \neq a} \sum_{b \in \Delta^+(j), b \neq a} y^k_{ajb} \leq 1, \forall a \in N_0, k \in K \tag{4.13}$$

$$\sum_{j \in S_g{}', j \neq b} \sum_{a \in \Delta^-(j), a \neq b} y^k_{ajb} \leq 1, \forall b \in N_+, k \in K \tag{4.14}$$

$$2y^k_{ajb} \leq \sum_{h \in \Delta^+(a)} x^k_{ah} + \sum_{l \in \Delta^-(b)} x^k_{lb}, \forall a \in N_0, j \in \left\{S_g{}' : j \neq a\right\}, b \in \left\{\Delta^+(j) : b \neq a\right\}, k \in K \tag{4.15}$$

$$y^k_{0,j,2|P|+|G|+1} = 0, \forall j \in S_g{}', k \in K \tag{4.16}$$

$$t^k_0 = 0, \forall k \in K \tag{4.17}$$

$$t^k_{2|P|+|G|+1} \leq T_{\mathsf{max}} \sum_{i \in N_0} x^k_{i,2|P|+|G|+1}, \forall k \in K \tag{4.18}$$

$$t'^k_a \geq t^k_a, \forall a \in N, k \in K \tag{4.19}$$

$$t'^k_0 + T^V_{0b} + SL \sum_{h \in S_g{}'} \sum_{l \in \Delta^+(h)} y^k_{0hl} + SR \sum_{g \in S_g{}', g \neq b} \sum_{f \in \Delta^-(g), f \neq b} y^k_{fgb} \leq t^k_b + T_{\mathsf{max}}\left(1 - x^k_{0b}\right), \forall b \in N_+, k \in K \tag{4.20}$$

$$t'^k_a + T^V_{ab} + \mathsf{max}\left(1 - \sum_{\substack{h \in S_g{}' \\ h \neq a}} \sum_{\substack{l \in \Delta^+(h) \\ l \neq a}} y^k_{ahl} - \sum_{\substack{n \in S_g{}' \\ n \neq a}} \sum_{\substack{m \in \Delta^-(n) \\ m \neq a}} y^k_{mna}, 0\right) ST^V_a + SL \sum_{\substack{h \in S_g{}' \\ h \neq a}} \sum_{\substack{l \in \Delta^+(h) \\ l \neq a}} y^k_{ahl}$$
$$+ SR \sum_{g \in S_g{}', g \neq b} \sum_{f \in \Delta^-(g), f \neq b} y^k_{fgb} \leq t^k_b + T_{\mathsf{max}}\left(1 - x^k_{ab}\right), \forall a \in S, b \in \Delta^+(a), k \in K \tag{4.21}$$

$$t'^k_i + T^D_{ij} + SL - T_{\mathsf{max}}\left(1 - \sum_{b \in \Delta^+(j), b \neq i} y^k_{ijb}\right) \leq t^k_j, \forall j \in S_g{}', i \in \Delta^-(j), k \in K \tag{4.22}$$

$$t'^k_j + T^D_{jb} + ST^D_j + SR - T_{\mathsf{max}}\left(1 - \sum_{a \in \Delta^-(j), a \neq b} y^k_{ajb}\right) \leq t^k_b, \forall j \in S_g{}', b \in \Delta^+(j), k \in K \tag{4.23}$$

$$\lambda^k_b \geq \left(t'^k_0 + T^V_{0b} + SL \sum_{h \in S_g{}'} \sum_{l \in \Delta^+(h)} y^k_{0hl} - T_{\mathsf{max}}\left(1 - x^k_{0b}\right) - L_b\right)^+, \forall b \in S, k \in K \tag{4.24}$$

$$\lambda^k_b \geq \left(\begin{array}{l} t'^k_a + T^V_{ab} + \mathsf{max}\left(1 - \sum\limits_{\substack{h \in S_g{}' \\ h \neq a}} \sum\limits_{\substack{l \in \Delta^+(h) \\ l \neq a}} y^k_{ahl} - \sum\limits_{\substack{n \in S_g{}' \\ n \neq a}} \sum\limits_{\substack{m \in \Delta^-(n) \\ m \neq a}} y^k_{mna}, 0\right) ST^V_a \\ + SL \sum\limits_{\substack{h \in S_g{}' \\ h \neq a}} \sum\limits_{\substack{l \in \Delta^+(h) \\ l \neq a}} y^k_{ahl} - T_{\mathsf{max}}\left(1 - x^k_{ab}\right) - L_b \end{array}\right)^+, \tag{4.25}$$
$$\forall a \in S, b \in \Delta^+(a), k \in K$$

$$\lambda_j^k \geq \left({t'}_i^k + T_{ij}^D + SL - T_{\max} \left(1 - \sum_{b \in \Delta^+(j), b \neq i} y_{ijb}^k \right) - L_j \right)^+, \forall j \in {S_g}', i \in \Delta^-(j), k \in K \tag{4.26}$$

$${t'}_a^k - ST_a^V \sum_{n \in {S_g}', n \neq a} \sum_{m \in \Delta^-(n), m \neq a} y_{mna}^k \geq E_a, \forall a \in S, k \in K \tag{4.27}$$

$$t_b^k - {t'}_a^k \leq E + T_{\max} \left(1 - \sum_{j \in {S_g}', j \neq a, j \neq b} y_{ajb}^k \right), \forall a \in N_0, b \in \Delta^+(a), k \in K \tag{4.28}$$

$$1 - M\left(1 - x_{ij}^k\right) \leq u_j^k - u_i^k, \forall i \in N_0, j \in \Delta^+(i), k \in K \tag{4.29}$$

$$u_j^k - u_i^k \leq 1 - M\left(x_{ij}^k - 1\right), \forall i \in N_0, j \in \Delta^+(i), k \in K \tag{4.30}$$

$$u_j^k \leq M \sum_{i \in \Delta^-(j)} x_{ij}^k, \forall j \in N_+, k \in K \tag{4.31}$$

$$u_j^k - u_i^k \leq M p_{ij}^k, \forall i \in N_0, j \in S \backslash \{i\}, k \in K \tag{4.32}$$

$$u_j^k - u_i^k \geq M(p_{ij}^k - 1) + 1, \forall i \in N_0, j \in S \backslash \{i\}, k \in K \tag{4.33}$$

$$t_b^k - T_{\max} \left(3 - \sum_{j \in {S_g}'} y_{ajb}^k - \sum_{\substack{m \in {S_g}', m \neq l \\ m \neq a, m \neq b}} \sum_{\substack{n \in \Delta^+(m) \\ n \neq a, n \neq b}} y_{lmn}^k - p_{al}^k \right) \leq t_l^k, \forall k \in K, a \in N_0, b \in N_+, l \in S \backslash \{a, b\} \tag{4.34}$$

$$u_{i+|P|}^k - u_i^k \geq 0, \forall i \in S_p^o, k \in K \tag{4.35}$$

$$u_{i+|P|}^k - u_i^k - 1 \leq \eta, \forall i \in S_p^o, k \in K \tag{4.36}$$

$$x_{ij}^k \in \{0, 1\}, \forall i \in N_0, j \in \Delta^+(i), k \in K \tag{4.37}$$

$$y_{ajb}^k \in \{0, 1\}, \forall k \in K, a \in N_0, j \in \left\{ {S_g}' : j \neq a \right\}, b \in \left\{ \Delta^+(j) : b \neq a \right\} \tag{4.38}$$

$$u_i^k, t_i^k, {t'}_i^k \geq 0, \forall i \in N, k \in K \tag{4.39}$$

$$p_{ij}^k \in \{0, 1\}, \forall i \in N_0, j \in S \backslash \{i\}, k \in K \tag{4.40}$$

The objective function (4.1) is to minimize the sum of transportation costs of DRBs and drones and the delay penalty at each node. Constraints are classified into three categories.

- Routing and flow constraints (constraints (4.2)-(4.16) and (4.29) - (4.36)).

  Regarding DRB operations, constraints (4.2) ensure that nodes that can only be served by DRBs are visited by DRBs exactly once. Constraints (4.3) ensure the pickup and delivery points of a passenger request are visited by the same vehicle, and constraints (4.35) ensure that the origin of a passenger request is visited before its destination. Constraints (4.5) - (4.7) state that each DRB leaves and returns to the depot at most once, and DRBs do not travel between depots. Constraints (4.8) ensure flow conservation. Constraints (4.9) - (4.12) ensure that the DRB load does not exceed the capacity for passengers and goods. Constraints (4.29) - (4.33) define the position of each node that DRB visits and eliminate the sub-tours of DRBs. Constraints (4.36) ensure at most η intermediate stops between one passenger request service.

  Regarding drone operations, constraints (4.13) - (4.14) ensure that a drone can be launched or recovered at each location at most once. Constraints (4.16) prohibit the

drone from picking up a parcel from the depot, visiting the customer, and returning to the depot. Constraints (4.34) ensure that a drone can perform another delivery task only after finishing the previous one.

Regarding the cooperation between DRBs and drones, constraints (4.4) ensure that nodes eligible for drone service are visited exactly once, either by a DRB or a drone. Constraints (4.15) ensure that the DRB must visit nodes where its corresponding drone takes off and lands.

- Scheduling and synchronization constraints (constraints (4.17) - (4.28)). Constraints (4.17) state that DRBs and drones are ready at the depot at time 0, and constraints (4.18) ensure that DRBs and drones must return to the depot before exceeding the maximum working time of a DRB. Constraints (4.19) - (4.23) calculate t_a^k and t'^k_a and regulate their relations. Constraints (4.24) - (4.26) calculate the delay time at each node. Constraints (4.27) ensure that DRBs and drones can only start services after the earliest service start time. Constraints (4.28) regulate the maximum flying time of a flight.
- Decision variable domain constraints (constraints (4.37) - (4.40)).

4.3.4 Path-based formulation

This study proposes a path-based formulation that can be solved via a column generation approach.

$$\min \sum_{r \in R} c_r \chi_r \tag{4.41}$$

s.t.

$$\sum_{r \in R} a_{ir} \chi_r \geq 1, \forall i \in S_p \cup S_g \tag{4.42}$$

$$\chi_r \in \{0, 1\}, \forall r \in R \tag{4.43}$$

The objective function (4.41) minimizes the total operation cost. Constraints (4.42) ensure that each node is served exactly once. Note that "$=$" in constraints (4.42) is replaced with "$\geq$" to reduce the computation time (Danna & Le Pape, 2005). Constraints (4.43) define the domains of variables.

4.4 Column generation algorithm

Since it is impossible to enumerate all paths for large-scale instances, we developed a column generation (CG) approach to solve the path-based SARP-D model. The CG algorithm involves solving two problems: a restricted master problem (RMP) that selects the combination of paths that has the minimum objective value, and a pricing problem (PP) that aims to find new paths having the potential to reduce the objective value.

Initially, the RMP includes columns generated by the heuristic described in Section 4.4.4. The CG first solves the linear RMP in each iteration and passes the dual variables to the PP. Then, the PP is solved by algorithms introduced in Sections 4.4.1 and 4.4.3 to find feasible paths with negative reduced costs. If the PP finds new paths with negative reduced costs, all new paths are added to the RMP. The RMP and PP are solved iteratively until the PP cannot identify paths with negative reduced costs. A validated lower bound of the original problem is obtained in this situation. If the optimal solution at the last iteration of the CG is fractional, an integer programming model of the RMP is solved to get an upper bound of the original problem; otherwise, the optimal solution at the last iteration of CG is the optimal solution of the original problem.

The RMP is the linear relaxation of the path-based model, and the set of all possible paths, i.e., R, is replaced by a subset of possible paths $R' \subseteq R$. Let $\beta_i, i \in S_p \cup S_g$ be the dual variables associated with constraints (4.42), the reduced cost of path $r \in R$ is calculated as $\bar{c}_r = c_r - \sum_{i \in S_p \cup S_g} a_{ir}\beta_i$. The pricing problem of the SARP-D is an elementary shortest path problem with resource constraints (ESPPRC), which can be solved efficiently by a labeling algorithm. Inspired by Feillet et al. (2004), We developed a tailored labeling algorithm to solve the PP of the SARP-D.

4.4.1 Label correcting algorithm

We define Φ_i and Π_i are the sets of labels and temporary labels associated with node i. Then, given a (partial) path $p(*)$[5] where the last node visited by a DRB (independently or together with a drone) is node $i \in N$, we define two concepts, $\phi_i \in \Phi_i$ and $\pi_i \in \Pi_i$. ϕ_i is a label denoting path $p(\phi_i)$ when node i is a combined node. π_i is a temporary label denoting path $p(\pi_i)$ when node i is a DRB node.

For each π_i, a drone leg between the last combined node and DRB node i on path $p(\pi_i)$ is added to constitute a feasible path in a SARP-D solution. By adding the drone leg, node i becomes a combined node and π_i is transferred to ϕ_i. For example, let π_1 be a temporary label of the partial path (0→1), if a drone leg <0,9,1> is added to the partial path (0→1), we get a new label ϕ_1 denoting the partial path ([0→1, <0,9,1>]). Both ϕ_i and π_i have the following attributes:

- $c(*)$: the last combined node on path $p(*)$.
- $v(*)$: the last node that a DRB visits on path $p(*)$. It could be a combined node or a DRB node.
- $dr(*)$: the last drone node on path $p(*)$.
- $pos(*)$: a vector that records the position of each node except for the drone node on path $p(*)$. $pos(*)_j$ is the position of node j on path $p(*)$.
- $tp(*)$: a vector that records the type of each node on path $p(*)$, i.e., common node, launch node, recovery node, recovery-launch node, drone node. $tp(*)_j$ represents the type of node j on path $p(*)$.
- $\tau(*)$: a vector that records the arrival time at each node on path $p(*)$. If node j is a drone node, $\tau(*)_j$ is the arrival time of the drone at node j; otherwise, $\tau(*)_j$ is the arrival time of the DRB at node j.
- $\tau'(*)$: the time point that the drone finishes landing at $c(*)$.
- $\tau''(*)$: a vector that records time-related attributes of each node on path $p(*)$. Let j be a node on path $p(*)$, if j is a common node or drone node, $\tau''(*)_j$ is the start service time at node j; if j is a launch node or recovery-launch node, $\tau''(*)_j$ is the time point that the drone starts taking off at node j; if j is a recovery node, $\tau''(*)_j$ is the time point that the DRB finishes all tasks at node j (including serving the corresponding request and recovering the drone) and leaves node j.
- $fly(*)$: the flying duration of the last flight of the drone on path $p(*)$.
- $pl(*)$: the occupied passenger capacity after vising all nodes on path $p(*)$.
- $gl(*)$: the occupied goods capacity after visiting all nodes on path $p(*)$.

[5] The notation of "$*$" represents ϕ_i or π_i explained later in this paragraph.

- $\Omega(*)$: the set of visited nodes on path $p(*)$.
- $O(*)$: the set of open passenger requests whose origin is included on $p(*)$ but the destination is not. $O(*)_0$ is the first passenger request in $O(*)$, if $O(*)$ is not empty.
- $V(*)$: the set of nodes that could be visited by the DRB from $v(*)$ without considering the time windows and vehicle capacity constraint.
- $D(*)$: the set of nodes that could be visited by a drone from $c(*)$ without considering the time windows, vehicle capacity, and drone battery endurance constraints.
- $\kappa(*)$: the accumulated dual value of path $p(*)$.
- $cost(*)$: the cost of path $p(*)$.
- $\overline{rc}(*)$: the reduced cost of path $p(*)$.

Algorithm 1 presents the procedure of the labeling algorithm to solve the PP of SARP-D. In Algorithm 1, Γ represents the list of pending examination nodes. The function $AddDroneLeg(\pi_i, j)$ appends a drone leg $< c(\pi_i), j, i >$ to path $p(\pi_i)$, creating a new label ϕ_i, if the extension is feasible. Here, j belongs to set $D(\pi_i)$. Function $AddCombinedArc(\phi_i, j)$ extends path $p(\phi_i)$ by adding a combined arc $(i \Rightarrow j)$, resulting in a new label ϕ_j, provided the extension is viable. The value of j is a member of set $V(\phi_i)$. Function $AddDRBArc(\phi_i, j)$ introduces a temporary label π_j by incorporating a DRB arc $(i \rightarrow j)$ into path $p(\phi_i)$, given that the extension is feasible. Here, j belongs to set $V(\phi_i)$. Function $AddDRBArc(\pi_i, j)$ generates a temporary label π_j by incorporating a DRB arc $(i \rightarrow j)$ into path $p(\pi_i)$, if the extension is achievable. The value of j is within the set $V(\pi_i)$. The function $checkDominance(\phi_i, \Phi_i)$ determines whether the label ϕ_i dominates other labels within Φ_i, or if it is dominated by any of them. It then returns Φ_i, which solely contains non-dominated labels.

The sets of labels and temporary labels associated with each node $i \in N$ are initialized as follows. $\Phi_0 \leftarrow \{(0, 0, /, \{0\}, \{\text{common node}\}, \{0\}, 0, \{0\}, 0, 0, 0, \{0\}, \varnothing, S_p^o \cup S_g, {S_g}', 0, 0, 0)\}$ and $\Pi_0 \leftarrow \varnothing$. For node $i \in N \backslash \{0\}$, $\Phi_i \leftarrow \varnothing$ and $\Pi_i \leftarrow \varnothing$. In addition, the list of nodes waiting to be examined Γ is initialized as $\{0\}$.

The following steps are repeated while Γ is not empty. First, choose the first node, denoted by i, from Γ as the node to be treated. Second, extend each temporary label $\pi_i \in \Pi_i$ to new labels of node i and new temporary label of node $j \in V(\pi_i)$ by adding drone legs $< c(\pi_i), d, i >, d \in D(\pi_i)$ and DRB arc $(i \rightarrow j)$ to path $p(\pi_i)$, respectively, if the extensions are feasible; otherwise, do nothing. After that, π_i is deleted from Π_i. Third, extend each untreated label ϕ_i in Φ_i to new label and temporary label of $j \in V(\phi_i)$ by adding combined arc $(i \Rightarrow j)$ and DRB arc $(i \rightarrow j)$ to path $p(\phi_i)$, respectively, if the extensions are feasible. Then ϕ_i is marked as a treated label. In both the second the third steps, two additional works based on the two propositions that will explain later have been done to reduce the number of generated temporary labels and labels: 1) whenever $cost(*)$ is updated, the lower bound of the reduced cost of label ϕ_{dep}, denoted by $LB_{\overline{rc}(\phi_{dep})}$, where ϕ_{dep} is extended from $*$ and $c(\phi_{dep})$ is the returning depot, is calculated. If $LB_{\overline{rc}(\phi_{dep})} \geq 0$, $*$ is discarded. 2) When a new label ϕ_j of node j is generated, it will be compared with each label in Φ_j. If ϕ_j is not dominated by any label in Φ_j, ϕ_j will be added to Φ_j. If ϕ_j dominates some labels in Φ_j, the dominated labels will be deleted. In addition, if Π_j or Φ_j has changed and node j is not in Γ, node j will be added to Γ. Fourth, node i is deleted from Γ.

As illustrated within Algorithm 1, a label extension exists for both temporary labels (Case

Algorithm 1: Label correcting algorithm

```
//Initialization ;
Φ_0 ← {(0, 0, /, {0}, {common node}, {0}, 0, {0}, 0, 0, 0, {0}, ∅, S_p^o ∪ S_g, S_g', 0, 0, 0)} ;
Π_0 ← ∅ ;
for i ∈ N\{0} do
    Φ_i ← ∅, Π_i ← ∅ ;
Γ ← {0} ;
//Search ;
while Γ ≠ ∅ do
    choose the first node i in Γ ;
    //Case 1 ;
    for π_i ∈ Π_i do
        for j ∈ D(π_i) do
            φ_i ← AddDroneLeg(π_i, j) ;
            Φ_i ← CheckDominance(φ_i, Φ_i) ;
        for j ∈ V(π_i) do
            π_j ← AddDRBArc(π_i, j) ;
            Π_j ← Π_j ∪ {π_j} ;
            if Π_j has changed then
                Γ ← Γ ∪ {j} ;
        Π_i ← Π_i\{π_i} ;
    //Case 2 ;
    for φ_i ∈ Φ_i do
        if φ_i has not been treated then
            for j ∈ V(φ_i) do
                φ_j ← AddCombinedArc(φ_i, j) ;
                Φ_j ← CheckDominance(φ_j, Φ_j) ;
                if Φ_j has changed then
                    Γ ← Γ ∪ {j} ;
                π_j ← AddDRBArc(φ_i, j) ;
                Π_j ← Π_j ∪ {π_j} ;
                if Π_j has changed then
                    Γ ← Γ ∪ {j} ;
            Mark φ_i has been treated ;
    Γ ← Γ\{i} ;
```

1) and regular labels (Case 2). When dealing with Case 1 and 2, our initial action involves matching the attributes' values of $*^2$ to those of $*^1$ if the attributes of $*^2$ are derived from $*^1$. Subsequently, specific attributes' values of $*^2$ undergo modification. After getting the attributes of $*^2$, we check its feasibility. For an extensive elaboration on these label extensions, please refer to Appendices 4.A and 4.B.

4.4.2 Label elimination

As the instance size expands, the number of temporary labels and labels experiences exponential growth, resulting in substantial memory consumption and extended computation durations. To address this issue, we introduce two propositions aimed at diminishing the

volume of generated temporary labels and labels within the labeling algorithm. Initially, we suggest eliminating temporary labels and labels that do not culminate in a finalized path with a negative reduced cost. This proactive approach can contribute to a reduction in computational burden and enhance efficiency.

Proposition 1. Let ϕ_{dep} denote a label of the returning depot that is extended from temporary label π_i, the lower bound of $\overline{rc}(\phi_{dep})$, denoted by $LB_{\overline{rc}(\phi_{dep})}$, is calculated by $LB_{\overline{rc}(\phi_{dep})} = cost(\pi_i) + \min_{j \in D(\pi_i)}\{C^D_{c(\pi_i),j} + C^D_{j,v(\pi_i)}\} + \overline{cost}^V(\pi_i) - \sum_{a \in S} \beta_a$, where $\overline{cost}^V(\pi_i)$ is the minimum cost of a DRB traveling from $v(\pi_i)$, visiting all destinations of $O(\pi_i)$, and returning to the depot. If $LB_{\overline{rc}(\phi_{dep})} \geq 0$, the extension of temporary label π_i could not constitute a completed path with a negative reduced cost and therefore π_i can be discarded.

Note that getting the value of $\overline{cost}^V(\pi_i)$ requires to solve a traveling salesman problem. In this study, we can afford to enumerate all paths that start from $v(\pi_i)$, visiting all destinations of $O(\pi_i)$, and ending at the depot, because the number of $O(\pi_i)$ is small, specifically, less than or equal to $\eta+1$ due to the constraint of maximum intermediate stops between serving one passenger request.

Proof 1. To construct a completed path $p(\phi_{dep})$ by extending $p(\pi_i)$, a drone node in $D(\pi_i)$ and all destinations of passenger requests in $O(\pi_i)$ should be visited at least. The minimum drone flight cost is calculated by $\min_{j \in D(\pi_i)}\{C^D_{c(\pi_i),j} + C^D_{j,v(\pi_i)}\}$. Because of the triangle inequality of cost matrix, when more nodes that do not belong to destinations of passenger requests in $O(\pi_i)$ are added to $p(\pi_i)$, the calculation of $\overline{cost}^V(\pi_i)$ still holds. Since $cost(\phi_{dep}) \geq cost(\pi_i) + \min_{j \in D(\pi_i)}\{C^D_{c(\pi_i),j} + C^D_{j,v(\pi_i)}\} + \overline{cost}^V(\pi_i)$ and $\kappa(\phi_{dep}) = \sum_{a \in \Omega(\phi_{dep})} \beta_a \leq \sum_{a \in S} \beta_a$, $\overline{rc}(\phi_{dep}) = cost(\phi_{dep}) - \kappa(\phi_{dep}) \geq cost(\pi_i) + \min_{j \in D(\pi_i)}\{C^D_{c(\pi_i),j} + C^D_{j,v(\pi_i)}\} + \overline{cost}^V(\pi_i) - \sum_{a \in S} \beta_a$. The lower bound of the reduced cost of ϕ_{dep} is $LB_{\overline{rc}(\phi_{dep})} = cost(\pi_i) + \min_{j \in D(\pi_i)}\{C^D_{c(\pi_i),j} + C^D_{j,v(\pi_i)}\} + \overline{cost}^V(\pi_i) - \sum_{a \in S} \beta_a$.

A similar proposition is applied to label ϕ_i as well. The difference is that the lower bound of reduced cost of label ϕ_{dep} extended from ϕ_i is calculated by $LB_{\overline{rc}(\phi_{dep})} = cost(\phi_i) + \overline{cost}^V(\phi_i) - \sum_{a \in S} \beta_a$, where $\overline{cost}^V(\phi_i)$ is the minimum travel cost of a DRB traveling from $v(\phi_i)$, visiting all destinations of $O(\phi_i)$, and returning to the depot.

Second, dominance rules are applied to determine whether a newly generated label will be added to the label set.

For two labels of node i, ϕ_i^1 and ϕ_i^2, ϕ_i^1 dominates ϕ_i^2, if the following two conditions are satisfied. 1) Any extensions of label ϕ_i^2 used to construct a completed path can be connected to ϕ_i^1 as well; 2) $\overline{rc}(\phi_i^1) \leq \overline{rc}(\phi_i^2)$ (Ropke & Cordeau, 2009). Using this definition, we propose the following dominance rules for the SARP-D.

Proposition 2. ϕ_i^1 dominates ϕ_i^2 if the following conditions are satisfied:

(i) $c(\phi_i^1) = c(\phi_i^2)$

(ii) $tp(\phi_i^1) = tp(\phi_i^2)$

(iii) $\tau''(\phi_i^1) \leq \tau''(\phi_i^2)$

(iv) $\Omega(\phi_i^1) \subseteq \Omega(\phi_i^2)$

(v) $O(\phi_i^1) = O(\phi_i^2)$

(vi) $V(\phi_i^1) \supseteq V(\phi_i^2)$

(vii) $\overline{rc}(\phi_i^1) \leq \overline{rc}(\phi_i^2)$

Proof 2. Given two labels ϕ_i^1 and ϕ_i^2 that satisfy the conditions in **Proposition 2**, condition (i) implies that both partial path $p(\phi_i^1)$ and $p(\phi_i^2)$ ending at the same node. Conditions (iv), (v), and (vi) ensure that any nodes that can be extended by ϕ_i^2 can also be extended by ϕ_i^1. We do not require $D(\phi_1) \supseteq D(\phi_2)$, because $\Omega(\phi_1) \subseteq \Omega(\phi_2)$ implies $D(\phi_1) \supseteq D(\phi_2)$. Conditions (iv) and (v) also ensure that the remaining load capacity for both passengers and parcels of path $p(\phi_i^1)$ is equal to or large than that of $p(\phi_i^2)$. Conditions (ii), (iii), and (vii) guarantee that every feasible extension of ϕ_i^2 is a feasible extension of ϕ_i^1 with a smaller or equal reduced cost.

4.4.3 Heuristic column generation

Recognizing the typically time-intensive nature of the label correcting algorithm, we introduce a Large Neighborhood Search (LNS) heuristic to expedite the CG procedure. The LNS heuristic unfolds through the following steps: Initially, all paths with zero reduced cost are chosen, as modifications to these paths can easily yield paths with negative reduced costs. For each zero reduced cost path ($\overline{r'}$), a set $\bar{\Omega}$ is formulated, encompassing all nodes from $S_p \cup S_g$, except those already incorporated in the path. The nodes within $\bar{\Omega}$ are arranged in descending order based on their dual values. Subsequently, a request is randomly removed from $\overline{r'}$, and nodes from $\bar{\Omega}$ are progressively inserted into path $\overline{r'}$ at their optimal positions. This process generates new paths with negative reduced costs until all nodes in $\bar{\Omega}$ have been integrated or further node insertions no longer yield paths with negative reduced costs.

When tackling the pricing problem, the initial application involves the LNS heuristic. In cases where paths with negative reduced costs cannot be discovered, the label correcting algorithm is employed.

4.4.4 Initial columns

We adopt the initial column generation approach proposed by Cheng et al. (2023b), known as the greedy DRB-first drone-second repair method, to generate the starting columns for the CG process. This heuristic comprises two distinct stages. In the first stage, all requests are inserted greedily into a DRB route. Subsequently, in the second stage, parcel requests that meet the criteria for drone service are selectively moved from a DRB route to a drone flight in a greedy manner. To comprehensively understand this heuristic, readers should refer to the details provided in Cheng et al. (2023b).

4.5 Computational results

This section presents a comprehensive array of numerical experiments to assess the effectiveness of the CG approach. Our algorithm implementation used C++, and we employed CPLEX 12.10 as the solver for optimization tasks. The experiments were conducted on a machine featuring an Intel(R) Xeon(R) CPU E5-2660 V3 clocked at 2.60 GHz. Each CG run was subject to a time limit of 3 hours, with a memory allocation of 300 GB.

4.5.1 Instance design

We employed instances from the vehicle routing problem with drones (VRP-D) dataset provided by Sacramento et al. (2019) and adapted them to our specific SARP-D. Specifically, we utilized nodes' coordinates from Sacramento et al. (2019) instances involving 6, 10, 12, 20, and 50 nodes, labeled as "1". Instances with node counts of 6, 10, and 12 were categorized as small. In comparison, those with 20 and 50 nodes were considered

medium-size instances. Subsequently, we generated passenger and parcel requests for each node, along with time windows, using the methodology proposed by Cheng et al. (2023b). For instances up to 20 nodes, we distributed nodes across 5, 10, and 20 square miles. For the 50-node instances, the distribution areas were 10, 20, 30, and 40 square miles. Within each distribution category, we created ten instances by varying the ratios of passenger requests (r^P) from $\{0, 1/3, 2/3, 1\}$ and drone-eligible parcel requests (r^D) from $\{0, 0.25, 0.5, 0.75\}$. Instances with $r^P = 0$ or $r^P = 1$ corresponded to VRP-D and pickup and delivery problem (PDP) instances, respectively. Notably, SARP-D instances in Section 4.5 exclusively featured $r^P = 1/3$ or $r^P = 2/3$.

We formulated 79 networks, each characterized by the number of nodes, distribution (Dim), passenger requests, and drone-eligible parcel requests. Both soft and hard time windows were considered for each network. Distances traveled by DRBs adhered to Manhattan distances, while drone travel distances were based on Euclidean distances. The parameter configuration mirrored that of Cheng et al. (2023b). Specifically, the DRB speed was set at 35 miles/h, and the drone speed was set at 50 miles/h. The service time for DRBs and drones at each node was 1 minute, with an additional 1-minute setup time for drone launch and recovery. Penalty costs of 1 $/min and 0.5 $/min were assigned to passenger and parcel requests' delay, respectively. The DRB transportation cost was 0.2 $/mile, with the drone transportation cost constituting 10%. Passenger and parcel capacities, varying by instance size, were set at 6 for instances up to 20 nodes and 10 for 50-node instances. The maximum travel times for DRBs and drones were 480 and 30 minutes, respectively. Parameter η encompassed values of 0, 1, and 2, while E was uniformly set to 30 minutes. Consequently, 390 instances were created to comprehensively assess CG's performance, as summarized in Table 4.4.

Table 4.4: Summary of the instances used

(a) Small-size instances

# nodes	Dim	$\|P\|$	$\|S_g'\|$	η	TW type	E
6	{5, 10, 20}	2	2	{0,1,2}	{soft, hard}	{30}
10	{5, 10, 20}	3	3	{0,1,2}	{soft, hard}	{30}
12	{5, 10, 20}	4	3	{0,1,2}	{soft, hard}	{30}

(b) Medium-size instances

# nodes	Dim	r^P	r^D	η	TW type	E	Problem
20	{5, 10, 20}	0	{0.25, 0.5, 0.75}	{0}	{soft, hard}	{30}	VRP-D
		1/3	{0.25, 0.5, 0.75}	{0,1,2}	{soft, hard}	{30}	SARP-D
		2/3	{0.25, 0.5, 0.75}	{0,1,2}	{soft, hard}	{30}	SARP-D
		1	{0}	{0,1,2}	{soft, hard}	{30}	PDP
50	{10, 20, 30, 40}	0	{0.25, 0.5, 0.75}	{0}	{soft, hard}	{30}	VRP-D
		1/3	{0.25, 0.5, 0.75}	{0,1,2}	{soft, hard}	{30}	SARP-D
		2/3	{0.25, 0.5, 0.75}	{0,1,2}	{soft, hard}	{30}	SARP-D
		1	{0}	{0,1,2}	{soft, hard}	{30}	PDP

4.5.2 Algorithm performance

In this section, we comprehensively evaluated the CG approach. We began by conducting a comparative analysis between CG outcomes and those obtained from the arc-based model solved by CPLEX, focusing on small-size instances. Subsequently, we extended

our assessment to medium-size instances. In both cases, we utilized z_{lb} and z_{ub}, denoting the lower and upper bounds, respectively, as outlined in Table 4.5 and Table C1 in Appendix 4.C. To quantify the disparity between these bounds, we computed the relative gap (Gap) using the formula: $Gap = (z_{ub} - z_{lb})/z_{ub} \times 100\%$. Furthermore, in Table 4.5, we introduced Gap^*, computed as $Gap^* = (z_{ub} - z^*)/z^* \times 100\%$, where z^* denotes the optimal solution obtained by CPLEX for the arc-based model. This metric captures the relative difference between the upper bound attained through the CG and the optimal solution given by CPLEX.

4.5.2.1 Small-size instances

Table 4.5 displays CG and CPLEX results for small-size instances, denoted by $|S|\_|P|\_|G|\_|D|$—Dim, where $|S|$ represents the node count, $|P|$ the passenger requests, $|G|$ the parcel requests, $|D|$ the drone-eligible requests, and Dim indicates node distribution. As evident in Table 4.5, the CG surpassed CPLEX in solution quality and computation time. Solution-wise, the CG matched CPLEX's optimal solution in 53 of 54 instances, except for instance 6_2_2_2—10, featuring $\eta = 2$ and soft TW, where the CG achieved a 1.62% gap for a near-optimal integer solution. For 48 of 53 cases, the CG yielded a 0.00% gap between its lower and upper bounds. In terms of computation time, the CG significantly outperformed CPLEX.

Table 4.5: Comparison results of CPLEX and CG on small-size instances

Instance	η	Soft TW							Hard TW						
		CPLEX		CG				Gap^*	CPLEX		CG				Gap^*
		z^*	CPU time (s)	z_{lb}	z_{ub}	Gap	CPU time (s)		z^*	CPU time (s)	z_{lb}	z_{ub}	Gap	CPU time (s)	
6_2_2_2—5	0	4.0834	33.02	3.7921	4.0834	7.13%	1.49	0.00%	4.2965	31.23	3.7921	4.2965	11.74%	0.35	0.00%
6_2_2_2—5	1	3.3346	4.06	3.3346	3.3346	0.00%	0.04	0.00%	3.3346	12.72	3.3346	3.3346	0.00%	0.06	0.00%
6_2_2_2—5	2	3.2699	4.83	3.2699	3.2699	0.00%	0.06	0.00%	3.2699	12.28	3.2699	3.2699	0.00%	0.08	0.00%
6_2_2_2—10	0	8.3111	8.91	8.3111	8.3111	0.00%	0.03	0.00%	8.3111	2.86	8.3111	8.3111	0.00%	0.03	0.00%
6_2_2_2—10	1	8.3111	29.73	7.7785	8.3111	6.41%	0.25	0.00%	8.3111	37.98	7.7785	8.3111	6.41%	0.12	0.00%
6_2_2_2—10	2	8.179	16.86	7.7785	8.3111	6.41%	1.11	1.62%	8.3111	26.44	7.7785	8.3111	6.41%	0.35	0.00%
6_2_2_2—20	0	10.4419	3.47	10.4419	10.4419	0.00%	0.03	0.00%	10.4419	6.97	10.4419	10.4419	0.00%	0.04	0.00%
6_2_2_2—20	1	10.4419	4.83	10.4419	10.4419	0.00%	0.03	0.00%	10.4419	5.72	10.4419	10.4419	0.00%	0.04	0.00%
6_2_2_2—20	2	10.4419	5.47	10.4419	10.4419	0.00%	0.03	0.00%	10.4419	5.34	10.4419	10.4419	0.00%	0.04	0.00%
10_3_4_3—5	0	5.2563	1103.75	5.2563	5.2563	0.00%	0.11	0.00%	5.2563	375.78	5.2563	5.2563	0.00%	0.2	0.00%
10_3_4_3—5	1	4.5126	264.98	4.5126	4.5126	0.00%	0.13	0.00%	4.5126	338.69	4.5126	4.5126	0.00%	0.22	0.00%
10_3_4_3—5	2	4.4476	272.45	4.4476	4.4476	0.00%	0.61	0.00%	4.4476	231.09	4.4476	4.4476	0.00%	0.59	0.00%
10_3_4_3—10	0	12.5398	101.27	12.5398	12.5398	0.00%	0.19	0.00%	12.5398	66.78	12.5398	12.5398	0.00%	0.15	0.00%
10_3_4_3—10	1	10.7309	65.89	10.7309	10.7309	0.00%	0.09	0.00%	10.7309	30.02	10.7309	10.7309	0.00%	0.1	0.00%
10_3_4_3—10	2	10.7309	70.36	10.7309	10.7309	0.00%	0.1	0.00%	10.7309	40.58	10.7309	10.7309	0.00%	0.13	0.00%
10_3_4_3—20	0	17.6415	91.73	17.6415	17.6415	0.00%	0.09	0.00%	17.6415	31.48	17.6415	17.6415	0.00%	0.1	0.00%
10_3_4_3—20	1	17.5246	74.02	17.5246	17.5246	0.00%	0.15	0.00%	17.5246	31.72	17.5246	17.5246	0.00%	0.11	0.00%
10_3_4_3—20	2	17.5246	56.81	17.5246	17.5246	0.00%	0.13	0.00%	17.5246	396.66	17.5246	17.5246	0.00%	0.16	0.00%
12_4_4_3—5	0	7.1948	3127.16	7.1948	7.1948	0.00%	0.14	0.00%	7.1948	1568.45	7.1948	7.1948	0.00%	0.18	0.00%
12_4_4_3—5	1	6.6085	7558.72	6.6085	6.6085	0.00%	0.46	0.00%	6.6085	7241.67	6.6085	6.6085	0.00%	0.43	0.00%
12_4_4_3—5	2	6.4138	6116.78	6.4138	6.4138	0.00%	0.79	0.00%	6.4138	1357.89	6.4138	6.4138	0.00%	0.5	0.00%
12_4_4_3—10	0	10.6261	292.77	10.6261	10.6261	0.00%	0.17	0.00%	10.6261	188.3	10.6261	10.6261	0.00%	0.15	0.00%
12_4_4_3—10	1	10.5319	222.86	10.5319	10.5319	0.00%	0.14	0.00%	10.5319	173.48	10.5319	10.5319	0.00%	0.1	0.00%
12_4_4_3—10	2	10.5319	389.36	10.5319	10.5319	0.00%	0.32	0.00%	10.5319	168.19	10.5319	10.5319	0.00%	0.11	0.00%
12_4_4_3—20	0	25.2007	216.89	25.2007	25.2007	0.00%	0.09	0.00%	25.2007	43.84	25.2007	25.2007	0.00%	0.08	0.00%
12_4_4_3—20	1	25.2007	168.63	25.2007	25.2007	0.00%	0.11	0.00%	25.2007	44.03	25.2007	25.2007	0.00%	0.09	0.00%
12_4_4_3—20	2	25.2007	226.73	25.2007	25.2007	0.00%	0.14	0.00%	25.2007	121.36	25.2007	25.2007	0.00%	0.11	0.00%

4.5.2.2 Medium-size instances

Table 4.6 provides an overview of CG results for medium-size instances. The "# solved instances" column enumerates instances considered and how many were resolved by CG within a 3-hour limit, distinguished by their time window (TW) types. The "# optimal instances" column details instances solved optimally ($Gap = 0$). The last column denotes the average gap for solved instances by CG. Table C1 in Appendix 4.C offers in-depth computation results for each instance.

Table 4.6: Summary of computation results of medium-size instances

Problem	# nodes	Dim	r^P	r^D	η	# solved instances		# optimal instances		CPU time (s)		Average gap	
						Soft TW	Hard TW	Soft TW	Hard TW	Soft TW	Hard TW	Soft TW	Hard TW
VRP-D	20	{5, 10, 20}	0	{0.25, 0.5, 0.75}	{0}	9/9	9/9	0/9	0/9	807.01	830.12	1.90%	2.11%
	50	{10, 20, 30, 40}	0	{0.25, 0.5, 0.75}	{0}	6/12	7/12	2/6	0/7				
SARP-D	20	{5, 10, 20}	1/3	{0.25, 0.5, 0.75}	{0,1,2}	27/27	27/27	15/27	15/27	335.82	136.56	0.59%	0.53%
		{5, 10, 20}	2/3	{0.25, 0.5, 0.75}	{0,1,2}	27/27	27/27	21/27	22/27				
	50	{10, 20, 30, 40}	1/3	{0.25, 0.5, 0.75}	{0,1,2}	29/36	34/36	21/29	23/34				
		{10, 20, 30, 40}	2/3	{0.25, 0.5, 0.75}	{0,1,2}	36/36	36/36	20/36	24/36				
PDP	20	{5, 10, 20}	1	{0}	{0,1,2}	9/9	9/9	8/9	8/9	1.99	0.69	0.46%	0.65%
	50	{10, 20, 30, 40}	1	{0}	{0,1,2}	12/12	12/12	9/12	9/12				

Following Table 4.6, CG effectively tackled all 20-node instances (144 instances) and a substantial number of 50-node instances (172 out of 192 instances). In sum, across the 316 solved instances, the average gap remained at 0.70%. Various factors influence CG's efficacy, broadly categorized into the two types discussed below.

Network and operation features. As mentioned before, network features include the instance size, Dim, r^P, and r^D. The operation features refer to η and TW types. As expected, the computation difficulty and time increased with the increase in instance size, r^P, r^D, and η, and the decrease in Dim. In addition, instances with hard TW were easier to solve than instances with soft TW. The average computation time for VRP-D instances with hard TW is slightly longer than that of VRP-D instances with soft TW. This is because the computation time for the solved hard TW VRP-D instance with 50 nodes, $r^D = 0.75$, $Dim = 30$ is 8706 seconds, while the soft TW instance with the same network setting is not solvable.

Problem classification. PDP instances had the largest percentage of solved instances (100%), followed by SARP-D instances (96%). VRP-D instances were the most difficult to solve. Notably, the proposed CG could solve 66% of SARP-D instances and 81% of PDP instances to optimality. In terms of computation time, VRP-D instances took the longest computation time. The computation time for SARP-D instances was around half of the computation time for VRP-D instances. The PDP instances could be solved within a few seconds. The main difference between the three types of problems is the ratio of passenger requests to total requests. Due to the precedence requirement for the origin and destination nodes of passengers and the limited number of intermediate stops between serving one passenger request, instances with more passenger requests have smaller solution space. They are easier to solve than instances with fewer passenger requests. Overall, if we look at the average gaps, the proposed CG produces high-quality solutions to the SARP-D, with an average gap of 0.59% for soft TW instances and 0.53% for hard TW instances.

4.6 Sensitivity analysis and managerial insights

In this section, we conducted sensitivity analyses on Dim, η, TW types, and E, to investigate the properties of the integrated transportation system. All instances presented in this section are solved to optimality by the CG.

4.6.1 Node distribution

We selected 50-node instances characterized by $r^P = 2/3$, $r^D = 0.5$, $\eta = 0$, $E = 30$ min, and soft TW to investigate the influence of distribution on system performance. The outcomes of the chosen instances are presented in Table 4.7. From the results in Table 4.7, it becomes evident that an increased number of DRBs is necessary to fulfill all requests with a more expansive distribution of customers. This augmentation in DRBs leads to higher total costs, DRB-traveled and drone-traveled miles.

Table 4.7: Impact of distribution

Dim	Total costs	# used vehicles	DRB-traveled miles	Drone-traveled miles
10	53.0490	6	263.6576	15.8748
20	89.7376	8	441.1657	25.2210
30	156.1879	9	766.2628	46.7663
40	240.9552	12	1197.2296	75.4653

4.6.2 Number of intermediate stops between one passenger request

We conducted experiments using two sets of instances to examine how the maximum number of intermediate stops between passenger request services, denoted as η, impacts the system. In Set 1, we utilized 20-node instances with $Dim = 10$, $r^P = 1/3$, $r^D = 0.75$, and $E = 30$ min. Meanwhile, Set 2 comprised 20-node instances with $Dim = 20$, $r^P = 2/3$, $r^D = 0.5$, and $E = 30$ min. The values of η ranged from 0 to 5, where lower η values indicated less inconvenience caused by shared rides among passengers. For $\eta = 0$, a passenger request wasn't combined with any other request, whether passenger or parcel.

Table 4.8 showcases the effects of varying η on the system's performance. About instances with $\eta = 0$ as the baseline, the columns "Δ_TC" and "Δ_DRB miles" display the percentage changes in total costs and DRB-traveled miles, respectively, for different η values. The table reveals that allowing more intermediate stops during passenger request servicing leads to savings in total costs and DRB-traveled miles, albeit to varying extents across the two sets. A comparison between the percentage changes in total costs and DRB-traveled miles for the same instances from Set 1 indicates minor differences, while instances from Set 2 exhibit more significant variations when η exceeds 2. This variance can be attributed to the composition of total costs, encompassing DRB transportation costs, drone transportation costs, and delay penalties. Particularly, for the last three instances in Set 2, a noteworthy reduction in DRB-traveled miles is counterbalanced by a 6-minute delay at passenger stops.

Furthermore, the number of used vehicles experiences a decrease of one when transitioning from $\eta = 0$ to $\eta = 1$ within Set 1. However, in Set 2, the number of used vehicles remains constant as η increases. This phenomenon can be attributed to a minimum number of vehicles required to fulfill all requests while satisfying all stipulated constraints.

No specific conclusion can be drawn when it comes to drone-related indicators such as the number of flights, flying time, and drone-traveled miles. Nevertheless, an elevated value of η broadens the solution space, enabling more advantageous drone flights that contribute to cost reduction.

4.6.3 Hard versus Soft time windows

The CG successfully determined lower bounds for 243 out of 252 SARP-D instances. Moreover, 77 out of 119 instances with soft time windows (TW) and 84 out of 124 instances with hard TW were solved optimally with a gap of 0%. Among these solved instances,

Table 4.8: Impact of the maximum number of intermediate stops between one passenger request service

Instance	η	Total costs	Δ_TC	# used vehicles	# flights	Flying time	DRB-traveled miles	Δ_DRB miles	Drone-traveled miles	Passenger delay (min)	Goods delay (min)
Set 1	0	15.6833		4	2	21	77.7561		6.6041	0	0
	1	13.9275	-11.20%	3	5	113	66.3061	-14.73%	33.3163	0	0
	2	13.6314	-13.08%	3	4	55	66.3061	-14.73%	18.5105	0	0
	3	13.5725	-13.46%	3	3	46	66.4050	-14.60%	14.5743	0	0
	4	13.5725	-13.46%	3	3	46	66.4050	-14.60%	14.5743	0	0
	5	13.5725	-13.46%	3	3	46	66.4050	-14.60%	14.5743	0	0
Set 2	0	54.1807		4	1	30	270.2217		6.8168	0	0
	1	53.7319	-0.83%	4	1	30	267.9777	-0.83%	6.8168	0	0
	2	53.7319	-0.83%	4	1	30	267.9777	-0.83%	6.8168	0	0
	3	52.7747	-2.60%	4	1	30	233.1916	-13.70%	6.8168	6	0
	4	52.7747	-2.60%	4	1	30	233.1916	-13.70%	6.8168	6	0
	5	52.7747	-2.60%	4	1	30	233.1916	-13.70%	6.8168	6	0

Δ_TC: Percentage change in total costs; Δ_DRB miles: Percentage change in DRB-traveled miles

74 pairs[6] achieved optimality. Notably, for 60 out of these 74 instance pairs, the TW type had no impact, implying that the objective value of an instance with soft TW was identical to that of its hard TW counterpart. These findings suggest that, in scenarios with ample vehicles, simultaneous achievement of cost reduction and on-time delivery satisfaction is achievable for most cases. Nevertheless, there are instances where cost savings might be attained at the expense of compromising on-time delivery performance.

From Table 4.9, it is apparent that the objective value for instances with soft TW is frequently smaller than that of instances with hard TW for 14 pairs of instances. Additionally, allowing TW violations can reduce the number of used DRBs, indicating potential operational cost savings.

Table 4.9: Impact of TW type

# nodes	Dim	r^P	r^D	η	Soft TW					Hard TW		
					Total costs	# used vehicles	DRB-traveled miles	Passenger delay (min)	Goods delay (min)	Total costs	# used vehicles	DRB-traveled miles
20	10	2/3	0.75	1	17.5621	3	82.3260	1	0	18.0266	4	90.1331
20	10	2/3	0.75	2	17.4271	3	81.6509	1	0	17.8916	4	89.4580
50	20	1/3	0.5	0	85.1959	7	417.9187	0	1	86.1498	8	425.1883
50	20	2/3	0.5	0	89.7376	8	441.1657	1	0	90.1728	8	448.2851
50	30	2/3	0.25	1	145.3158	8	707.8330	2	3	151.4486	9	755.9968
50	30	2/3	0.5	0	156.1879	9	766.2628	2	0	158.1425	10	786.3918
50	30	2/3	0.5	1	144.5343	8	709.6336	2	0	145.8197	9	726.5047
50	30	2/3	0.5	2	138.3083	7	682.5471	1	0	139.3776	8	692.8938
50	40	1/3	0.25	1	164.4680	7	790.2199	3	6	166.6772	8	831.2659
50	40	1/3	0.25	2	162.8553	7	782.3964	3	6	165.8123	8	827.1816
50	40	1/3	0.75	0	176.0732	10	865.2115	0	1	177.5712	10	875.9731
50	40	2/3	0.5	2	207.2107	9	1004.7700	5	2	214.3914	10	1070.2105
50	40	2/3	0.75	1	221.1591	10	1091.5211	2	0	226.5568	11	1128.9106
50	40	2/3	0.75	2	221.1591	10	1091.5211	2	0	226.5568	11	1128.9106

4.6.4 Maximum flight time of drones

We selected a 20-node instance with $Dim = 20$, $r^P = 1/3$, $r^D = 0.75$, and $\eta = 2$ to investigate the influence of varying drone flight times by altering the value of E to 5, 10, 20, and 60 minutes. The summarized system performance under different drone endurance levels is provided in Table 4.10, while Figure 4.2 illustrates the solutions for each scenario.

For the case of $E = 5$, the drone had just 2 minutes for the journey from launch to customer and back to recovery. This constraint severely limited flight possibilities. Compared to this baseline scenario, as E increased to 10, 20, 30, and 60 minutes, total costs were successively reduced by 1.04%, 8.79%, 18.68%, and 19.20%. When E reached 20 min-

[6] In Section 4.6.3, a pair of instances includes two instances sharing the same features such as node size, distribution, r^P, r^D, η, and E, with one having soft TW and the other hard TW.

utes, a DRB could be spared, resulting in a 14.24% reduction in total DRB-traveled miles. However, with further increases in E to 30 and 60 minutes, drone flight times notably increased, although the reduction in DRB-traveled miles became more gradual. When comparing solutions for $E = 30$ and $E = 60$, an intriguing observation emerges: the DRB routes remained consistent for both cases.

Regarding drone flights, the main distinction lies in serving request 17, specifically <16,17,3> for $E = 30$ and <0,17,10> for $E = 60$. Although the drone-traveled miles for <0,17,10> were shorter than <16,17,3>, the total flying time for <0,17,10> exceeded that of <16,17,3>. This discrepancy arises from the comprehensive drone flying time, encompassing travel between locations and waiting times at customer sites and recovery nodes. The results from Table 4.10 and Figure 4.2 affirm that extending the maximum drone flight time enables more advantageous drone flights, facilitating long-distance travel or extended hovering periods, ultimately contributing to cost reduction.

Table 4.10: Impact of the maximum flight time of drones

E	Total costs	# used vehicles	# flights	Flying time	DRB-traveled miles	Drone-traveled miles	Passenger delay (min)	Goods delay (min)
5	40.7340	4	0	0	196.1697	0	0	3
10	40.3111	4	1	10	193.4886	5.6703	0	3
20	37.1527	3	3	42	168.2418	25.2146	0	6
30	33.1232	3	4	112	161.1567	44.5912	0	0
60	32.9111	3	4	153	161.1567	33.9894	0	0

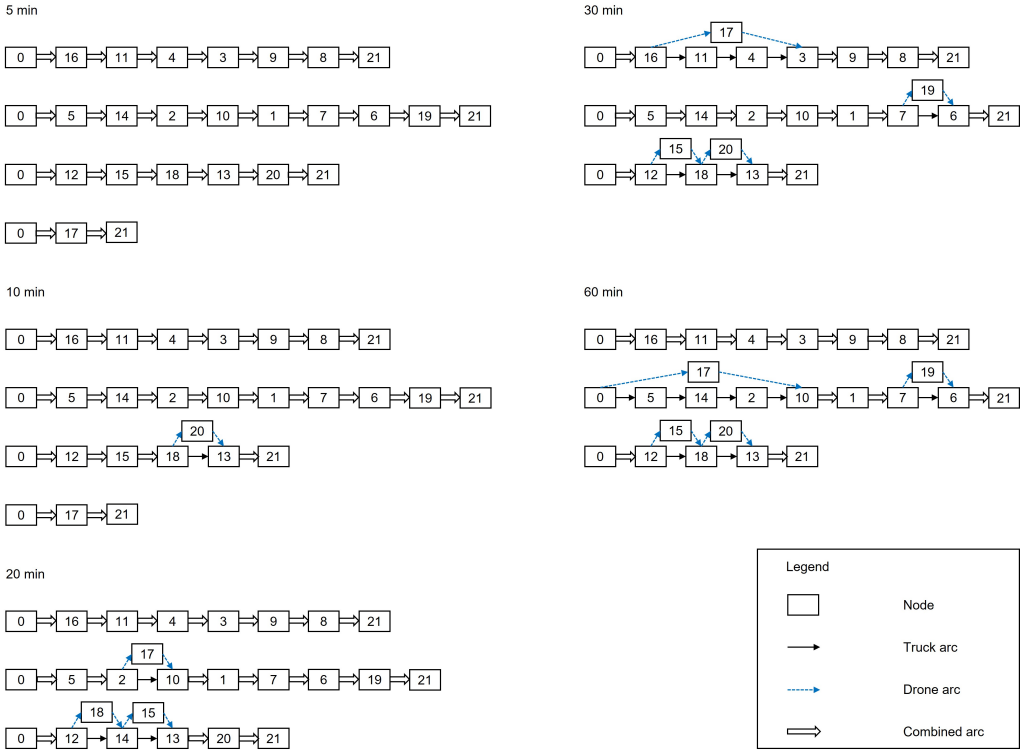

Figure 4.2: Solutions for 20-node instance with $Dim = 20$, $r^P = 1/3$, $r^D = 0.75$, and $\eta = 2$ under different drone battery endurance level

4.7 Conclusions

This study delves into a route planning dilemma centered on an integrated passenger and parcel transportation system, intertwining demand-responsive vehicles (DRBs) and

drones. The primary objective is to curtail operational expenses while accommodating the varied transportation requests by amalgamating these two modes. We introduced a path-based optimization model coupled with a column generation (CG) algorithm for exact solutions to address this. A notable feature of the model is its adaptability, permitting a shift from the integrated problem to simpler configurations such as vehicle routing problems with drones (VRP-D) and pickup and delivery problems (PDP) by adjusting the passenger request ratio. The CG algorithm is complemented by a custom label correcting procedure for pricing problems and further enhanced by a large neighborhood search heuristic and optimization strategies to expedite the CG process.

Extensive computational experiments were undertaken to evaluate the CG's efficacy. The outcomes showcased that the proposed CG solved all 20-node instances and 90% of the 50-node instances for the three problem variations (SARP-D, VRP-D, PDP), promptly yielding optimal solutions. The mean discrepancy between the lower and upper bounds across all resolved instances was a mere 0.7%. In-depth sensitivity analyses were conducted on pivotal parameters within the SARP-D framework, yielding insightful findings. For instance, allowing more intermediate stops during passenger service, relaxing hard time windows to soft ones, and augmenting drone endurance were identified to expand solution possibilities, leading to more efficient DRB routes or drone flights, ultimately curtailing overall costs. Consequently, the count of employed DRBs and DRB-traveled distances witnessed reductions. However, such reductions sometimes entailed service delays at specific stops, contingent on specific circumstances. Furthermore, when vehicle resources are ample, it is highly probable to reduce total costs while preserving a robust, on-time delivery service.

Future research can be directed toward several key areas. Firstly, explore further application scenarios involving intricate drone operations within the SARP-D framework, like incorporating advanced energy consumption models for drones or accommodating multiple drones for each DRB, and secondly, devising strategies to tackle the SARP-D challenge in uncertain environments, where factors such as unpredictable road travel times and variable request locations come into play. Lastly, focus on developing more efficient algorithms, either exact or metaheuristic, to efficiently handle larger and more complex instances, thus enhancing the scalability of the proposed approach.

Acknowledgements

The first author acknowledges financial support from the China Scholarship Council (No. 202107940012) and the Otto Moensted Foundation.

Appendix

4.A Label extensions

Case 1. Extend a temporary label π_i.

Subcase 1.1. Transfer π_i to ϕ_i by applying function $AddDroneLeg(\pi_i, j)$, where $j \in D(\pi_i)$. The attributes of ϕ_i inherit those from π_i and some of them are updated using the following equations.

$c(\phi_i) = i$

$dr(\phi_i) = j$

$tp(\phi_i)_j \leftarrow$ *drone node*

$tp(\phi_i)_{c(\phi_i)} \leftarrow$ *recovery node*

$\tau(\phi_i)_j = \tau''(\pi_i)_{c(\pi_i)} + SL + T^D_{c(\pi_i),j}$

$\tau'(\phi_i) = \max\{\max\{\tau(\phi_i)_j, E_j\} + ST^D_j + T^D_{j,c(\phi_i)} + SR, \tau(\pi_i)_{c(\phi_i)} + SR\}$

$\tau''(\phi_i)_j = \max\{\tau(\phi_i)_j, E_j\}$

$\tau''(\phi_i)_{c(\phi_i)} = \max\{\tau'(\phi_i), \tau''(\pi_i)_{v(\phi_i)} + ST^V_{v(\phi_i)}\}$

$fly(\phi_i) = \tau'(\phi_i) - \tau''(\phi_i)_{c(\pi_i)}$

$gl(\phi_i) = gl(\pi_i) + 1$

$\Omega(\phi_i) = \Omega(\pi_i) \cup \{j\}$

$V(\phi_i) = V(\pi_i) \backslash \{j\}$

$D(\phi_i) = D(\pi_i) \backslash \{j\}$

$\kappa(\phi_i) = \kappa(\pi_i) + \beta_j$

$cost(\phi_i) = cost(\pi_i) + C^D_{c(\pi_i),j} + C^D_{j,c(\phi_i)} + \alpha_j * \max\{0, \tau(\phi_i)_j - L_j\}$

$\overline{rc}(\phi_i) = cost(\phi_i) - \kappa(\phi_i)$

Note that if $fly(\phi_i) > E$, a time slack strategy that allows postponing the departure time at some nodes (Li et al., 2016a; Savelsbergh, 1992) will be applied. In the SARP-D context, the time slack strategy refers to postponing the time the drone starts taking off at the launch or recovery-launch node. Consequently, the values of $\tau(\phi_i)$ and $\tau'(\phi_i)$ for nodes associated with the newly added drone leg, $fly(\phi_i)$, $cost(\phi_i)$, and $\overline{rc}(\phi_i)$, will be updated. For a more detailed description of the time slack strategy for SARP-D, readers are referred to Cheng et al. (2023b).

Subcase 1.2. Extend π_i to π_j by applying function $AddDRBArc(\pi_i, j)$, where $j \in V(\pi_i)$. The attributes of π_j inherit those from π_i and are updated using the following equations.

$v(\pi_j) = j$

$pos(\pi_j)_j = pos(\pi_i)_{v(\pi_i)} + 1$

$tp(\pi_j)_j \leftarrow$ *common node*

$$\tau(\pi_j)_j = \tau''(\pi_i)_{v(\pi_i)} + ST^V_{v(\pi_i)} + T^V_{v(\pi_i),j}$$

$$\tau''(\pi_j)_j = \max\{\tau(\pi_j)_j, E_j\}$$

$$pl(\pi_j) = \begin{cases} pl(\pi_i) + Q_j & \text{if } j \in S_p \\ pl(\pi_i) & \text{if } j \notin S_p \end{cases}$$

$$gl(\pi_j) = \begin{cases} gl(\pi_i) + 1 & \text{if } j \in S_g \\ gl(\pi_i) & \text{if } j \notin S_g \end{cases}$$

$$\Omega(\pi_j) = \Omega(\pi_i) \cup \{j\}$$

$$O(\pi_j) = \begin{cases} O(\pi_i) & \text{if } j \notin S_p \\ O(\pi_i) \cup \{j\} & \text{if } j \in S^o_p \\ O(\pi_i) \backslash \{j - |P|\} & \text{if } j \in S^d_p \end{cases}$$

$$V(\pi_j) = \begin{cases} \{O(\pi_j)_0 + |P|\} & \text{if } pos(\pi_j)_j - pos(\pi_j)_{O(\pi_j)_0} = \eta \\ S^o_p \cup S_g \cup S^d_{O(\pi_j)} \backslash \Omega(\pi_j) & \text{else, where } S^d_{O(\pi_j)} \text{ is the set of destinations of } O(\pi_j) \end{cases}$$

$$D(\pi_j) = \begin{cases} D(\pi_i) \backslash \{j\} & \text{if } j \in S_g{}' \\ D(\pi_i) & \text{if } j \notin S_g{}' \end{cases}$$

$$\kappa(\pi_j) = \kappa(\pi_i) + \beta_j$$

$$cost(\pi_j) = cost(\pi_i) + C^V_{v(\pi_i),j} + \alpha_j * \max\{0, \tau(\pi_j)_j - L_j\}$$

$$\overline{rc}(\pi_j) = cost(\pi_j) - \kappa(\pi_j)$$

Case 2. Extend a label ϕ_i

Subcase 2.1. Extend ϕ_i to π_j by applying function $AddDRBArc(\phi_i, j)$, where $j \in V(\phi_i)$. The attributes of π_j inherit those from ϕ_i and are updated using the following equations.

$$v(\pi_j) = j$$

$$pos(\pi_j)_j = pos(\phi_i)_{v(\phi_i)} + 1$$

$$tp(\pi_j)_{c(\phi_i)} \leftarrow \begin{cases} \textit{launch node} & \text{if } tp(\phi_i)_{c(\phi_i)} \text{ is } \textit{common node} \\ \textit{recovery-launch node} & \text{if } tp(\phi_i)_{c(\phi_i)} \text{ is } \textit{recovery node} \end{cases}$$

$$tp(\pi_j)_j \leftarrow \textit{common node}$$

$$\tau''(\pi_j)_{c(\phi_i)} = \begin{cases} \tau''(\phi_i)_{c(\phi_i)} & \text{if } tp(\phi_i)_{c(\phi_i)} \text{ is } \textit{common node} \\ \max\{E_{c(\phi_i)}, \tau'(\phi_i)\} & \text{if } tp(\phi_i)_{c(\phi_i)} \text{ is } \textit{recovery node} \end{cases}$$

$$\tau(\pi_j)_j = \tau''(\pi_j)_{c(\phi_i)} + SL + T^V_{c(\phi_i),j}$$

$$\tau''(\pi_j)_j = \max\{\tau(\pi_j)_j, E_j\}$$

$$pl(\pi_j) = \begin{cases} pl(\phi_i) + Q_j & \text{if } j \in S_p \\ pl(\phi_i) & \text{if } j \notin S_p \end{cases}$$

$$gl(\pi_j) = \begin{cases} gl(\phi_i) + 1 & \text{if } j \in S_g \\ gl(\phi_i) & \text{if } j \notin S_g \end{cases}$$

$$\Omega(\pi_j) = \Omega(\phi_i) \cup \{j\}$$

$$O(\pi_j) = \begin{cases} O(\phi_i) & \text{if } j \notin S_p \\ O(\phi_i) \cup \{j\} & \text{if } j \in S_p^o \\ O(\phi_i) \backslash \{j - |P|\} & \text{if } j \in S_p^d \end{cases}$$

$$V(\pi_j) = \begin{cases} \{O(\pi_j)_0 + |P|\} & \text{if } pos(\pi_j)_j - pos(\pi_j)_{O(\pi_j)_0} = \eta \\ S_p^o \cup S_g \cup S_{O(\pi_j)}^d \backslash \Omega(\pi_j) & \text{else,where } S_{O(\pi_j)}^d \text{ is the set of destinations of } O(\pi_j) \end{cases}$$

$$D(\pi_j) = \begin{cases} D(\phi_i) \backslash \{j\} & \text{if } j \in S_g{}' \\ D(\phi_i) & \text{if } j \notin S_g{}' \end{cases}$$

$$\kappa(\pi_j) = \kappa(\phi_i) + \beta_j$$

$$cost(\pi_j) = cost(\phi_i) + C_{v(\phi_i),j}^V + \alpha_j * \text{max}\{0, \tau(\pi_j)_j - L_j\}$$

$$\overline{rc}(\pi_j) = cost(\pi_j) - \kappa(\pi_j)$$

Subcase 2.2. Extend ϕ_i to ϕ_j by applying function $AddCombinedArc(\phi_i, j)$, where $j \in V(\phi_i)$. The attributes of ϕ_j inherit those from ϕ_i and are updated using the following equations.

$$c(\phi_j) = j$$

$$v(\phi_j) = j$$

$$pos(\phi_j)_j = pos(\phi_i)_{v(\phi_i)} + 1$$

$$tp(\phi_j)_j \leftarrow \textit{common node}$$

$$\tau(\phi_j)_j = \begin{cases} \tau''(\phi_i)_{c(\phi_i)} + ST_{c(\phi_i)}^V + T_{c(\phi_i),j}^V & \text{if } tp(\phi_i)_{c(\phi_i)} \text{ is } \textit{common node} \\ \tau''(\phi_i)_{c(\phi_i)} + T_{c(\phi_i),j}^V & \text{if } tp(\phi_i)_{c(\phi_i)} \text{ is } \textit{recovery node} \end{cases}$$

$$\tau''(\phi_j)_j = \text{max}\{\tau(\phi_j)_j, E_j\}$$

$$pl(\phi_j) = \begin{cases} pl(\phi_i) + Q_j & \text{if } j \in S_p \\ pl(\phi_i) & \text{if } j \notin S_p \end{cases}$$

$$gl(\phi_j) = \begin{cases} gl(\phi_i) + 1 & \text{if } j \in S_g \\ gl(\phi_i) & \text{if } j \notin S_g \end{cases}$$

$$\Omega(\phi_j) = \Omega(\phi_i) \cup \{j\}$$

$$O(\phi_j) = \begin{cases} O(\phi_i) & \text{if } j \notin S_p \\ O(\phi_i) \cup \{j\} & \text{if } j \in S_p^o \\ O(\phi_i) \backslash \{j - |P|\} & \text{if } j \in S_p^d \end{cases}$$

$$V(\phi_j) = \begin{cases} \{O(\phi_j)_0 + |P|\} & \text{if } pos(\phi_j)_j - pos(\phi_j)_{O(\phi_j)_0} = \eta \\ S_p^o \cup S_g \cup S_{O(\phi_j)}^d \backslash \Omega(\phi_j) & \text{else, where } S_{O(\phi_j)}^d \text{ is the set of destinations of } O(\phi_j) \end{cases}$$

$$D(\phi_j) = \begin{cases} D(\phi_i) \backslash \{j\} & \text{if } j \in S_g{}' \\ D(\phi_i) & \text{if } j \notin S_g{}' \end{cases}$$

$$\kappa(\phi_j) = \kappa(\phi_i) + \beta_j$$

$$cost(\phi_j) = cost(\phi_i) + C_{v(\phi_i),j}^V + \alpha_j * \text{max}\{0, \tau(\phi_j)_j - L_j\}$$

$$\overline{rc}(\phi_j) = cost(\phi_j) - \kappa(\phi_j)$$

4.B Extension feasibility check

After getting the attributes of a new label ϕ_i (**Subcase 1.1** and **Subcase 2.2**), we check the feasibility of this label. There are two situations.

Situation 1. i is the returning depot. Then, the newly generated label ϕ_i is feasible when the following constraints are satisfied.

$gl(\phi_i) \leq Cap^G$

$O(\phi_i) = \varnothing$

$\tau''(\phi_i)_i \leq T_{\text{max}}$

$fly(\phi_i) \leq E$

Situation 2. i is not the returning depot. Then, the newly generated label ϕ_i is feasible when the following constraints are satisfied.

$pl(\phi_i) \leq Cap^P$

$gl(\phi_i) \leq Cap^G$

$$\tau''(\phi_i)_i \leq \begin{cases} T_{\text{max}} - ST_i^V & \text{if } tp(\phi_i)_i \text{ is } \textit{common node} \\ T_{\text{max}} & \text{if } tp(\phi_i)_i \text{ is } \textit{recovery node} \end{cases}$$

$fly(\phi_i) \leq E$

If the new label ϕ_i is feasible, ϕ_i will be added to Φ_i. Otherwise, ϕ_i will be discarded.

Similarly, when the attributes of a temporary label $\pi_i, i \in N\backslash\{0\}$(**Subcase 1.2** and **Subcase 2.1**) are obtained, the feasibility of this temporary label should be checked. There are two situations as well.

Situation 1. i is the returning depot. Then, the newly generated label π_i is feasible when the following constraints are satisfied.

$gl(\pi_i) \leq Cap^G$

$O(\pi_i) = \varnothing$

$\tau''(\pi_i)_i \leq T_{\text{max}}$

$D(\pi_i) \neq \varnothing$

Situation 2. i is not the returning depot. Then, the newly generated label ϕ_i is feasible when the following constraints are satisfied.

$pl(\pi_i) \leq Cap^P$

$gl(\pi_i) \leq Cap^G$

$\tau''(\pi_i)_i + ST_i^V \leq T_{\text{max}}$

$D(\pi_i) \neq \varnothing$

If the new temporary label π_i is feasible, π_i will be added to Π_i. Otherwise, π_i will be discarded.

4.C Results of medium-size instances

Table C1: Results of medium-size instances

Problem	# nodes	Dim	r^P	r^D	η	Soft TW				Hard TW			
						z_{lb}	z_{ub}	Gap	CPU time (s)	z_{lb}	z_{ub}	Gap	CPU time (s)
VRP-D	20	5	0	0.25	0	6.6553	7.0856	6.07%	89.61	6.6553	7.1305	6.66%	26.55
VRP-D	20	10	0	0.25	0	12.0594	12.0699	0.09%	26.87	12.0594	12.0755	0.13%	4.2
VRP-D	20	20	0	0.25	0	28.0932	29.8253	5.81%	1.16	29.147	30.646	4.89%	0.22
VRP-D	50	10	0	0.25	0	-	-	-	10800	-	-	-	10800
VRP-D	50	20	0	0.25	0	47.0622	47.4364	0.79%	5337.29	47.0622	47.5055	0.93%	3124.53
VRP-D	50	30	0	0.25	0	77.2029	77.204	0.00%	267.29	77.2029	77.2513	0.06%	60.13
VRP-D	50	40	0	0.25	0	101.0624	102.0028	0.92%	114.53	101.4771	102.2591	0.76%	12.52
VRP-D	20	5	0	0.5	0	6.2485	6.4534	3.17%	265.98	6.2485	6.4534	3.17%	101.86
VRP-D	20	10	0	0.5	0	10.4082	10.4691	0.58%	32.87	10.4082	10.4498	0.40%	10.54
VRP-D	20	20	0	0.5	0	22.5445	23.1894	2.78%	3.57	22.5445	23.1894	2.78%	0.64
VRP-D	50	10	0	0.5	0	-	-	-	10800	-	-	-	10800
VRP-D	50	20	0	0.5	0	-	-	-	10800	-	-	-	10800
VRP-D	50	30	0	0.5	0	63.6924	64.5836	1.38%	5031.25	63.6924	65.2339	2.36%	957.6
VRP-D	50	40	0	0.5	0	86.9388	86.9388	0.00%	278.82	88.4921	91.1479	2.91%	23.17
VRP-D	20	5	0	0.75	0	5.1079	5.263	2.95%	358.89	5.1079	5.263	2.95%	179.31
VRP-D	20	10	0	0.75	0	7.4671	7.5123	0.60%	121.36	7.4671	7.5123	0.60%	63.76
VRP-D	20	20	0	0.75	0	21.4281	22.1704	3.35%	6.3	21.4281	22.1704	3.35%	1.04
VRP-D	50	10	0	0.75	0	-	-	-	10800	-	-	-	10800
VRP-D	50	20	0	0.75	0	-	-	-	10800	-	-	-	10800
VRP-D	50	30	0	0.75	0	-	-	-	10800	62.0905	62.5598	0.75%	8705.88
VRP-D	50	40	0	0.75	0	87.1101	87.1101	0.00%	169.47	88.0818	88.9985	1.03%	9.98
SARP-D	20	5	1/3	0.25	0	11.0488	11.0488	0.00%	7.82	11.0488	11.0488	0.00%	1.36
SARP-D	20	5	1/3	0.25	1	9.1479	10.0371	8.86%	11.85	9.1479	10.0371	8.86%	3.77
SARP-D	20	5	1/3	0.25	2	8.9569	9.9544	10.02%	30.4	8.9569	9.7223	7.87%	17.63
SARP-D	20	10	1/3	0.25	0	16.8669	16.8669	0.00%	0.79	16.8669	16.8669	0.00%	0.16
SARP-D	20	10	1/3	0.25	1	14.8341	14.8341	0.00%	2.13	14.8341	14.8341	0.00%	0.47

Table C1 continued from previous page

Problem	# nodes	Dim	r^P	r^D	η	Soft TW				Hard TW			
						z_{lb}	z_{ub}	Gap	CPU time (s)	z_{lb}	z_{ub}	Gap	CPU time (s)
SARP-D	20	10	1/3	0.25	2	14.4962	14.8341	2.28%	3.09	14.4962	14.6775	1.24%	0.67
SARP-D	20	20	1/3	0.25	0	49.3038	49.3038	0.00%	0.07	49.3038	49.3038	0.00%	0.07
SARP-D	20	20	1/3	0.25	1	46.4389	47.2249	1.66%	0.2	46.7922	49.4463	5.37%	0.21
SARP-D	20	20	1/3	0.25	2	44.1062	44.1062	0.00%	0.21	44.1062	44.1062	0.00%	0.14
SARP-D	50	10	1/3	0.25	0	41.3696	41.728	0.86%	4450.6	41.3696	41.4571	0.21%	58.96
SARP-D	50	10	1/3	0.25	1	-	-	-	10800	33.5478	33.5478	0.00%	372.73
SARP-D	50	10	1/3	0.25	2	-	-	-	10800	31.4321	31.4321	0.00%	8429.41
SARP-D	50	20	1/3	0.25	0	97.7212	97.7212	0.00%	72.92	97.9468	98.0646	0.12%	6.56
SARP-D	50	20	1/3	0.25	1	77.3696	77.953	0.75%	175.72	77.6227	78.6893	1.36%	9.11
SARP-D	50	20	1/3	0.25	2	72.6495	72.7514	0.14%	433.94	72.7957	72.8898	0.13%	18.99
SARP-D	50	30	1/3	0.25	0	144.7892	144.7892	0.00%	10.23	144.7892	144.7892	0.00%	6.98
SARP-D	50	30	1/3	0.25	1	134.6192	134.6192	0.00%	13.8	134.6192	134.6192	0.00%	7.01
SARP-D	50	30	1/3	0.25	2	134.4776	134.4776	0.00%	36.09	134.4776	134.4776	0.00%	7.4
SARP-D	50	40	1/3	0.25	0	177.2972	178.4884	0.67%	3.21	178.0366	178.0366	0.00%	4.13
SARP-D	50	40	1/3	0.25	1	164.468	164.468	0.00%	5.45	166.6772	166.6772	0.00%	4.99
SARP-D	50	40	1/3	0.25	2	162.8553	162.8553	0.00%	15.36	165.8123	165.8123	0.00%	6.13
SARP-D	20	5	1/3	0.5	0	11.3479	11.7551	3.46%	19.09	11.3479	11.6212	2.35%	3.52
SARP-D	20	5	1/3	0.5	1	8.7723	8.9777	2.29%	56.97	8.7723	8.9777	2.29%	23.71
SARP-D	20	5	1/3	0.5	2	7.6344	7.8343	2.55%	306.72	7.6344	7.8492	2.74%	99.78
SARP-D	20	10	1/3	0.5	0	16.9026	16.9026	0.00%	4.68	16.9026	16.9026	0.00%	0.41
SARP-D	20	10	1/3	0.5	1	15.5326	15.5326	0.00%	4.87	15.5326	15.5326	0.00%	1.03
SARP-D	20	10	1/3	0.5	2	15.064	15.1497	0.57%	13.82	15.064	15.1497	0.57%	1.16
SARP-D	20	20	1/3	0.5	0	47.8678	47.8678	0.00%	0.26	47.8678	47.8678	0.00%	0.15
SARP-D	20	20	1/3	0.5	1	41.5054	41.5054	0.00%	0.39	41.5054	41.5054	0.00%	0.14
SARP-D	20	20	1/3	0.5	2	41.5054	41.5054	0.00%	0.59	41.5054	41.5054	0.00%	0.16
SARP-D	50	10	1/3	0.5	0	41.8564	41.8695	0.03%	3923.23	41.8564	41.8695	0.03%	73.6
SARP-D	50	10	1/3	0.5	1	34.9456	34.9587	0.04%	9994.16	34.9456	34.9587	0.04%	367.22
SARP-D	50	10	1/3	0.5	2	-	-	-	10800	32.4385	32.6379	0.61%	2594.31

Table C1 continued from previous page

Problem	# nodes	Dim	r^P	r^D	η	Soft TW				Hard TW			
						z_{lb}	z_{ub}	Gap	CPU time (s)	z_{lb}	z_{ub}	Gap	CPU time (s)
SARP-D	50	20	1/3	0.5	0	85.1959	85.1959	0.00%	58.36	86.1498	86.1498	0.00%	7.71
SARP-D	50	20	1/3	0.5	1	73.849	73.849	0.00%	646.09	73.849	73.849	0.00%	11.36
SARP-D	50	20	1/3	0.5	2	69.6332	69.6332	0.00%	1970.51	69.6332	69.6332	0.00%	63.57
SARP-D	50	30	1/3	0.5	0	132.8691	132.8691	0.00%	21.44	132.8691	132.8691	0.00%	8.47
SARP-D	50	30	1/3	0.5	1	118.1943	118.1943	0.00%	56.71	118.1943	118.1943	0.00%	4.55
SARP-D	50	30	1/3	0.5	2	113.2683	113.2683	0.00%	239.53	113.2683	113.2683	0.00%	6.61
SARP-D	50	40	1/3	0.5	0	168.6409	168.6409	0.00%	7.01	168.6409	168.6409	0.00%	14.76
SARP-D	50	40	1/3	0.5	1	154.2936	154.2936	0.00%	15.33	154.2936	154.2936	0.00%	4.74
SARP-D	50	40	1/3	0.5	2	151.5366	151.5366	0.00%	32.95	151.5366	151.5366	0.00%	9.3
SARP-D	20	5	1/3	0.75	0	10.1312	10.2144	0.81%	30.87	10.1312	10.2434	1.10%	6.39
SARP-D	20	5	1/3	0.75	1	9.2222	9.3729	1.61%	103.71	9.2222	9.3782	1.66%	13.4
SARP-D	20	5	1/3	0.75	2	8.796	8.812	0.18%	244.71	8.796	8.812	0.18%	96.45
SARP-D	20	10	1/3	0.75	0	15.6833	15.6833	0.00%	2.91	15.6833	15.6833	0.00%	1.38
SARP-D	20	10	1/3	0.75	1	13.9275	13.9275	0.00%	7.82	13.9275	13.9275	0.00%	1.96
SARP-D	20	10	1/3	0.75	2	13.6314	13.6314	0.00%	8.56	13.6314	13.6314	0.00%	1.36
SARP-D	20	20	1/3	0.75	0	44.9683	44.9683	0.00%	0.28	44.9683	44.9683	0.00%	0.17
SARP-D	20	20	1/3	0.75	1	36.1248	39.1278	7.67%	0.28	36.1248	38.6892	6.63%	0.13
SARP-D	20	20	1/3	0.75	2	33.1232	33.1232	0.00%	0.44	33.1232	33.1232	0.00%	0.15
SARP-D	50	10	1/3	0.75	0	-	-	-	10800	38.6227	38.6298	0.02%	2066.42
SARP-D	50	10	1/3	0.75	1	-	-	-	10800	-	-	-	10800
SARP-D	50	10	1/3	0.75	2	-	-	-	10800	-	-	-	10800
SARP-D	50	20	1/3	0.75	0	96.7609	96.7609	0.00%	692.96	96.7609	96.7609	0.00%	13.67
SARP-D	50	20	1/3	0.75	1	75.2667	75.5923	0.43%	8013.03	77.3212	77.7663	0.57%	1077.8
SARP-D	50	20	1/3	0.75	2	-	-	-	10800	74.8225	74.8225	0.00%	890.3
SARP-D	50	30	1/3	0.75	0	127.7182	127.7182	0.00%	25.1	127.7182	127.7182	0.00%	5.71
SARP-D	50	30	1/3	0.75	1	112.1805	112.1805	0.00%	41.47	114.4067	116.2508	1.59%	5.59
SARP-D	50	30	1/3	0.75	2	111.0402	112.1805	1.02%	389.89	112.337	113.3445	0.89%	13.59
SARP-D	50	40	1/3	0.75	0	176.0732	176.0732	0.00%	18.77	177.5712	177.5712	0.00%	7.6

Table C1 continued from previous page

Problem	# nodes	Dim	r^P	r^D	η	Soft TW				Hard TW			
						z_{lb}	z_{ub}	Gap	CPU time (s)	z_{lb}	z_{ub}	Gap	CPU time (s)
SARP-D	50	40	1/3	0.75	1	164.2103	164.2103	0.00%	13.18	164.2103	164.2103	0.00%	7.08
SARP-D	50	40	1/3	0.75	2	159.1861	159.1861	0.00%	29.31	159.1861	159.1861	0.00%	5.21
SARP-D	20	5	2/3	0.25	0	12.5727	12.6874	0.90%	0.1	12.5727	12.6874	0.90%	0.1
SARP-D	20	5	2/3	0.25	1	9.7641	9.7641	0.00%	0.66	9.7641	9.7641	0.00%	0.29
SARP-D	20	5	2/3	0.25	2	9.1289	9.4438	3.33%	2.25	9.1289	9.4494	3.39%	0.78
SARP-D	20	10	2/3	0.25	0	18.2172	18.2172	0.00%	0.1	18.2172	18.2172	0.00%	0.07
SARP-D	20	10	2/3	0.25	1	17.8772	17.8772	0.00%	0.17	17.8772	17.8772	0.00%	0.17
SARP-D	20	10	2/3	0.25	2	17.7177	17.7177	0.00%	0.45	17.7177	17.7177	0.00%	0.15
SARP-D	20	20	2/3	0.25	0	52.5338	52.5338	0.00%	0.04	52.5338	52.5338	0.00%	0.04
SARP-D	20	20	2/3	0.25	1	49.6744	50.1466	0.94%	0.08	50.1466	50.1466	0.00%	0.07
SARP-D	20	20	2/3	0.25	2	47.6478	48.0682	0.87%	0.1	48.6196	50.1466	3.05%	0.07
SARP-D	50	10	2/3	0.25	0	56.0785	56.0785	0.00%	17.27	56.0785	56.0785	0.00%	12.22
SARP-D	50	10	2/3	0.25	1	44.8392	45.06	0.49%	68.11	44.8392	45.0421	0.45%	9.65
SARP-D	50	10	2/3	0.25	2	40.9945	41.0227	0.07%	455.98	40.9945	41.0227	0.07%	29.11
SARP-D	50	20	2/3	0.25	0	97.5598	97.8903	0.34%	2.25	97.5598	98.0157	0.47%	2.14
SARP-D	50	20	2/3	0.25	1	80.5515	80.5515	0.00%	6.29	80.6581	80.709	0.06%	6.45
SARP-D	50	20	2/3	0.25	2	77.7051	79.3188	2.03%	28.45	78.5975	79.9533	1.70%	6.4
SARP-D	50	30	2/3	0.25	0	162.7961	162.7961	0.00%	1.9	162.7961	162.7961	0.00%	5.74
SARP-D	50	30	2/3	0.25	1	145.3158	145.3158	0.00%	3.55	151.4486	151.4486	0.00%	2.85
SARP-D	50	30	2/3	0.25	2	144.5427	144.6272	0.06%	18.89	149.3249	149.3249	0.00%	8.37
SARP-D	50	40	2/3	0.25	0	240.9338	240.9338	0.00%	0.64	240.9338	240.9338	0.00%	0.83
SARP-D	50	40	2/3	0.25	1	214.7797	216.0614	0.59%	1.31	218.2388	218.2388	0.00%	0.69
SARP-D	50	40	2/3	0.25	2	212.3029	213.0543	0.35%	7.44	212.5103	212.5103	0.00%	2.06
SARP-D	20	5	2/3	0.5	0	13.1666	13.1666	0.00%	0.26	13.1666	13.1666	0.00%	0.14
SARP-D	20	5	2/3	0.5	1	10.8066	10.8066	0.00%	1.06	10.8066	10.8066	0.00%	0.25
SARP-D	20	5	2/3	0.5	2	10.1468	10.1468	0.00%	4.96	10.1468	10.1468	0.00%	0.65
SARP-D	20	10	2/3	0.5	0	19.7813	19.7813	0.00%	0.12	19.7813	19.7813	0.00%	0.09
SARP-D	20	10	2/3	0.5	1	18.115	18.115	0.00%	0.35	18.115	18.115	0.00%	0.15

Table C1 continued from previous page

Problem	# nodes	Dim	r^P	r^D	η	Soft TW				Hard TW			
						z_{lb}	z_{ub}	Gap	CPU time (s)	z_{lb}	z_{ub}	Gap	CPU time (s)
SARP-D	20	10	2/3	0.5	2	18.115	18.115	0.00%	1.04	18.115	18.115	0.00%	0.16
SARP-D	20	20	2/3	0.5	0	54.1807	54.1807	0.00%	0.04	54.1807	54.1807	0.00%	0.05
SARP-D	20	20	2/3	0.5	1	53.7319	53.7319	0.00%	0.08	53.7319	53.7319	0.00%	0.07
SARP-D	20	20	2/3	0.5	2	53.7319	53.7319	0.00%	0.06	53.7319	53.7319	0.00%	0.05
SARP-D	50	10	2/3	0.5	0	53.049	53.049	0.00%	68.97	53.049	53.049	0.00%	6.4
SARP-D	50	10	2/3	0.5	1	43.0142	43.0142	0.00%	266.39	43.0142	43.0142	0.00%	11.84
SARP-D	50	10	2/3	0.5	2	41.6533	41.7312	0.19%	2498.28	41.6533	41.7312	0.19%	98.07
SARP-D	50	20	2/3	0.5	0	89.7376	89.7376	0.00%	9.2	90.1728	90.1728	0.00%	2.81
SARP-D	50	20	2/3	0.5	1	74.0608	74.0608	0.00%	17.98	74.0608	74.0608	0.00%	5.07
SARP-D	50	20	2/3	0.5	2	73.7704	73.7704	0.00%	74.93	73.7704	73.7704	0.00%	7.97
SARP-D	50	30	2/3	0.5	0	156.1879	156.1879	0.00%	1.69	158.1425	158.1425	0.00%	1.29
SARP-D	50	30	2/3	0.5	1	144.5343	144.5343	0.00%	4.65	145.8197	145.8197	0.00%	2.48
SARP-D	50	30	2/3	0.5	2	138.3083	138.3083	0.00%	25.59	139.3776	139.3776	0.00%	3.41
SARP-D	50	40	2/3	0.5	0	240.9552	240.9552	0.00%	1.41	240.9552	240.9552	0.00%	0.83
SARP-D	50	40	2/3	0.5	1	221.5501	222.0294	0.22%	2.39	225.8197	225.8197	0.00%	1.41
SARP-D	50	40	2/3	0.5	2	207.2107	207.2107	0.00%	9.14	214.3914	214.3914	0.00%	1.37
SARP-D	20	5	2/3	0.75	0	12.1618	12.1618	0.00%	0.36	12.1618	12.1618	0.00%	0.18
SARP-D	20	5	2/3	0.75	1	9.8026	9.8026	0.00%	2.12	9.8026	9.8026	0.00%	0.54
SARP-D	20	5	2/3	0.75	2	9.1964	9.3271	1.40%	8.22	9.1964	9.3276	1.41%	2.46
SARP-D	20	10	2/3	0.75	0	19.959	21.3671	6.59%	0.14	19.959	20.4613	2.45%	0.13
SARP-D	20	10	2/3	0.75	1	17.5621	17.5621	0.00%	0.46	18.0266	18.0266	0.00%	0.17
SARP-D	20	10	2/3	0.75	2	17.4271	17.4271	0.00%	0.41	17.8916	17.8916	0.00%	0.22
SARP-D	20	20	2/3	0.75	0	54.1807	54.1807	0.00%	0.04	54.1807	54.1807	0.00%	0.06
SARP-D	20	20	2/3	0.75	1	53.7319	53.7319	0.00%	0.08	53.7319	53.7319	0.00%	0.06
SARP-D	20	20	2/3	0.75	2	53.7319	53.7319	0.00%	0.16	53.7319	53.7319	0.00%	0.08
SARP-D	50	10	2/3	0.75	0	52.7585	52.7585	0.00%	36.96	52.7585	52.7585	0.00%	4.62
SARP-D	50	10	2/3	0.75	1	42.7486	43.0801	0.77%	299.31	42.7486	43.1589	0.95%	26.88
SARP-D	50	10	2/3	0.75	2	39.5607	39.6473	0.22%	3427.38	39.5607	39.6624	0.26%	156.26

Table C1 continued from previous page

Problem	# nodes	Dim	r^P	r^D	η	Soft TW				Hard TW			
						z_{lb}	z_{ub}	Gap	CPU time (s)	z_{lb}	z_{ub}	Gap	CPU time (s)
SARP-D	50	20	2/3	0.75	0	89.2275	89.2275	0.00%	12.31	89.2275	89.2275	0.00%	3.1
SARP-D	50	20	2/3	0.75	1	76.9903	77.8905	1.16%	35.8	76.9903	78.0504	1.36%	6.39
SARP-D	50	20	2/3	0.75	2	76.6173	78.1969	2.02%	190.01	76.6173	78.4003	2.27%	11.6
SARP-D	50	30	2/3	0.75	0	150.2841	150.4479	0.11%	3.4	153.4046	153.4046	0.00%	3.24
SARP-D	50	30	2/3	0.75	1	143.7704	144.7228	0.66%	9.22	144.4064	144.6678	0.18%	3.79
SARP-D	50	30	2/3	0.75	2	143.0263	144.9627	1.34%	49.78	144.303	144.6678	0.25%	6.08
SARP-D	50	40	2/3	0.75	0	242.6529	242.6529	0.00%	2.42	242.6529	242.6529	0.00%	3.4
SARP-D	50	40	2/3	0.75	1	221.1591	221.1591	0.00%	2.17	226.5568	226.5568	0.00%	2.29
SARP-D	50	40	2/3	0.75	2	221.1591	221.1591	0.00%	7.75	226.5568	226.5568	0.00%	2.15
PDP	20	5	1	0	0	13.8597	13.8597	0.00%	0.03	13.8597	13.8597	0.00%	0.02
PDP	20	5	1	0	1	11.2838	11.2838	0.00%	0.04	11.2838	11.2838	0.00%	0.04
PDP	20	5	1	0	2	10.3529	10.9221	5.21%	0.11	10.3529	11.1781	7.38%	0.05
PDP	20	10	1	0	0	24.1166	24.1166	0.00%	0.03	24.1166	24.1166	0.00%	0.02
PDP	20	10	1	0	1	21.3134	21.3134	0.00%	0.03	21.3134	21.3134	0.00%	0.04
PDP	20	10	1	0	2	20.6259	20.6259	0.00%	0.08	20.6259	20.6259	0.00%	0.05
PDP	20	20	1	0	0	57.5111	57.5111	0.00%	0.03	57.5111	57.5111	0.00%	0.02
PDP	20	20	1	0	1	51.8543	51.8543	0.00%	0.02	57.5111	57.5111	0.00%	0.03
PDP	20	20	1	0	2	47.5389	47.5389	0.00%	0.07	51.1403	51.1403	0.00%	0.04
PDP	50	10	1	0	0	64.9869	64.9869	0.00%	1.29	64.9869	64.9869	0.00%	0.99
PDP	50	10	1	0	1	48.2688	48.7303	0.95%	2.5	48.2688	50.0424	3.54%	1.45
PDP	50	10	1	0	2	43.9433	44.6711	1.63%	11.38	43.9433	44.3051	0.82%	4.05
PDP	50	20	1	0	0	120.1893	120.1893	0.00%	0.6	120.1893	120.1893	0.00%	0.64
PDP	50	20	1	0	1	99.1423	99.1423	0.00%	0.66	99.1423	99.1423	0.00%	1.71
PDP	50	20	1	0	2	97.9655	99.8965	1.93%	12.34	97.9655	99.7764	1.81%	1.53
PDP	50	30	1	0	0	194.7624	194.7624	0.00%	0.26	195.2373	195.2373	0.00%	0.33
PDP	50	30	1	0	1	166.0724	166.0724	0.00%	0.47	167.3267	167.3267	0.00%	1.32
PDP	50	30	1	0	2	158.7501	158.7501	0.00%	7.32	160.8342	160.8342	0.00%	0.78
PDP	50	40	1	0	0	255.9041	255.9041	0.00%	0.39	255.9041	255.9041	0.00%	0.14

Table C1 continued from previous page

Problem	# nodes	Dim	r^P	r^D	η	Soft TW				Hard TW			
						z_{lb}	z_{ub}	Gap	CPU time (s)	z_{lb}	z_{ub}	Gap	CPU time (s)
PDP	50	40	1	0	1	242.0272	242.0272	0.00%	1.2	242.0272	242.0272	0.00%	0.67
PDP	50	40	1	0	2	238.3889	238.3889	0.00%	2.94	238.3889	238.3889	0.00%	0.57

References

Agatz, N., Bouman, P., & Schmidt, M. (2018). Optimization approaches for the traveling salesman problem with drone. *Transportation Science*, *52*(4), 965–981.

Anderson, J. M., Nidhi, K., Stanley, K. D., Sorensen, P., Samaras, C., & Oluwatola, O. A. (2014). *Autonomous vehicle technology: A guide for policymakers*. Rand Corporation.

Bouman, P., Agatz, N., & Schmidt, M. (2018). Dynamic programming approaches for the traveling salesman problem with drone. *Networks*, *72*(4), 528–542.

Cavani, S., Iori, M., & Roberti, R. (2021). Exact methods for the traveling salesman problem with multiple drones. *Transportation Research Part C: Emerging Technologies*, *130*, 103280.

Cheng, R., Jiang, Y., & Nielsen, O. A. (2023a). Integrated people-and-goods transportation systems: From a literature review to a general framework for future research. *Transport Reviews*, 1–24.

Cheng, R., Jiang, Y., Nielsen, O. A., & Pisinger, D. (2023b). An adaptive large neighborhood search metaheuristic for a passenger and parcel share-a-ride problem with drones. *Transportation Research Part C: Emerging Technologies*, *153*, 104203.

Cochrane, K., Saxe, S., Roorda, M. J., & Shalaby, A. (2017). Moving freight on public transit: Best practices, challenges, and opportunities. *International Journal of Sustainable Transportation*, *11*(2), 120–132.

Coindreau, M.-A., Gallay, O., & Zufferey, N. (2021). Parcel delivery cost minimization with time window constraints using trucks and drones. *Networks*, *78*(4), 400–420.

Danna, E., & Le Pape, C. (2005). Branch-and-price heuristics: A case study on the vehicle routing problem with time windows. *Column generation* (pp. 99–129). Springer.

Di Puglia Pugliese, L., Guerriero, F., & Scutellá, M. G. (2021). The last-mile delivery process with trucks and drones under uncertain energy consumption. *Journal of Optimization Theory and Applications*, *191*(1), 31–67.

European Commission. (2007). Green paper, towards a new culture for urban mobility, Luxembourg: Publications Office of the European Union.

Feillet, D., Dejax, P., Gendreau, M., & Gueguen, C. (2004). An exact algorithm for the elementary shortest path problem with resource constraints: Application to some vehicle routing problems. *Networks: An International Journal*, *44*(3), 216–229.

Ghilas, V., Cordeau, J.-F., Demir, E., & Woensel, T. V. (2018). Branch-and-price for the pickup and delivery problem with time windows and scheduled lines. *Transportation Science*, *52*(5), 1191–1210.

Ghilas, V., Demir, E., & Van Woensel, T. (2016). A scenario-based planning for the pickup and delivery problem with time windows, scheduled lines and stochastic demands. *Transportation Research Part B: Methodological*, *91*, 34–51.

Golbabaei, F., Yigitcanlar, T., & Bunker, J. (2021). The role of shared autonomous vehicle systems in delivering smart urban mobility: A systematic review of the literature. *International Journal of Sustainable Transportation*, *15*(10), 731–748.

Ha, Q. M., Deville, Y., Pham, Q. D., & Hà, M. H. (2018). On the min-cost traveling salesman problem with drone. *Transportation Research Part C: Emerging Technologies*, *86*, 597–621.

Jeong, H. Y., Song, B. D., & Lee, S. (2019). Truck-drone hybrid delivery routing: Payload-energy dependency and no-fly zones. *International Journal of Production Economics*, *214*, 220–233.

Kuo, R., Lu, S.-H., Lai, P.-Y., & Mara, S. T. W. (2022). Vehicle routing problem with drones considering time windows. *Expert Systems with Applications*, *191*, 116264.
Li, B., Krushinsky, D., Reijers, H. A., & Van Woensel, T. (2014). The share-a-ride problem: People and parcels sharing taxis. *European Journal of Operational Research*, *238*(1), 31–40.
Li, B., Krushinsky, D., Van Woensel, T., & Reijers, H. A. (2016a). An adaptive large neighborhood search heuristic for the share-a-ride problem. *Computers & Operations Research*, *66*, 170–180.
Li, B., Krushinsky, D., Van Woensel, T., & Reijers, H. A. (2016b). The share-a-ride problem with stochastic travel times and stochastic delivery locations. *Transportation Research Part C: Emerging Technologies*, *67*, 95–108.
Li, H., Chen, J., Wang, F., & Bai, M. (2021). Ground-vehicle and unmanned-aerial-vehicle routing problems from two-echelon scheme perspective: A review. *European Journal of Operational Research*, *294*(3), 1078–1095.
Li, H., & Wang, F. (2023). Branch-price-and-cut for the truck–drone routing problem with time windows. *Naval Research Logistics (NRL)*, *70*(2), 184–204.
Lu, C.-C., Diabat, A., Li, Y.-T., & Yang, Y.-M. (2022). Combined passenger and parcel transportation using a mixed fleet of electric and gasoline vehicles. *Transportation Research Part E: Logistics and Transportation Review*, *157*, 102546.
Luo, Q., Wu, G., Ji, B., Wang, L., & Suganthan, P. N. (2021). Hybrid multi-objective optimization approach with pareto local search for collaborative truck-drone routing problems considering flexible time windows. *IEEE Transactions on Intelligent Transportation Systems*, *23*(8), 13011–13025.
Macrina, G., Di Puglia Pugliese, L., Guerriero, F., & Laporte, G. (2020). Drone-aided routing: A literature review. *Transportation Research Part C: Emerging Technologies*, *120*, 102762.
Mourad, A., Puchinger, J., & Van Woensel, T. (2021). Integrating autonomous delivery service into a passenger transportation system. *International Journal of Production Research*, *59*(7), 2116–2139.
Murray, C. C., & Chu, A. G. (2015). The flying sidekick traveling salesman problem: Optimization of drone-assisted parcel delivery. *Transportation Research Part C: Emerging Technologies*, *54*, 86–109.
Murray, C. C., & Raj, R. (2020). The multiple flying sidekicks traveling salesman problem: Parcel delivery with multiple drones. *Transportation Research Part C: Emerging Technologies*, *110*, 368–398.
Othman, K. (2022). Exploring the implications of autonomous vehicles: A comprehensive review. *Innovative Infrastructure Solutions*, *7*(2), 165.
Poikonen, S., & Golden, B. (2020). Multi-visit drone routing problem. *Computers & Operations Research*, *113*, 104802.
Poikonen, S., Wang, X., & Golden, B. (2017). The vehicle routing problem with drones: Extended models and connections. *Networks*, *70*(1), 34–43.
Roberti, R., & Ruthmair, M. (2021). Exact methods for the traveling salesman problem with drone. *Transportation Science*, *55*(2), 315–335.
Ropke, S., & Cordeau, J.-F. (2009). Branch and cut and price for the pickup and delivery problem with time windows. *Transportation Science*, *43*(3), 267–286.
Sacramento, D., Pisinger, D., & Ropke, S. (2019). An adaptive large neighborhood search metaheuristic for the vehicle routing problem with drones. *Transportation Research Part C: Emerging Technologies*, *102*, 289–315.

Salama, M. R., & Srinivas, S. (2022). Collaborative truck multi-drone routing and scheduling problem: Package delivery with flexible launch and recovery sites. *Transportation Research Part E: Logistics and Transportation Review*, *164*, 102788.

Savelsbergh, M. W. (1992). The vehicle routing problem with time windows: Minimizing route duration. *ORSA journal on computing*, *4*(2), 146–154.

Tamke, F., & Buscher, U. (2021). A branch-and-cut algorithm for the vehicle routing problem with drones. *Transportation Research Part B: Methodological*, *144*, 174–203.

Tiniç, G. O., Karasan, O. E., Kara, B. Y., Campbell, J. F., & Ozel, A. (2023). Exact solution approaches for the minimum total cost traveling salesman problem with multiple drones. *Transportation Research Part B: Methodological*, *168*, 81–123.

Wang, X., Poikonen, S., & Golden, B. (2017). The vehicle routing problem with drones: Several worst-case results. *Optimization Letters*, *11*, 679–697.

Wang, Y., Wang, Z., Hu, X., Xue, G., & Guan, X. (2022). Truck–drone hybrid routing problem with time-dependent road travel time. *Transportation Research Part C: Emerging Technologies*, *144*, 103901.

Wang, Z., & Sheu, J.-B. (2019). Vehicle routing problem with drones. *Transportation research part B: methodological*, *122*, 350–364.

Xia, Y., Zeng, W., Zhang, C., & Yang, H. (2023). A branch-and-price-and-cut algorithm for the vehicle routing problem with load-dependent drones. *Transportation Research Part B: Methodological*, *171*, 80–110.

Yang, Y., Yan, C., Cao, Y., & Roberti, R. (2023). Planning robust drone-truck delivery routes under road traffic uncertainty. *European Journal of Operational Research*, *309*(3), 1145–1160.

Yao, R., & Bekhor, S. (2023). A general equilibrium model for multi-passenger ridesharing systems with stable matching. *Transportation Research Part B: Methodological*, *175*.

Yin, Y., Li, D., Wang, D., Ignatius, J., Cheng, T., & Wang, S. (2023a). A branch-and-price-and-cut algorithm for the truck-based drone delivery routing problem with time windows. *European Journal of Operational Research*, *309*(3), 1125–1144.

Yin, Y., Yang, Y., Yu, Y., Wang, D., & Cheng, T. (2023b). Robust vehicle routing with drones under uncertain demands and truck travel times in humanitarian logistics. *Transportation Research Part B: Methodological*, *174*, 102781.

Yu, V. F., Indrakarna, P. A., Redi, A. A. N. P., & Lin, S.-W. (2021). Simulated annealing with mutation strategy for the share-a-ride problem with flexible compartments. *Mathematics*, *9*(18), 2320.

Yu, V. F., Purwanti, S. S., Redi, A. P., Lu, C.-C., Suprayogi, S., & Jewpanya, P. (2018). Simulated annealing heuristic for the general share-a-ride problem. *Engineering Optimization*, *50*(7), 1178–1197.

Yu, V. F., Zegeye, M. M., Gebeyehu, S. G., Indrakarna, P. A., & Jodiawan, P. (2023). A matheuristic algorithm for the share-a-ride problem. *Expert Systems with Applications*, 120569.

Zhang, S., Markos, C., & James, J. (2022). Autonomous vehicle intelligent system: Joint ride-sharing and parcel delivery strategy. *IEEE Transactions on Intelligent Transportation Systems*, *23*(10), 18466–18477.

Zhen, L., Gao, J., Tan, Z., Wang, S., & Baldacci, R. (2023). Branch-price-and-cut for trucks and drones cooperative delivery. *IISE Transactions*, *55*(3), 271–287.

Zhou, H., Qin, H., Cheng, C., & Rousseau, L.-M. (2023). An exact algorithm for the two-echelon vehicle routing problem with drones. *Transportation Research Part B: Methodological*, *168*, 124–150.

5 Assessing the impacts of public transport-based crowdshipping: A case study in a central district in Copenhagen

Cheng, R., Fessler, A., Nielsen, O. A., Larsen. A., Jiang, Y., (2023). Assessing the impacts of public transport-based crowdshipping: A case study in a central district in Copenhagen. To be submitted to Frontiers of Engineering Management.

Abstract

The rapid development of E-commerce and sharing economy has created an opportunity for crowdshipping as a novel solution to last-mile delivery. Prior research and applications on crowdshipping mainly focus on private vehicle-based crowdshipping, which often generates rebound effects resulting in traffic congestion and emission increases due to the dedicated trips performed for crowdsourced deliveries. To mitigate the rebound effects, this paper proposes a public transport (PT)-based crowdshipping concept as a complementary solution to the traditional parcel delivery system, where public transport users utilize their existing trips to carry out crowdsourced deliveries. We propose a methodology comprising a parcel locker location model and a vehicle routing model to analyze the impact of PT-based crowdshipping. It is worth noting that the parcel locker location model not only helps to plan the PT-based crowdshipping network but also helps to understand the barriers to the development of PT-based crowdshipping. A case study in a central district in Copenhagen using real-world data is conducted to estimate the impacts of PT-based crowdshipping. Our results indicate that PT-based crowdshipping could reduce the total vehicle kilometers traveled, the total working time of drivers, and the number of used vans (drivers) to perform last-mile deliveries, which would contribute to mitigating traffic congestion and environmental pollution. However, the development of PT-based crowdshipping might be restricted by the number of crowdshippers. Thus, our research suggests that efforts should be made to increase the number of crowdshippers.

Keywords: Last-mile delivery; Crowdshipping; Public transport-based crowdshipping; Integrated passenger and freight transportation; Impact assessment

5.1 Introduction

E-commerce has been growing exponentially in the last decade, with global E-commerce sales reaching 5.717 trillion dollars in 2022, compared to 1.336 trillion in 2014. The number is expected to grow by 50 percent by 2025 (Statista, 2022). With the growth comes not only business opportunities but also great challenges for both retailers and logistics services providers. On the one hand, the increased demand will bring more revenues to companies. On the other hand, last-mile delivery, which is the most expensive and inefficient part of the supply chain, becomes a pivotal factor in securing market share in the competitive environment, as consumers are more and more sensitive to delivery speed and flexibility. Moreover, the rising transportation demand has resulted in a surge of delivery vans entering the urban areas, exacerbating traffic congestion and environmental issues. Consequently, both practitioners and academics are actively seeking viable solutions to provide last-mile delivery in an efficient and sustainable manner.

One relatively new solution to last-mile delivery is the introduction of parcel lockers, offering various benefits. Parcel lockers allow logistics companies to deliver parcels to centralized facilities, capitalizing on economies of scale and reducing the cost caused by "Not-at-Home" delivery. They allow recipients to collect their parcels in a flexible time without having to wait for a delivery person or risking missing a delivery attempt. Furthermore, parcel lockers offer a way to deliver parcels without physical interaction between the delivery man and customer, which facilitates delivery in situations where contactless interaction is preferred, e.g., during a pandemic. According to a report by the European Regulators Group for Postal Services (ERGP) (European Regulators Group for Postal Services, 2022), the count of parcel lockers has witnessed substantial growth across many countries, particularly in Denmark (465 in 2017 and 1740 in 2021), Finland (487 in 2017 and 2288 in 2021), and Norway (191 in 2020 and 2800 in 2021).

In recent years, the concept of crowdshipping, inspired by successful business models under the sharing economy (e.g., Uber and Airbnb), has presented another novel solution to last-mile delivery. In a crowdshipping system, ordinary people utilize their free capacity regarding time and/or space to perform parcel delivery with monetary compensation. Both logistics services providers and E-retailers have conducted experiments with crowdshipping (Alnaggar et al., 2021). For example, in 2013, DHL piloted a project, "Myways" in Stockholm, which allowed individuals to deliver parcels on the way to their destination. In 2015, Amazon introduced a service named "Amazon Flex", where ordinary people use their own cars to deliver Amazon orders to final customers. This service is now active in more than 50 cities.

Crowdshipping can be implemented in various ways. The main body of prior research and practical applications related to crowdshipping has focused on private personal vehicle use, where dedicated trips or detours are often unavoidable (Allahviranloo & Baghestani, 2019; Punel & Stathopoulos, 2017). These personal vehicle-based concepts often entail rebound effects resulting in emission increases instead of decreases (Buldeo Rai et al., 2018). Additionally, sharing economic concepts have often been criticized for undermining the rights of workers and creating a 'gig-economy' precariat (Paus, 2018).

To harness the benefits of parcel lockers and crowdshipping while mitigating the drawbacks of personal vehicle-based crowdshipping, this paper focuses on public transport (PT)-based crowdshipping. This concept is regarded as a form of integrating people and goods transportation (Cheng et al., 2023a), which aligns with the European Commission's call for the integration of passenger and freight transportation (European Commission, 2007). Figure 5.1 presents a schematic overview of the PT-based crowdshipping. Before

delving into the details of our PT-based crowdshipping, we first explain the terminologies used in this context. Note that parcel lockers in our PT-based crowdshipping concept are all installed in PT stations.

- **Recipients:** Customers who buy a PT-based crowdshipping service. They are also the owners of the parcels.
- **Pickup Parcel Lockers (P-PL):** Parcel lockers that crowdshippers use to pick up parcels. In this study, they are positioned at PT stations close to the distribution center and are predetermined.
- **Delivery Parcel Lockers (D-PL):** Parcel lockers that crowdshippers use to drop off parcels. These parcel lockers are also parcel lockers where the final recipients pick up the parcels. Locations of D-PL are determined by the model presented in Section 5.3.3.

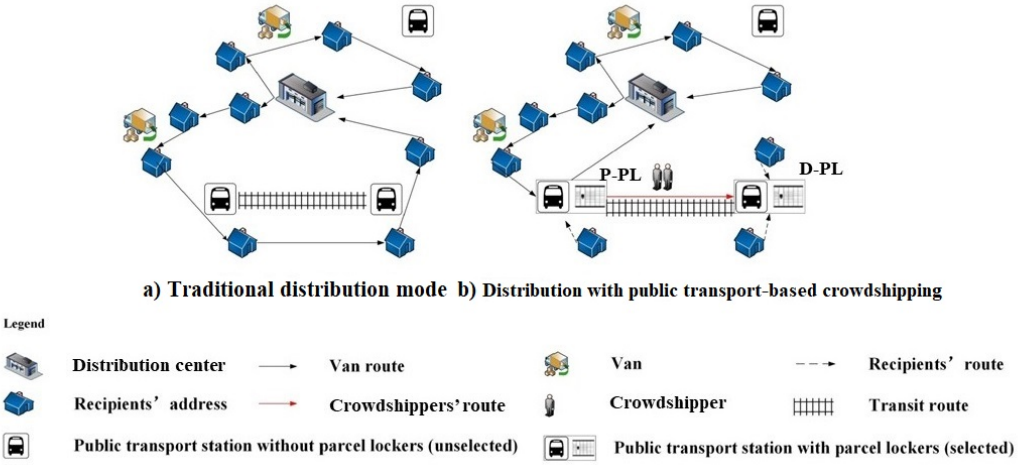

Figure 5.1: An illustration of PT-based crowdshipping

In the traditional distribution mode, all parcels are delivered by vans owned and operated by logistics companies. In PT-based crowdshipping, parcel lockers are installed in some PT stations to store small parcels. A proportion of parcels, termed crowdshipped parcels, are shifted from vans to crowdshippers. The journey of these crowdshipped parcels from the distribution center to their final destinations comprises three legs. In the first leg, crowdshipped parcels are transported by trucks from the distribution center to P-PLs positioned at PT stations near the distribution center. In the second leg, crowdshippers, who are PT users, transport parcels between different PT stations. They pick up crowdshipped parcels from P-PLs at their origin PT stations, take the PT trips, and drop off parcels to D-PLs at their destination PT stations. The final leg is completed by recipients who collect their parcels from D-PLs positioned at PT stations near their homes. Note that crowdshippers are compensated with credit for the transit system. This could ensure that only trips that would be taken anyway are utilized, preventing crowdshipping from creating a new precarious job market lacking workers' right.

It is expected that PT-based crowdshipping could bring positive impacts on mitigating traffic congestion and reducing environmental pollution by reducing the number of vans entering the city center and the total vehicle traveled miles. Prior to implementing a PT-based crowdshipping service, operators should explore their target customers' attitudes and preferences, as well as assess the potential benefits of this service. By doing the for-

mer, operators could tailor the service to meet customers' needs and enhance its adoption rate. Fessler et al. (2022) have conducted a study in this domain. They analyzed passengers' preference for PT-based crowdshipping within the Greater Copenhagen Area. This study, on the other hand, focuses on evaluating the impacts of this service to explore its viability.

The contributions of this paper are summarized as follows. First, we enrich the limited studies on PT-based crowdshipping. Second, we develop an approach to estimate the impacts of PT-based crowdshipping. This approach consists of a parcel locker location model and a vehicle routing model. The parcel locker location model not only assists in the strategic planning of the PT-based crowdshipping network but also provides insights into the efforts required to achieve various development objectives for PT-based crowdshipping. Third, we present the potential benefits of PT-based crowdshipping based on a case study using real-world data.

The remainder of the paper is organized as follows. Section 5.2 reviews related works on PT-based crowdshipping. Section 5.3 introduces the methodology for assessing the impacts of PT-based crowdshipping. Section 5.4 presents the results of a case study. Finally, Section 5.5 concludes this paper and provides future research directions.

5.2 Related works

While PT-based crowdshipping is not a completely new concept, studies on PT-based crowdshipping are still relatively limited compared with personal vehicle-based crowdshipping. In this section, we present an overview of related works on PT-based crowdshipping.

As we introduced in Section 5.1, there are three legs in PT-based crowdshipping: the first leg delivery (from the parcel's origin to P-PLs), the PT trip (from P-PLs to D-PLs), and the last leg delivery (from D-PLs to the parcel's destination). We categorize three ways of organizing PT-based crowdshipping, depending on which legs involve crowdshippers' participation.

- **Crowdshippers involved in the first and last legs (P1)**

  Kızıl and Yıldız (2023) proposed a system where crowdshippers are responsible for the first and last legs, which are usually short distances. Parcels that cannot be handled by crowdshippers are transported by backup delivery vehicles. They presented an optimization model to determine parcel locker locations and backup delivery vehicle routes. The objective is to minimize the total transportation cost of backup delivery vehicles. The simulation result of a case study in Istanbul demonstrated that making use of public transport as a backbone of the crowdshipping system could alleviate the negative externalities of last-mile delivery operations.

- **Crowdshippers involved in the PT trip and the last leg (P2)**

  Zhang and Cheah (2023) and Zhang et al. (2023) investigated a PT-based crowdshipping system where crowdshippers are involved in the PT trip and the last leg. Crowdshipped parcels are first transported by logistics companies from the distribution center to parcel lockers at PT stations, from where crowdshippers pick up the parcels, take PT trips, and deliver parcels to the parcels' final destinations. They developed approaches consisting of a parcel allocation model and a vehicle routing model to assess the impacts of their proposed PT-based crowdshipping. The results from a case study in Singapore showcased this PT-based crowdshipping could reduce vehicle kilometers traveled and associated air emissions.

- **Crowdshippers involved only in the PT trip (P3)**

  Different from the previous two PT-based crowdshipping systems where customers wait for their parcels at home, in this system, customers should pick up their parcels from D-PLs at PT stations. Logistics companies and crowdshippers are responsible for the first leg and PT trips, respectively. Several studies on this concept have been conducted from various perspectives. Gatta et al. (2019) estimated people's willingness to act as a crowdshipper and to buy a PT-based crowdshipping service based on a survey in Rome. The results highlighted the importance of flexible delivery time for customers and compensation for passengers to participate in PT-based crowdshipping. This observation aligns with Fessler et al. (2022), which analyzed passengers' willingness to act as crowdshippers based on a survey in Copenhagen. Assuming that the locations of P-PLs and D-PLs are predetermined, Karakikes and Nathanail (2022) estimated the impacts of PT-based crowdshipping by developing a city-scale traffic freight microsimulation model in PTV Vissim, taking a middle-sized Greek city as an example. Simulation results demonstrated the positive impacts of PT-based crowdshipping on reducing traffic congestion and air pollution.

Table 5.1: Different PT-based crowdshipping systems

	First leg	PT trip	Last leg	References
P1	Crowdshipper and backup delivery vans	PT lines	Crowdshipper and backup delivery vans	Kızıl & Yıldız (2023)
P2	Logistics company	Crowdshipper	Crowdshipper	Zhang et al. (2022); Zhang and Cheah (2023)
P3	Logistics company	Crowdshipper	Recipient	Gatta et al. (2019); Fessler et al. (2022); Karakikes and Nathanail (2022); This study

Each PT-based crowdshipping system has its own advantages and challenges. P1 may make the most significant impact on reducing delivery vehicles traveled miles by utilizing PT lines, but it poses several practical challenges. For example, retrofitting passenger vehicles (or carriages) and PT stations to facilitate and ensure the safety of the movement of parcels. Moreover, dedicated operators might be required to handle parcels at PT stations. P2 and P3 are easier to implement in practice compared to P1. Comparing P2 and P3, P3 is more likely to attract more passengers to act as crowdshippers. This is because P3 does not require crowdshippers to make the final delivery to customers, the direction of which might be opposite to the crowdshippers' own destinations. This requirement in P2 reduces the passengers' willingness to act as crowdshippers. However, P3 may have lower crowdshipping demand because P3 requires customers to collect parcels from D-PLs at PT stations near their homes instead of receiving parcels at their homes. Nevertheless, this drawback could be mitigated by optimizing the locations of D-PLs, as a case study in Rome (Iannaccone et al., 2021) has shown that more than 72% of customers would like to opt for picking up parcels from parcel lockers, if parcel lockers are characterized by a short distance (less than 500m) from home/work, 24h accessibility, and a small incentive (€ 1); even without a small incentive, the probability of a customer willing to collect parcels from parcel lockers exceeds 60%. Given that PT stations are 24-hour accessible and parcel lockers are cost-effective, and many countries plan to expand their parcel locker networks, we believe that P3 is a promising and sustainable solution for last-mile delivery, provided that locations of parcel lockers are well-designed.

5.3 Methodology

5.3.1 Overview of the methodology

Figure 5.2 presents the overview of the modeling framework to assess the impacts of PT-based crowdshipping. Within this framework, the entire parcels are categorized into crowdshipped parcels and van delivery parcels (Arrows 1 and 2 in Figure 5.2). The number of crowdshipped parcels is influenced by various factors from both the demand and

supply sides.

From the demand side, primary influencing factors include:

DF1) parcels' attributes such as weight, size, and type;

DF2) customers' willingness to collect their parcels from parcel lockers instead of home, which is mainly influenced by distance between parcel lockers and home and accessibility of parcels lockers.

From the supply side, primary influencing factors include:

SF1) the number of passengers traveling between specific PT stations;

SF2) passengers' willingness to act as crowdshippers, which is mainly influenced by passengers' social-demographic characteristics and compensation;

SF3) the deployment of parcel lockers.

It is essential to note that this study aims to assess the impacts of PT-based crowdshipping instead of investigating customers' and passengers' preferences for this service. Thus, crowdshippers and deliveries are predetermined to be "matched" based on given levels of demand for such service and passenger volumes between specific PT stations (Arrows 1 and 3 in Figure 5.2). The compensation cost of PT-based crowdshipping is influenced by the number of matched crowdshipped parcels (Arrow 11 in Figure 5.2). To prevent D-PLs from constraining the number of crowdshipped parcels, we develop a D-PL location model (see Section 5.3.3) to determine the locations of D-PLs. This model ensures that each customer can be served by at least one D-PL within a short distance of their homes. The inputs of this model include PT stations, passenger origin-destination pairs, and crowdshipped parcels (Arrows 4, 5, and 6 in Figure 5.2). The outputs of this model are the selected PT stations to install D-PLs and the allocation of D-PLs to customers (Arrow 7 in Figure 5.2). Moreover, by conducting sensitivity analysis on certain parameters within this model, we can get insights into potential actions and strategies that can be implemented to achieve the objectives of shifting varying percentages of parcels from vans to crowdshippers (see Section 5.4.2).

For van delivery parcels, we develop a vehicle routing model (see Section 5.3.3) to determine the routes of vans (Arrow 8 in Figure 5.2). According to solutions provided by the vehicle routing model, we could calculate various indicators related to vans, e.g., vehicle kilometers traveled by vans and traveling time of vans (Arrow 9 in Figure 5.2).

Since the first journey of crowdshipper parcels (from the distribution center to P-PLs) is transported by trucks, indicators related to trucks, which are associated with the locations of P-PLs, are also counted when assessing the impacts of PT-based crowdshipping (Arrow 10 in Figure 5.2).

5.3.2 Notations and assumptions

Table 5.2: Notations

Sets	
K	Set of homogeneous delivery vans, $K = \{1, 2, ..., \|K\|\}$, where $\|K\|$ is the number of vans.
S^o	Set of PT stations to install P-PLs, $S^o = \{1, 2, ..., \|S^o\|\}$, where $\|S^o\|$ is the number of candidate PT stations to install P-PLs.
S^d	Set of candidate PT stations to install D-PLs, $S^d = \{1, 2, ..., \|S^d\|\}$, where $\|S^d\|$ is the number of candidate PT stations to install D-PLs.

V_{cs}	Set of crowdshipping customers, $V_{cs} = \{1, 2, ..., \|V_{cs}\|\}$, where $\|V_{cs}\|$ is the number of crowdshipping customers.
V_h	Set of van delivery customers, $V_h = \{1, 2, ..., \|V_h\|\}$, where $\|V_h\|$ is the number of home delivery customers.
N	$N = V_h \cup \{0, \|V_h\| + 1\}$, where 0 and $\|V_h\| + 1$ are the distribution center nodes indicating the start and end nodes of a van route.
Parameters	
Cap	Capacity of a van.
T_{ij}	Travel time between nodes $i \in N$ and $j \in N$.
ST_j	Service time at node $j \in V_h$.
T_{max}	Maximum travel time of a van route.
Q_j^{cs}	Demand value at node $j \in V_{cs}$.
Q_j^h	Demand value at node $j \in V_h$.
D_{ij}	Distance between nodes $i \in S^d$ and $j \in V_{cs}$.
D_{max}	Service range of a D-PL. It also represents the maximum walking distance that customers are willing to travel to pick up their parcels.
L_{ij}	The number of passengers traveling between $i \in S^o$ and $j \in S^d$.
η	The average number of parcels a crowdshipper takes per trip.
$Pr_{csshipper}$	The probability of a passenger acting as a crowdshipper.
Variables	
w_{aij}	Amount of crowdshipped parcels traveling from $a \in S^o$ to $i \in S^d$ and finally picked up by customer $j \in V_{cs}$
y_i	$y_i = 1$, if a D-PL is installed at $i \in S^d$; otherwise $y_i = 0$.
x_{ijk}	$x_{ijk} = 1$, if van k travels from nodes $i \in N$ to $j \in N$; otherwise, $x_{ijk} = 0$.
t_{jk}	The arrival time of van k at node $j \in N$.

We make the following assumptions.

- All parcels are delivered on the same day.
- Only one parcel locker is installed at each selected PT station, but the capacity of parcel lockers is infinite. In reality, the capacity of each parcel locker can be estimated according to the results of the D-PL location model.
- Given a specific compensation level, passengers' willingness to act as crowdshippers $Pr_{csshipper}$ is uniform. The value of $Pr_{csshipper}$ is set as the smallest value provided in Fessler et al. (2022).
- The speed of the vans is constant.
- The distance matrix is obtained by finding the shortest path between two nodes using a Julia Package (OpenStreetMapX.jl).

5.3.3 Delivery parcel locker location model

The D-PL location model is formulated as follows:

$$\min \sum_{i \in S^d} y_i \tag{5.1}$$

s.t.

$$\sum_{a \in S^o} \sum_{i \in S^d} w_{aij} = Q_j^{cs}, \forall j \in V_{cs} \tag{5.2}$$

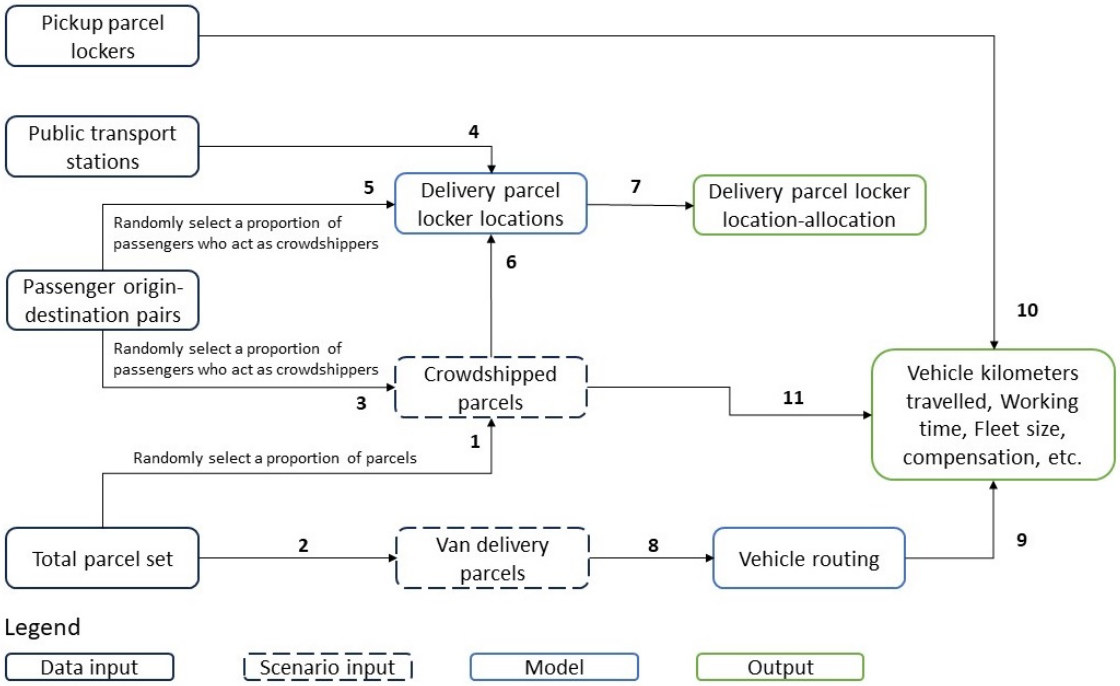

Figure 5.2: Overview of the modeling framework

$$\sum_{j \in V_{cs}} w_{aij} \leq y_i L_{ai} \eta Pr_{csshipper}, \forall a \in S^o, i \in S^d \tag{5.3}$$

$$w_{aij} \geq 0, \forall a \in S^o, i \in S^d, j \in V_{cs} \tag{5.4}$$

$$w_{aij} = 0, \forall a \in S^o, i \in S^d, j \in V_{cs}, \text{if } D_{ij} > D_{\text{max}} \tag{5.5}$$

$$y_i \in \{0, 1\} \tag{5.6}$$

The objective function (5.1) minimizes the number of D-PLs. Constraints (5.2) ensure that the total crowdshipped parcel flow to node $j \in V_{cs}$ satisfies all demands. Constraints (5.3) ensure that if there is no D-PL at PT station $i \in S^d$, the crowdshipped parcels flow through $i \in S^d$ is zero; otherwise, the crowdshipped parcel flow between $a \in S^o$ and $i \in S^d$ does not exceed the product of the number of crowdshippers traveling between nodes $a \in S^o$ and $i \in S^d$ and the average number of parcels carried per crowdshipper. Constraints (5.4) - (5.6) define the domains of decision variables. Constraints (5.5) state that if the distance between nodes $i \in S^d$ and $j \in V_{cs}$ is larger than D_{max}, the crowdshipper parcel flow routed between nodes $i \in S^d$ and $j \in V_{cs}$ is zero.

The model was solved by CPLEX in our case study.

5.3.4 Vehicle routing model

Similar to Zhang et al. (2023), we develop a vehicle routing model to determine the routes of vans. The model is formulated as follows:

$$\min \sum_{(i,j)\in N} \sum_{k\in K} T_{ij} x_{ijk} \tag{5.7}$$

s.t.

$$\sum_{k\in K} \sum_{i\in N, i\neq j} x_{ijk} = 1, \forall j \in V_h \tag{5.8}$$

$$\sum_{j\in N\setminus\{0\}} x_{0jk} \leq 1, \forall k \in K \tag{5.9}$$

$$\sum_{i\in N\setminus\{|V_h|+1\}} x_{i,|V_h|+1,k} \leq 1, \forall k \in K \tag{5.10}$$

$$\sum_{i\in N\setminus\{|V_h|+1\}, i\neq j} x_{ijk} - \sum_{i\in N\setminus\{0\}, i\neq j} x_{jik} = 0, \forall j \in V_h, k \in K \tag{5.11}$$

$$\sum_{i\in N\setminus\{|V_h|+1\}} \sum_{j\in N\setminus\{0\}, i\neq j} Q_j^h x_{ijk} \leq Cap, \forall k \in K \tag{5.12}$$

$$t_{0k} = 0, \forall k \in K \tag{5.13}$$

$$t_{ik} + ST_i + T_{ij} - T_{\text{max}}(1 - x_{ijk}) \leq t_{jk}, \forall i \in N\setminus\{|V_h|+1\}, j \in N\setminus\{0\}, j \neq i, k \in K \tag{5.14}$$

$$t_{|V_h|+1,k} \leq T_{\text{max}}, \forall k \in K \tag{5.15}$$

$$x_{ijk} \in \{0,1\}, \forall k \in K, (i,j) \in N \tag{5.16}$$

The objective function (5.7) minimizes the total travel time of vans. Note that this objective function also minimizes distance-based cost because of our assumption of the constant speed of vans. Constraints (5.8) ensure that each home delivery customer is visited exactly once. Constraints (5.9) ensure that all vans depart from the depot at most once. Constraints (5.10) ensure that all vans return to the depot at most once. Constraints (5.11) ensure flow conservation. Constraints (5.12) ensure the sum of demand at customers served by van k does not exceed the capacity of that van. Constraints (5.13) state that all vans are ready at time 0. Constraints (5.14) calculate the arrival time of van k at node $j \in N\setminus\{0\}$. They also eliminate subtours. Constraints (5.15) ensure that all vans should return to the depot before exceeding the maximum travel time of a route. Constraints (5.16) define the domains of decision variables.

The vehicle routing problem is NP-hard, which means that it is difficult to get the optimal solution to large instances within an acceptable time using exact methods. In this study, we develop an adaptive large neighborhood search (ALNS) metaheuristic to solve the routing problem, considering that the ALNS performs very well in many variants of vehicle routing problems (Cheng et al., 2023b; Li et al., 2016; Ropke & Pisinger, 2006). The ALNS was coded in C++.

5.4 Case study

5.4.1 Study area and data sources

This study used a central district located in the northwest of Copenhagen as the study area. It has a high population density at 18,820 persons per square kilometer. The district also has good PT coverage with 3 S-train[1] stations, 5 metro stations, and 56 bus stops. The reasons for selecting this district as our study area are as follows: 1) It faces serious traffic congestion due to its dense urban environment; 2) It has good PT coverage, which makes it suitable for PT-based crowdshipping; 3) There is a dedicated team in an anonymous logistics services provider in Denmark responsible for last-mile delivery in this district and this team validated our simulation results.

The total parcel data was provided by a major logistics services provider in Denmark. The data set includes the coordinates and demand values of each customer in the selected central district served by last-mile delivery vans. We extracted the data between October 11th – October 17th in 2021 for our study, representing a normal operation week, without the pandemic restrictions, Black Friday, public holidays, etc. On average, 864 parcels with 492 delivery points are delivered per weekday and 480 parcels with 146 delivery points are delivered on the weekend. We also extracted the smart card data (Rejsekort) from the same timeframe from Rejsekort & Rejseplanen A/S, which runs an electronic ticketing system for traveling by bus, train, and metro on behalf of the transport operators in Denmark. The data includes information on public transport users' selected trips and routes through the public transport network in Copenhagen. It represents approximately 40% of all public transport trips, excluding many monthly travel pass holders whose specific travel patterns were not known. The geospatial data, including the road map and PT stations, is from OpenStreetMap.

The anonymous logistics services provider's parcels distributed to the Copenhagen metropolitan area are sorted in a distribution center in a southwestern suburb of Copenhagen. Vans with smaller capacities depart from this distribution center, visit their designated areas for last-mile delivery, and finally return to the distribution center. There are two S-train stations near this distribution center. We assume P-PLs are installed in the two S-train stations. The locations of D-PLs in the selected central district are determined by the D-PL location model.

5.4.2 Scenario development and analysis

To assess the impacts of PT-based crowdshipping, we created four scenarios. The base scenario (S0) mirrors the current delivery mode, where all parcels are delivered by vans. In contrast, scenarios S1, S2, and S3 entail a transition of 10%, 20%, and 30% of parcels, respectively, from vans to crowdshippers. To mitigate the stochastic effects of randomly selecting crowdshipped parcels, we generate 15 samples for each scenario to obtain a comprehensive understanding of the crowdshipping scenarios. The compensation for crowdshippers is 10 DKK per parcel, aligning with the field test conducted in Denmark (Fessler et al., 2023).

As highlighted in Section 5.3, the volume of crowdshipped parcels is shaped by influencing factors from both the demand and supply sides. While our data sets lack information on demand-side factors (DF1 and DF2), we have drawn insights from other studies. Regarding DF1, a case study in Singapore indicates that approximately 74.9% of parcels are suitable for crowdshipping (Zhang et al., 2023). Regarding DF2, findings from a case study in Rome reveal that more than 60% of customers would opt to collect their parcels

[1] S-train serves the Copenhagen metropolitan area. It has 86 stations that connect the suburban and urban areas. The S-train system carries more than 357,000 passengers a day.

from parcel lockers if parcel lockers are installed within 500 m of their residences and are accessible 24h a day. According to these studies, we believe that achieving a 30% share of crowdshipped parcels is not insurmountable from the demand perspective, provided that the deployment of D-PLs is well-designed.

Turning to influencing factors on the supply side (SF1, SF2, and SF3), we have access to SF1 information through the Rejsekort data. For SF2, we set $Pr_{csshipper} = 30\%$ in this study. As reported by Fessler et al. (2022), when the compensation to the crowdshipper is 10 DKK per parcel, the probability of a passenger bringing a parcel during his/her trip is about 30%. To prevent SF3 from limiting the supply of PT-based crowdshipping, we do not impose a maximum limit on the number of D-PLs that could be installed. Inputting this data to the D-PL location model, we could acquire valuable insights into the feasibility of achieving scenarios S1, S2, and S3, and evaluate the ease or difficulty associated with each of them.

Ideally, the values of D_{max} and η should be set to 500m and 1, respectively. However, these ideal values could lead to infeasible solutions under some scenarios. Hence, we conducted a sensitivity analysis on D_{max} and η to explore the challenges of achieving corresponding scenarios. We consider three values of D_{max}: 500m, 600m, and 700m. Given a value of D_{max}, we initially set $\eta = 1$ and solve the D-PL model. If there is no feasible solution, we increase the value of η by 0.1 and re-run the model until there is a feasible solution. By doing this, we ascertain the minimum number of parcels a passenger should take under a specific value of D_{max}. The corresponding objective value indicates the minimum number of required D-PLs under the combination of (D_{max}, η). Table 5.3 presents a view of the minimum number of parcels per crowdshipper should take and the corresponding number of delivery parcel lockers to achieve varying scenarios under different values of D_{max}.

Table 5.3: The minimum number of parcels per crowdshipper should take and the corresponding number of delivery parcel lockers to achieve varying scenarios under different values of D_{max}

Scenario	D_{max}	The minimum number of parcels per crowdshipper should take	Number of delivery parcel lockers
S1	500 m	1	19
S1	600 m	1	16
S1	700 m	1	13
S2	500 m	1.5	30
S2	600 m	1.3	32
S2	700 m	1	30
S3	500 m	2.2	35
S3	600 m	1.9	37
S3	700 m	1.5	30

According to Table 5.3, S1 is very easy to achieve given current passenger volumes. This is facilitated by the acceptability of a 500-meter distance to transit and the practice of a crowdshipper carrying just one parcel per trip. When D_{max} increases, the required number of D-PLs decreases.

In contrast, the realization of S2 and S3 presents more challenges compared to S1. When $D_{\text{max}} = 500$m, each crowdshipper needs to carry 1.5 and 2.2 parcels per trip to achieve S2 and S3, respectively. Although increasing D_{max} leads to a reduction of the minimum number of parcels a crowdshipper needs to carry, it may cause inconvenience for customers and consequently affect the demand for PT-based crowdshipping. Certain measures should be implemented to cope with the challenges arising from higher D_{max} values. One such solution is to lower prices for PT-crowdshipping customers. Alternatively, if we keep $D_{\text{max}} = 500$ m and look at parameters on the supply side, there are two ideas to

address the challenges to achieve S2 and S3. First, assuming that passenger volumes remain unchanged, efforts could be made to increase passengers' willingness to participate as crowdshippers or to bring more than one parcel. This could be achieved by increasing the compensation level. As demonstrated by Fessler et al. (2022), increasing the compensation level results in a higher likelihood of passengers acting as crowdshippers. Moreover, a crowdshipper would like to carry an additional parcel if the compensation is increased by 2.67 DKK. Second, if we maintain the compensation level unchanged and each crowdshipper continues to carry only one parcel per trip, actions could be taken to increase the number of PT users. This is beyond the capacity of logistics companies but is congruent with the policies employed by numerous nations that advocate for a shift from private car utilization towards the utilization of public transport.

5.4.3 Impacts

Using the methodology introduced in Section 5.3, we simulate the delivery operation of the anonymous carrier across various scenarios. Three key performance indicators, vehicles kilometers traveled per day (including the travel distance of trucks that transport crowdshipped parcels from the distribution center to P-PLs), total working time of drivers, and the number of used vans to serve the selected central district, are used to describe the performance of each scenario. The simulation results of the base scenario were validated by the anonymous carrier, which confirms that the three indicators obtained from our simulation are very close to their actual operations on those days. The value of each indicator for each scenario is equal to the average value of the 15 samples of the scenario. The impacts of PT-based crowdshipping are presented below.

- **Impacts on vehicle kilometers traveled**

  Figure 5.3 presents the percentage change of vehicle kilometers traveled during the study period under different crowdshipping scenarios. All signs are negative, indicating that using PT-based crowdshipping as a complementary solution to last-mile delivery could effectively reduce the vehicle kilometers traveled to deliver the parcels, even if some distances are needed to transport the crowdshipped parcels from the distribution center to P-PLs. Moreover, there is a direct correlation between the number of crowdshipped parcels and the percentage reduction of vehicle kilometers traveled. Specifically, it is shown that the average percentage reduction of vehicle kilometers traveled is 6%, 11%, and 20% under scenarios S1, S2, and S3, respectively. In addition, the percentage reduction of vehicle kilometers traveled on the weekdays (8%, 14%, and 25% for scenarios S1, S2, and S3, respectively) is more significant than that on the weekend (2%, 4%, and 6% for scenarios S1, S2, and S3, respectively).

- **Impacts on total working time of drivers**

  Figure 5.4 demonstrates the percentage change in drivers' total working time under different scenarios. On average, a substantial reduction in drivers' total working time is evident, with scenarios S1, S2, and S3 leading to reductions of 11%, 20%, and 30% on weekdays, and 7%, 15%, and 21% on weekends, respectively. These observations underscore that PT-based crowdshipping is able to alleviate the growing labor intensity of drivers.

- **Impacts on the number of used vans**

  Figure 5.5 shows the change in the number of used vans to serve the selected central district across different scenarios. The simulation results are in line with our intuition that when parcels are progressively shifted from vans to crowdshippers,

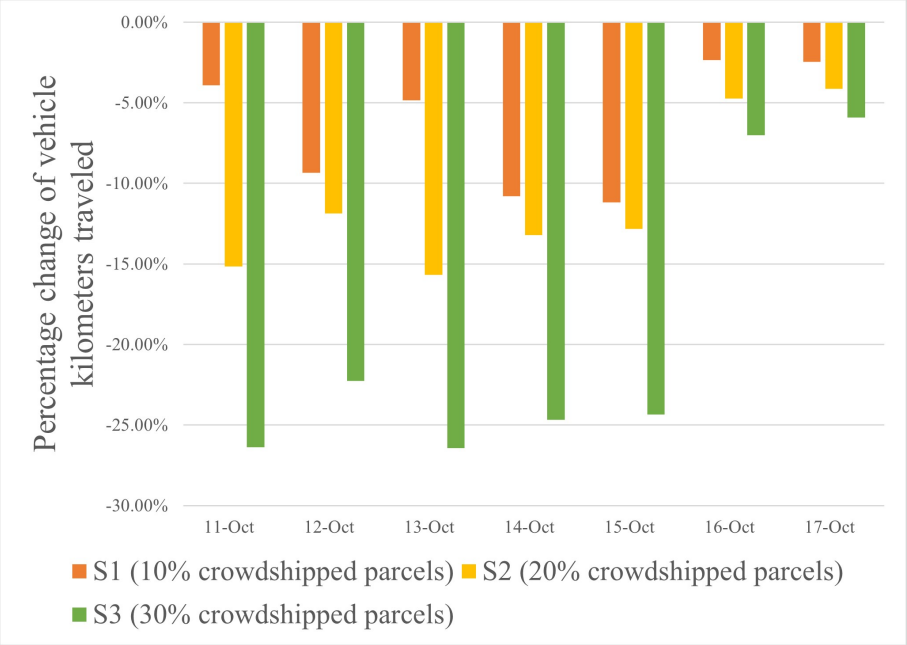

Figure 5.3: Percentage change of vehicle kilometers traveled under different scenarios

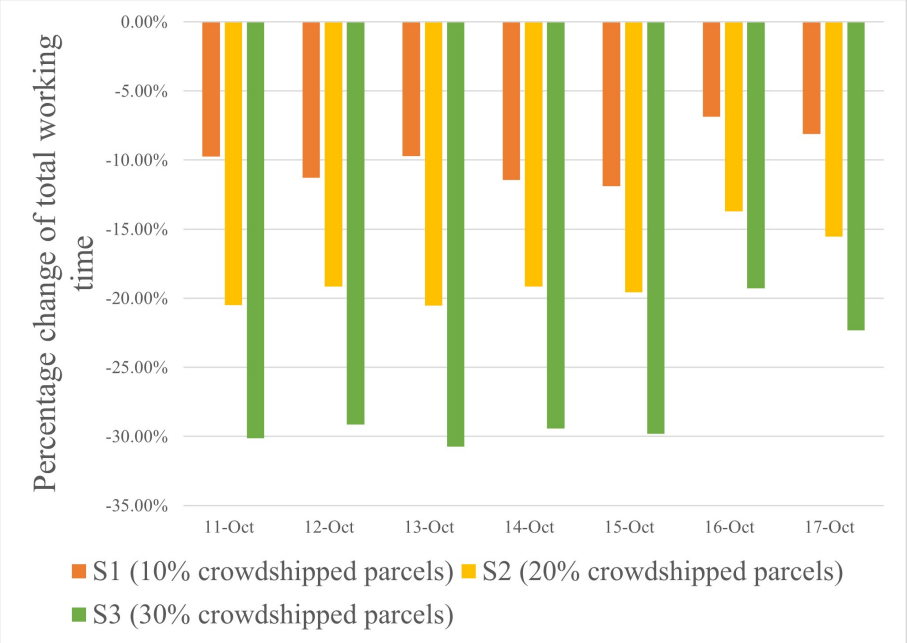

Figure 5.4: Percentage change of total working time under different scenarios

the number of used vans should be less than or equal to that of the base scenario. Notably, the number of used vans on weekends remains uniform under the four scenarios. Additionally, the number of used vans remains unchanged in S1 on October 11th and October 13th. This intriguing phenomenon is attributed to the limited capacity of vans. In these cases, the number of used vans is equal to the minimum number of vans required to serve the selected central district, which is calculated by dividing the total demands in this district by the van's capacity. This observation indicates that realizing meaningful reductions in the number of required vans (drivers) is contingent on the transition of a substantial parcel volume from vans to crowd-

shippers. Generally, if 20% of the parcels could be delivered by crowdshippers, it facilitates the release of one van (driver). If the percentage of crowdsourced parcels reaches 30%, two vans (drivers) are released.

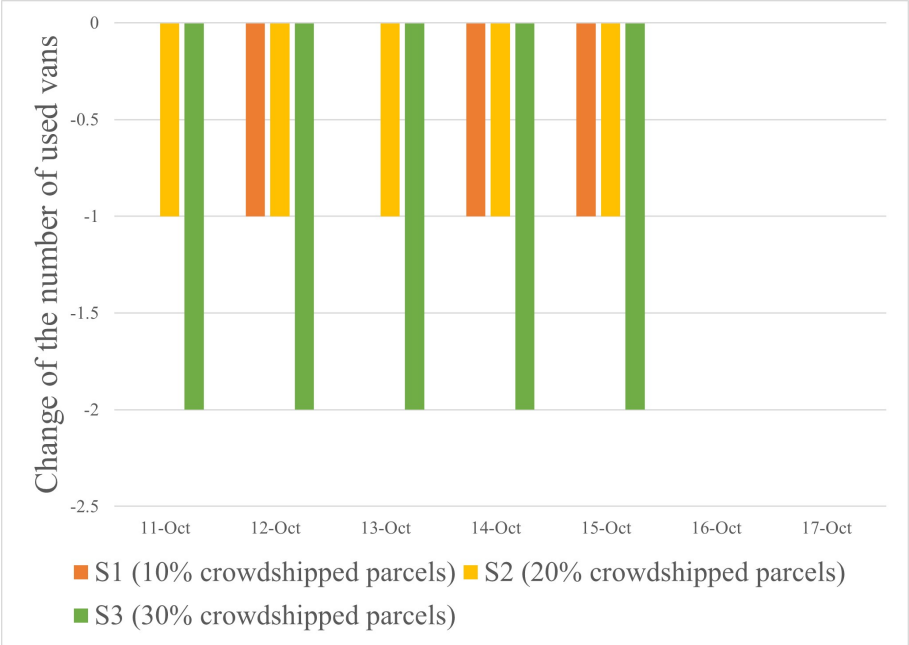

Figure 5.5: Change of the number of used vans under different scenarios

- **Cost analysis**

  Our cost analysis accounts for four distinct types of costs, i.e., driving costs of vans and trucks, external costs of traffic (e.g., marginal costs of air pollution and traffic congestion), labor cost, and compensation paid to crowdshippers. This section presents the potential benefits of PT-based crowdshipping based on the transport economic unit prices (TEUP) of 2022 prepared by Transport DTU and COWI for the Ministry of Transport (Denmark) (https://www.man.dtu.dk/forskningsbaseret-raadgivning/teresa-og-transportoekonomiske-enhedspriser).

  – **Driving costs.** The driving costs of vans and trucks encompass expenses related to fuel, tires, repair and maintenance, and depreciation. These costs are split into fixed and variable costs per hour and per kilometer, respectively, in TEUP. Fixed costs for vans and trucks are 529 DKK/hour and 542 DKK/hour, respectively. Variable costs for vans and trucks are 1.82 DKK/km and 4.19 DKK/km, respectively.

  – **External costs.** The negative externalities of transport account for air pollution, climate change, noise, accidents, congestion, and wear on the infrastructure. The marginal external costs are used to estimate the cost per kilometer for the external effects. The marginal external costs for vans and trucks are 1.46 DKK/km and 6.01 DKK/km, respectively.

  – **Labor cost.** The average salary for a postal delivery worker is 24,274 DKK per month (https://www.paylab.com/dk/salaries-in-country?lang=en).

  – **Compensation paid to crowdshippers.** This stands at 10 DKK per parcel, the same as the field test in Fessler et al. (2023).

Table 5.4 presents the four types of costs under different crowdshipping scenarios. The distribution of each type of cost among various scenarios is similar. Figure 5.6 illustrates the percentage distribution of each cost category. As shown in Figure 5.6, the labor cost accounts for most of the total costs (71%), followed by the driving cost (25%), the external cost (3%), and the compensation (1%). Since labor cost is the predominant factor of total costs, a significant reduction in total costs occurs only when at least one van is saved. On average, the total costs of S1, S2, and S3 are reduced by 8%, 13%, and 24% on weekdays and 1%, 3%, and 4% on the weekend, respectively, compared to the base scenario. Based on Table 5.4, we conclude that PT-based crowdshipping has great potential to reduce last-mile delivery's labor cost and driving cost by providing small compensation. This will definitely benefit logistics companies by reducing operational costs, while its impacts on employment opportunities could be negative for markets oversaturated with delivery workers or positive for markets lacking delivery workers.

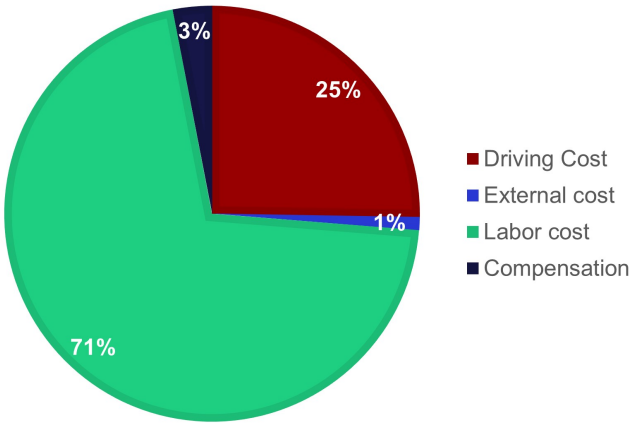

Figure 5.6: Percentage of each cost type

5.5 Conclusions

In this study, we proposed a methodology consisting of a parcel locker location model and a vehicle routing model to investigate the impact of implementing the PT-based crowdshipping as a complementary solution to the traditional last-mile solution. We selected a central district in Copenhagen as study area because of its high population density and good coverage of public transport. Three crowdshipping scenarios with varying percentages of crowdshipped parcels were created to compare against the traditional delivery method.

We evaluated the performance of different scenarios using three indicators, i.e., vehicle kilometers traveled, total working time of drivers, and the number of used vans. All indicators obtained reductions, with larger decreases corresponding to higher proportions of crowdshipped parcels. In the most optimistic scenario, where 30% of the parcels are delivered by crowdshippers, we observe an average reduction of 20% and 27% in vehicle kilometers traveled and the total working time of drivers, respectively; two vans (drivers) were released. The cost analysis reveals that substantial savings in labor and driving costs could be achieved by offering small compensations to crowdshippers. However, the challenge lies in achieving the shift of 30% of parcels from vans to crowdshippers. Considering customers' high willingness to collect parcels from parcel lockers within 500m of their homes, we believe the bottleneck that restricts the development of PT-based crowdshipping is not from the demand side but the supply side. Efforts could be made to increase

Table 5.4: Cost analysis of public transport-based crowdshipping under different scenarios

		11-Oct	12-Oct	13-Oct	14-Oct	15-Oct	16-Oct	17-Oct
Driving costs (DKK)	S0	16,123	17,275	17,010	16,239	15,230	2,717	7,747
	S1	14,117	15,431	14,882	14,502	13,558	2,487	6,965
	S2	12,569	13,648	13,228	12,887	12,034	2,256	6,228
	S3	11,239	12,192	11,806	11,529	10,780	2,082	5,618
External costs (DKK)	S0	288	314	292	282	279	58	140
	S1	281	289	283	255	252	57	138
	S2	253	286	255	253	251	56	137
	S3	225	259	228	225	223	56	137
Labor costs (DKK)	S0	42,480	48,548	42,480	42,480	42,480	6,069	18,206
	S1	42,480	42,480	42,480	36,411	36,411	6,069	18,206
	S2	36,411	42,480	36,411	36,411	36,411	6,069	18,206
	S3	30,343	36,411	30,343	30,343	30,343	6,069	18,206
Compensation (DKK)	S0	0	0	0	0	0	0	0
	S1	870	970	870	830	800	120	360
	S2	1,730	1,930	1,740	1,650	1,600	240	720
	S3	2,600	2,900	2,610	2,480	2,390	360	1,080
Total costs (DKK)	S0	58,890	66,137	59,782	59,000	57,989	8,843	26,092
	S1	57,747	59,169	58,514	51,998	51,021	8,732	25,668
	S2	50,962	58,344	51,634	51,201	50,297	8,621	25,291
	S3	44,407	51,761	44,987	44,576	43,735	8,566	25,041
Percentage change in total costs	S1	-2%	-11%	-2%	-12%	-12%	-1%	-2%
	S2	-13%	-12%	-14%	-13%	-13%	-3%	-3%
	S3	-25%	-22%	-25%	-24%	-25%	-3%	-4%

the number of crowdshippers from several angles. For example, encouraging people to take PT instead of driving private cars; increasing the compensation level to attract more passengers to act as crowdshippers or to motivate crowdshippers to carry more parcels per trip.

While our study provides valuable insights into the potential benefits and impacts of PT-based crowdshipping and how to push its development, it has several limitations that can be investigated in further studies. First, expanding the study area to encompass larger regions. Second, developing optimization models to further optimize the deployment of the system. For example, instead of merely choosing PT stations near the distribution center to place P-PLs, an optimization model could be developed to optimize the location of P-PLs to maximize the potential benefits of PT-based crowdshipping, especially when expanding this service to a larger area. Third, developing more accurate methodologies and using advanced software to simulate the actual traffic in a city and using more indicators to describe the system performance may be needed to scale the results to a regional/city level rather than a district level only.

Acknowledgment

The first author acknowledges financial support from the China Scholarship Council (No. 202107940012). We thank the anonymous logistics services provider and Rejsekort & Rejseplanen A/S for providing the data.

References

Allahviranloo, M., & Baghestani, A. (2019). A dynamic crowdshipping model and daily travel behavior. *Transportation Research Part E: Logistics and Transportation Review*, *128*, 175–190.

Alnaggar, A., Gzara, F., & Bookbinder, J. H. (2021). Crowdsourced delivery: A review of platforms and academic literature. *Omega*, *98*, 102139.

Buldeo Rai, H., Verlinde, S., & Macharis, C. (2018). Shipping outside the box. environmental impact and stakeholder analysis of a crowd logistics platform in belgium. *Journal of Cleaner Production*, *202*, 806–816.

Cheng, R., Jiang, Y., & Nielsen, O. A. (2023a). Integrated people-and-goods transportation systems: From a literature review to a general framework for future research. *Transport Reviews*, 1–24.

Cheng, R., Jiang, Y., Nielsen, O. A., & Pisinger, D. (2023b). An adaptive large neighborhood search metaheuristic for a passenger and parcel share-a-ride problem with drones. *Transportation Research Part C: Emerging Technologies*, *153*, 104203.

European Commission. (2007). Green paper, towards a new culture for urban mobility, Luxembourg: Publications Office of the European Union.

European Regulators Group for Postal Services. (2022). ERGP PL II (22) 12 ERGP report on core indicators 2021 for monitoring the European postal market.

Fessler, A., Cash, P., Thorhauge, M., & Haustein, S. (2023). A public transport based crowdshipping concept: Results of a field test in denmark. *Transport Policy*, *134*, 106–118.

Fessler, A., Thorhauge, M., Mabit, S., & Haustein, S. (2022). A public transport-based crowdshipping concept as a sustainable last-mile solution: Assessing user preferences with a stated choice experiment. *Transportation Research Part A: Policy and Practice*, *158*, 210–223.

Gatta, V., Marcucci, E., Nigro, M., & Serafini, S. (2019). Sustainable urban freight transport adopting public transport-based crowdshipping for b2c deliveries. *European Transport Research Review*, *11*(1), 1–14.

Iannaccone, G., Marcucci, E., & Gatta, V. (2021). What young e-consumers want? forecasting parcel lockers choice in rome. *Logistics*, *5*(3), 57.

Karakikes, I., & Nathanail, E. (2022). Assessing the impacts of crowdshipping using public transport: A case study in a middle-sized greek city. *Future Transportation*, *2*(1), 55–83.

Kızıl, K. U., & Yıldız, B. (2023). Public transport-based crowd-shipping with backup transfers. *Transportation Science*, *57*(1), 174–196.

Li, B., Krushinsky, D., Van Woensel, T., & Reijers, H. A. (2016). An adaptive large neighborhood search heuristic for the share-a-ride problem. *Computers & Operations Research*, *66*, 170–180.

Paus, E. (2018). *Confronting dystopia: The new technological revolution and the future of work*. Cornell University Press.

Punel, A., & Stathopoulos, A. (2017). Modeling the acceptability of crowdsourced goods deliveries: Role of context and experience effects. *Transportation Research Part E: Logistics and Transportation Review*, *105*, 18–38.

Ropke, S., & Pisinger, D. (2006). An adaptive large neighborhood search heuristic for the pickup and delivery problem with time windows. *Transportation science*, *40*(4), 455–472.

Statista. (2022). *Worldwide retail e-commerce sales. statista*. https://www.statista.com/statistics/379046/worldwide-retail-e-commerce-sales/

Zhang, M., & Cheah, L. (2023). Prioritizing outlier parcels for public transport-based crowdshipping in urban logistics. *Transportation Research Record*, 03611981231182429.

Zhang, M., Cheah, L., & Courcoubetis, C. (2023). Exploring the potential impact of crowdshipping using public transport in singapore. *Transportation Research Record*, *2677*(2), 173–189.

6 Conclusions

Transportation plays a vital role in society and the economy. It facilitates the movement of people and goods, enabling economic activities and providing people with access to essential services such as education and healthcare. Over recent decades, factors such as population growth and urbanization and the boom of E-commerce have led to a significant increase in urban transportation demands. While this has undoubtedly boosted the economy, it has also exacerbated traffic congestion and environmental pollution. In response to the European Commission's (2007) advocacy for the integration of passenger and freight transportation, this thesis delves into the feasibility of mitigating negative externalities of transportation by merging the two transportation flows. Initially, we provide an overview of the development of integrated transportation systems and propose a general framework for planning such a system. Subsequently, we introduce two novel forms of integrating passengers and goods and validate their viability. The contributions of this thesis are not limited to advancing the comprehension of the development of integrated people-and-goods transportation but also enhancing mathematical optimization within related fields such as VRP and crowdshipping.

This chapter concludes the thesis by responding to the research questions we proposed in Chapter 1, summarizing the contributions, and presenting future research directions.

6.1 Research questions revisited

Research question 1 (Q1). Which framework can comprehensively represent and guide the planning and operation of an integrated people-and-goods transportation system?

In Chapter 2, we present such a framework comprising three interconnected modules. The first module encompasses physical components in the integrated transportation system, including people and goods transportation demands, transportation supply (e.g., public transport and private vehicles), and infrastructure underpinning the transportation system (e.g., road and information and communications technology). The second module relates to planning and operating the integrated transportation system, covering demand management, supply management, and demand-supply matching. The third module includes key performance indicators for evaluating the effectiveness of the integrated transportation system on both the demand and supply sides. There is a dynamic feedback loop between the three modules. Module 1 serves as the input for Module 2, where the actions taken by operators according to the demand and supply status in Module 1 directly influence the system performance (Module 3). The performance of the system (Module 3), in turn, influences the demand and supply in Module 1.

Research question 2 (Q2). Are there innovative solutions that incorporate other last-mile solutions with the concept of integrating people and goods transportation?

This thesis investigates two innovative solutions that couple other prevailing last-mile solutions with integrated people-and-goods transportation, presenting the concept and identifying the key planning problems involved.

Chapter 3 proposes our first solution: utilizing DRBs and drones to combine passenger and parcel transportation. A passenger request is characterized by its origin, destination,

and associated demand value, while parcel requests share unified demand values and are characterized solely by their destinations. All requests have specified time windows. Delay is allowed with a penalty. DRBs can serve both passengers and parcels, while drones are exclusively responsible for parcel delivery. To ensure passengers have a higher priority than parcel requests, we impose constraints on the maximum number of intermediate stops between one passenger service request. The central challenge within this concept is optimizing the routes for both DRBs and drones. We term the corresponding problem as passenger and parcel share-a-ride problem with drones (SARP-D).

Chapter 5 introduces our second solution: public transport (PT)-based crowdshipping. This innovative approach acts as a complementary solution to traditional delivery. Within this framework, a portion of the parcels are delivered by crowdshippers, while the rest of the parcels are delivered by logistics companies using their vans. Crowdshippers are PT users who utilize their planned trips to transport parcels between parcel lockers positioned at their origin and destination PT stops. This solution represents a potential synergy between urban PT and logistics systems. Two key problems are involved in this concept. The first one is the parcel locker location problem: optimizing the locations of parcel lockers while considering the accessibility and efficiency for both crowdshippers and parcel recipients. The second one is the vehicle routing problem for vans that distribute parcels that cannot be accommodated by crowdshippers, considering constraints on the vehicle capacity, drivers' maximum working time, etc.

Research question 3 (Q3). What are the benefits of the proposed innovative solutions, and how can they be quantified?

The main key performance indicators considered in this thesis are total operations costs, the number of used vehicles, and the total vehicle kilometers traveled. The results in Chapters 3,4, and 5 demonstrate that both SARP-D and PT-based crowdshipping contribute to a significant reduction in these three indicators. The reduction degree depends on several factors, varying between the two solutions. For the SARP-D, it depends on the distribution of the requests, the maximum intermediate stops between one passenger request, etc. For PT-based crowdshipping, it depends on the number and percentage of parcels that are delivered by crowdshippers.

Chapters 3 and 4 provide two distinct approaches to quantify the benefits of the SARP-D. Specifically, Chapter 3 presents an arc-based mixed integer programming model solvable by CPLEX for small instances with up to 12 nodes. Larger instances with up to 200 nodes are solved by the ALNS metaheuristic. Remarkably, our ALNS also demonstrates exceptional performance in solving the VRP-D, comparable to a metaheuristic designated for the VRP-D. In contrast, Chapter 4 reformulates the SARP-D into a path-based model, which is solved by the CG. The CG provides a verified lower bound and an upper bound for the SARP-D. If the lower and upper bounds are the same, the problem is solved optimally. Computation results show that the CG could solve SARP-D instances with up to 50 nodes, and 66% of SARP-D instances were solved optimally. Overall, the average gap between the upper and lower bounds for all SARP-D instances is less than 0.6%. If the ratio of passenger requests to the total requests is set to 0% and 100%, the SARP-D is simplified to VRP-D and one-to-one PDP, respectively. Our CG could solve the VRP-D and one-to-one PDP as well. The instances used in Chapters 3 and 4 are created based on VRP-D instances presented by Sacramento et al. (2019).

In Chapter 5, we present a mixed integer programming model to optimize the locations of parcel lockers. The model can be solved by CPLEX. We further devise an ALNS metaheuristic to optimize the vans' routes for delivering parcels that are not delivered by crowd-

shippers. To evaluate the impacts of PT-based crowdshipping, we create four scenarios. The base scenario is the existing distribution mode, where all parcels are delivered by vans. In other scenarios, we shift 10%, 20%, and 30% of parcels from vans to crowdshippers. Initially, we seek validation from an anonymous logistics company for the vehicle routes derived from our algorithm in the baseline scenario. Then, we apply our parcel locker location model and vehicle routing model to calculate the total vehicle kilometers traveled, the total working time of drivers, and the number of used vehicles in other scenarios. The case study conducted in Chapter 5 is based on real-world data, with the parcel data provided by a major logistics services provider in Denmark and the public transport travel card data provided by Rejsekort & Rejseplanen A/S, which runs an electronic ticketing system for traveling by bus, train, and metro on behalf of the transport operators in Denmark.

6.2 Contributions

Contributions to integrated people-and-goods transportation

This thesis's contributions to the realm of integrated people-and-goods transportation are twofold.

Comprehensive review and a general framework.

We provide a comprehensive review of integrated people-and-goods transportation by categorizing various integration forms, exemplifying their applications, highlighting key issues for different forms, and introducing corresponding solutions. Furthermore, we propose a general framework for describing, planning, and operating an integrated transportation system. This review advances the understanding of integrated people-and-goods transportation for the public, scholars, and practitioners in this field.

Innovative integration forms.

We enrich studies on integrated people-and-goods transportation by proposing two innovative integration forms that harness opportunities presented by emerging technologies and last-mile solutions: integrating passenger and parcel transportation by DRBs and drones and PT-based crowdshipping. Meanwhile, we validate the feasibility of the two integration forms. In Chapter 3, we elaborate on the operation of the first integrated transportation system, identify the key problem of the system (SARP-D), provide a mathematical formulation for the SARP-D, and develop an ALNS metaheuristic for the SARP-D. An alternative method for the SARP-D is presented in Chapter 4. Chapter 5 introduces the concept of PT-based crowdshipping, provides an approach to planning such a system, and analyzes its potential impacts by conducting a case study using real-world data.

Contributions to the VRP

Introduction of a distinctive variant of the VRP.

Fundamentally, the VRP-D and one-to-one PDP are established variants of the VRP due to their distinctive features. While the SARP-D bears some similarities with the VRP-D and one-to-one PDP, it has special features that set it apart and could become a new variant of the VRP. In particular, the SARP-D differs from the VRP-D because the ground vehicles in the VRP-D do not serve passengers, whereas the SARP-D involves passenger service. Furthermore, the SARP-D distinguishes itself from the one-to-one PDP because the SARP-D necessitates coordination and synchronization between ground and aerial vehicles, while the one-to-one PDP does

not. More importantly, what truly sets the SARP-D apart from the VRP-D and one-to-one PDP is that the ground vehicles in the SARP-D serve requests with different features, i.e., pickup and delivery for passenger requests and delivery tasks for parcel requests, while the ground vehicles perform only delivery tasks in the VRP-D and only pickup and delivery tasks in the one-to-one PDP. The different characteristics of one-to-one pickup and delivery tasks and only delivery tasks make the model different because the one-to-one PDP involves pairing and precedence constraints, whereas the delivery-only tasks do not. Overall, the hybrid tasks of one-to-one pickup and delivery and delivery-only tasks in the SARP-D make it more complicated than the VRP-D and one-to-one PDP and establish the SARP-D as a new variant of the VRP.

Solution methods and benchmark instances.

In addition to introducing a new variant of the VRP, this thesis also provides solution methods and benchmark instances that can serve as valuable resources for future studies on the SARP-D.

Contributions to crowdshipping

Exploration of PT-based Crowdshipping.

Crowdshipping has been regarded as a complementary solution for last-mile logistics in recent years. It has various application ways. Most of them rely on personal vehicles, where dedicated trips or subtours are unavoidable, which leads to increases in the number of trips, vehicle kilometers traveled, etc. To avoid this, we present the idea of PT-based crowdshipping, which utilizes passengers' trips that will be taken anyway to perform crowdsourced delivery. While PT-based crowdshipping is not a completely new concept, it remains an underexplored area with limited prior research. In this thesis, we delve deeper into the concept, drawing inspiration from the following two works.

Optimization models for parcel locker location.

Existing studies on PT-based crowdshipping focus on analyzing passengers' preferences or assessing the impacts of PT-based crowdshipping based on a given network, i.e., the locations of parcel lockers are determined. In contrast, we develop an optimization model to determine the ideal PT stations for installing parcel lockers to maximize the benefits of PT-based crowdshipping.

Real-world case study.

We conduct a case study in a central district in Copenhagen using real-world data. The dataset includes actual parcel data provided by a major logistics services provider in Denmark, public transport travel card data provided by Rejsekort & Rejseplanen A/S, and geographic data from OpenStreetMap.

6.3 Future research

For SARP-D

Future research directions on SARP-D could be considered from modeling, solution methods, and operation aspects.

Extended models accounting for dynamics and uncertainties.

Chapters 3 and 4 consider static and deterministic SARP-D. These models can be extended to accommodate dynamics and uncertainties. In practice, passenger and

parcel requests might occur dynamically. In addition, there are lots of uncertainties in real life. For example, travel time on the road may be influenced by the weather, traffic congestion, or some unexpected events. A customer location's suitability for drone taking-off or landing might be influenced by the weather. Developing models that can adapt to these real-world fluctuations will lead to more robust and adaptable solutions.

Advanced solution methods.

Chapter 3 offers a metaheuristic, while Chapter 4 provides an alternative method that is not exact but could yield solutions very close to optimality. Since the SARP-D is quite a new problem, there is room for developing faster solution methods, whether exact methods or heuristics, especially for solving large instances. Moreover, it would also be interesting to embed machine learning and reinforcement learning with exact or heuristics, given that they have shown good performance in solving some combinatorial optimization problems (Karimi-Mamaghan et al., 2022; Nazari et al., 2018).

Complex drone operations.

In Chapters 3 and 4, we assume that each drone is capable of performing only one delivery task during each flight. It is worth considering scenarios where this assumption is relaxed, e.g., a drone has a larger load capacity and extended battery life. Meanwhile, integrating a function that calculates the drone energy consumption into the SARP-D model could provide valuable insights into energy-efficient drone deployment. Moreover, it would be intriguing to replace aerial drones with ground-based counterparts, i.e., autonomous delivery robots, because they are more politically acceptable.

Electric vehicle integration.

With people's growing concern about GHG emissions, numerous countries around the world are actively striving to transition from conventional vehicles to electric vehicles as part of their climate action plans. Consequently, the DRBs in our SARP-D could be replaced with electric vehicles, and our SARP-D models could be expanded to incorporate considerations associated with electric vehicles, e.g., the charging location and charging strategy of electric vehicles. It is also valuable to consider a fleet of DRBs comprising both electric and conventional vehicles, recognizing that transforming from conventional vehicles to electric vehicles takes a long time.

For PT-based crowdshipping

In Chapter 5, we explore PT-based crowdshipping from a high level. There exist several limitations that could be studied in the future.

Extending the study area.

The study area in Chapter 5 is a district in Copenhagen. An extension of the study area will produce a more comprehensive understanding of PT-based crowdshipping because first, the impacts of PT-based crowdshipping in areas that have short, medium, and long distances to the distribution center might vary significantly; second, implementing this service in larger areas may produce scale benefits by involving more PT passengers. Moreover, extending this service to rural areas would enhance the economic viability of transport services in such regions.

Optimization of origin PT stations of crowdshipped parcels.

We assume all parcels designated for delivery by crowdshippers are transported by trucks from the distribution center to S-train stations near the depot, from where crowdshippers pick up the parcels. However, since distribution centers are usually located in suburban areas, it might be more advantageous to consider transporting crowdsourced parcels to some major PT stations having more passenger volume. This results in a research problem of selecting PT stations, where the parcels are transferred from trucks to crowdshippers, to maximize the utilization of both PT and crowdshippers' capacities and ultimately maximize the benefits of PT-based crowdshipping.

Handling unsuccessful deliveries.

We assume all crowdsourced parcels could be delivered by crowdshippers successfully. However, in practice, there may be situations where some crowdshippers do not complete deliveries. Future research should explore the management of undelivered parcels to enhance the overall effectiveness of PT-based crowdshipping.

References

European Commission. (2007). Green paper, towards a new culture for urban mobility, Luxembourg: Publications Office of the European Union.

Karimi-Mamaghan, M., Mohammadi, M., Meyer, P., Karimi-Mamaghan, A. M., & Talbi, E.-G. (2022). Machine learning at the service of meta-heuristics for solving combinatorial optimization problems: A state-of-the-art. *European Journal of Operational Research*, *296*(2), 393–422.

Nazari, M., Oroojlooy, A., Snyder, L., & Takác, M. (2018). Reinforcement learning for solving the vehicle routing problem. *Advances in neural information processing systems*, *31*.

Sacramento, D., Pisinger, D., & Ropke, S. (2019). An adaptive large neighborhood search metaheuristic for the vehicle routing problem with drones. *Transportation Research Part C: Emerging Technologies*, *102*, 289–315.